

**MODULATING CYTOCHROME P450-MEDIATED ARACHIDONIC ACID METABOLISM AS  
A POTENTIAL NEW TREATMENT MODALITY FOR CARDIAC HYPERTROPHY**

by

Ahmed Abd El-Hakeem El-Sherbeni

A thesis submitted in partial fulfillment of the requirements for the degree of

**DOCTOR OF PHILOSOPHY  
IN  
PHARMACEUTICAL SCIENCES**

Faculty of Pharmacy and Pharmaceutical Sciences  
University of Alberta

© Ahmed Abd El-Hakeem El-Sherbeni, 2017

## Abstract

Arachidonic acid (AA) metabolism has long been a very appealing target for drug discovery and development efforts. Beside cyclooxygenase and lipoxygenase pathways, AA is also metabolized by the recently recognized cytochrome P450 (P450) pathway, forming several biologically-active epoxyeicosatrienoic acids (EETs) and hydroxyeicosatetraenoic acids (HETEs). Already, drugs that are targeting cyclooxygenase- and lipoxygenase-mediated AA metabolism are remarkably successful medicines. For P450-derived AA metabolites, recent data demonstrated their potent and multifaceted roles in cardiovascular pathophysiology, albeit no drug was clinically approved to target these metabolites. Our focus was on cardiac hypertrophy, which is a prelude for heart failure estimated to affect 2.2% of US population. Once heart failure develops from cardiac hypertrophy, the condition is irreversible and is associated with a high death rate. Accordingly, our aims were; 1) to characterize AA metabolism by microsomes separated from different rat organs and by individual recombinant rat P450 enzymes, 2) to determine the alterations in P450-mediated AA metabolism in the heart during cardiac hypertrophy, 3) to identify novel drug targets in the P450-mediated AA metabolic cascade, and 4) to extrapolated animal and human in vitro data to identify an effective and safe modulator of P450-mediated AA metabolism. Our results showed that microsomes from different rat organs can mediate the formation of their own P450-derived AA metabolites with organ-distinct metabolic and kinetic profiles. In addition, our data suggest that the major P450-epoxygenases are CYP2C11, CYP2Bs, CYP2C23 and CYP2C11/ CYP2C23 for the heart, lungs, kidneys and liver, respectively, while CYP4As may be the major  $\omega$ -hydroxylase in the heart and kidneys, and CYP4As and/or CYP4Fs may be the major hydroxylases in the lungs and liver. Cardiac P450 enzymes that were altered and significantly impacted P450-mediated AA metabolism during cardiac hypertrophy were identified in SD rats to be, CYP1B1, CYP2B2, CYP2J3 and CYP4As, which may have a role in the development and progression of pressure overload-induced cardiac hypertrophy, by

mediating the formation and degradation of 12-, 19- and 20-HETEs and EETs. Furthermore, our results showed that certain rat P450 enzymes could be exceptionally good candidates for drug targeting based on their high activity, narrow regioselectivity and high inducibility, most importantly CYP1As, CYP2C11, and CYP2E1, that may be useful for several diseases, such as heart and renal diseases. Finally, our data suggest that P450 modulation by clinically-approved drugs could be employed to effectively and selectively modulate P450-mediated AA metabolism in humans, comparable to investigational drugs, of which resveratrol and fluconazole could be good candidates to be repurposed as new P450-based treatments. In conclusion, we identified several potentially critical drug targets in the cascade of AA metabolism that could be used to counterbalance the alterations of P450-mediated AA metabolism in the heart during cardiac hypertrophy. These drug targets may be effectively and selectively modulated by agents that are already approved for clinical use, and therefore, they are readily available to clinical trials.

## Preface

This thesis is an original work by Ahmed El-Sherbeni. All experimental animal procedures were approved by the University of Alberta Health Sciences Animal Policy and Welfare Committee. Chapter 1 of this thesis has been published as 2 review papers: El-Sherbeni, Ahmed A., and Ayman OS El-Kadi. "Microsomal cytochrome P450 as a target for drug discovery and repurposing." *Drug Metabolism Reviews* just-accepted (2016): 1-40, and El-Sherbeni, Ahmed A., and Ayman OS El-Kadi. "The role of epoxide hydrolases in health and disease." *Archives of toxicology* 88.11 (2014): 2013-2032. I was responsible for summarizing published reports on the topic and manuscript composition. Ayman OS El-Kadi was the supervisory author and was involved with concept formation and manuscript composition. Section 1 in chapter 3 and 4 has been published as El-Sherbeni, Ahmed A., Aboutabl ME, Zordoky BN, Anwar-Mohamed A, and Ayman OS El-Kadi. "Determination of the dominant arachidonic acid cytochrome P450 monooxygenases in rat heart, lung, kidney, and liver: protein expression and metabolite kinetics." *The AAPS journal* 15.1 (2013): 112-122. I was responsible for performing experiments, data analysis, and manuscript composition. Aboutabl ME, Zordoky BN, and Anwar-Mohamed A performed experiments and assisted in data analysis and manuscript edits. Ayman OS El-Kadi was the supervisory author and was involved with concept formation and manuscript composition. Section 2 in chapter 3 and 4 has been published as El-Sherbeni, Ahmed A., and Ayman OS El-Kadi. "Alterations in cytochrome P450-derived arachidonic acid metabolism during pressure overload-induced cardiac hypertrophy." *Biochemical pharmacology* 87.3 (2014): 456-466. I was responsible for performing experiments, data analysis and manuscript composition. Ayman OS El-Kadi was the supervisory author and was involved with concept formation and manuscript composition. Section 3 in chapter 3 and 4 has been published as El-Sherbeni, Ahmed A., and Ayman OS El-Kadi. "Characterization of arachidonic acid metabolism by rat cytochrome P450 enzymes: the involvement of CYP1As." *Drug Metabolism and Disposition* 42.9 (2014): 1498-

1507. I was responsible for performing experiments, data analysis and manuscript composition. Ayman OS El-Kadi was the supervisory author and was involved with concept formation and manuscript composition. Section 4 in chapter 3 and 4 has been published as El-Sherbeni, Ahmed A., and Ayman OS El-Kadi. "Repurposing resveratrol and fluconazole to modulate human cytochrome P450-mediated arachidonic acid metabolism." *Molecular pharmaceutics* 13.4 (2016): 1278-1288. I was responsible for performing experiments, data analysis and manuscript composition. Ayman OS El-Kadi was the supervisory author and was involved with concept formation and manuscript composition.

***This work is dedicated to***

***my beloved parents, better half, and daughters,***

***Samaa, Farida and Safa.***

## **ACKNOWLEDGEMENTS**

I would like to express my sincere appreciation to my supervisor and mentor, Dr. Ayman El-Kadi, for his support and guidance. He was always accessible and encouraging along my PhD.

I am grateful to my supervisory committee member, Dr. Dion Brocks, whose logical way of thinking and insightful suggestions were of great value to me. I also would like to thank my supervisory committee member, Dr. Paul Jurasz, for his support and his kind and constructive feedbacks.

I would like to express my gratitude to Dr. Vishwa Somayaji and my senior lab members, Drs. Beshay Zordoky, Anwar Anwar-Mohamed, Mona Aboutabl, Mohamed El Gendy and Ghada Abdelhamid, for their guidance through lab techniques and being great mentors to me. My sincere gratitude is extended to Drs. John Seubert and Arno Siraki for their amazing academic support, Dr. Randy Whittal and Mrs. Jing Zheng for the training kindly provided on the triple quadrupole mass spectrometry, and Mrs. Jody Levasseur and Dr. Jason Dyck for the training I have received on the aortic constriction procedure. Also, I would like to thank Mrs. Sandra Kelly and Donna Beker for performing the animal surgery and the echocardiography.

I would like to thank the Egyptian government and Alberta-Innovates-Health Solutions for the financial support they provided to me, and the Canadian Institutes of Health Research for funding my PhD project. Finally, I wish to thank my entire extended family, friends and lab members for their help and for providing a loving environment for me.

## TABLE OF CONTENTS

---

<b>CHAPTER 1: INTRODUCTION</b>	<b>1</b>
<hr/>	
<b>1. Cytochrome P450</b>	<b>2</b>
<b>1.1. Nomenclature and Classification</b>	<b>3</b>
<b>1.2. Molecular Mechanism</b>	<b>8</b>
<b>1.2.1. Chain of Electron Transfer</b>	<b>8</b>
1.2.1.1. <i>NADPH-Cytochrome P450 Reductase</i>	9
<b>1.2.2. The Catalytic Cycle of Cytochrome P450</b>	<b>10</b>
<b>1.3. Cellular Location and Tissue Expression</b>	<b>13</b>
<b>1.4. Physiological Functions of Microsomal Cytochrome P450</b>	<b>16</b>
<b>1.4.1. Elimination of Xenobiotics</b>	<b>16</b>
<b>1.4.2. Metabolism of Polyunsaturated Fatty Acids</b>	<b>17</b>
<b>2. Arachidonic Acid Metabolism</b>	<b>20</b>
<b>2.1. Cytochrome P450-Derived Arachidonic Acid Metabolites</b>	<b>22</b>
<b>2.1.1. Epoxy-Metabolites of Arachidonic Acid</b>	<b>23</b>
<b>2.1.2. Hydroxy-Metabolites of Arachidonic Acid</b>	<b>25</b>
<b>3. Soluble Epoxide Hydrolase</b>	<b>28</b>
<b>3.1. Tissue and Species Expression</b>	<b>28</b>
<b>3.2. Molecular Mechanism</b>	<b>29</b>
<b>3.3. Regulation</b>	<b>31</b>
<b>3.4. Physiological Functions</b>	<b>32</b>
<b>3.4.1. The Epoxides of Linoleic Acid</b>	<b>32</b>
<b>4. The pharmacological Modulation of Cytochrome P450-Mediated Arachidonic Acid Metabolism</b>	<b>34</b>
<b>4.1. Modulators of Soluble Epoxide Hydrolase</b>	<b>34</b>

<b>4.2. Microsomal Cytochrome P450 Modulators</b>	<b>37</b>
<b>4.2.1. Development of New Cytochrome P450 Modulators</b>	<b>37</b>
<b>4.2.2. Repurposing of Old Cytochrome P450 Modulators</b>	<b>41</b>
4.2.2.1. <i>Drug-Drug Interactions</i>	41
4.2.2.2. <i>Cytochrome P450 Inhibitors</i>	42
4.2.2.3. <i>Cytochrome P450 Inducers</i>	46
<b>4.3. Receptor Agonists and Antagonists</b>	<b>47</b>
<b>5. Cardiac Hypertrophy</b>	<b>50</b>
<b>5.1. The Burden of Cardiac Hypertrophy</b>	<b>50</b>
<b>5.2. Cardiac Remodeling</b>	<b>51</b>
<b>5.3. Cytochrome P450-Mediated Arachidonic Acid Metabolism and Cardiac Hypertrophy</b>	<b>52</b>
<b>6. Rationale, Hypotheses and Objectives</b>	<b>55</b>
<b>6.1. Rationale</b>	<b>55</b>
<b>6.2. Hypotheses</b>	<b>56</b>
<b>6.3. Objectives</b>	<b>56</b>
<hr/>	
<b>CHAPTER 2: MATERIALS AND METHODS</b>	<b>58</b>
<hr/>	
<b>1. Chemicals and Materials</b>	<b>59</b>
<b>2. Methods</b>	<b>61</b>
<b>2.1. Analysis of Cytochrome P450-Derived Arachidonic Acid Metabolites</b>	<b>61</b>
<b>2.2. Method Validation</b>	<b>63</b>
<b>2.3. Animals and Treatment</b>	<b>64</b>
<b>2.4. Echocardiography</b>	<b>65</b>
<b>2.5. Tissue Collection and Microsomal Preparation</b>	<b>66</b>
<b>2.6. RNA Extraction and cDNA Synthesis</b>	<b>67</b>

2.7. Quantification by Real Time-PCR	67
2.8. Western Blot Analysis	68
2.9. The Extraction of Arachidonic Acid Metabolites from Heart Tissue	69
2.10. sEH Activity Assay	70
2.11. Measuring CYP1A1 and CYP1A2 Activity	70
2.12. Arachidonic Acid Metabolism	71
2.12.1. Microsomal-Mediated AA Metabolism	71
2.12.2 Recombinant Cytochrome P450-Mediated AA Metabolism	73
2.13. Chromatographic Purification and Structural Elucidation	74
2.14. Selective Chemical Inhibition of Cytochrome P450-Mediated AA Metabolism	74
2.15. Immunoinhibition of Cytochrome P450-Mediated AA Metabolism	75
2.16. Selective Induction of CYP1As-Mediated AA Metabolism	76
2.17. Data Fitting	76
2.18. Monte Carlo Simulation	78
2.19. Statistical analysis	79
<hr/>	
<b>CHAPTER 3: RESULTS</b>	<b>80</b>
<hr/>	
1. Determination of the Dominant Arachidonic Acid Cytochrome P450 Monooxygenases in Rat Heart, Lungs, Kidneys and Liver	81
1.1. Protein Expression of Cytochrome P450 Enzymes in Rat Heart, Lungs, Kidneys and Liver	81
1.2. Determination of the Kinetic Parameters of Cytochrome P450-Mediated AA Metabolism in Rat Heart, Lungs, Kidneys and Liver	84
1.3. Determination of the Regioselectivity of AA Metabolism in Rat Heart, Lungs, Kidneys and Liver	89
1.4. Immunoinhibition of Cytochrome P450-Mediated AA Epoxygenation and Hydroxylation Activity	91

<b>2. Alterations in Cytochrome P450-Derived Arachidonic Acid Metabolism During Pressure Overload-Induced Cardiac Hypertrophy</b>	<b>93</b>
2.1. Effect of DAC on the Development of Cardiac Hypertrophy	93
2.2. Effect of Cardiac Hypertrophy on the Levels of AA Metabolites in Heart Tissue	95
2.3. Effect of Cardiac Hypertrophy on the Formation and Degradation of EETs	98
2.4. Effect of Cardiac Hypertrophy on the Formation of HETEs	100
2.5. Effect of Cardiac Hypertrophy on Cytochrome P450 Protein Expression	102
2.6. Role of CYP1B1 and CYP2J2 in Mid-Chain HETEs Metabolism	106
<b>3. Characterization of Arachidonic Acid Metabolism by Rat Cytochrome P450 Enzymes</b>	<b>109</b>
3.1. LC-ESI-MS Method Development and Validation	109
3.2. Determination of AA-Metabolizing Activity and Metabolic Profile of Cytochrome P450 Enzymes	112
3.3. Determination of the Kinetic Profile of CYP1A1/2- and CYP2C6/11-Mediated AA Metabolism	117
3.4. Determination of AA Metabolic Profile of Rat Heart, Lungs, Kidneys and Liver Microsomes	119
3.5. Determination of the Contribution of CYP1A1/2 to AA Metabolism in Rat Heart, Lungs, Kidneys and Liver	122
<b>4. Repurposing Resveratrol and Fluconazole to Modulate Human Cytochrome P450-Mediated Arachidonic Acid Metabolism</b>	<b>129</b>
4.1. AA-Metabolizing Activity and Metabolic Profile of Recombinant Cytochrome P450 Enzymes	129
4.2. AA-Metabolizing Activity and Metabolic Profile of Human Microsomes	133
4.3. Effect of Cytochrome P450 Inhibition on AA-Metabolism Mediated by Human Liver Microsomes	135
4.4. Kinetics of Cytochrome P450-Mediated AA Metabolism Inhibition	140
4.5. Simulating the Inhibition of Cytochrome P450-Mediated AA Metabolism after Safe Oral Doses of Res and Flu	143
<hr/> <b>CHAPTER 4: DISCUSSION</b>	<hr/> <b>145</b>

---

<b>1. Determination of the Dominant Arachidonic Acid Cytochrome P450 Monooxygenases in Rat Heart, Lungs, Kidneys and Liver</b>	<b>146</b>
<b>2. Alterations in Cytochrome P450-Derived Arachidonic Acid Metabolism During Pressure Overload-Induced Cardiac Hypertrophy</b>	<b>151</b>
<b>3. Characterization of Arachidonic Acid Metabolism by Rat Cytochrome P450 Enzymes</b>	<b>157</b>
<b>4. Repurposing Resveratrol and Fluconazole to Modulate Human Cytochrome P450-Mediated Arachidonic Acid Metabolism</b>	<b>162</b>
<b>5. Summary and General Conclusions</b>	<b>167</b>
<b>6. Limitations and Pitfalls</b>	<b>171</b>
<b>7. Future Research Directions</b>	<b>172</b>

---

<b>REFERENCES</b>	<b>174</b>
-------------------	------------

---

<b>Appendix: Supplement Materials</b>	<b>206</b>
---------------------------------------	------------

---

## LIST OF TABLES

Table 1.1. Statistics of the Named Sequences of P450 Enzymes.	3
Table 1.2. The Major Substrate Class of Human P450 Enzymes.	13
Table 1.3. The Main Cellular Location of Human P450 Enzymes.	14
Table 1.4. The Chemical Structure and Characterization of the Common Polyunsaturated Fatty Acid.	19
Table 1.5. FDA Recommended <i>In Vivo</i> and <i>In Vitro</i> Inhibitors of Specific P450 Enzymes.	44
Table 1.6. FDA Recommended <i>In Vivo</i> and <i>In Vitro</i> Inducers of Specific P450 Enzymes.	47
Table 2.1. Primers Sequences Used for Real-Time PCR Reactions.	68
Table 3.1. Enzyme Kinetic Parameters (mean $\pm$ S.E.E) for the Formation of EETs and HETEs by Microsomes Separated from Untreated Rat Heart, Lungs, Kidneys and Liver.	88
Table 3.2. Immunoinhibition of P450-Mediated AA Epoxygenation and Hydroxylation in Untreated Rat Heart, Lung, Kidney and Liver Microsomes. Data are the Mean $\pm$ S.E.M. Each point was measured in triplicate.	92
Table 3.3. The Retention Times and Ions Monitored for the P450-Derived AA Metabolites Analyzed.	95
Table 3.4. The Retention Times ( $R_t$ ), Ions Monitored, Sensitivity and Linearity Results of P450-Derived AA Metabolites Analysis.	110
Table 3.5. Precision and Accuracy Results of Representative P450-Derived AA Metabolites.	111
Table 3.6. Enzyme Kinetic Parameters (mean $\pm$ S.E.E) for the Formation of Major Metabolites of CYP1A1/2 and CYP2C6/11.	118
Table 3.7. The Formation Rate of P450-derived AA Metabolites Mediated by Heart, Lung, Kidney and Liver Microsomal Fractions Separated from Untreated Rat.	120
Table 3.8. The Inhibitory Effect of CYP1As Inhibitor, $\alpha$ -Naphthoflavone on P450-Mediated AA Metabolism by Heart, Lung, Kidney and Liver Microsomal Fractions Separated from Untreated Rat.	123

<b>Table 3.9. The Inhibitory Effect of Anti-CYP1As Antibodies on P450-Mediated AA Metabolism by Heart, Lung, Kidney and Liver Microsomal Fractions Separated from Untreated Rat.</b>	<b>125</b>
<b>Table 3.10. Effect (Mean <math>\pm</math> S.E.M.) of Different Selective Investigational P450 Inhibitors on P450-Mediated AA Metabolism by Human Liver Microsomes Based on at Least 3 Individual Experiments.</b>	<b>136</b>
<b>Table 3.11. Effect (mean <math>\pm</math> S.E.M) of Different Selective Clinically-approved P450 Inhibitors on P450-Mediated AA Metabolism by Human Liver Microsomes Based on at Least 3 Individual Experiments.</b>	<b>139</b>

## LIST OF FIGURES

<b>Figure 1.1. P450 Classification According to the International Union of Biochemistry and Molecular Biology.</b>	<b>5</b>
<b>Figure 1.2. The P450 Phylogenetic Tree of the 60 Known Human P450 Enzymes.</b>	<b>7</b>
<b>Figure 1.3. The Electron Transfer Chain of NADPH-P450 Reductase from NADPH to P450.</b>	<b>10</b>
<b>Figure 1.4. The Catalytic Cycle of Microsomal P450.</b>	<b>12</b>
<b>Figure 1.5. Site of Action of Phospholipase A<sub>1</sub>, A<sub>2</sub>, B, C and D on Phosphoglycerides.</b>	<b>21</b>
<b>Figure 1.6. The Metabolism of Arachidonic Acid by Cyclooxygenase-, Lipoxygenase and P450-Mediated Pathways.</b>	<b>22</b>
<b>Figure 1.7. The Formation and Degradation of EETs by P450 and sEH-Mediated Pathways, Respectively.</b>	<b>25</b>
<b>Figure 1.8. The P450-Mediated Metabolism of AA to Form HETEs.</b>	<b>27</b>
<b>Figure 1.9. The Mechanism of the Hydrolysis of Epoxide Substrates by sEH.</b>	<b>30</b>
<b>Figure 1.10. The Chemical Structures of Representative Examples of sEH Inhibitors.</b>	<b>36</b>
<b>Figure 1.11. The Mechanism of sEH Inhibition by Carbamide-Based Inhibitors.</b>	<b>36</b>
<b>Figure 1.12. The Chemical Structures of Representative of Inhibitors of P450-AA Monooxygenases.</b>	<b>40</b>
<b>Figure 1.13. The Chemical Structures of Representative of inducers of P450 enzymes.</b>	<b>46</b>
<b>Figure 1.14. The Chemical Structures of Representative of EETs and 20-HETE stable analogues and antagonists.</b>	<b>49</b>
<b>Figure 3.1. P450 Protein Expression in Untreated Rat Heart, Lungs, Kidneys and Liver.</b>	<b>83</b>
<b>Figure 3.2. Kinetic Profiles of EET Formation by Microsomes Separated from Healthy Rat Heart, Lungs, Kidneys and Liver.</b>	<b>85</b>
<b>Figure 3.3. Kinetic Profiles of 19- and 20-HETE Formation by Microsomes Separated from Healthy Rat Heart, Lungs, Kidneys and Liver.</b>	<b>86</b>

<b>Figure 3.4. Regioselectivity of Arachidonic Acid Epoxygenation and Hydroxylation Mediated by Microsomes Separated from Untreated Rat Heart, Lungs, Kidneys and Liver.</b>	<b>90</b>
<b>Figure 3.5. Assessment of Cardiac Hypertrophy.</b>	<b>94</b>
<b>Figure 3.6. Effect of Cardiac Hypertrophy on Rat Cardiac AA Metabolites Levels.</b>	<b>97</b>
<b>Figure 3.7. Effect of Cardiac Hypertrophy on the Formation and Degradation of EETs by Microsomes Separated from Rat Heart.</b>	<b>99</b>
<b>Figure 3.8. Effect of Cardiac Hypertrophy on the Formation of HETEs by Microsomes Separated from Rat Heart.</b>	<b>101</b>
<b>Figure 3.9. Effect of Cardiac Hypertrophy on P450 Protein Expression in Rat Heart.</b>	<b>103</b>
<b>Figure 3.10. Correlation between P450 Protein Expression Levels and the Formation Rate of P450-Derived AA Metabolites by Microsomes Separated from Rat Heart.</b>	<b>105</b>
<b>Figure 3.11. Formation of Mid-Chain HETEs by Recombinant Human CYP1B1.</b>	<b>107</b>
<b>Figure 3.12. Degradation of 12-HPETE by Recombinant Human CYP2J2.</b>	<b>108</b>
<b>Figure 3.13. P450-Mediated AA-Metabolizing Activity of Rat Recombinant P450 Enzymes.</b>	<b>113</b>
<b>Figure 3.14. The Metabolic Profile/Regioselectivity of P450-Mediated AA Metabolism by Rat CYP1A1/2, CYP2B1 and CYP2C6/11.</b>	<b>115</b>
<b>Figure 3.15. The Metabolic Profile/Regioselectivity of P450 Mediated AA Metabolism by Rat CYP2A1, CYP2C13, CYP2D1, CYP2E1 and CYP3A1.</b>	<b>116</b>
<b>Figure 3.16. P450-Mediated AA Metabolite Formation by Heart, Lung, Kidney and Liver Microsomes Separated from Untreated Rats.</b>	<b>121</b>
<b>Figure 3.17. The Effect of 3-MC Treatment on CYP1A1 and CYP1A2 Activity of Rat Heart, Lung, Kidney and Liver Microsomes.</b>	<b>127</b>
<b>Figure 3.18. The Effect of 3-MC Treatment on P450-mediated AA Metabolism by Rat Heart, Lung, Kidney and Liver Microsomes.</b>	<b>128</b>
<b>Figure 3.19. The Metabolizing Activity of Human Recombinant P450 Enzymes: AA Consumption, and EETs, Mid-Chain HETEs (mHETE) and Terminal and Subterminal HETEs (<math>\omega/\omega-1</math> HETEs) Formation.</b>	<b>131</b>

<b>Figure 3.20. Heat Map of the Activities of P450-Derived AA Metabolite Formation of Human Recombinant P450 Enzymes.</b>	<b>132</b>
<b>Figure 3.21. The Formation of P450-Derived AA Metabolites Mediated by Human Liver and Kidney Microsomes.</b>	<b>134</b>
<b>Figure 3.22. Concentration-Dependent Inhibition of CYP4A11-, CYP4F2- and CYP4F3B-Mediated 20-HETE Formation by Res.</b>	<b>141</b>
<b>Figure 3.23. Concentration-Dependent Inhibition of Hepatic Microsomal-Mediated Formation of P450-Derived AA Metabolites by Res and Flu.</b>	<b>142</b>
<b>Figure 3.24. Box Plot Showing Monte Carlo Simulations of P450-Mediated AA Metabolism Modulation by Different Doses of Res and Flu.</b>	<b>144</b>

## GLOSSARY OF TERMS

<b>%EF</b>	<b>Percentage of ejection fraction</b>
<b>%FS</b>	<b>Percentage of fractional shortening</b>
<b>17-ODYA</b>	<b>17-octadecynoic acid</b>
<b>3-MC</b>	<b>3-methylcholanthrene</b>
<b>7-ER</b>	<b>7-ethoxyresorufin</b>
<b>7-MR</b>	<b>7-methoxyresorufin</b>
<b>AA</b>	<b>Arachidonic acid</b>
<b>ANP</b>	<b>Atrial natriuretic peptide</b>
<b>APAU</b>	<b>1-(1-acetypiperidin-4-yl)-3-adamantanylurea</b>
<b>BNP</b>	<b>Brain natriuretic peptide</b>
<b>Cl<sub>int</sub></b>	<b>Intrinsic clearance</b>
<b>cyb5</b>	<b>Cytochrome b5</b>
<b>DAC</b>	<b>Descending aortic constriction</b>
<b>Dan</b>	<b>Danazol</b>
<b>DHET</b>	<b>Dihydroxyeicosatrienoic acid</b>
<b>EET</b>	<b>Epoxyeicosatrienoic acid</b>
<b>FAD</b>	<b>Flavin adenine dinucleotide</b>
<b>FDA</b>	<b>The Food and Drug Administration</b>
<b>Flu</b>	<b>Fluconazole</b>
<b>FMN</b>	<b>Flavin mononucleotide</b>
<b>HET0016</b>	<b>N-Hydroxy-N'-(4-butyl-2-methylphenyl) formamidine</b>
<b>HETE</b>	<b>Hydroxyeicosatetraenoic acid</b>
<b>HpETE</b>	<b>Hydroperoxyeicosatetraenoic acid</b>
<b>HPLC</b>	<b>High performance liquid chromatography</b>

<b>IC<sub>50</sub></b>	<b>Inhibitor concentration required for 50% inhibition</b>
<b>I<sub>max</sub></b>	<b>Maximal inhibition</b>
<b>IVS</b>	<b>Interventricular septal wall thickness</b>
<b>K<sub>m</sub></b>	<b>The affinity constant</b>
<b>K<sub>si</sub></b>	<b>The inhibition constant</b>
<b>LC-ESI-MS</b>	<b>Liquid chromatography-electrospray ionization-mass spectrometry</b>
<b>LV wt/tl</b>	<b>Left ventricular weight to tibial length</b>
<b>LVPW</b>	<b>Left ventricle posterior wall thickness</b>
<b>LVV</b>	<b>Left ventricle volume</b>
<b>mEH</b>	<b>Microsomal epoxide hydrolase</b>
<b>MS-PPOH</b>	<b>N-methylsulfonyl-6-(2-propargyloxyphenyl)hexanamide</b>
<b>NADPH</b>	<b>Nicotinamide adenine dinucleotide phosphate</b>
<b>P450</b>	<b>Cytochrome P450</b>
<b>PPOH</b>	<b>6-(2-propargyloxyphenyl)hexanoic acid</b>
<b>PTU</b>	<b>Propylthiouracil</b>
<b>r</b>	<b>Spearman correlation coefficient</b>
<b>Res</b>	<b>Resveratrol</b>
<b>R<sub>t</sub></b>	<b>Retention time</b>
<b>sEH</b>	<b>Soluble epoxide hydrolase</b>
<b>Ser</b>	<b>Sertraline</b>
<b>Tic</b>	<b>Ticlopidine</b>
<b>TMS</b>	<b>2,4,3',5'-tetramethoxystilbene</b>
<b>TS-011</b>	<b>N-(3-Chloro-4-morpholin-4-yl)Phenyl-N'-hydroxyimido Formamide</b>
<b>TUPS</b>	<b>1-(1-methanesulfonyl-piperidin-4-yl)-3-(4-trifluoromethoxy-phenyl)-urea</b>
<b>V<sub>max</sub></b>	<b>The maximal rate of formation</b>

<b><math>\alpha</math>-MHC</b>	<b><math>\alpha</math>-myosin heavy chain</b>
<b><math>\alpha</math>-NF</b>	<b>A-naphthoflavone</b>
<b><math>\beta</math>-MHC</b>	<b><math>\beta</math>-myosin heavy chain</b>
<b><math>\omega</math></b>	<b>Terminal</b>
<b><math>\omega</math>-1</b>	<b>Subterminal</b>

## **CHAPTER 1: INTRODUCTION**

## 1. Cytochrome P450

Cytochrome P450 (P450) is a superfamily of heme-thiolate enzymes that are ubiquitous in almost all biological systems. 3.5 billion years ago, earth's organisms were primitive strict anaerobes, and P450 may have developed then to detoxify the earliest traces of free oxygen entering the cell (Wickramashighe and Vilee 1975, Lewis, Watson et al. 1998, Deng, Carbone et al. 2007). Thereafter, P450 enzymes were evolved to extend their original protective role to include the inactivation of a wide array of xenobiotics, in addition to mediating key biological reactions in the cascade of biosynthesis of endogenous compounds. The evolutionary conservation and abundance of P450 in nature underscore the importance of biological functions mediated by P450 enzymes (Werck-Reichhart and Feyereisen 2000). There are more than 35,000 P450 enzymes that have been isolated from all biological organisms (Table 1.1), with exception of some primitive prokaryotes, such as *Escherichia coli*, which are believed to have emerged before the evolution of P450 (Ioannides 2008, Nelson 2009). P450 consists of heme group, which represents the center of the active site, covalently or noncovalently bound to apoprotein that dictates substrate selectivity and affinity (Ioannides 2008). All P450 enzymes share the same heme group, albeit different in the amino acid sequence of their apoproteins; however, interestingly, few differences have been noted in the tertiary structure of P450 enzymes (Ioannides 2008).

Historically, P450 was believed to be a mixed function oxidase partnering with nicotinamide adenine dinucleotide phosphate (NADPH)-P450 reductase and lipids from cell membrane, because of the capability of this function unit to oxidize two substrates by one catalytic cycle (Ortiz de Montellano 2005). However, on the light of the wide variety of organic reactions that can be mediated by P450, considering P450 as a mixed function oxidases has been greatly diminished, and rendering the term monooxygenases more accepted (Ortiz de Montellano 2005). Nowadays, P450 enzymes are in the mainstream of drug development

studies as the most important phase I xenobiotic-metabolizing enzymes, and moreover, as a lipid signaling enzyme mediating the transformation of polyunsaturated fatty acids, notably, arachidonic acid (AA), to highly bioactive molecules (Roman 2002).

**Table 1.1. Statistics of the Named Sequences of P450 Enzymes, adapted from (Nelson 2009).**

<b>Animals</b>	<b>Number of P450 enzymes</b>
<b>Mammals</b>	1666
<b>Other vertebrates</b>	1344
<b>Non-insect invertebrates</b>	1348
<b>Insects</b>	6119
<b>Plants</b>	13,978
<b>Fungi</b>	7,873
<b>Protozoa</b>	602
<b>Bacteria</b>	2,156
<b>Archaea</b>	52
<b>Viruses</b>	28
<b>Total</b>	35,166

### 1.1. Nomenclature and Classification

Until now, the International Union of Biochemistry and Molecular Biology disagrees on the term “cytochrome P450” and suggests “heme-thiolate enzymes” as a more appropriate name; the Union classifies heme-thiolate enzymes as external monooxygenases (Hannemann, Bichet et al. 2007, Room 2013) (Fig. 1.1). P450 was discovered in the early 1950s. Brodie’s laboratory was one of the first to show that a NADPH-dependent enzyme system, associated with the microsomal fraction of the liver, mediates the oxidation of many drugs (Brodie, Gillette et al. 1958). In 1958, Klingenberg

and Garfinkel independently reported a CO-binding pigment in liver microsomes, which was reducible by either NADPH or dithionite, and displayed a typical absorption maximum of the reduced CO-binding complex at 450 nm (Garfinkel 1958, Klingenberg 1958). In 1962, Omura and Sato demonstrated that this pigment was a hemoprotein, assigning for the first time the term “cytochrome P450” to the active form of the hemoprotein (calling the degraded form “P420”) (Omura and Sato 1962). The first successful efforts to solubilize and separate the P450 fraction from mammalian microsomes were performed by Lu et al in 1969 (Lu, Junk et al. 1969). At this point, nomenclature of P450 was according to the origin of the separated microsomes/purified enzymes, viz., human, rat, mouse, bacterial; also, P450 was separated from cellular fractions other than microsomes, leading to auxiliary nomenclature/classification of microsomal, mitochondrial and cytosolic P450 (Jefcoate, Hume et al. 1970). In 1971, Lu et al reported that the microsomes from phenobarbital-treated and 3-methylcholanthrene (3-MC)-treated rats showed different activity in the N-demethylation of benzphetamine and chlorcyclizine, and the hydroxylation of pentobarbital, 3,4-Benzpyrene and testosterone (Lu, Kuntzman et al. 1971, Lu, Levin et al. 1973). Based on differences in the catalytic, spectral and gel electrophoretic properties, and sensitivity toward inhibitors of hepatic microsomes after the pretreatment with certain compounds, the existence of different types of P450 has been evident (Sladek and Mannering 1966, Alvares and Siekevitz 1973). These new P450 types were generally indicated by their inducers, such as the phenobarbital-, 3-methylcholanthrene-, isoniazid- and clofibrate-induced P450 enzymes, or by light absorbance, such as the P-448, P-450 and P-452 forms of P450 (Tamburini, Masson et al. 1984, Tse, Aboutabl et al. 2013).

In the 1980s, great progress was accomplished with respect to the purification, sequencing and cloning of several P450 enzymes (Nebert, Adesnik et al. 1987, Nebert, Wikvall et al. 2013). Accordingly, new nomenclature of P450 enzymes based on evolution

of P450 was first suggested by Nebert et al in 1987, which was quickly and widely accepted by P450 workers (Nebert, Adesnik et al. 1987). In this classification, P450 enzymes were divided into families and subfamilies according to evolutionary relationships in phylogenetic trees (Fig. 1.2), which are basically dictated by amino acid sequence of P450 apoproteins; members of the same P450 family share  $\geq 40\%$  sequence homology, whereas, members of the same P450 subfamily share  $\geq 55\%$  sequence homology (Nelson 2006, Nelson 2009, Nebert, Wikvall et al. 2013). However, “The actual decision to include a sequence in an existing group largely depends on how it clusters on a tree and not so much on the absolute percentage of identity, which is more or less a rule of thumb.”, as underscored by Dr. David Nelson in his 2006 publication on P450 nomenclature (Nelson 2006).

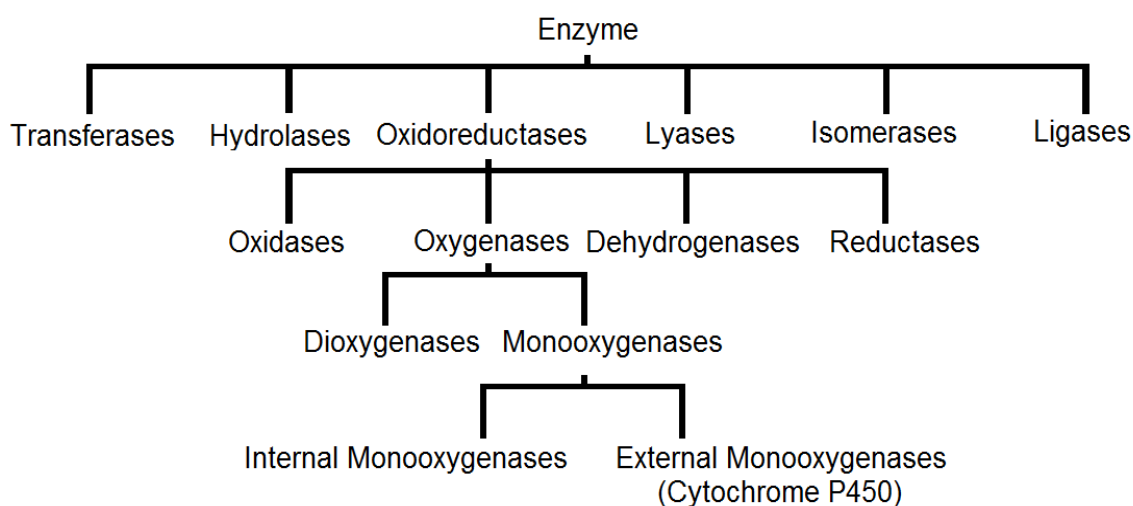


**Figure 1.1. P450 Classification According to the International Union of Biochemistry and Molecular Biology (Hannemann, Bichet et al. 2007).**

So far, more than 120 families and 500 subfamilies have been sequenced in animals alone. There are 18 P450 families in humans, of which CYP2, CYP3 and CYP4 families contain the majority of the 60 P450 enzymes identified in humans (Fig. 1.2), for example CYP2 family comprises A, B, C, D, E, F, G, J, R, S, T, U and W subfamilies

(Nelson 2009, Nebert, Wikvall et al. 2013). To facilitate handling of this increasing number of P450 enzymes, P450 families that consistently cluster together on phylogenetic trees were suggested to be further gathered in a new group called “P450 clan” (Nelson 2006). However, this new P450 group is not routinely used among P450 researchers. Instead, grouping P450 families, subfamilies and members according to their predominant substrate into xenobiotic, fatty-acids, sterols and vitamins P450 enzymes has been more commonly used.

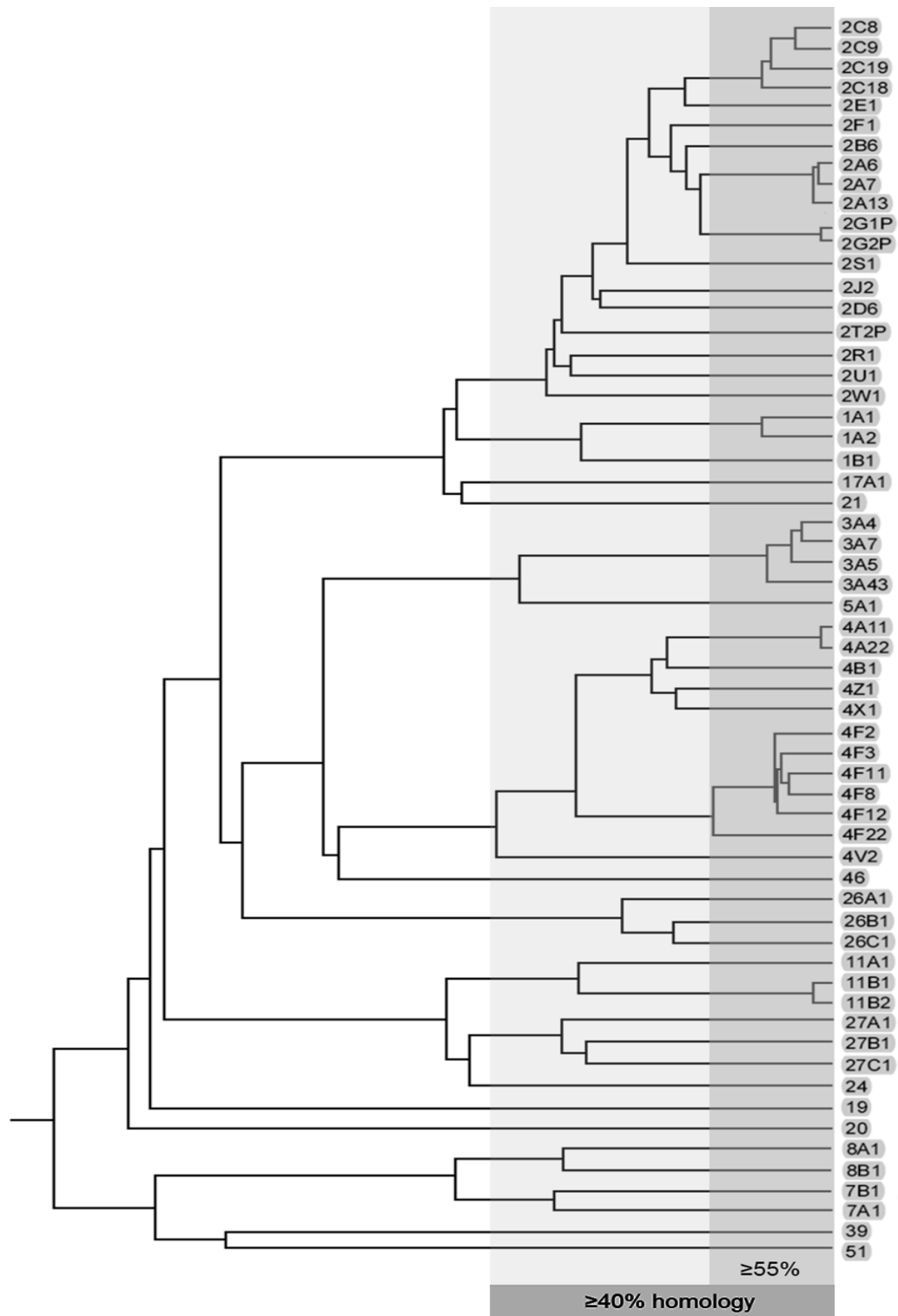


Figure 1.2. The P450 Phylogenetic Tree of the 60 Known Human P450 Enzymes, adapted from (Nelson 2009).

## 1.2. Molecular Mechanism

The tertiary structure of P450 enzymes has been greatly conserved during evolution, albeit less than 20% of the gene sequence is shared among the P450 superfamily (Denisov, Makris et al. 2005). The core structure of P450 is based on four helix bundles, three are described as parallel and the fourth is antiparallel, indicated by the letters D, L and I, and E, respectively (Denisov, Makris et al. 2005). The heme group, Fe-protoporphyrin IX, is trapped between the I- and L-helices by non-covalent bonding, with exception of CYP4 family members, which have heme group covalently-bonded to glutamate residue of the I-helix (Hoch and Ortiz De Montellano 2001, LeBrun, Hoch et al. 2002). Substrates of P450 are positioned by the apoprotein in the active site, where the heme group activates the molecular oxygen to initiate the oxidation reaction (Denisov, Makris et al. 2005, Bernhardt 2006, Ioannides 2008).

### 1.2.1. Chain of Electron Transfer

As mentioned before, P450 enzymes are external monooxygenases, which means they rely on an external reducing partner that extract electrons from reducing equivalents (cofactor) to form an electron transfer chain: reducing equivalent  $\rightarrow$  reducing partner  $\rightarrow$  P450 (Bernhardt 2006, Hannemann, Bichet et al. 2007). In animal mitochondrial P450, a pair of electrons is transferred from NADPH through ferredoxin reductase and iron-sulphur cluster to P450; whereas, in animal microsomal P450, a pair of electrons is transferred from NADPH through microsomal NADPH-P450 reductase and cytochrome b5 (cyb5) to P450 (Bernhardt 2006, Hannemann, Bichet et al. 2007). When P450 enzymes receive the pair of electrons, the following general reaction will be catalyzed:  $2e^- + 2H^+ + O_2 + \text{Substrate} \rightarrow H_2O + \text{Substrate-O}$  (Bernhardt 2006, Ioannides 2008). The

redox couple  $\text{Fe}^{3+}/\text{Fe}^{2+}$  in the center of the heme group is responsible for the catalysis of the reaction, whose reduction potential is maintained low (-170 – -400 mV) by forming a thiolate complex with proximal cysteine, and whence the name “heme-thiolate” (Denisov, Makris et al. 2005, Ioannides 2008). The reducing equivalents are two electron donors, while P450 enzymes need the pair of electrons to be given sequentially; therefore, the reducing partner organizes the electron transfer to accept the pair of electrons from the reducing equivalent and give one electron at a time to P450 (Ortiz de Montellano 2005, Stuehr, Tejero et al. 2009). Our focus will be on NADPH-P450 reductase and microsomal P450 enzymes.

#### **1.2.1.1. NADPH-Cytochrome P450 Reductase**

NADPH-P450 reductase is a 70 kDa, intrinsic and highly evolutionary conserved enzyme, and it is co-localized with microsomal P450 on the smooth endoplasmic reticulum in about 10:1 ratio (Voznesensky and Schenkman 1992, Vincent, Morellet et al. 2012). Electrons are transferred by the prosthetic groups, flavin adenine dinucleotide (FAD) and flavin mononucleotide (FMN), of NADPH-P450 reductase (Hannemann, Bichet et al. 2007, Stuehr, Tejero et al. 2009, Vincent, Morellet et al. 2012). Interestingly, NADPH-P450 reductase has evolved from the combination of two ancestral enzymes, the FMN-containing bacterial flavodoxins at the N-terminal with the FAD-containing ferredoxin NADP+ reductases at the C-terminal (Porter and Kasper 1986). Briefly, the molecular mechanism of the electron transfer starting by FAD accepting the pair of electrons, thereafter, one electron is transferred to FMN to be passed to P450 in two sequential steps (Hannemann, Bichet et al. 2007, Stuehr, Tejero et al. 2009) (Fig. 1.3). Noteworthy, there is some evidence that cyb5 helps mediating the

transfer of the second electron, from NADPH-P450 reductase to P450 (Hannemann, Bichet et al. 2007, Dorokhov, Shindyapina et al. 2015). The binding of the substrate to P450 apoprotein has been reported to activate NADPH-P450 reductase to initiate the electron transfer cycle (Sligar 1976, Daff, Chapman et al. 1997, Ortiz de Montellano 2005). This is a cellular protective mechanism in order to prevent unplanned activation of NADPH-P450 reductase, and the consequent production of reactive oxygen species and unproductive waste of NADPH (Ortiz de Montellano 2005). It has been previously reported that cyb5 is specifically important for  $\omega$ -hydroxylation of fatty acids by CYP4 family members (Wang, Stec et al. 1996, Adas, Salaun et al. 1999, Xu, Falck et al. 2004).

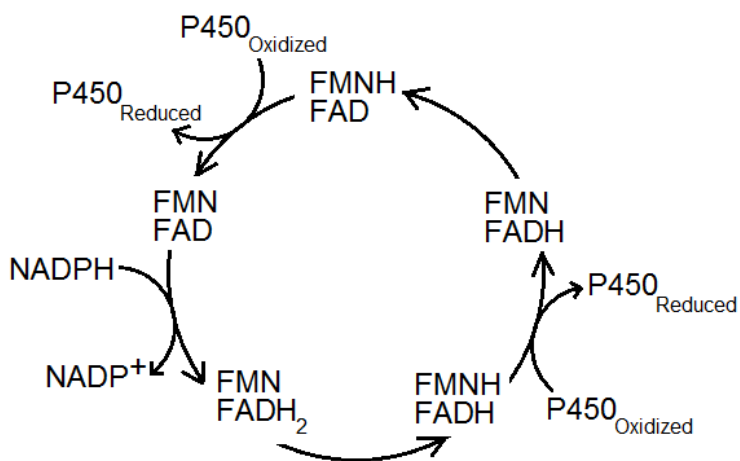


**Figure 1.3. The Electron Transfer Chain of NADPH-P450 Reductase from NADPH to P450. FAD, flavin adenine dinucleotide; FMN, flavin mononucleotide.**

### 1.2.2. The Catalytic Cycle of Cytochrome P450

After the binding of the substrate to P450 apoprotein, and the proper positioning of the substrate at the active site, the Fe<sup>3+</sup> of the heme group binds to the imminent part of the substrate to form ferric P450-substrate adduct (Fig. 1.4-(2)) (Denisov, Makris et al. 2005, Guengerich 2008). The first electron transfer

reduces the ferric P450 into ferrous state (Fig. 1.4-(3)), enabling the binding of one molecule of oxygen to give ferric-dioxygen complex (Fig. 1.4-(4)) (Denisov, Makris et al. 2005, Guengerich 2008). Then, the second electron is accepted by the iron to produce a ferric-peroxy anion (Fig. 1.4-(5a)), which is easily protonated to ferric-hydroperoxy complex (Fig. 1.4-(5b)) (Denisov, Makris et al. 2005, Guengerich 2008). This complex rapidly accepts proton to undergo proton-assisted heterolytic oxygen–oxygen bond scission, resulting in the release of one molecule of water, and oxo-ferryl  $\pi$ -cation complex coupled with a porphyrin radical cation, also known as “Compound I” (Fig. 1.4-(6)) (Denisov, Makris et al. 2005, Guengerich 2008). Compound I is very reactive and oxidizes the substrate (Fig. 1.4-(7)), and then the oxidized product, and the initial ferric P450 (Fig. 1.4-(1)) are then generated (Denisov, Makris et al. 2005).

The catalytic cycle of P450-mediated oxidation of the substrate can be prematurely terminated by three different abortive reactions (Denisov, Makris et al. 2005, Bernhardt 2006): (i) the autoxidation of ferric-dioxygen complex (Fig. 1.4-(4)) to release superoxide anion, (ii) generation of hydrogen peroxide from ferric-hydroperoxy complex (Fig. 1.4-(5b)) to (iii) the oxidase uncoupling by compound I (Fig. 1.4-(6)) accepting another pair of electrons and with two proton, one molecule of water is formed. These reactions are called “uncoupling” or “shunt” reactions as they are produced by “uncoupling” of P450 enzyme with the substrate or the “uncoupling” of substrate oxidation from electron transfer (Denisov, Makris et al. 2005, Bernhardt 2006), and it has been reported that they are induced by the improper positioning of the substrate in the active site (Denisov, Makris et al. 2005, Ortiz de Montellano 2005).

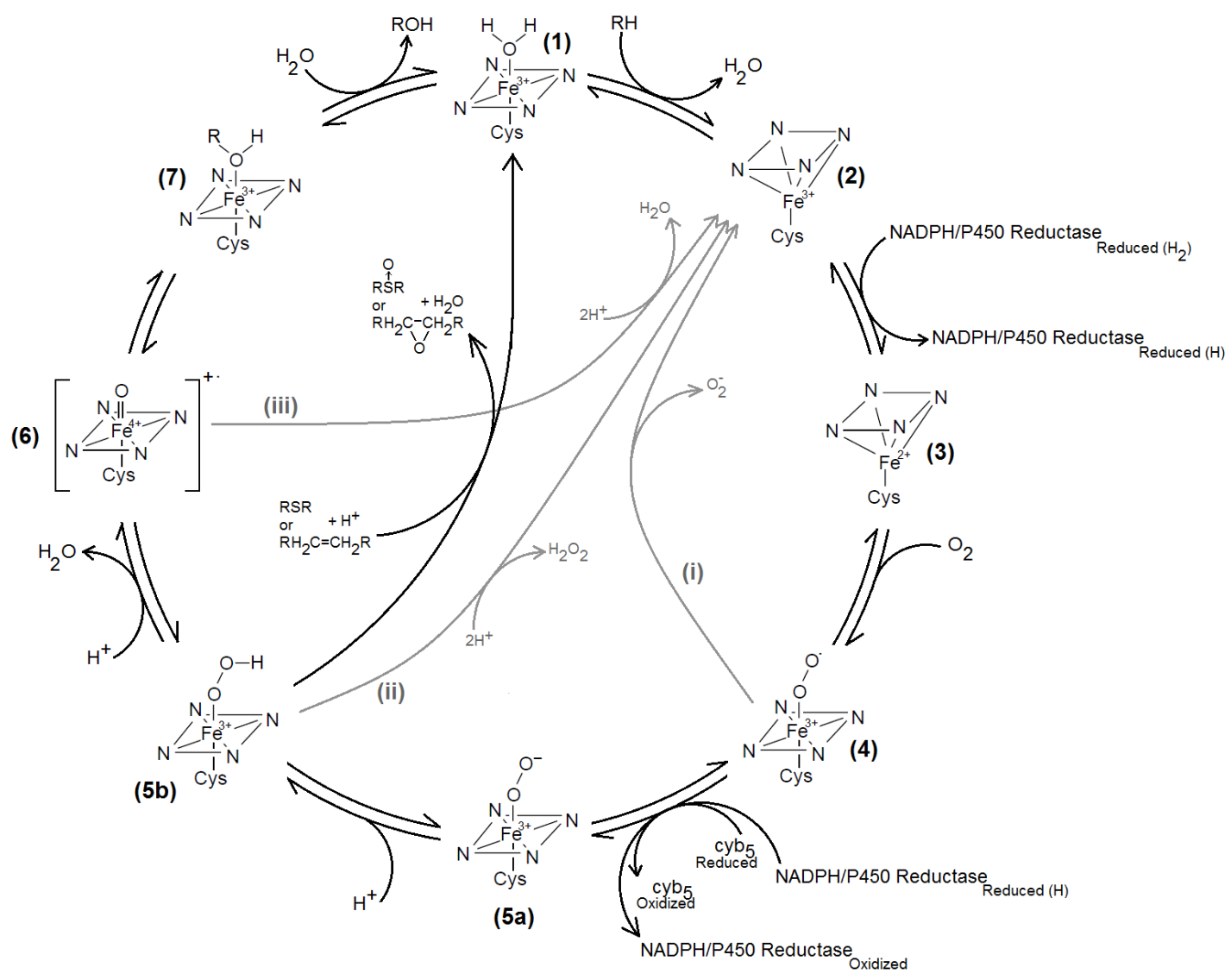


Figure 1.4. The Catalytic Cycle of Microsomal P450.

**Table 1.2. The Major Substrate Class of Human P450 Enzymes.**

<b>Xenobiotics</b>	CYP1As and 1B1 (Ioannides 2008) CYP2As, 2B6, 2Cs, 2D1, 2E1, 2F1 and 2G1 (Ioannides 2008) CYP3As (Ioannides 2008)
<b>Fatty acids</b>	CYP2J2, 4As, 4Bs, and 4Fs (Ioannides 2008) CYP2U1 (Chuang, Helvig et al. 2004) CYP5A1 (Ruan, Li et al. 1994) CYP8A1 (Chevalier, Allorge et al. 2002)
<b>Sterols</b>	CYP1B1 (Murray, Melvin et al. 2001) CYP7A1 and 7B1 (Pandak, Hylemon et al. 2002, Dubrac, Lear et al. 2005) CYP8B1 (Inoue, Yu et al. 2006) CYP11A1 and 11Bs (Schwarz, Chernogolov et al. 1999, Bureik, Schiffler et al. 2002, Midzak, Akula et al. 2011) CYP17A1 (Mizrachi, Wang et al. 2011) CYP19A1 (Pandey, Kempna et al. 2007) CYP21A (Mizrachi, Wang et al. 2011) CYP24A1 (Annalora, Goodin et al. 2010) CYP27A1, 27B1 and 27C1 (Dubrac, Lear et al. 2005) CYP39A1 (Alexander, Fabbro et al. 2015) CYP46A1 (Alexander, Fabbro et al. 2015) CYP51A1 (Alexander, Fabbro et al. 2015)
<b>Vitamins</b>	CYP2R1 (Shinkyō, Sakaki et al. 2004) CYP24A1 (Annalora, Goodin et al. 2010) CYP26A1, 26B1 and 26C1 (Slavotinek, Mehrotra et al. 2013, Tripathy, Chapman et al. 2016) CYP27A1 and 27B1 (Axen, Postlind et al. 1994, Araya, Norlin et al. 1996)

No information was available for CYP2S1, CYP2Ts, CYP2W1, CYP4V2, CYP4X1, CYP4Z1 and CYP20A1.

#### **1.4. Cellular Location and Tissue Expression**

P450 enzymes, according to the cellular fraction they are mainly reside in, can be classified to microsomal, mitochondrial and cytosolic (soluble). Mammalian P450 enzymes are all membrane-attached (intrinsic), either attached to the mitochondrial inner membrane at the matrix side, or attached to the endoplasmic reticulum (Table 1.3).

Membrane-attached P450 have a membrane-anchoring sequence at the N-terminal. This sequence consists of a distal hydrophobic part of 40-50 amino acids that, when inserted in the cell membrane, forms a helix called transmembrane helix and a proximal part of about 20 amino acid rich in positively-charged amino acids and connects the transmembrane helix with the core structure of P450 (Ortiz de Montellano 2005, Anandatheerthavarada, Sepuri et al. 2009). Cytosolic P450 enzymes are soluble proteins and found in more primitive organisms, such as fungi, (Stundl, Schmidt et al. 1998), and therefore, they are out of our current scope. The P450 enzymes that mediate sterols and bile acid synthesis are mitochondrial, whereas, xenobiotic-metabolizing P450 enzymes are microsomal (Tables 1.2 and 1.3).

**Table 1.3. The Main Cellular Location of Human P450 Enzymes.**

<b>Endoplasmic reticulum (Microsomes)</b>		<b>Mitochondria</b>
CYP1As, 1B1, 2As, 2B6, 2Cs, 2D1, 2E1, 2F1, 2G1, 2J2, 3As, 4As, 4Bs and 4Fs (Ioannides 2008)	CYP7B1 (Pandak, Hylemon et al. 2002)	CYP7A1 (Dubrac, Lear et al. 2005)
CYP2R1 (Shinkyō, Sakaki et al. 2004)	CYP8A1 and 8B1 (Ullrich, Brugger et al. 1997, Inoue, Yu et al. 2006)	CYP11A1 and 11Bs (Schwarz, Chernogolov et al. 1999, Bureik, Schiffler et al. 2002, Midzak, Akula et al. 2011)
CYP2S1 (Deb and Bandiera 2009)	CYP17A1 (Mizrachi, Wang et al. 2011)	CYP24A1 (Annalora, Goodin et al. 2010)
CYP2U1 (Chuang, Helvig et al. 2004)	CYP19A1 (Pandey, Kempna et al. 2007)	CYP26A1, 26B1 and 26C1 (Slavotinek, Mehrotra et al. 2013, Tripathy, Chapman et al. 2016)
CYP2W1 (Karlgrén, Gomez et al. 2006)	CYP21A (Mizrachi, Wang et al. 2011)	CYP27A1, 27B1 and 27C1 (Axen, Postlind et al. 1994, Dubrac, Lear et al. 2005)
CYP5A1 (Ruan, Li et al. 1994)		

No information was available for CYP2Ts, 4V2, 4X1, 4Z1, 20A1, 39A1, 46A1 and 51A1.

In mammals, microsomal P450 expressions were thought to be limited to the liver a few decades ago. Certainly, liver, as the organ responsible for xenobiotic detoxification, has the highest P450 content in the body. However, several P450 genes have been shown to be constitutively expressed in different organs (Imaoka, Hashizume et al. 2005, Zordoky, Aboutabl et al. 2008). In our laboratory, we have shown that several P450 are expressed in rat heart, lungs and kidneys, as well as liver (Zordoky, Aboutabl et al. 2008); CYP2Bs, CYP2C11, CYP2J3, CYP2E1, CYP4As and CYP4Fs were found to have relatively high mRNA levels in the heart (Zordoky, Aboutabl et al. 2008), while in the lungs, CYP2B1, CYP2J3, CYP2E1 and CYP4Fs genes were found to be predominant (Zordoky, Aboutabl et al. 2008). In the kidneys, high gene expression of almost all of P450 enzymes was found (Zordoky, Aboutabl et al. 2008). However, assessing P450 distribution in organs via gene expression has an innate imperfection, as it measures only mRNA levels that may not reflect the final protein levels. P450 protein level is a function of transcriptional regulation in addition to translational and posttranslational regulation. Similarly, discrepancies between mRNA and protein levels of CYP2J2 and CYP2C8 have been previously reported (Delozier, Kissling et al. 2007); it has been reported that although CYP2J2 mRNA was about 1000 times higher than CYP2C8, both enzymes had comparable protein levels in human heart tissue (Delozier, Kissling et al. 2007). Though, studies evaluating P450 expression across different tissues by the actual measuring of protein levels are relatively limited.

It is worth to note that, since P450 activity is dependent on other cofactors such as NADPH-P450 reductase and cyb5, correlation between P450 enzymes expression and activity is not always guaranteed. Marji *et al.* (Marji, Wang et al. 2002) described a lack of correlation between CYP4A enzymes expression and their activities due to insufficient P450 reductase in rat kidneys (Marji, Wang et al. 2002). Naturally, P450 are greatly varied

in their catalytic activities (Imaoka, Hashizume et al. 2005). Therefore, a P450 enzyme of high activity, despite its low expression level, may dominate a reaction in a tissue more efficiently than a highly expressed P450 but with low activity.

## **1.5. Physiological Functions of Microsomal Cytochrome P450**

### **1.5.1. Elimination of Xenobiotics**

Xenobiotics are relatively small, non-nutrient compounds that are exogenous to the species in question (Ioannides 2002). Accordingly, xenobiotics include drugs and environmental factors, such as pollutants, pesticides and natural occurring chemicals (Ioannides 2002). Naturally, xenobiotics are persistently entering the body, which responds with the elimination processes, namely excretion and metabolism, to limit the exposure to foreign compounds (Ioannides 2002). Metabolism aims to alter the chemical structure of xenobiotics by a wide array of biological reactions, mostly enzyme mediated, leading to increase the hydrophilicity of xenobiotics, and therefore their excretion (Golan 2012). In addition, metabolism frequently leads to inactivation of xenobiotic biological effect, albeit, in certain cases, the bioactivation of inactive xenobiotics to give biologically-active molecules can also occur (Guengerich 2008). Xenobiotic metabolism is usually divided to phase I and II, where polar function groups are unmasked or introduced in the chemical structure (phase I or activation), followed by the conjugation between this polar group of the xenobiotic and endogenous molecules, notably glucuronic acid, to further improve hydrophilicity (phase II or conjugation) (Golan 2012). Hepatic microsomal P450 are the enzymes that dominate the catalysis of phase I metabolism of xenobiotics (Anzenbacher and Anzenbacherova 2001). Therefore, P450-mediated metabolism plays a critical role determining the onset and duration of drug action. Hepatic microsomal P450 enzymes, typically CYP1A2, CYP2A6, CYP2B6, CYP2C8, CYP2C9, CYP2C18, CYP2C19, CYP2D6, CYP2E1 and CYP3A4,

determine how much will be the half-life in the body for most of drugs (Anzenbacher and Anzenbacherova 2001, Anzenbacher and Zanger 2012). Also, P450 enzymes, notably CYP3As, influence the extent of absorption from gastrointestinal tract by what is called first-pass effect for drugs with high-extraction ratios (Dufek, Bridges et al. 2013). The liver, as the organ with the highest P450 content, dominates drug metabolism; however, it has been reported that the P450 at local tissues, such as brain, can affect the biological activity of drugs away from the liver (Miksys and Tyndale 2013). Due to the critical role of microsomal P450 in drug metabolism, alterations in P450 activity during drug treatments could lead to therapeutic failure or exacerbation of adverse effects/toxicity incidence (Shorr, Ray et al. 1993). Therefore, factors that can alter P450 activity, such as, age, genetic variation, disease and most importantly co-administered drugs, have been extensively studied (Shorr, Ray et al. 1993).

### **1.5.2. Metabolism of Polyunsaturated Fatty Acids**

Beside their critical role in xenobiotic metabolism, the endogenous roles of P450 enzymes were reported as early as 1968 (Wilson, Oldham et al. 1968), when the role of P450 was first reported in mediating the steroidal 11 $\beta$ -hydroxylation, identified later to be CYP11Bs converting 11-deoxycortisol to cortisol, as well as 11-deoxycorticosterone to corticosterone (Ortiz de Montellano 2005). CYP11Bs and all other P450 enzymes mediating steroidal reactions are mitochondrial, except the microsomal CYP1B1, whose substrates include 17 $\beta$ -estradiol and testosterone, as well as xenobiotics, such as polycyclic aromatic hydrocarbons (Shimada, Watanabe et al. 1999, Murray, Melvin et al. 2001). However, microsomal P450 are more important than mitochondrial forms in the monooxygenation of polyunsaturated fatty acids, mediating the formation of several bioactive metabolites (Oliw 1994). Polyunsaturated fatty acids are aliphatic monocarboxylic acids with two or more cis-double bonds, which are normally found esterified in cell membranes (Table 1.4) (Rustan

and Drevon 2001). They are indicated by the number of carbons, as well as the number and sometimes the location of double bonds, for example AA is 20:4, cis,cis,cis,cis- $\Delta$ 5,8,11,14 (Table 1.4) (Rustan and Drevon 2001). Also, polyunsaturated fatty acids are classified according to the position of their last double bond in the carbon chain to  $\omega$ -3 and  $\omega$ -6 (Table 1.4) (Rustan and Drevon 2001). Two of the polyunsaturated fatty acids cannot be synthesized by human body, and therefore, it is essential to be supplied from external sources (Rustan and Drevon 2001, Russo 2009). These essential polyunsaturated fatty acids are the linoleic acid and  $\alpha$ -linolenic acid, and their main dietary sources are plant and fish oils (Rustan and Drevon 2001, Russo 2009).

Microsomal P450 enzymes can either insert epoxide or hydroxyl function groups to the polyunsaturated fatty acids, to give epoxy- or hydroxy-fatty acids, respectively; according to the function group, epoxide or hydroxide, of the major metabolite(s) P450 enzymes are divided into either P450 epoxygenases or hydroxylases, respectively (Oliw 1994, Spector and Kim 2015, Westphal, Konkel et al. 2015). AA, in addition to other polyunsaturated fatty acids, notably linoleic acid, eicosapentaenoic acid and docosahexaenoic acid, have been reported to be metabolized by P450 enzymes to give the corresponding epoxy- or hydroxy-fatty acids (Spector and Kim 2015, Westphal, Konkel et al. 2015). However, AA is considered the most significant polyunsaturated fatty acid substrate for P450 epoxygenases and hydroxylases to form several bioactive metabolites that have been extensively studied (Oliw 1994, Spector and Kim 2015, Westphal, Konkel et al. 2015).

**Table 1.4. The Chemical Structure and Characterization of the Common Polyunsaturated Fatty Acid.**

Common name	Chemical structure	Characterization
Linoleic acid		$\omega$ -6    18:2
$\alpha$ -Linolenic acid		$\omega$ -3    18:3
Arachidonic acid		$\omega$ -6    20:4
Eicosapentaenoic acid		$\omega$ -3    20:5
Docosahexaenoic acid		$\omega$ -3    22:6

## 2. Arachidonic Acid Metabolism

AA is an  $\omega$ -6 polyunsaturated fatty acid, which is abundant in all body organs. In normal condition, a small portion of AA is maintained in its free form (unesterified), while the majority of AA is stored in the cellular membranes, mostly esterified at the sn-2 position of phosphoglycerides (Buczynski, Dumlao et al. 2009, Imig 2012). Glycerol, which is a trihydroxyl propyl alcohol, is esterified to a phosphoric acid derivative at the C3 hydroxyl group; whereas, the two other hydroxyl groups at C1 and C2, or sn-1 and sn-2, respectively, are esterified to carboxylic acids to give the phosphoglycerides (Fig. 1.5) (Xu, Valenzuela et al. 2013). Enzymes responsible for the hydrolysis of these ester linkages are called phospholipases, and categorized according to the regioselectivity of their esterase activity on the phosphoglycerides (Fig. 1.5). Phospholipases that act on sn-1, sn-2 and both sn-1 and sn-2 are called phospholipase A<sub>1</sub>, phospholipase A<sub>2</sub> and phospholipase B, respectively, to give free fatty acids and lysophosphoglycerides (Fig. 1.5) (Zolk, Munzel et al. 2004). Accordingly, the release of AA, which is kept at lower rate, is mediated by phospholipase A<sub>2</sub> (Buczynski, Dumlao et al. 2009, Imig 2012). Phospholipase A<sub>2</sub> is a superfamily that contains at least four different clusters: the secreted, the cytosolic, the calcium-independent and the platelet-activating-factor phospholipase A<sub>2</sub> (Burke and Dennis 2009). The dominant AA-releasing phospholipase A<sub>2</sub> in the mammals is the cytosolic type, notably group IVA (Buczynski, Dumlao et al. 2009); whereas, the platelet-activating-factor phospholipase A<sub>2</sub> has been linked to coronary heart disease in humans (Burke and Dennis 2009).

Intracellular concentration of the unesterified AA is widely believed to be in  $\mu$ M range, based on reports where the total concentration of unesterified AA has been determined in different tissues. For example, while the unesterified form of AA is in nM range in blood (Brash 2001), its concentration has been reported to be 13-44  $\mu$ M in umbilical cord and intervillous space (Benassayag, Mignot et al. 1997), 18.9  $\mu$ g/g (approximately equivalent to 60  $\mu$ M) in skin

(Hammarstrom, Hamberg et al. 1975), and 75 µg/g (approximately equivalent to 250 µM) in liver (Edpuganti and Mehvar 2013). Therefore, 50-100 µM of AA was used in several published studies performed AA- P450 incubation experiments (Xu, Falck et al. 2004, Imaoka, Hashizume et al. 2005). Furthermore, in response to stimuli, the release of the free AA has been reported to be remarkably increased (Buczynski, Dumlao et al. 2009). Regardless, the unesterified AA is then metabolized into several biologically active metabolites, termed eicosanoids, by one of three groups of enzymes: cyclooxygenases, lipoxygenases, or microsomal P450 enzymes (Buczynski, Dumlao et al. 2009).

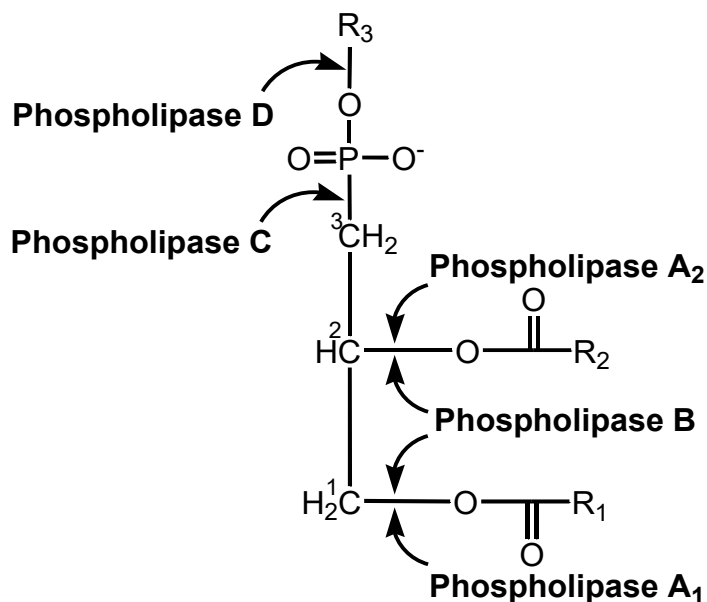


**Figure 1.5. Site of Action of Phospholipase A<sub>1</sub>, A<sub>2</sub>, B, C and D on Phosphoglycerides.**

In contrast to microsomal P450, cyclooxygenase and lipoxygenase enzymes are soluble enzymes (Buczynski, Dumlao et al. 2009). Cyclooxygenase enzymes, as the name implies, form a cyclic structure out of AA by forming a bond between C8 and C12 of AA, in addition to oxygen insertion (Fig. 1.6) (Buczynski, Dumlao et al. 2009, Rouzer and Marnett 2009). Cyclooxygenase enzymes have two active sites, the peroxidase and cyclooxygenase active sites. The cyclooxygenase active site metabolizes AA to prostaglandin G<sub>2</sub>, then the peroxidase active site metabolizes prostaglandin G<sub>2</sub> to prostaglandin H<sub>2</sub> (Fig. 1.6) (Rouzer and

Marnett 2009). By prostaglandin synthases, prostaglandin H<sub>2</sub> is converted to large array of bioactive prostaglandins, such as prostaglandin E<sub>2</sub> and F<sub>2α</sub>, thromboxane A<sub>2</sub> and prostacyclin (Fig. 1.6) (Rouzer and Marnett 2009). On the other hand, lipoxygenase enzymes are lipid peroxidizing enzymes, which insert hydroperoxy group in AA to form hydroperoxyeicosatetraenoic acids (Fig. 1.6) (HPETEs) (Kuhn, Banthiya et al. 2015). The 5-HPETE is the substrate of leukotrienes synthases to give different leukotrienes, viz., A<sub>4</sub>, B<sub>4</sub>, C<sub>4</sub>, D<sub>4</sub> and E<sub>4</sub> (Fig. 1.6) (Buczynski, Dumlao et al. 2009, Kuhn, Banthiya et al. 2015). In humans, lipoxygenase is represented by six enzymes, 12/15-, 15-, 12R-, 5-, platelet-type 12- and epidermis-type lipoxygenases (Kuhn, Banthiya et al. 2015).

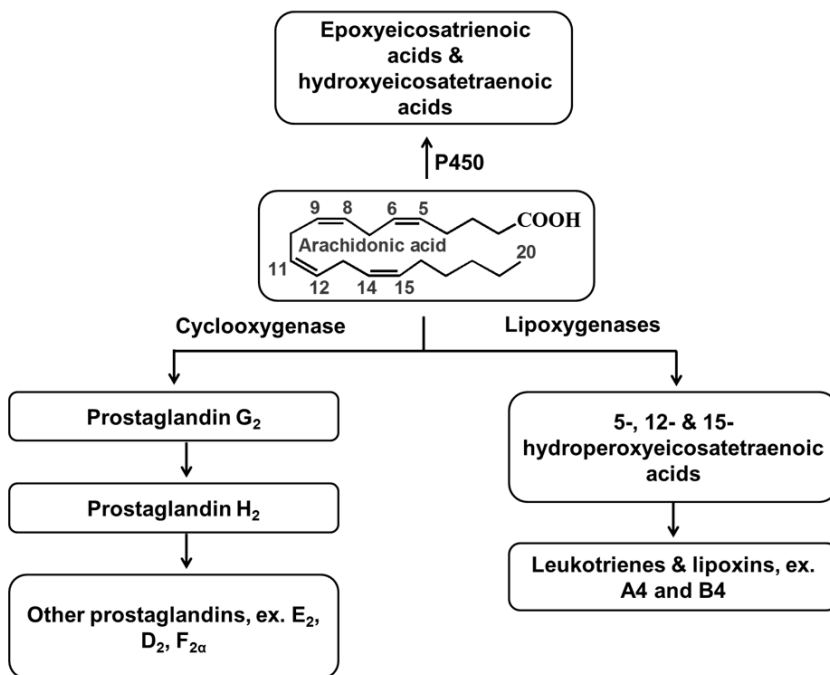


**Figure 1.6. The Metabolism of Arachidonic Acid by Cyclooxygenase-, Lipoxygenase- and P450-Mediated Pathways.**

### 2.1. Cytochrome P450-Derived Arachidonic Acid Metabolites

Microsomal P450 enzymes catalyze mid-chain and terminal oxygen insertion to AA to give several epoxy- and hydroxy-metabolites in the presence of oxygen and NADPH (Capdevila, Falck et al. 2000). Despite the fact that P450-mediated AA metabolism was

reported about 30 years ago, P450-derived AA metabolites have only recently garnered a lot of attention (Roman 2002). The significant and multifaceted roles of P450-derived AA metabolites have been recognized in the regulation of biological functions, especially in the cardiovascular system (Roman 2002). Several studies have shown the substantial association between the alterations in P450-derived AA metabolites levels and several pathological conditions (Alonso-Galicia, Falck et al. 1999, Roman 2002, Morisseau 2013). In our laboratory, we have previously reported that cardiac hypertrophy and cardiomyopathy, induced by arsenic, isoproterenol, doxorubicin or benzo(a)pyrene in rats and mice, is accompanied by definitive alterations in P450-mediated AA-metabolism (Zordoky, Aboutabl et al. 2008, Aboutabl, Zordoky et al. 2009, Alsaad, Zordoky et al. 2012, Anwar-Mohamed, El-Sherbeni et al. 2012). Also, to clarify the cause-effect relationship, several studies have shown that by modulating the levels of P450-derived AA metabolites, heart damage can be induced or controlled (Imig 2012, Alsaad, Zordoky et al. 2013, Morisseau and Hammock 2013). Moreover, it has been shown that number of P450-derived AA metabolites have a direct detrimental effect on cardiomyocytes (Maayah, Abdelhamid et al. 2015, Maayah and El-Kadi 2016), or have a protective effect on cardiomyocytes against chemical insults, such as angiotensin II and isoproterenol (Tse, Aboutabl et al. 2013, Elkhatali, El-Sherbeni et al. 2015).

### **2.1.1. Epoxy-Metabolites of Arachidonic Acid**

P450 enzymes mediate epoxidation of AA at any of its four cis-double bonds, keeping the cis conformation, to give 5,6-, 8,9-, 11,12-, or 14,15-cis-epoxyeicosatrienoic acids (EETs); the insertion of the epoxide function group can occur at any of the two flanks of AA double bond, leading to either R,S or S,R cis-EETs (Fig. 1.7). The formation of EETs is mediated mostly by CYP2 family, notably, CYP2Bs, CYP2Cs and CYP2Js enzymes, which are collectively called P450-AA epoxygenases (Fig. 1.7) (Capdevila, Falck et al.

2000, Imig 2012). Thereafter, an enzyme called soluble epoxide hydrolase (sEH) catalyzes the hydration of EET to dihydroxyeicosatrienoic acids (DHETs) (Imig 2012) (Fig. 1.7). The sEH mediates the main pathway for EETs deactivation; however, there are several other pathways for the deactivation of EETs, namely  $\beta$ -oxidation, incorporation to plasma membrane, diffusion and binding to plasma and tissue proteins, cyclooxygenase- and P450-mediated metabolism and chain elongation that are minor compared to sEH pathway (Roman 2002, Imig 2012).

EETs exhibit several beneficial effects on biological system, such as anti-inflammatory, analgesic, vasodilatory, anti-platelet, fibrinolytic and vascular smooth muscle anti-migratory effects (Sudhahar, Shaw et al. 2010, Imig 2012). Because DHETs are less-biologically-active, EET hydrolysis by sEH is considered a deactivation process. Recently, DHETs have been reported to exhibit a pro-inflammatory effect, and, in contrast to EETs, sEH is the main pathway for DHETs formation (Norwood, Liao et al. 2010). Therefore, it is believed that sEH activity is deleterious by decreasing the cytoprotective EETs and increasing the pro-inflammatory DHETs.

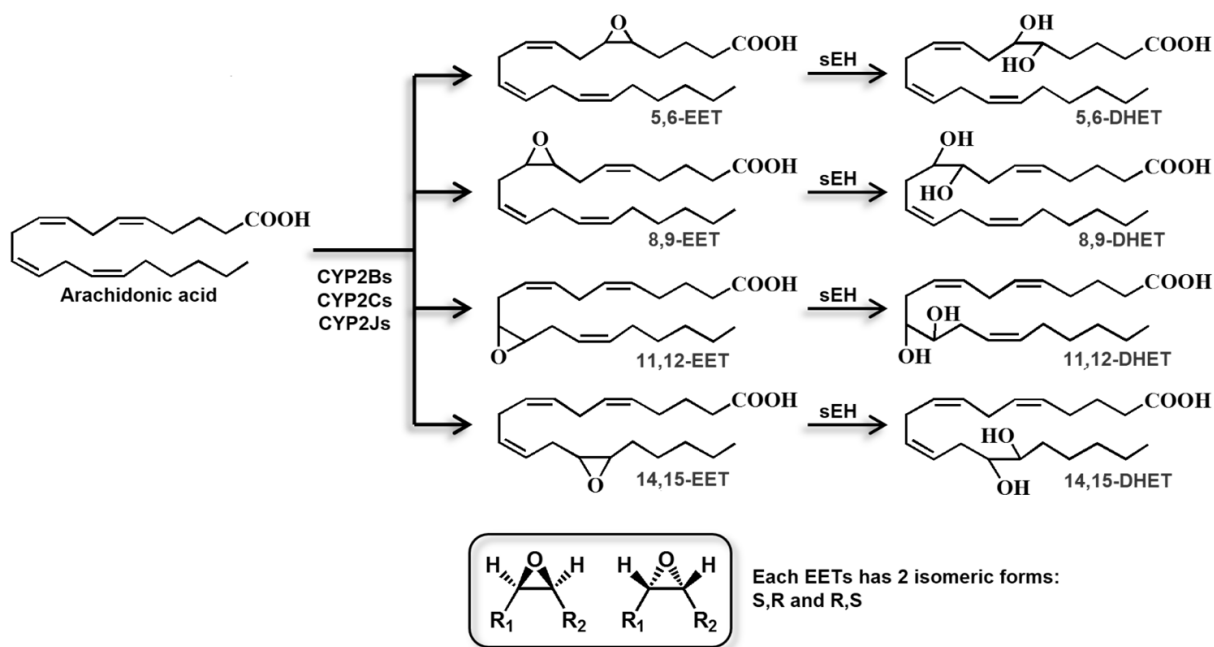


**Figure 1.7. The Formation and Degradation of EETs by P450 and sEH-Mediated Pathways, Respectively.**

### 2.1.2. Hydroxy-Metabolites of Arachidonic Acid

The hydroxy-metabolites of AA are divided into mid-chain and terminal/subterminal hydroxyeicosatetraenoic acids (HETEs) (Fig. 1.8) (Capdevila, Falck et al. 2000). The insertion of hydroxyl group mediated by CYP450 produces chiral center in HETEs, leading to S/R enantiomers in all HETEs except the terminal, C20, HETE (Fig. 1.8). The formation of mid-chain HETEs, namely 5-, 8-, 9-, 11-, 12- and 15-HETEs, is believed to be catalyzed by CYP1B1, and to a lower extent CYP1As and CYP3As, most probably through hydroperoxy-intermediates (Bylund, Kunz et al. 1998, Choudhary, Jansson et al. 2004, Zhao and Funk 2004). It has been reported that CYP4 family predominantly catalyzes 20-HETE formation (Xu, Falck et al. 2004). On the other hand, a heterogeneous group of P450 catalyzes the formation of subterminal HETEs, namely 16-, 17-, 18- and 19-HETEs, including CYP1As and CYP4As (Falck, Lumin et al. 1990, Laethem, Balazy et al. 1993, Capdevila, Falck et al. 2000). P450 enzymes mediating HETE formation are collectively

called P450-AA hydroxylases, and similar to EETs, there are several pathways for HETE deactivation:  $\beta$ -oxidation, incorporation to plasma membrane, diffusion and binding to plasma and tissue proteins, cyclooxygenase- and P450-mediated metabolism and chain elongation (Roman 2002, Imig 2012).

In contrast to EETs, 20-HETE is reported to exhibit vasoconstrictor, pro-inflammatory and pro-fibrotic activities (Zou, Fleming et al. 1996, Stec, Gannon et al. 2007). However, contrary to EETs and 20-HETE, the other HETEs are generally overlooked despite their reported biological activities. It has been reported that subterminal HETEs induce renal vasodilation and inhibit neutrophil adhesion, in addition to the suggested role of 19-HETE as the endogenous antagonist of 20-HETE (Alonso-Galicia, Falck et al. 1999, Bednar, Gross et al. 2000, Zhang, Deng et al. 2005); while mid-chain HETEs have been reported to induce cellular hypertrophy, inflammation and fibrosis (Reddy, Thimmalapura et al. 2002, Kayama, Minamino et al. 2009).

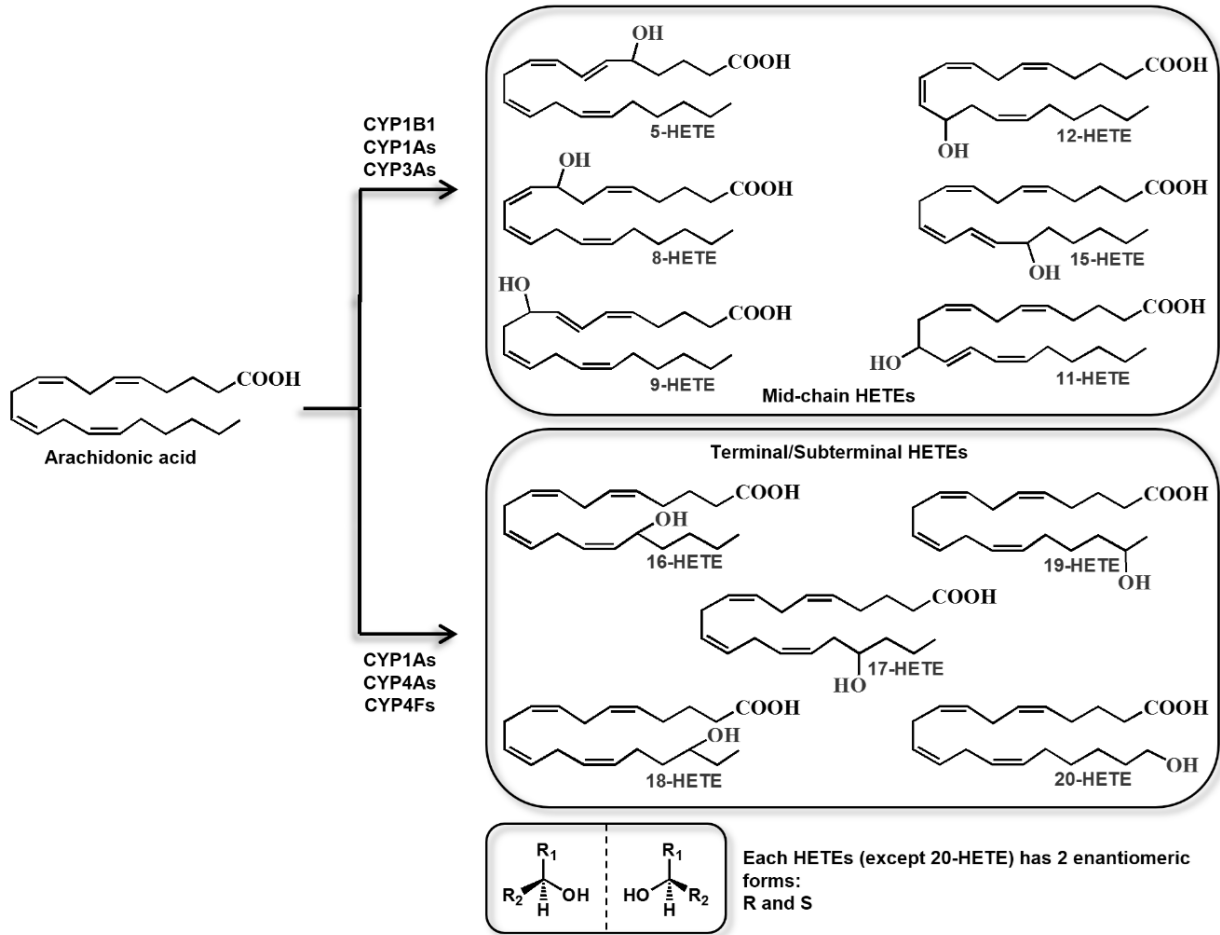


Figure 1.8. The P450-Mediated Metabolism of AA to Form HETEs.

### 3. Soluble Epoxide Hydrolase

As we mentioned previously, P450 and sEH are the dominant players controlling the levels of P450-derived AA metabolites in the tissues. Therefore, in this section, we will reveal more details about sEH characteristics. There are two main types of epoxide hydrolase, soluble and microsomal, and they play a significant role in *in vivo* detoxification of reactive metabolites, by catalyzing the hydrolysis of epoxides to more soluble and easily excretable metabolites (Kodani and Hammock 2015). Moreover, epoxide hydrolase regulates several physiological and pathological functions through controlling tissue levels of biologically-active epoxide mediators (Fretland and Omiecinski 2000, Imig 2012).

There is a clear overlap in substrate selectivity between soluble and microsomal epoxide hydrolases, however, sEH is generally more oriented toward epoxy-fatty acid metabolism; whereas microsomal epoxide hydrolase (mEH) is more oriented toward the metabolism of xenobiotics (Decker, Arand et al. 2009). In contrast to mEH, which is attached to cellular membranes as a monomer, sEH presents as a homodimer in solution (Gomez, Morisseau et al. 2004). sEH molecular weight is about 62 kDa, formed of 554 amino acid residues and belongs to the large family of  $\alpha/\beta$  hydrolase fold enzymes (Grant, Storms et al. 1993). The C-terminal of sEH is similar to mEH and accommodates the active site for the epoxide hydrolase activity (Newman, Morisseau et al. 2005). Contrary to the N-terminal of mEH, which acts as a membrane anchor, the N-terminal of sEH carries a second catalytic site that was found to be a functional phosphatase (Gomez, Morisseau et al. 2004, Newman, Morisseau et al. 2005).

#### 3.1. Tissue and Species Expression

Interestingly, tissue distribution of sEH and mEH is independent. sEH is expressed in all organs and tissues but at different levels. The organ of highest sEH level

is the liver, followed by kidneys, heart, lungs and brain (Gill and Hammock 1980); while for mEH, its expression is generally the highest in the liver, followed by adrenal gland, lungs, kidneys and intestine in mammals (Oesch, Raphael et al. 1977). sEH expression is confined to vascular tissue of kidneys, lungs and brain, contrary to other organs, such as liver and pituitary gland, where its expression is diffused in all tissues (Morisseau and Hammock 2005). It has been previously reported that sEH is exclusively localized in the cytosol in all organs, except for liver, where sEH is localized in both cytosol and peroxisome (Enayetallah, French et al. 2006). However, sEH activity has been commonly observed in mitochondrial and microsomal fractions. For a long time, this activity was attributed to the cytosolic sEH trapped in these fractions; only recently, Decker et al identified two new epoxide hydrolases, EH3 and EH4, that exhibit sEH activity, but they are attached to cellular membranes (Decker, Adamska et al. 2012). On the other hand, there are only sparse studies that have investigated the species-dependent expression of sEH. Despite that sEH gene expression in liver was comparable among mouse, rat and human, there was a 100-fold difference in sEH activity between rat and mouse liver (Hammock, Grant et al. 1997). Also, the hepatic content of sEH has been reported to be in the following order, mice > human > rat (Ioannides 2002).

### **3.2. Molecular Mechanism**

In contrast to mEH, the quaternary structure of human sEH has been identified. There are some differences in the structure between sEH and mEH as we mentioned before; however, the molecular mechanism of epoxides hydration by sEH and mEH is identical (Zou, Hallberg et al. 2000, Gomez, Morisseau et al. 2004, Morisseau and Hammock 2005). Epoxide hydrolases are characterized by high substrate affinity and low turnover number, usually smaller than 1 molecule per second, with most of its substrates (Oesch, Hengstler et al. 2004). Epoxide hydrolases catalyze the overall reaction of the

addition of a water molecule to an epoxide ring to ultimately yield a trans-dihydrodiol (Newman, Morisseau et al. 2005). It was found that labeled water molecules in the reaction medium are incorporated into the enzyme itself rather than the generated dihydrodiol from the epoxide substrate (Lacourciere, Vakharia et al. 1993). This was the first indication of an unusual mechanism for epoxide hydrolases. Thereby, it was concluded that the molecular mechanism of epoxide hydrolysis involves two chemical steps (Fretland and Omiecinski 2000, Decker, Arand et al. 2009). The epoxide hydrolases form an ester intermediate with the epoxide substrate; thereafter the final hydrolysis of the ester intermediate to the dihydrodiol is occurred (Borhan, Jones et al. 1995, Decker, Arand et al. 2009) (Fig. 1.9).

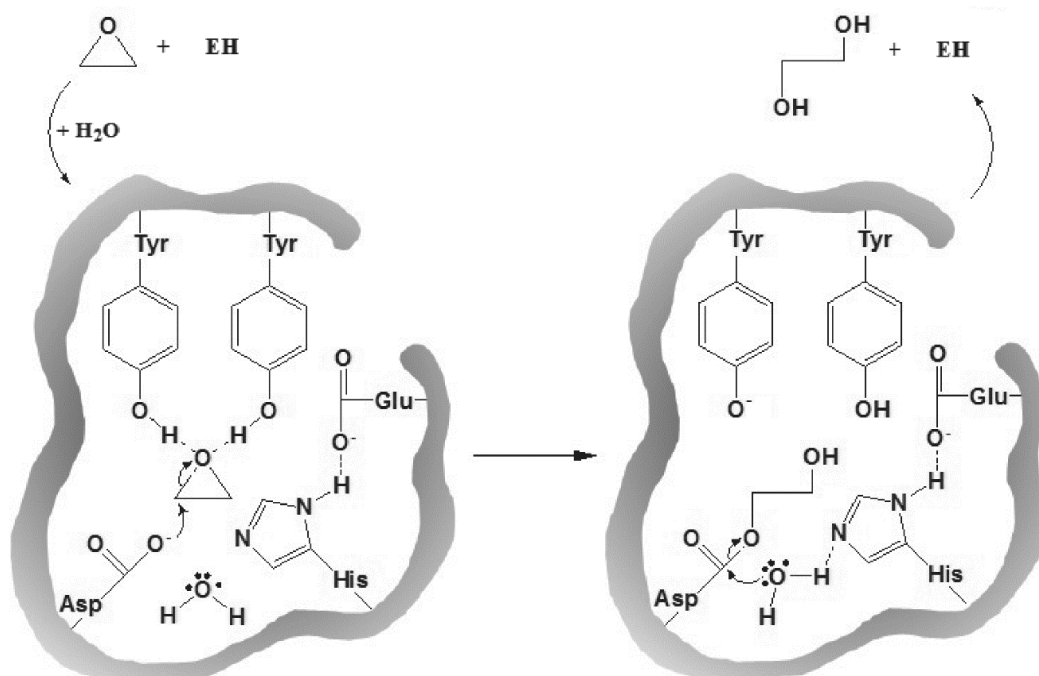


**Figure 1.9. The Mechanism of the Hydrolysis of Epoxide Substrates by sEH.**

The sEH catalytic site contains the essential histidine (His<sup>523</sup>) and aspartate (Asp<sup>333</sup>, and Asp<sup>495</sup>) residues, in addition to two tyrosine (Tyr<sup>382</sup> and Tyr<sup>465</sup>) residues that provide an essential support to the catalytic triad (Fig. 1.9) (Gomez, Morisseau et al. 2004,

Morisseau and Hammock 2005). Epoxide hydrolases recognize the substrate that is positioned in the active site by trapping the epoxide oxygen between the two tyrosine residues via hydrogen bonding (Fretland and Omiecinski 2000, Decker, Arand et al. 2009). Due to the position of the catalytic triad at the end of the substrate access tunnel, hydrophobic interactions between the substrate and the enzyme dictate certain stereo- and enantioselectivity (Zou, Hallberg et al. 2000, Decker, Arand et al. 2009). The first chemical step is very rapid and involving a nucleophilic substitution reaction between the epoxide ring activated by hydrogen bonding and the catalytic nucleophile, which is the aspartic acid (Fretland and Omiecinski 2000). An ester is formed between aspartate and the substrate to displace the C-O bond in the epoxide ring, simultaneously, one of the two tyrosine residues gives a proton to the resulted activated oxygen (Zou, Hallberg et al. 2000, Decker, Arand et al. 2009) (Fig. 1.9). In the second step, the ester formed between substrate and epoxide hydrolases is subsequently hydrolyzed by so called activated “charge relay system” composed of a histidine, as well as aspartate or glutamate residues (Zou, Hallberg et al. 2000, Decker, Arand et al. 2009).

### **3.3. Regulation**

sEH regulation is mediated by peroxisome proliferator-activated receptor responsive element in the 5'-flanking region of sEH gene (Pinot, Grant et al. 1995). Therefore, it has been reported that peroxisome proliferator-activated receptor- $\alpha$  agonist, fenofibrate, induced sEH activity by thirteen fold in rat liver and two folds in rat kidneys (Schladt, Hartmann et al. 1987). On the other hand, the peroxisome proliferator-activated receptor- $\gamma$  agonist, rosiglitazone, has been reported to downregulate sEH in cardiomyocytes (Pang, Li et al. 2011). Furthermore, a significant increase in sEH expression has been reported in male rats and mice compared with females, suggesting a hormonal domain in the regulation of sEH (Newman, Morisseau et al. 2005). Recently,

angiotensin II, as well as homocysteine was reported to upregulate sEH expression (Zhang, Xie et al. 2012).

### **3.4. Physiological Functions**

In addition to EETs, there are other epoxides of fatty acids that have also a reported potent biological activity and are found in significant levels in all tissues (Ioannides 2002, Decker, Arand et al. 2009). Most importantly, epoxides of linoleic acid, namely the epoxyoctadecenoic acids, have been proposed, similar to EETs, to regulate several physiological functions, notably cardiovascular, pulmonary and renal functions (Moran, Nowak et al. 2001, Fleming 2014, Vangaveti, Jansen et al. 2016). Also, sEH contribution to the metabolism of drugs and other xenobiotics has been reported, but it is considered minor compared with the microsomal epoxide hydrolase (Kodani and Hammock 2015).

#### **3.4.1. The Epoxides of Linoleic Acid**

Linoleic acid is an essential fatty acid and represents the major part of our dietary unsaturated fatty acids. It is epoxidized *in vivo* to 9,10- and 12,13- epoxyoctadecenoic acids. Historically, epoxyoctadecenoic acids were first identified as neutrophil-derived fatty acid epoxides, and therefore epoxyoctadecenoic acids are also termed leukotoxins (Ozawa, Nishikimi et al. 1988). The epoxidation can be enzyme-mediated, by P450 or cytochrome c, or can occur by spontaneous reaction of linoleic acid with reactive oxygen species. The most prominent P450- linoleic acid epoxygenase was reported to be CYP2C9 in human liver (Draper and Hammock 2000). On the other hand, sEH is the enzyme responsible for the hydrolysis of epoxyoctadecenoic acids, similar to EETs, to the corresponding dihydroxyoctadecenoic acids. In contrast to EETs, Epoxyoctadecenoic acids are

cytotoxic as proven *in vivo* and *in vitro*; They inhibit mitochondrial respiration leading to multiple organ failure such as cardiotoxicity, renal failure and adult respiratory distress syndrome (Moran, Weise et al. 1997). However, several reports have suggested that the cytotoxic effect of epoxyoctadecenoic acids is less potent than of their corresponding dihydroxyoctadecenoic acids (Draper and Hammock 2000, Mitchell, Moran et al. 2002). Dihydroxyoctadecenoic acids also inhibit mitochondrial respiration, yet by a different mechanism, epoxyoctadecenoic acids uncouple oxidative phosphorylation, whereas dihydroxyoctadecenoic acids additionally inhibit the electron transport chain itself (Mitchell, Moran et al. 2002). Dihydroxyoctadecenoic acids mediate the inhibition of Na<sup>+</sup>/K<sup>+</sup>-ATPase, and the induction of nuclear factor kappa B, in addition to mitochondrial dysfunction, consequently, they are potent cytotoxic agents (Moran, Weise et al. 1997, Slim, Hammock et al. 2001).

#### **4. The pharmacological Modulation of Cytochrome P450-Mediated Arachidonic Acid Metabolism: Drug Discovery vs. Drug Repurposing**

AA metabolism has long been a very appealing target for drug discovery and development efforts. Historically, modulating the activity of AA-metabolism cascade led to very successful medicines, most importantly nonsteroidal anti-inflammatory drugs and leukotriene antagonists, which attenuate cyclooxygenase- and lipoxygenase-cascade activity, respectively. These cyclooxygenase- and lipoxygenase-targeting drugs have been used in heart diseases, such as aspirin, lung diseases, such as montelukast, inflammation, pain and fever, such as ibuprofen and ketorolac. Accordingly, there is great enthusiasm to similarly develop new drugs based on the P450-mediated AA pathway. As we have already shown, microsomal P450 enzymes and sEH are the main players in this AA metabolic pathway; therefore, efforts have been paid to develop effective and safe P450 and sEH modulators to control tissue levels of P450-derived AA metabolites, as we will illustrate afterwards. With this respect, the attention has been directed more to sEH than P450, because sEH is an individual enzyme vs. the multiplicity of P450, and partially because EETs are more studied compared with HETEs (Capdevila 2007, Imig 2012).

##### **4.1. Modulators of Soluble Epoxide Hydrolase**

The first generation sEH inhibitors worked as competitive reversible inhibitors that rapidly bind to sEH but slowly dissociate from it (Morisseau, Du et al. 1998). The most important examples of these epoxide-based inhibitors is chalcone oxide derivatives, such as 4-fluorochalcone oxide (Fig. 1.10) (Morisseau and Hammock 2005, Newman, Morisseau et al. 2005). Morisseau et al were the first to report that carbamide compounds with appropriate substituents can exhibit potent sEH inhibitory activity (Figs. 1.9 and 1.10) (Morisseau, Goodrow et al. 1999). Accordingly, several urea-, amide- and carbamate-

compounds have been derived and identified to exhibit nanomolar sEH inhibition (Morisseau, Goodrow et al. 1999). One important urea-based sEH inhibitor is 1-(1-acetypiperidin-4-yl)-3-adamantanylurea (APAU) (Fig. 1.10 & 11), which was taken to Phase IIA clinical trial (Morisseau and Hammock 2013). Urea derivatives were the most successful sEH carbamate inhibitors, which were worked on to give new sEH classes of benzamide and benzoxazole sEH inhibitors (Fig. 1.10) (Eldrup, Soleymanzadeh et al. 2009). These inhibitors have comparatively more rigid structure than the older sEH inhibitors, and, show more selectivity toward sEH (Shen and Hammock 2012). New sEH inhibitors exhibit much more potency and better pharmacokinetics than the old epoxide-based inhibitors (Morisseau 2013). GlaxoSmithKline developed sEH inhibitor, GSK2256294 (Fig. 1.10), that has entered Phase I clinical trial for chronic obstructive pulmonary disease in male, obese, smoking patients (Podolin, Bolognese et al. 2013). Very recently, the dimerization of sEH was found to be crucial for sEH activity, introducing a novel target for allosteric sEH inhibitors that has not been explored yet (Nelson, Subrahmanyam et al. 2013). It has been reported in several studies that sEH inhibitors have multiple beneficial effects on the cardiovascular system, lungs, kidneys, diabetes, inflammation and pain typically through increasing EETs levels (Imig and Hammock 2009, Podolin, Bolognese et al. 2013, He, Wang et al. 2016).

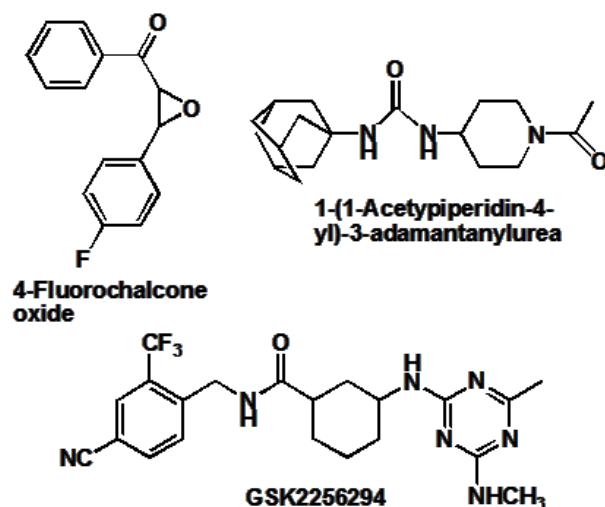


**Figure 1.10. The Chemical Structures of Representatives of sEH Inhibitors.**

On the other hand, the induction of sEH has been observed as a consequence of exposing to peroxisome proliferator-activated receptor- $\alpha$  agonists, such as clofibrate, fenofibrate and acetylsalicylic acid (Pinot, Grant et al. 1995). Diabetes and starvation cause an increase in sEH activity in rat liver that was corrected by insulin administration (Thomas, Schladt et al. 1989). Moreover, male mice kidneys and liver constitutively have a higher sEH content compared with female mice (Pinot, Grant et al. 1995).

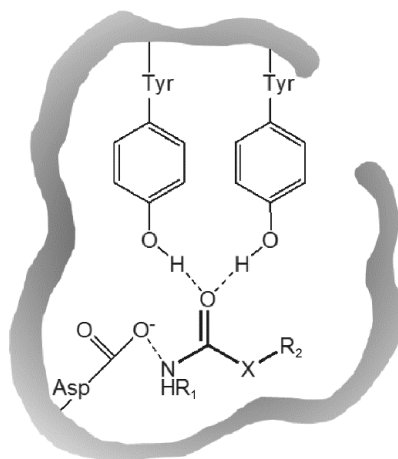


**Figure 1.11. The Mechanism of sEH Inhibition by Carbamide-Based Inhibitors; X is CH<sub>2</sub>, O or NH.**

## **4.2. Microsomal Cytochrome P450 Modulators**

Microsomal P450 mediating AA metabolism represent a big group of enzymes that makes the development of a modulator that is both effective and selective relatively difficult (Capdevila, Falck et al. 2000). Therefore, this approach to control P450-mediated AA metabolism attracted less interest, despite its promising potential, compared with sEH inhibition approach. For a P450 approach, it is imperative to pin-point the target P450 enzymes, and to do so, knowledge about two things is needed: 1) to determine which P450 enzyme is dominating AA metabolism based on AA-metabolizing activity and metabolic profile in different organs, and 2) to attribute metabolic alterations associated with pathological conditions to certain P450 enzyme. However, only sparse studies have tried to compare P450 enzymes with respect to AA-metabolism under the same experimental conditions (Imaoka, Hashizume et al. 2005). Also, previously published studies on P450-mediated AA metabolism focused mainly on EETs and 20-HETE, as a result, mid-chain and subterminal HETEs have been largely ignored (Fan, Muroya et al. 2015, Huang, Al-Shabrawey et al. 2016). This is due mainly to the lack of simple method for the simultaneous measuring of mid-chain and subterminal HETEs along with EETs and 20-HETE (Blewett, Varma et al. 2008). As a result, our knowledge on the critical points that can be targeted to correct the alteration of P450-mediated AA metabolism during pathological conditions is incomplete.

### **4.2.1. Development of New Cytochrome P450 Modulators**

Regardless, a numbers of inhibitors of fatty acid monooxygenation have been developed. The early inhibitors used to inhibit P450-mediated AA metabolism were not directed toward specific P450 enzymes, but, simply, they contained a suicidal function groups, such as allylic and acetylenic groups, that are known to

become activated and form a non-functional adduct with P450 (Gan, Acebo et al. 1984, Capdevila, Gil et al. 1988, Muerhoff, Williams et al. 1989, Sacerdoti, Gatta et al. 2003). The most used of these inhibitors is the 17-octadecynoic acid (17-ODYA), which is a long-chain (18 carbons) carboxylic acid, with a terminal triple bond (Fig. 1.12) (Muerhoff, Williams et al. 1989, Miyata, Taniguchi et al. 2001). 17-ODYA is potent in inhibiting P450-mediated AA metabolism, however, it has poor selectivity (Wang, Brand-Schieber et al. 1998, Miyata, Taniguchi et al. 2001). Based on 17-ODYA, the most advanced inhibitors of P450-mediated fatty acid monooxygenation were developed (Fig. 1.12) (Wang, Brand-Schieber et al. 1998), with the exception of HET0016 and its close relative TS-011, which have been independently identified by high throughput screening (Miyata, Taniguchi et al. 2001). These inhibitors are proven to be both selective and potent. Most importantly, the 6-(2-propargyloxyphenyl)hexanoic acid (PPOH) and N-methylsulfonyl-6-(2-propargyloxyphenyl)hexanamide (MS-PPOH), which have been shown to selectively inhibit the formation of EETs with an  $IC_{50}$  value of about 10  $\mu$ M, but not the 20-HETE formation by rat renal microsomes (Fig. 1.12) (Wang, Brand-Schieber et al. 1998). While other compounds, N-methylsulfonyl-12,12-dibromododec-11-enamide and 12,12-dibromododec-11-enoic acid, inhibit the formation of 20-HETE more potently than EET, with a 25-30-fold difference in  $IC_{50}$  values (Fig. 1.12) (Wang, Brand-Schieber et al. 1998). For the inhibition of 20-HETE formation, HET0016 (N-Hydroxy-N'-(4-butyl-2-methylphenyl) formamidine), and TS-011 (N-(3-Chloro-4-morpholin-4-yl)Phenyl-N'-hydroxyimido Formamide) were developed by Taisho Pharmaceutical Co to be more selective and potent toward 20-HETE formation (Fig. 1.12). For HET0016, the  $IC_{50}$  value for 20-HETE formation was 35 nM and for EET formation was 2800 nM in rat kidney microsomes, (Miyata, Taniguchi et al. 2001). TS-011 is even more selective toward 20-HETE formation

with  $IC_{50}$  value of 9 nM with no inhibition of EET formation being observed in spontaneous hypertensive rat kidney microsomes (Miyata, Seki et al. 2005). The effect of HET0016 and TS-011 was attributed to inhibition of CYP4s (Miyata, Taniguchi et al. 2001, Miyata, Seki et al. 2005). Moreover, based on the chemical structure of resveratrol (Chang, Chen et al. 2001), which is known to inhibit the CYP1 family, the compound 2,4,3',5'-tetramethoxystilbene (TMS), was developed as an inhibitor of CYP1B1 (Fig. 1.12) (Chun, Kim et al. 2001, Kim, Ko et al. 2002). CYP1B1 is believed to be a predominant P450 enzyme in mid-chain HETE formation (Choudhary, Jansson et al. 2004, Zhao and Funk 2004), therefore, a decrease in mid-chain HETE formation is expected by TMS-mediated inhibition of CYP1B1 activity.

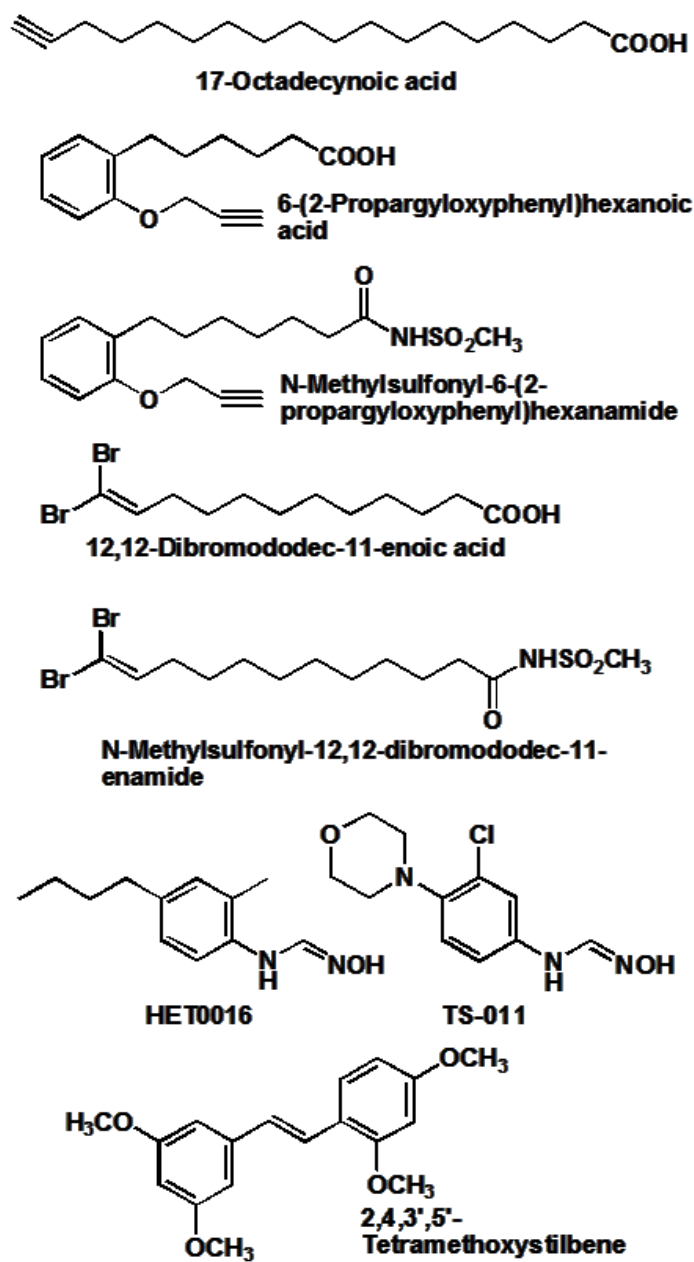


Figure 1.12. The Chemical Structures of Representatives of Inhibitors of P450-AA Monooxygenases.

## **4.2.2. Repurposing of Old Cytochrome P450 Modulators**

With the first efforts to develop new modulators for P450-mediated formation of AA metabolites, it was realized that modulators of xenobiotic-metabolizing P450 enzymes also have an effect on AA metabolism (Capdevila, Gil et al. 1988). The long interest in P450 as the main xenobiotic inactivators has led to the recognition that certain clinically-approved drugs have the capacity to alter P450 activity. These drugs can result in drug-drug interactions due to the alteration in the elimination of co-administered drugs, exposing the patient to a serious health risk (Anzenbacher and Anzenbacherova 2001, Ioannides 2008).

### **4.2.2.1. Drug-Drug Interactions**

Drug-drug interaction describes the situation when the expected effect of a drug is altered by the concurrent administration of another drug (Vangaveti, Jansen et al. 2016). Obviously, two drugs are interacting when they have opposite effects on the body, such as antidiabetic drugs and glucocorticoids “antagonistic” effect on blood glucose level (Vangaveti, Jansen et al. 2016), or have same/similar effects, such as warfarin and nonsteroidal anti-inflammatory drugs “synergistic” effect that increases the risk of bleeding (Shorr, Ray et al. 1993, Knijff-Dutmer, Schut et al. 2003), which are collectively called “pharmacodynamic interactions” because they occur at the receptor level (Shorr, Ray et al. 1993). On the other hand, there are “pharmacokinetic interactions” where the concentration of a drug in the body is decreased or increased, causing therapeutic failure or drug toxicity, respectively (Shorr, Ray et al. 1993, Vangaveti, Jansen et al. 2016). This happens when one or more of the pharmacokinetic processes, namely absorption, distribution, metabolism and excretion, are altered by an interacting drug, such as the inhibition of absorption of

co-administered drugs by antacids (Gugler and Allgayer 1990), the displacement of drugs from the plasma protein binding sites affecting drug distribution (Vangaveti, Jansen et al. 2016), and the inhibition of excretion of acidic drugs by probenecid (Shorr, Ray et al. 1993, Imig and Hammock 2009). Altering drug metabolism causes the most dramatic alteration in drug concentration, because almost all metabolic reactions are enzyme mediated, and enzymes are present in limited amounts that make them easily saturable. Any changes in enzyme levels, either by inactivation or induction, readily affect the rate of the reaction they mediate (Andersen 1981). Certainly, facilitated diffusion and active transport have a role in drug absorption and excretion; however, in contrast to drug metabolism, passive processes (namely, passive diffusion and glomerular filtration) have the major contribution to absorption and excretion, respectively (Doligalski, Tong Logan et al. 2012). Accordingly, metabolism-mediated drug interactions are the most probable and severe among drug-drug interactions (Shorr, Ray et al. 1993, Doligalski, Tong Logan et al. 2012). Today's drug dispensing practice requires good knowledge on drug-drug interactions (Knijff-Dutmer, Schut et al. 2003, Zhang, Luo et al. 2012). Because P450 enzymes are the most important drug-metabolizing enzymes, the potential to alter P450 activity has been studied for different drugs, and consequently, effective and selective microsomal P450 enzymes inhibitors and inducers are already available and clinically approved (Tables 1.5 and 1.6).

#### **4.2.2.2. Cytochrome P450 Inhibitors**

Drugs exhibiting P450 inhibitory activity are often reversible in nature; however, some potent inhibitors of P450 are irreversible (Bibi 2008). Reversible inhibitors of P450, as the name implies, are transient in their effect, contrary to the irreversible inhibitors, and are divided according to their enzyme inhibition kinetics

into: competitive, non-competitive and uncompetitive (Doligalski, Tong Logan et al. 2012). Competitive inhibition can occur when two drugs are metabolized by the same P450 enzyme, and consequently they are competing for the active site of the enzyme (Bibi 2008). Drugs that have a remarkably higher affinity toward P450 and/or achieve higher molar concentration *in vivo* are more effective competitive inhibitors (Kramer and Tracy 2008, Caterina, Antonello et al. 2013). This type of inhibition causes an increase in the  $K_m$  with no change in the  $V_{max}$  of the metabolism of the substrate (Kramer and Tracy 2008). Generally, competitive inhibition cannot provide a very effective inhibitor for *in vivo* use, because the inhibition of a substrate metabolism normally leads to an increase in substrate concentration, displacing the inhibitor from the active site and ceasing the inhibition. Examples for competitive P450 inhibitors include fluoxetine (CYP2D6 inhibitor) and clotrimazole (CYP3A4 inhibitor) (Preskorn, Alderman et al. 1994, Zhang, Ramamoorthy et al. 2002). Non-competitive inhibition is rarely observed and occurs when the inhibitor binds to an allosteric site that regulates the activity of the enzyme, leading to a decrease in the  $V_{max}$  with no change in the  $K_m$  of substrate metabolism, such as tranlycypromine inhibition of CYP2C9, and resveratrol inhibition of CYP2E1 (Piver, Berthou et al. 2001, Salsali, Holt et al. 2004, Bibi 2008, Kramer and Tracy 2008). For uncompetitive inhibition, the inhibitor binds to the enzyme-substrate complex, leading to a decrease in both  $K_m$  and  $V_{max}$  of substrate metabolism (Kramer and Tracy 2008). Cotinine, which is the major metabolite of nicotine, inhibits CYP2E1 by an uncompetitive mechanism (Van Vleet, Bombick et al. 2001). Notably, several reversible P450 inhibitors do not show pure kinetics of any of the aforementioned types, but show mixed kinetics of inhibition, and are characterized by a decrease in  $V_{max}$  and an increase in  $K_m$  of substrate metabolism (Kramer and Tracy 2008).

**Table 1.5. FDA Recommended *In Vivo* and *In Vitro* Inhibitors of Specific P450 Enzymes (Huang, Temple et al. 2007, Food-and-Drug-Administration 2014).**

Pharmacological agent	Selectivity	Safe use	Effectiveness
<b><math>\alpha</math>-Naphthoflavone</b>	CYP1A2	<i>In vitro</i>	Ki = 0.01 $\mu$ m
<b>Amiodarone</b>	CYP2C9	<i>In vivo</i>	Decrease Cl <sub>int</sub> by 50-80%
<b>Bupropion</b>	CYP2D6	<i>In vivo</i>	Decrease Cl <sub>int</sub> by >80%
<b>Ciprofloxacin</b>	CYP1A2	<i>In vitro</i>	Decrease Cl <sub>int</sub> by >80%
<b>Clarithromycin</b>	CYP3A4	<i>In vivo</i>	Decrease Cl <sub>int</sub> by >80%
<b>Clomethiazole</b>	CYP2E1	<i>In vitro</i>	Ki = 12 $\mu$ m
<b>Clopidogrel</b>	CYP2B6	<i>In vitro</i>	Ki = 0.5 $\mu$ m
<b>Clopidogrel,</b>	CYP2B6	<i>In vivo</i>	Decrease Cl <sub>int</sub> by 20-50%
<b>Diallyldisulfide</b>	CYP2E1	<i>In vitro</i>	Ki = 150 $\mu$ m
<b>Diethyldithiocarbamate</b>	CYP2E1	<i>In vitro</i>	Ki = 9.8-34 $\mu$ m
<b>Enoxacin</b>	CYP1A2	<i>In vitro</i>	Decrease Cl <sub>int</sub> by >80%
	CYP2C8	<i>In vitro</i>	Ki = 7 $\mu$ m
<b>Fluconazole</b>	CYP2C9	<i>In vivo</i>	Decrease Cl <sub>int</sub> by 50-80%
	CYP2C19	<i>In vivo</i>	Decrease Cl <sub>int</sub> by >80%
<b>Fluoxetine</b>	CYP2C9	<i>In vitro</i>	Ki = 18-41 $\mu$ m
	CYP2D6	<i>In vivo</i>	Decrease Cl <sub>int</sub> by >80%
<b>Fluvoxamine</b>	CYP1A2	<i>In vitro</i>	Decrease Cl <sub>int</sub> by >80%
	CYP2C9	<i>In vitro</i>	Ki = 6.4-19 $\mu$ m
	CYP2C19	<i>In vivo</i>	Decrease Cl <sub>int</sub> by >80%
<b>Furafylline</b>	CYP1A2	<i>In vitro</i>	Ki = 0.6-0.73 $\mu$ m
<b>Gemfibrozil</b>	CYP2C8	<i>In vivo</i>	Decrease Cl <sub>int</sub> by >80%
	CYP2C8	<i>In vitro</i>	Ki = 69-75 $\mu$ m
<b>Indinavir</b>	CYP3A4	<i>In vivo</i>	Decrease Cl <sub>int</sub> by >80%
<b>Itraconazole</b>	CYP3A4	<i>In vivo</i>	Decrease Cl <sub>int</sub> by >80%
	CYP3A4	<i>In vitro</i>	Ki = 0.27-2.3 $\mu$ m
	CYP2C9	<i>In vivo</i>	Decrease Cl <sub>int</sub> by 50-80%
<b>Ketoconazole</b>	CYP3A4	<i>In vivo</i>	Decrease Cl <sub>int</sub> by >80%
	CYP3A4	<i>In vitro</i>	Ki = 0.0037- 0.18 $\mu$ m
<b>Montelukast</b>	CYP2C8	<i>In vitro</i>	Ki = 1.1 $\mu$ m
<b>Nootkatone</b>	CYP2C19	<i>In vitro</i>	Ki = 0.5 $\mu$ m
<b>Oxandrolone</b>	CYP2C9	<i>In vivo</i>	Decrease Cl <sub>int</sub> by 50-80%
<b>Paroxetine</b>	CYP2D6	<i>In vivo</i>	Decrease Cl <sub>int</sub> by >80%
<b>Phencyclidine</b>	CYP2B6	<i>In vitro</i>	Ki = 10 $\mu$ m
<b>Pioglitazone</b>	CYP2C8	<i>In vitro</i>	Ki = 1.7 $\mu$ m
<b>Prasugrel</b>	CYP2B6	<i>In vivo</i>	Decrease Cl <sub>int</sub> by 20-50%
<b>Quercetin</b>	CYP2C8	<i>In vitro</i>	Ki = 1.1 $\mu$ m
<b>Quinidine</b>	CYP2D6	<i>In vivo</i>	Decrease Cl <sub>int</sub> by >80%
	CYP2D6	<i>In vitro</i>	Ki = 0.027-0.4 $\mu$ m
<b>Rosiglitazone</b>	CYP2C8	<i>In vitro</i>	Ki = 5.6 $\mu$ m
<b>Sertraline</b>	CYP2B6	<i>In vitro</i>	IC50 = 3.2 $\mu$ m
<b>Sulfaphenazole</b>	CYP2C9	<i>In vitro</i>	Ki = 0.3 $\mu$ m
<b>Ticlopidine</b>	CYP2B6	<i>In vivo</i>	Decrease Cl <sub>int</sub> by 20-50%
	CYP2B6	<i>In vitro</i>	Ki = 0.2 $\mu$ m
	CYP2C19	<i>In vivo</i>	Decrease Cl <sub>int</sub> by >80%
	CYP2C19	<i>In vitro</i>	Ki = 1.2 $\mu$ m
<b>Trimethoprim</b>	CYP2C8	<i>In vitro</i>	Ki = 32 $\mu$ m
<b>Verapamil</b>	CYP3A4	<i>In vitro</i>	Ki = 10-24 $\mu$ m

The permanent aspect of P450 inhibition by irreversible inhibitors is due to covalent bonding formed between the inhibitor and the enzyme, either occupying the active site, or neutralizing an essential functional part of the enzyme (de Montellano and Correia 1995). This type of inhibitor needs to be activated before binding to the enzyme, and therefore, they are also known as mechanism-based or suicidal inhibitors (Bibi 2008, Fowler and Zhang 2008). Noteworthy, compounds forming a metabolic intermediate complex with P450 leading to quasi-irreversible inhibition are considered a subtype of the mechanism-based inhibitors (Taxak, Desai et al. 2012). The kinetics of inhibition are characterized by a time-dependent decrease in the  $V_{max}$  with no change in the  $K_m$  of substrate metabolism (Fowler and Zhang 2008). Examples of irreversible inhibitors include amphetamine, cimetidine, isoniazid, methadone and sulfanilamide (Riviere 2011).

The Food and Drug Administration (FDA) recommends certain drugs that can safely, selectively and effectively inhibit P450 enzymes (Table 1.5) (Huang, Temple et al. 2007, Food-and-Drug-Administration 2014). These probe-drugs are routinely used to perform drug metabolism and drug interaction studies for new drugs (Huang, Temple et al. 2007, Food-and-Drug-Administration 2014). Repurposing these clinically-approved agents could provide safe and rapid means to control EETs and HETEs levels in humans. For P450 enzymes that have low contribution to the metabolism of drugs, and therefore, not considered to be important for drug metabolism, such as CYP4 family, individual efforts are being performed to identify their selective inhibitors, by screening already clinically-approved drugs. In this context, it has been reported that danazol and 4-hydroxyamiodarone selectively inhibit CYP2J2 (Lee, Jones et al. 2012).

Drug repurposing can be a very successful approach to identify new modulators of P450-mediated AA metabolism; however, more effort is needed to: 1) examine a large array of purified animal and human xenobiotic- and AA-metabolizing P450 enzymes to determine their contribution to AA metabolism, 2) develop simple and rapid assays to measure the full P450-mediated AA metabolic profile to accurately determine the selectivity of the agents, and 3) optimize the dosage regimen for the new use of these agents by utilizing advanced animal-to-human and in-vitro-to-in-vivo translational techniques.

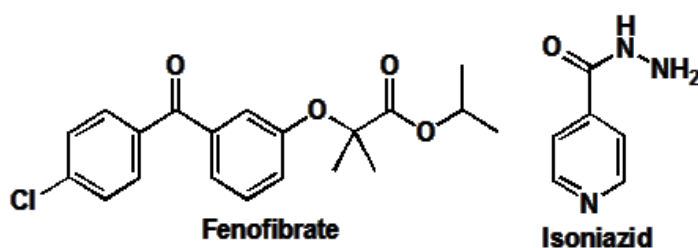


**Figure 1.13. The Chemical Structures of Representative Examples of inducers of P450 enzymes.**

#### 4.2.2.3. Cytochrome P450 Inducers

Compared with the inhibitors of P450 enzymes, our cumulative experience with the induction of xenobiotic-metabolizing P450 enzymes has been used more often to increase the formation rates of P450-derived AA metabolites. Fibrates have been successfully used as P450 enzymes inducers in rat, to produce alterations in P450-mediated AA metabolism; this seems to be dependent on the specific fibrate member, dose and duration of treatment (Fig. 1.13) (Lozada and Dujovne 1994, Muller, Theuer et al. 2004, Althurwi, Elshenawy et al. 2014, Makia and Goldstein 2016). In our lab, an increase in the tissue level of 19-HETE was achieved by utilizing the previously-reported inductive effect of isoniazid on CYP2E1 (Fig. 1.13) (Palakodety, Clejan et al. 1988, Elkhatali, El-Sherbeni et al. 2015). Also, there is some evidence for

rosiglitazone to be used as CYP2J2 inducer (Evangelista, Kaspera et al. 2013). FDA recommends certain drugs that can safely, selectively and effectively induce P450 enzymes (Table 1.6) (Huang, Temple et al. 2007, Food-and-Drug-Administration 2014). These probe-drugs are routinely used to perform drug metabolism and drug interaction studies for new drugs (Huang, Temple et al. 2007, Food-and-Drug-Administration 2014).

**Table 1.6. FDA Recommended *In Vivo* and *In Vitro* Inducers of Specific P450 Enzymes (Huang, Temple et al. 2007, Food-and-Drug-Administration 2014).**

Pharmacological agent	Selectivity	Safe use	Effectiveness
<b>Avasimibe</b>	CYP3A	<i>In vivo</i>	Increase $Cl_{int}$ by >500%
<b>Carbamazepine</b>	CYP2C9	<i>In vivo</i>	Increase $Cl_{int}$ by 200-500%
	CYP3A	<i>In vivo</i>	Increase $Cl_{int}$ by >500%
<b>Efavirenz</b>	CYP2B6	<i>In vivo</i>	Increase $Cl_{int}$ by 200-500%
<b>Lansoprazole</b>	CYP1A2	<i>In vitro</i>	10-fold increase at 10 $\mu$ M
<b>Montelukast</b>	CYP1A2	<i>In vivo</i>	Increase $Cl_{int}$ by 200-500%
<b>Omeprazole</b>	CYP1A2	<i>In vitro</i>	14-24-fold increase at 25-100 $\mu$ M
<b>Phenobarbital</b>	CYP2B6	<i>In vitro</i>	5-10-fold increase at 500-1000 $\mu$ M
<b>Phenytoin</b>	CYP1A2	<i>In vivo</i>	Increase $Cl_{int}$ by 200-500%
	CYP3A	<i>In vivo</i>	Increase $Cl_{int}$ by >500%
	CYP2B6	<i>In vivo</i>	Increase $Cl_{int}$ by 200-500%
	CYP2C8	<i>In vivo</i>	Increase $Cl_{int}$ by 200-500%
<b>Rifampin</b>	CYP2C8	<i>In vitro</i>	2-4-fold increase at 10 $\mu$ M
	CYP2C9	<i>In vivo</i>	Increase $Cl_{int}$ by 200-500%
	CYP2C9	<i>In vitro</i>	3.7-fold increase at 10 $\mu$ M
	CYP2C19	<i>In vivo</i>	Increase $Cl_{int}$ by 200-500%
	CYP2C19	<i>In vitro</i>	20-fold increase at 10 $\mu$ M
	CYP3A	<i>In vivo</i>	Increase $Cl_{int}$ by >500%
	CYP3A4	<i>In vitro</i>	24-31-fold increase at 10-50 $\mu$ M

#### 4.3. Receptor Agonists and Antagonists

Aside of modulating P450 or sEH enzymes, some researchers preferred to pursue a third avenue, which is to directly target the receptors of P450-derived AA metabolites using receptor agonists and antagonists. As with enzyme modulators, EETs and 20-HETEs have garnered most of the attention, and their agonists and antagonists have been

developed, despite their receptors still being unidentified. In fact, one evidence that EETs and 20-HETE receptors exist is how their structural analogues can block their biological effects (Roman 2002). Further evidences include the stereospecific effect of 11,12-EET on rat renal arterioles, as well as the necessity of intact cell membrane to exert an effect of 20-HETE on K<sup>+</sup> channels (Roman 2002). It was found that protecting the carboxyl group in the 14,15-EET by forming an imide with different sulfonamides: methylsulfonamide, phenyliodosulfonamide, biotinsulfonamide and benzoyldihydrocinnamide-sulfonamide, gives more stable analogues of 14,15-EET, such as the 14,15-EET-mSA (Fig. 1.14) (Yang, Holmes et al. 2007). Another way that has also been shown to improve EETs stability is by incorporating the epoxide group in the middle of the carbon chain of EETs to produce their ether analogue (Imig, Elmarakby et al. 2010). This group of EET agonists includes the 11,12-ether-EET-8-ZE and its amide derivative with aspartate, 11,12-ether-EET-5-ZE and NUDSA (Fig. 1.14) (Imig, Elmarakby et al. 2010). Most recently, a urea group was inserted in EETs structure to yield EETs agonists that simultaneously exhibit sEH inhibition activity, such as EET-Z (Fig. 1.14) (Hye Khan, Pavlov et al. 2014). On the other hand, partial saturation of 14,15-EET giving 14,15-epoxyeicosa-5-enoic acid, and its methylsulfonylimide derivative, which have been shown to behave as antagonists to 14,15-EET (Fig. 1.14) (Gauthier, Deeter et al. 2002). For 20-HETE, the agonists and antagonists are strikingly similar and all based on partial saturation of the 20-HETE. In this context, it has been previously reported that saturating the 8- and 11-double bonds of 20-HETE provides for a 20-HETE agonist, whereas, replacing the four bonds at C5, C8 C11 and C14 of the 20-HETE with 2 cis-double bonds at C6 and C15 gives a 20-HETE antagonist (Fig. 1.14) (Alonso-Galicia, Falck et al. 1999). The former is the 20-hydroxyeicosa-5,14-dienoic acid, and the latter is the 20-hydroxyeicosa-6,15-dienoic acid (Fig. 1.14) (Alonso-Galicia, Falck et al. 1999).

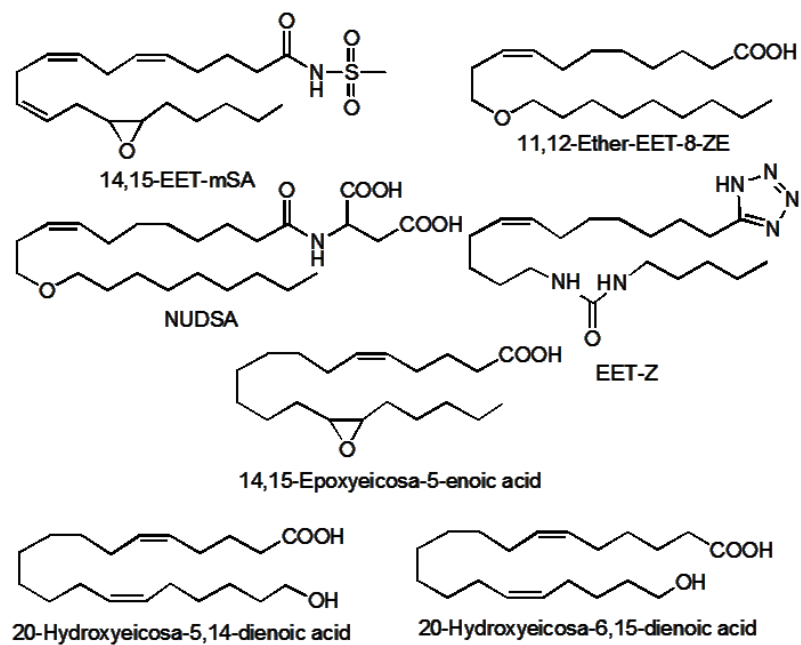


**Figure 1.14. The Chemical Structures of Representatives of EETs and 20-HETE stable analogues and antagonists.**

## **5. Cardiac Hypertrophy**

### **5.1. The Burden of Cardiac Hypertrophy**

Cardiac hypertrophy is the increase in the heart mass, due to the increase in the size, and not the number, of cardiomyocytes (Frey, Katus et al. 2004). There is no available statistical data about the incidence and prevalence of cardiac hypertrophy, as in most cases, cardiac hypertrophy does not cause substantial symptoms of its own. This makes cardiac hypertrophy hard to be diagnosed (Katholi and Couri 2011). It is true that cardiac hypertrophy is not a disease by itself, however, cardiac hypertrophy is a major risk factor for fatal heart diseases, most importantly heart failure (Frey and Olson 2003, Katholi and Couri 2011, Writing Group, Mozaffarian et al. 2016). Heart failure is a serious health problem, as there are more than 5.7 million heart failure patients in the US as estimated in 2012, which represents 2.2% of the US population, and the number is expected to rise to about 9.6 million by 2030 (Roger, Go et al. 2012, Writing Group, Mozaffarian et al. 2016). There are about one million new cases every year, and in Canada the number of deaths due to heart failure was 4,430 deaths per 100,000 population in 2004 (Public Health Agency of Canada. 2009), and the annual mortality rate associated with heart failure is 65,000 cases in the US (Writing Group, Mozaffarian et al. 2016). The health problem of heart failure costed US \$30.7 billion in 2012 and has risen due to the growth of the geriatric subpopulation and the increase in life expectancy (Writing Group, Mozaffarian et al. 2016). Also, in Canada, it was estimated that hospital admission for heart failure costed \$482 million in 2013, and the costs is expected to rise to \$722 million in 2030 (Tran, Ohinmaa et al. 2016). Therefore, better understanding of cardiac hypertrophy may lead to better diagnosis and treatment of heart failure.

## 5.2. Cardiac Remodeling

Cardiac hypertrophy begins as an adaptive response to a hemodynamic overload (Nagata, Liao et al. 1998, Frey and Olson 2003). The hemodynamic overload can be physiological, as in case of vigorous exercises, or pathological, as in case of hypertension, aortic stenosis, severe obesity and anemia (Lorell and Carabello 2000, McMullen and Jennings 2007). Cardiac hypertrophy initially meets the additional needs of the hemodynamic overload; however, prolonged hypertrophy is catastrophic, resulting in progressive deterioration in heart function that eventually leads to heart failure (Sasayama, Kihara et al. 1999, Frey and Olson 2003). The process of transforming a normal to hypertrophic heart is called cardiac remodeling, which involves changes at the biochemical, cellular and anatomical levels (Kehat and Molkentin 2010). Basically, cardiomyocytes undergo two changes at the biochemical level; 1) An increase in the number of their basic contractile units, sarcomeres, in series or parallel, leading to increase in the length or thickness of myofibrils, respectively (Kehat and Molkentin 2010), and 2) A reactivation of fetal gene program shifting energy production from fatty acid oxidation to glycolysis in addition to an increase in the expression of what are collectively called hypertrophic markers, such as atrial and brain natriuretic peptide (ANP and BNP, respectively) and  $\beta$ -myosin heavy chain ( $\beta$ -MHC) at the expense of  $\alpha$ -myosin heavy chain ( $\alpha$ -MHC) (Taegtmeyer, Sen et al. 2010). At the cellular level, cardiomyocytes are increased in their length or diameter to accommodate the bigger myofibrils, which is associated with the digestion and rebuilding of the extracellular matrix with the activation of fibrosis (Kehat and Molkentin 2010, Fan, Takawale et al. 2012). Anatomically, the heart becomes bigger (termed cardiomegaly). This occurs either by the increase in heart wall thickness and a decrease in heart chamber size, or by the increase in heart chamber sizes without affecting, or sometimes decreasing, heart wall thickness, (termed concentric or

eccentric cardiac hypertrophy, respectively) (Mihl, Dassen et al. 2008, Kehat and Molkentin 2010). Concentric cardiac hypertrophy is to cope with pressure overload, while, eccentric cardiac hypertrophy is to cope with volume overload (Frey and Olson 2003, Frey, Katus et al. 2004, Mihl, Dassen et al. 2008, Kehat and Molkentin 2010). Initially, heart function is maintained or even enhanced, and therefore it is called compensated cardiac hypertrophy; however, heart function is, then, slowly deteriorated to become decompensated cardiac hypertrophy, eventually leading to heart failure (Frey and Olson 2003, Frey, Katus et al. 2004).

### **5.3. Cytochrome P450-Mediated Arachidonic Acid Metabolism and Cardiac Hypertrophy**

The link between cardiac hypertrophy and P450-mediated AA metabolism was first established when the activation of phospholipase A<sub>2</sub> and P450 pathways was noticed to occur in cardiomyocytes exposed to mechanical stress, normally enough to induce cardiac hypertrophy (Sadoshima and Izumo 1993). More evidence was provided when Thum et al reported differences in cardiac P450 enzyme expression between normal and hypertension-induced hypertrophied rat hearts (Thum and Borlak 2002). Our laboratory was the first to report that the alteration in cardiac P450 expression is accompanied with an aberration in cardiac EETs and 20-HETE formation during isoproterenol-induced cardiac hypertrophy (Zordoky, Aboutabl et al. 2008). This observation was confirmed using several other models of cardiac hypertrophy and toxicity, viz., doxorubicin-, 3-methylcholanthrene-, benzo(a)pyrene-, arsenic-, pressure-overload-, and angiotensin II-induced cardiac hypertrophy (Aboutabl, Zordoky et al. 2009, Zordoky, Anwar-Mohamed et al. 2010, Alsaad, Zordoky et al. 2012, Anwar-Mohamed, El-Sherbeni et al. 2012). Also, the time course of the alterations in cardiac P450 expression by isoproterenol insult with the development of cardiac hypertrophy was then reported (Althurwi, Maayah et al. 2015).

Generally, in these studies, the cardiac EETs were decreased, while the cardiac 20-HETE and DHETs were increased. Interestingly, counterbalancing these alterations by sEH inhibition using 1-(1-methanesulfonyl-piperidin-4-yl)-3-(4-trifluoromethoxy-phenyl)-urea (TUPS), P450-AA epoxygenases induction by fenofibrate, or 20-HETE-formation inhibition by HET0016 were efficient interventions to prevent/control cardiac hypertrophy in rats (Aboutabl, Zordoky et al. 2011, Althurwi, Elshenawy et al. 2014). After identifying subterminal and mid-chain HETEs to be altered during cardiac hypertrophy, the effects of these AA metabolites have been investigated on cardiac hypertrophy, similar to EETs and 20-HETE. It has been found that exposing cardiomyocytes to mid-chain HETEs induces cellular hypertrophic markers (Maayah, Abdelhamid et al. 2015, Maayah and El-Kadi 2016). On the other hand, blocking the formation of mid-chain HETEs controlled cardiac hypertrophy induced in rats (Maayah, Althurwi et al. 2016). For subterminal HETEs, however, 19-HETE proved to have a cardioprotective effect against angiotensin II-induced cardiac hypertrophy both *in vivo* and *in vitro* in rats (Elkhatali, El-Sherbeni et al. 2015).

Accordingly, P450-derived AA metabolites have been shown to directly contribute to the pathogenesis and progression of cardiac hypertrophy, most probably by altering inflammation and fibrosis in the heart. In fact, inflammation and fibrosis represent key events in cardiac hypertrophy. Evidently, the expression of inflammatory markers has been shown to precede any manifestation of cardiac hypertrophy (Smeets, Teunissen et al. 2008). Also, several reports demonstrated the association between the magnitude of the expression of inflammatory markers and the deterioration of heart function (Bayes-Genis 2007, Frustaci, Verardo et al. 2007, Masiha, Sundstrom et al. 2013). Furthermore, the induction and prevention of cardiac hypertrophy were reported to be achievable by altering inflammatory mediators *in vivo* and *in vitro* (Bozkurt, Kribbs et al. 1998, Ha, Li et al. 2005, Smeets, Teunissen et al. 2008, Miguel-Carrasco, Zambrano et al. 2010). In contrast to inflammation,

fibrosis is not associated with the initial stages of cardiac hypertrophy, but is involved in the deterioration of heart function (Conrad, Brooks et al. 1995, Nicoletti and Michel 1999). The stiffness of the heart muscles due to fibrosis leads to an increase in the relative workload per myocyte, resulting in further damage (Nicoletti and Michel 1999). Thereby, progressive deterioration in the heart function may be occurring during the transition from compensated to decompensated cardiac hypertrophy, and eventually leads to heart failure. Furthermore, it has been reported that mid-chain HETEs can activate mitogen-activated protein kinases and nuclear factor kappa B pathways (Maayah, Abdelhamid et al. 2015, Maayah and El-Kadi 2016).

## **6. Rationale, Hypotheses and Objectives**

### **6.1. Rationale**

Cardiac hypertrophy is a major risk factor for several heart diseases, notably heart failure and sudden death. The prevention and control of cardiac hypertrophy may help to reduce the mortality and morbidity from cardiovascular causes, as well as to diminish health care costs.

P450-derived AA metabolites are present in measurable levels in cardiac tissue. These metabolites have been reported to impact inflammation, fibrosis and angiogenesis, which are important aspects in cardiac hypertrophy and heart failure (Oka, Akazawa et al. 2014). Increasing the cardioprotective P450-derived AA metabolites and decreasing the cardiotoxic P450-derived AA metabolites in the heart could provide promising interventions for the prevention and control of cardiac hypertrophy. In order to do so, critical points in the cascade of P450-mediated AA metabolism need to be identified by thoroughly studying the aberration in P450-mediated AA metabolism during the pathological incidence; this is achievable by finding the major players in P450-mediated AA metabolism at physiological conditions, as well as during the pathological incidence.

Because the central role of P450 enzymes in xenobiotic metabolism has long been recognized and extensively studied, several clinically-approved chemical molecules have been identified to affect xenobiotic metabolism through modulating P450 enzymes levels and activities. However, little is known about the effect of these modulators of P450-mediated xenobiotic metabolism on P450-mediated AA metabolism, and the consequent alteration in the cardiac levels of P450-derived AA metabolites. Using this approach of repurposing clinically-approved P450 modulators can identify new agents that are easily

introducible to clinical trials, sparing challenging problems in drug development, such as determination of drug tolerability and the optimization of drug dosing.

## **6.2. Hypotheses**

6.2.1. Different rat and human organs effectively metabolise AA to different regioisomers of epoxy- and hydroxy-AA metabolites.

6.2.2. Small group of P450 enzymes dominate the AA metabolism in rat and human organs, and the dominating P450 enzymes are different across organs.

6.2.3. Pressure-overload-induced cardiac hypertrophy is associated with alterations in the P450-mediated AA metabolism in the heart.

6.2.4. Alterations in AA metabolism associated with cardiac hypertrophy are due to alterations in the expression of certain P450 enzymes in the heart.

6.2.5. P450-derived AA metabolites are key regulators in the onset and progression of cardiac hypertrophy; EETs and subterminal HETEs are cytoprotective, whereas, mid-chain and 20-HETEs are cytotoxic.

6.2.6. Selective and effective regulation of the tissue levels of P450-derived AA metabolites is achievable by the utilization of specific P450 inhibitors.

## **6.3. Objectives**

6.3.1. To develop and validate a liquid chromatography-mass spectrometry method for the simultaneous determination of the P450-derived AA metabolites.

6.3.2. To determine the metabolic and kinetic profiles of P450-mediated AA metabolism in rat heart, lungs, kidneys and liver.

6.3.3. To determine the differential tissue expression of P450 in rat heart, lungs, kidneys and liver.

6.3.4. To determine the AA-metabolizing activity and metabolic and kinetic profiles of individual rat recombinant P450 enzymes.

6.3.5. To determine the contribution of different P450 enzymes to P450-mediated AA metabolism in rat heart, lungs, kidneys and liver.

6.3.6. To determine the AA-metabolizing activity and metabolic profile of human liver and kidney microsomes, as well as individual human recombinant P450 enzymes.

6.3.7. To determine the alterations in cardiac levels, as well as the formation and degradation rates of P450-derived AA metabolites associated with pressure overload-induced cardiac hypertrophy in rats.

6.3.8. To determine P450 enzymes involved in the alterations in P450-mediated AA metabolism associated with pressure overload-induced cardiac hypertrophy in rats.

6.3.9. To identify clinically-approved drugs and their dosage that would significantly and selectively modulate P450-mediated AA metabolism in humans.

## **CHAPTER 2: MATERIALS AND METHODS**

## 1. Chemicals and Materials

Butylated hydroxytoluene, formic acid, NADPH, triethylamine, sucrose, camphorsulfonic acid and ethylenediaminetetraacetic acid were purchased from Sigma-Aldrich Chemical Co. (St. Louis, MO). High performance liquid chromatography (HPLC) grade acetonitrile, methanol, isopropanol, water and ethyl acetate were purchased from EM Scientific (Gibbstawn, NJ). Acrylamide, *N,N'*-bis-methylene-acrylamide, ammonium persulphate,  $\beta$ -mercaptoethanol, glycine, nitrocellulose membrane (0.45  $\mu$ m) and TEMED were purchased from Bio-Rad Laboratories (Hercules, CA, USA). Chemiluminescence Western blotting detection reagents were purchased from GE Healthcare Life Sciences, Piscataway, NJ, USA. Oasis HLB (30 mg, 30  $\mu$ m) cartridges were purchased from Waters Corporation (Milford, MA, USA). P450 enzymes modulators: 3-methylcholanthrene (3-MC),  $\alpha$ -naphthoflavone ( $\alpha$ -NF), resveratrol (Res), fluconazole (Flu), ticlopidine (Tic), sertraline (Ser) and danazol (Dan) were purchased from Sigma-Aldrich Chemical Co. (St. Louis, MO). Propylthiouracil (PTU), MS-PPOH and HET0016, were purchased from Cayman Chemical (Ann Arbor, MI). Peroxide-free AA and AA metabolites standards: 5,6-, 8,9-, 11,12- and 14,15-EETs, 5,6-, 8,9-, 11,12- and 14,15-DHETs, 5-, 8-, 9-, 11-, 12-, 15-, 16-, 17-, 18-, 19- and 20-HETEs, and 12-hydroperoxyeicosatetraenoic acid (12-HPETE) as well as internal standards (AA-D8, 14,15-EET-D11 and 15-HETE-D8) were purchased from Cayman Chemical (Ann Arbor, MI). Internal standard, 4-hydroxybenzophenone, was purchased from Sigma-Aldrich Chemical Co. (St. Louis, MO). 8-hydroxy-11,12-epoxyeicosatrienoic acid (hepoxilin A3) was purchased from Santa Cruz Biotechnology, Inc. (Santa Cruz, CA).

Recombinant enzymes: Rat CYP1A1-, CYP1A2-, CYP2A1-, CYP2B1-, CYP2C6-, CYP2C11-, CYP2C13-, CYP2D1-, CYP2E1- and CYP3A1-containing cell microsomes supplemented with NADPH-P450 reductase (Supersomes), as well as human CYP1A1-, CYP1A2-, CYP1B1-, CYP2B6-, CYP2C8-, CYP2C9, CYP2C18-, CYP2C19-, CYP2E1-,

CYP2J2-, CYP3A4-, CYP4A11-, CYP4F2-, CYP4F3A-, CYP4F3B- and CYP4F12-containing cell microsomes supplemented with NADPH-P450 reductase (Supersomes) were obtained from Gentest (Woburn, MA), whereas cyb5 and NADPH-P450 reductase were from Oxford Biomedical Research (Oxford, MI).

Primary rabbit anti-rat CYP1A1 polyclonal antibody (cat #ab79819), rabbit anti-rat CYP1B1 polyclonal antibody (cat #ab78044), rabbit anti-rat CYP2C11 polyclonal antibody (cat #ab3571), rabbit anti-rat CYP2C23 polyclonal antibody (cat #ab53944), and rabbit anti-human CYP4F2 polyclonal antibody (cat #ab125399) were purchased from Abcam (Cambridge, UK). Primary rabbit anti-human/rat CYP2Js polyclonal antibody was a generous gift from Dr. Darryl Zeldin (National Institute of Environmental Health Sciences, National Institutes of Health, Research Triangle Park, NC). Primary mouse anti-rat CYP2Bs monoclonal antibody (cat #sc-53244), goat anti-rat CYP2E1 polyclonal antibody (cat #sc-26834), mouse anti-rat CYP4As monoclonal antibody (cat #sc-271983), goat anti-rat glyceraldehyde-3-phosphate dehydrogenase (GAPDH) monoclonal antibody (cat #sc-47724) and rabbit anti-rat actin polyclonal antibody (cat #sc-1616-R) were purchased from Santa Cruz Biotechnology, Inc. (Santa Cruz, CA). Secondary goat anti-rabbit (cat #sc-2004), goat anti-mouse (cat #sc-2031) and donkey anti-goat (cat #sc-2020) were purchased from Santa Cruz Biotechnology, Inc. (Santa Cruz, CA). Other chemicals were purchased from Fisher Scientific Co. (Toronto, ON, Canada).

Pooled human liver and kidney microsomes were obtained from BioreclamationIVT (Baltimore, MD). For liver microsomes, it was pooled from liver tissue of 10 non-smoker donors, whose age and weight mean  $\pm$  SD were  $53.4 \pm 22.5$  year and  $98 \pm 23.5$  kg, respectively. For kidney microsomes, it was pooled from kidney tissues of 3 male donors, whose age and weight mean  $\pm$  SD were  $40.3 \pm 17$  year and  $93.5 \pm 18.2$  kg, respectively.

## 2. Methods

### 2.1. Analysis of Cytochrome P450-Derived Arachidonic Acid Metabolites

AA and P450-derived AA metabolites were analyzed using liquid chromatography-electrospray ionization-mass spectrometry (LC-ESI-MS) (Waters Micromass ZQ 4000 spectrometer). Multiple chromatographic conditions were applied to allow the separation of the targeted compounds:

To determine the kinetic and metabolic profiles of P450-mediated AA metabolism by microsomes separated from untreated rats, a previously described method to simultaneously measure EETs, DHETs and 19- and 20-HETEs was adopted (Powell, Wolf et al. 1998, Nithipatikom, Grall et al. 2001). These AA metabolites were separated on reverse phase C18 column (Kromasil, 250 × 2.1 mm) using the mobile phase of water/acetonitrile mixture with 0.005% acetic acid. The mobile phase was delivered using a linear gradient method at a flow rate of 0.2 ml/min as follows: 60% to 80% acetonitrile in 30 min, 80% to 100% acetonitrile in 5 min, and 100% for 5 min. The internal standard was 4-hydroxybenzophenone. The mass spectrometer was run under negative ionization mode with selected ion monitoring. EETs and HETEs were monitored at  $m/z=319$ , DHETs at  $m/z=337$  and the internal standard, 4-hydroxybenzophenone, at  $m/z=197$ . The nebulizer gas was acquired from an in house high purity nitrogen source. The temperature of the source was set at 150 °C, and the capillary and cone voltage were 3.51 kV and 25 V, respectively.

To determine the alterations in P450-mediated AA metabolism during cardiac hypertrophy in rats, a modified version of previously published methods was developed to measure 5-, 8-, 12- and 15-HETEs as well as 16-, 17- and 18-HETEs, in addition to EETs, DHETs and 19- and 20-HETEs (Powell, Wolf et al. 1998, Roy, Joshua et al. 2005,

Blewett, Varma et al. 2008). Similarly, the mass spectrometer was run under negative ionization mode with selected ion monitoring. The nebulizer gas was acquired from an in house high purity nitrogen source. The temperature of the source was set at 150 °C, and the capillary and cone voltage were 3.51 kV and 25 V, respectively. The samples were separated on reverse phase C18 column (Kromasil, 250 × 2.1 mm) at 30°C. The mobile phase consisted of water/acetonitrile with 0.005% acetic acid and delivered using a linear gradient method at a flow rate of 200 µL/min, as follows: 50% to 80% acetonitrile in 35 min, 80% to 100% acetonitrile in 5 min, and 100% for 6 min. EETs and HETEs were monitored at  $m/z=319$ , DHETs at  $m/z=337$  and the internal standards, 15-HETE-D8 and 14,15-EET-D11, were monitored at  $m/z = 327$  and 330, respectively.

To determine the kinetic and metabolic profiles of P450-mediated AA metabolism by rat and human recombinant microsomes, a new method was developed that can simultaneously measure all P450-derived AA metabolites, the four EETs, 5,6-, 8,9-, 11,12- and 14,15-EETs, the six mid-chain HETEs, 5-, 8-, 9-, 11-, 12- and 15-HETEs, and the five terminal/subterminal HETEs, 16-, 17-, 18-, 19- and 20-HETEs. This was achieved by a gradient separation on a reverse phase C18 column (Alltima HP, 250 × 2.1 mm) at 35°C. Mobile phase A consisted of water with 0.01% formic acid and 0.005% triethylamine (v/v), whereas mobile phase B consisted of 8% methanol, 8% isopropanol and 84% acetonitrile with 0.01% formic acid and 0.005% triethylamine (v/v). Samples were subjected to linear gradient elution at a flow rate of 200 µL/min, as follows: 60 to 48% in 4 min, held isocratically at 48% for 24 min, 48 to 35% in 11 min, 35 to 0% in 11 min, and finally held isocratically at 0% for 7 min of mobile phase A. The internal standards were AA-D8, 15-HETE-D8 and 14,15-EET-D11. The mass spectrometer was run under negative ionization mode with selected ion monitoring; AA was monitored at  $m/z=303$ , EETs and HETEs at  $m/z=319$  and the internal standards at  $m/z = 311$ , 327 and 330 for AA-D8, 15-HETE-D8

and 14,15-EET-D11, respectively. The nebulizer gas was acquired from an in house high purity nitrogen source. The temperature of the source was set at 150 °C, and the capillary and cone voltage were 3.51 kV and 25 V, respectively.

## 2.2. Method Validation

Calibration samples of AA and its metabolites were prepared in acetonitrile containing 0.014, 0.069, 0.14, 0.69, 1.37, 6.9, 13.7, 24.4, 137 and 1370 µg/ml of AA or 0.0045, 0.0225, 0.045, 0.09, 0.225, 0.45, 0.9, 2.25, 3, 4.5 µg/ml of each of the 15 AA metabolites. Calibration curves constructed on three separate days were analyzed to evaluate the linearity. Accuracy and precision was determined using quality control samples at 4 levels in the range of the expected concentrations in the test samples, 0.14, 1.37, 13.7 and 68.5 µg/ml for AA and 0.005, 0.045, 0.45 and 4.5 µg/ml for AA metabolites. Quality control samples were prepared in 100 mM potassium phosphate buffer, pH 7.4, containing 0.5 mg/mL of heat-deactivated liver microsomes (60 µL final volume). After the addition of internal standards (AA-D8, 14,15-EET-D11 and 15-HETE-D8), samples were double extracted with 1 ml ethyl acetate; thereafter the organic extracts were combined, evaporated to dryness and reconstituted in 60 µL acetonitrile containing 0.01% formic acid. Each concentration had a replicate of three samples that were injected in the same day to determine the intraday accuracy and precision. The assay was also repeated in three different days to determine the interday accuracy and precision. Accuracy was determined by calculating the concentration of each quality control sample based on standard curves utilizing analyte to internal standard peak area (response ratio). Bias was assessed by calculating percent error ( $\%error = (C_{calculated} - C_{nominal}) / C_{nominal} \times 100$ ) for all injections at each level analyzed. Precision was assessed by calculating the coefficient of variation ( $CV\% = SD / Mean \times 100$ ) for all injections at each level analyzed.

### 2.3. Animals and Treatment

All animals were maintained and used in accordance with the animal protocol approved by the University of Alberta Health Sciences Animal Policy and Welfare Committee, Edmonton, Alberta, Canada. All animals were allowed free access to food and water.

Ten adult male SD rats (Charles River Canada, St. Constant, QC, Canada), with body weight ranging between 400-500 g were used as the source of organs needed afterwards for microsomal preparation. Animals were euthanized under isoflurane anesthesia. Hearts, lungs, kidneys, and livers were excised, washed in ice-cold potassium chloride (1.15%, w/v), and immediately frozen in liquid nitrogen and stored at  $-80^{\circ}\text{C}$ .

Eight adult male SD rats, with body weight ranging between 400-500 g, were used to determine the effect of 3-MC on CYP1As induction and the consequent alteration in the P450-mediated AA metabolism. A solution of 3-MC in corn oil (20 mg/mL) was prepared and used to inject 4 rats with 3-MC 20 mg/kg/day, ip, for 3 consecutive days. 4 weight matched rats received the same volume of corn oil, ip, served as the control group. In the fourth day, animals were euthanized under isoflurane anesthesia. Hearts, lungs, kidneys, and livers were excised, washed in ice-cold potassium chloride (1.15%, w/v), and immediately frozen in liquid nitrogen and stored at  $-80^{\circ}\text{C}$ .

For the descending aortic constriction (DAC) study, nine male SD weighing 150-200 g were subjected to the descending aortic constriction for induction of cardiac hypertrophy as described previously (Juric, Wojciechowski et al. 2007). Animals were anesthetized for surgery with isoflurane. The suprarenal abdominal aorta was exposed by a midline laparotomy. A blunt 21-gauge needle was used as a guide for tying off aorta by silk suture. Six sham-operated rats were subjected to the same procedure except for the

aortic constriction. The DAC procedure was externally performed by Mrs. Sandra Kelly at the small animal surgery core at the Cardiovascular Research Center, University of Alberta. After 5 weeks post-surgery, animals were euthanized under isoflurane anesthesia. Hearts and the right back legs were excised, washed in ice-cold potassium chloride (1.15%, w/v), and immediately frozen in liquid nitrogen and stored at  $-80^{\circ}\text{C}$ .

#### **2.4. Echocardiography**

In the DAC study, the development of cardiac hypertrophy was monitored using echocardiography externally performed by Mrs. Donna Beker at the echo core at the Cardiovascular Research Center, University of Alberta. At 5 weeks post-surgery, sham (n=6) and DAC (n=9) animals were weighed and mildly anesthetized using 1.5% isoflurane. Subsequently, transthoracic echocardiography was performed using a Vevo 770 Imaging System (VisualSonics, Toronto, ON). Heart dimensions, namely the left ventricle posterior wall thickness (LVPW), interventricular septal wall thickness (IVS), and left ventricle volume (LVV) during diastole, as well as systolic and diastolic functions, namely the percentage of fractional shortening (%FS), percentage of ejection fraction (%EF), and Tei index, were determined. Dimension and function parameters were determined using M-mode measurements taken from parasternal long- and short-axis views at the midpapillary level. Tei index was calculated as the sum of the isovolumic relaxation and contraction time divided by the ejection time. Measurements were averaged from 3 to 6 cardiac cycles according to the American Society of Echocardiography, and subsequently analyzed using VisualSonics software version 3.0.0.

#### **2.5. Tissue Collection and Microsomal Preparation**

Animals were euthanized under isoflurane anesthesia. Hearts, lungs, kidneys, and livers were excised, immediately frozen in liquid nitrogen and stored at  $-80^{\circ}\text{C}$ . For

DAC study, the tibia was separated and its length was measured by micro-CT (SkyScan NV, Kontich, Belgium). Microsomal fractions from hearts, lungs, kidneys and livers of SD rats were separated by differential centrifugation of homogenized tissues as described previously (Barakat, El-Kadi et al. 2001). Briefly, organs were washed in ice-cold potassium chloride (1.15%, w/v). Subsequently, they were cut into pieces, and homogenized in ice-cold 0.25 M sucrose solution (17%, w/v). Thereafter, microsomal fractions were separated by differential ultracentrifugation, as the following: In the first centrifugation step, the samples were centrifuged at 1000 x g, 4°C, for 8 min, in order to separate and discard tissue debris. Then, the supernatants were then centrifuged at 23,000 x g, 1°C, for 10 min to get the S9 fractions (the supernatants) and the pellets were discarded. In the final step, the S9 fractions were centrifuged at 130,000 x g, 1°C, for 60 min to separate the microsomal fraction (pellets) from cytosolic fraction (supernatants). The separated microsomal fractions were washed in ice-cold potassium chloride (1.15%, w/v), and re-suspended in cold sucrose and stored at -80°C. For the preparation of pooled microsomal fractions, organ homogenates from the untreated rats were pooled together; while, for animals used in DAC study as well as the 3-MC studies, the organs from each rat was processed separately to prepare individual microsomal and cytosolic fractions. The microsomal and cytosolic protein concentration was determined by the Lowry method using bovine serum albumin as a standard (Lowry, Rosebrough et al. 1951).

## **2.6. RNA Extraction and cDNA Synthesis**

Total RNA from the frozen tissues was isolated using TRIzol reagent (Invitrogen) according to the manufacturer's instructions. Briefly, 2 mL of TRIzol reagent was added to 200 mg of tissue. Tissue homogenates were then collected into 1.5 ml Eppendorf tubes and mixed with 400 µl chloroform followed by centrifugation at 15,000 x g for 15 min at 4 °C. The aqueous upper phase which contains the RNA was then transferred to a fresh tube and

400 µl of isopropyl alcohol was added to each tube to precipitate the RNA by cooling the samples at -20 °C for at least 4 h. Following centrifugation at 15,000 x g for 10 min at 4 °C, the RNA pellet was washed once with 75% ethanol in ultrapure water (DNase/RNase-Free), and then dissolved in ultrapure water (DNase/RNase-Free). RNA was then quantified by measuring the absorbance at 260 nm, and RNA quality was determined by measuring the 260/280 ratio. Thereafter, first-strand cDNA synthesis was performed by using the High-Capacity cDNA reverse transcription kit (Applied Biosystems) according to the manufacturer's instructions. 1.5 µg of total RNA from each sample was added to a mix of 2.0 µl 10X RT buffer, 0.8 µl 25X dNTP mix (100 mM), 2.0 µl 10X RT random primers, 1.0 µl MultiScribe™ reverse transcriptase and 3.2 µl nuclease-free water. The final reaction mix was kept at 25°C for 10 min, heated to 37°C for 120 min, heated for 85°C for 5 seconds, and finally cooled to 4°C.

## **2.7. Quantification by Real Time-PCR**

Quantitative analysis of specific mRNA expression was performed by real time-PCR, by subjecting the resulting cDNA to PCR amplification using 96-well optical reaction plates in the ABI Prism 7500 System (Applied Biosystems). Each 25-µL reaction mix contained 0.1 µL of 10 µM forward primer and 0.1 µL of 10 µM reverse primer, 12.5 µL of SYBR Green Universal Mastermix, 11.05 µL of nuclease-free water, and 1.25 µL of cDNA sample. The primers used in the current study were chosen from previously published studies (Muir, Chamberlain et al. 2001, Nakamura, Yoshimura et al. 2004, Zolk, Munzel et al. 2004, Sucharov, Dockstader et al. 2008, Althurwi, Tse et al. 2013) and are listed in Table 2.1. Thermocycling conditions were initiated at 95°C for 10 min, followed by 40 PCR cycles of denaturation at 95°C for 15 seconds, and annealing/extension at 60°C for 1 min. Dissociation curves were performed by the end of each cycle to confirm the specificity of the primers and the purity of the final PCR product. The real-time PCR data were analyzed

using comparative CT method, i.e. ( $\Delta\Delta CT$ ) method, as described in Applied Biosystems User Bulletin No.2 and explained further by Livak et al (Livak and Schmittgen 2001). The data are presented as the fold change in gene expression normalized to the endogenous reference gene, GAPDH and relative to a calibrator. The sham control was used as the calibrator when the change of gene expression by the treatment was studied.

**Table 2.1. Primers Sequences Used for Real-Time PCR Reactions.**

<b>Gene</b>	<b>Forward Primer</b>	<b>Reverse Primer</b>
<b>ANP</b>	GGAGCCTGCGAAGGTCAA	TATCTTCGGTACCGGAAGCTGT
<b>BNP</b>	CAGAAGCTGCTGGAGCTGATAAG	TGTAGGGCCTTGGTCCTTTG
<b><math>\alpha</math>-MHC</b>	ACAGAGTGCTTCGTGCCTGAT	CGAATTTCCGGAGGGTTCTGC
<b><math>\beta</math>-MHC</b>	CGCTCAGTCATGGCGGAT	GCCCCAAATGCAGCCAT
<b>EPHX2</b>	GATTCTCATCAAGTGGCTGAAGAC	GGACACGCCACTGGCTAAAT
<b>GAPDH</b>	CAAGGTCATCCATGACAACCTTTG	GGGCCATCCACAGTCTTCTG

## 2.8. Western Blot Analysis

Western blot analysis was performed using a previously described method (Gharavi and El-Kadi 2005). 20  $\mu$ g of microsomal preparations were separated by 10% sodium dodecyl sulfate-polyacrylamide gel, and then electrophoretically transferred to nitrocellulose membrane. Protein blots were then blocked overnight at 4°C in blocking solution containing 0.15 M sodium chloride, 3 mM potassium chloride, 25 mM Tris-base, 5% skim milk, 2% bovine serum albumin and 0.5% Tween-20. After blocking, the blots were incubated with the primary antibodies diluted in 0.15 M sodium chloride, 3 mM potassium chloride, 25 mM Tris-base and 0.1% Tween-20 as the following: rabbit anti-rat CYP1A1 (1:200), rabbit anti-rat CYP1B1 (1:1000), mouse anti-rat CYP2Bs (1:1000), rabbit anti-rat CYP2C11 (1:2000), rabbit anti-rat CYP2C23 (1:2000), rabbit anti-human/rat CYP2Js (1:500), goat anti-rat CYP2E1 (1:500), mouse anti-rat CYP4As (1:500), and rabbit anti-human CYP4F2 (1:1000); whereas, goat anti-rat GAPDH (1:200) and rabbit anti-rat actin (1:1000) antibodies were diluted in 0.15 M sodium chloride, 3 mM potassium

chloride, 25 mM Tris-base, 5% skim milk, 0.8% bovine serum albumin and 0.1% Tween-20. The blots were incubated with a primary antibody for a 2 h incubation period (24 h for CYP2B5 at 4°C). After incubation of the membrane with the primary antibody, rinsing was done for 3 times (5 min each) using washing buffer (0.15 M sodium chloride, 3 mM potassium chloride, 25 mM Tris-base and 0.1% Tween-20) to remove any residual antibodies. Thereafter, blots were incubated with a peroxidase-conjugated secondary antibody for 1 h at room temperature. Blots were stripped by incubating with stripping buffer (15% glycine [pH 2.2], 1% SDS, 1% Tween 20) for 2 times (10 min each), thereafter, washed and blocked as mentioned above, prior to reprobing. The bands were visualized using the enhanced chemiluminescence method according to the manufacturer's instructions (GE Healthcare Life Sciences, Piscataway, NJ, USA). The intensity of the protein bands were quantified, relative to the signals obtained for actin or GAPDH, using ImageJ software (National Institutes of Health, Bethesda, MD, <http://rsb.info.nih.gov/ij>).

## **2.9. The Extraction of Arachidonic Acid Metabolites from Heart Tissue**

Two hundred mg of heart tissue was homogenized on ice with 1 mL 100 mM potassium phosphate buffer (pH 7.4). The homogenates were centrifuged at 10,000 g for 15 min at 0°C. The separated supernatant was added to 1 mL of methanol containing the internal standards (15-HETE-D8 and 14,15-EET-D11), butylated hydroxytoluene and ethylenediaminetetraacetic acid. Samples were centrifuged again for 15 min at 10,000 g at 0°C. AA metabolites were extracted from the resultant supernatant by solid-phase cartridge (Oasis HLB). Conditioning and equilibration of solid-phase cartridge were performed with 1 mL of methanol, ethyl acetate, 0.2% formic acid (v/v), and 10% methanol, in sequence. After sample application, cartridges were washed by 1 mL of 0.2% formic acid (v/v), and 10% methanol in 0.2% formic acid (v/v), in sequence. Finally, AA metabolites were eluted by 1 mL of 1% formic acid in acetonitrile (v/v) and ethyl acetate,

in sequence. Thereafter, the samples were evaporated to dryness, reconstituted with 50  $\mu$ L acetonitrile and subjected to analysis. Epoxy-metabolites were measured as the sum of each EET and its corresponding DHET.

### **2.10. sEH Activity Assay**

sEH activity was measured using the previously published method by Morisseau and Hammock with modifications (Morisseau and Hammock 2007). The cytosolic fraction was diluted to 0.4 mg/mL with sodium phosphate buffer (76 mM, pH 7.4) supplemented with BSA (2.5 mg/mL) to final volume of incubates of 200  $\mu$ L. The assay was initiated by the addition of 14,15-EET (final concentration 2  $\mu$ g/ml), and the mixture was incubated at 37°C for 10 min. Thereafter, the reaction was terminated by the addition of 600  $\mu$ L ice cold acetonitrile followed by the internal standard, 14,15-EET-D11. Metabolites were extracted by 1 mL ethyl acetate twice and dried using speed vacuum (Savant, Farmingdale, NY). The P450-derived AA metabolites concentrations were measured by LC-ESI-MS, relative to standard curve. Three standard samples were prepared by spiking protein preparation with known amounts of tested compounds, as well as internal standards. Standard samples were subjected to the same extraction procedure as test samples to be analyzed at the beginning and at the end of the run. The concentrations of the 14,15-EET and its corresponding 14,15-DHET were determined from standard curves utilizing analyte to internal standard peak area (response ratio).

### **2.11. Measuring CYP1A1 and CYP1A2 Activity**

The O-dealkylation of 7-ethoxyresorufin (7-ER) or 7-methoxyresorufin (7-MR) by CYP1A1 or CYP1A2, respectively, was measured in incubation buffer consisting of 3 mM magnesium chloride hexahydrate in 100 mM potassium phosphate buffer (pH 7.4). In a total volume of 200  $\mu$ L, microsomal protein of rat heart (1 mg/mL), lungs (1 mg/mL),

kidneys (1 mg/mL) or liver (0.25 mg/mL) was incubated with 0, 10, 20, 40, 80, 160, 250 nM of  $\alpha$ -NF for 10 min on ice. Then, 0.4 nmole of 7-ER or 7-MR was added, followed by the addition of NADPH to initiate the reaction. Fluorescence associated with resorufin formation was measured every 2 min (excitation and emission wavelengths of 535 and 585 nm) for 30 min at 37°C using a BioTek Synergy H1 Hybrid Reader (BioTek Instruments, Inc., VT, USA). The initial rate of product formation in each well was determined by linear regression of fluorescence-time data.

## **2.12. Arachidonic Acid Metabolism**

Preliminary incubations were performed to ensure that the formation of AA metabolites was linear with respect to incubation time and protein content under assay conditions. AA was incubated in an incubation buffer composed of 3 mM magnesium chloride hexahydrate dissolved in 100 mM potassium phosphate buffer, pH 7.4. The P450-derived AA metabolite concentrations were measured by LC-ESI-MS, relative to standard curve. Three standard samples were prepared by spiking protein preparation with known amounts of tested compounds, as well as internal standards. Standard samples were subjected to the same extraction procedure as test samples to be analyzed at the beginning and at the end of the run. The concentrations of the AA metabolites were determined from standard curves utilizing analyte to internal standard peak area (response ratio).

### **2.12.1. Microsomal-Mediated AA Metabolism**

With respect to the determination of rat microsomal-mediated AA metabolism regioselectivity and kinetics, the total microsomal protein concentrations used were 1 mg/mL for heart and lungs, and 0.5 mg/mL for kidneys and liver. The total volume of microsomal incubates was 200  $\mu$ L of incubation buffer. AA was added at a final

concentration ranging between 16-922  $\mu\text{M}$  for heart and lungs and 16-182  $\mu\text{M}$  for kidneys and liver. For DAC study, a total rat heart microsomal protein concentration of 1 mg/mL was incubated with 50 or 100  $\mu\text{M}$  AA for 30 min. The total volume of microsomal incubates was 200  $\mu\text{L}$  of incubation buffer. All incubations were conducted at 37°C in a shaking water bath (90 rpm) after a 5-min pre-equilibration period. The reaction was initiated by the addition of the cofactor NADPH (final concentration 2 mM) and terminated by the addition of 600  $\mu\text{L}$  ice-cold acidified acetonitrile. AA metabolites were extracted twice by 1 mL ethyl acetate and dried using speed vacuum (Savant, Farmingdale, NY, USA), then reconstituted in 50-200  $\mu\text{L}$  acetonitrile. The microsomal incubations were performed without adding sEH inhibitor, since the inhibition of sEH may activate the other pathways of EETs degradation (Imig 2012). Therefore, EET formation rates were calculated based on the sum of each EET and its corresponding DHETs. All AA metabolites are stable in phosphate buffer except 5,6-EET, which has been reported to spontaneously transform to 5,6- $\delta$ -lactone. Therefore, the method of Fulton et al. (Fulton, Falck et al. 1998) was used to accurately measure 5,6-EET. Briefly, incubations were performed as aforementioned with 50  $\mu\text{M}$  AA, thereafter, 5,6-EET and 5,6- $\delta$ -lactone were transformed to the quite stable 5,6-DHET by camphorsulfonic acid and triethylamine, in sequence.

With respect to human microsomal-mediated AA-metabolism, AA (7.5, 75 and 750  $\mu\text{M}$ ) was incubated with 0.5 mg/mL of liver or kidney microsomes for 30 min in incubation buffer to a final volume of 300  $\mu\text{L}$ . After a 5-min pre-equilibration period, the reaction was initiated by the addition of the cofactor NADPH (final concentration 2 mM) and terminated by the addition of 600  $\mu\text{L}$  ice-cold acetonitrile containing 0.01% formic acid and 0.001% butylated hydroxytoluene. Incubations were conducted at 37°C in a shaking water bath (90 rpm). The incubation mixtures were double extracted with 1 ml ethyl

acetate; thereafter the organic extracts were combined, evaporated to dryness and reconstituted in 40  $\mu$ L acetonitrile containing 0.01% formic acid.

### **2.12.2. Recombinant Cytochrome P450-Mediated AA Metabolism**

With respect to rat recombinant P450 enzymes, P450-mediated AA metabolism was characterized in incubation mixture (200  $\mu$ L) containing incubation buffer, NADPH-P450 reductase, cyb5 (40 pmol), P450 and AA. AA (75  $\mu$ M) was incubated with 50 pmol/mL of CYP1A1, CYP1A2, CYP2C6, CYP2C11 for 15 min, or 50 pmol/mL CYP2C13 or 100 pmol/mL of CYP2A1, CYP2B1, CYP2D1, CYP2E1 or CYP3A1 was incubated with AA (75  $\mu$ M) for 25 min. For the kinetic experiments, AA concentrations varied from 15-320  $\mu$ M incubated for 15 min with 50 pmol/mL of CYP1A1, CYP1A2, CYP2C6 and CYP2C11. NADPH reductase or cyb5 alone did not mediate the formation of P450-derived AA metabolites. For human recombinant P450 enzymes, AA (75  $\mu$ M) was incubated with 50 pmol/mL of CYP2C19 or CYP4A11 for 15 min, 50 pmol/mL of CYP4F2, CYP4F3A, CYP4F3B or CYP4F12 for 20 min, 100 pmol/mL of CYP1A1 or CYP1A2 for 15 min, or 100 pmol/mL of CYP1B1, CYP2B6, CYP2C8, CYP2C9, CYP2C18, CYP2E1, CYP2J2 or CYP3A4 for 20 min in incubation buffer. cyb5 was added to AA-P450 incubates to achieve a molar ratio of 1:1 (final volume of 300  $\mu$ L) (Xu, Falck et al. 2004, Zhang, Im et al. 2007). NADPH reductase or cyb5 alone did not mediate the formation of P450-derived AA metabolites. After a 5-min pre-equilibration period, the reaction was initiated by the addition of the cofactor NADPH (final concentration 2 mM) and terminated by the addition of 600  $\mu$ L ice-cold acetonitrile containing 0.01% formic acid and 0.001% butylated hydroxytoluene. Incubations were conducted at 37°C in a shaking water bath (90 rpm). The incubation mixtures were double extracted with 1 ml ethyl acetate; thereafter the organic extracts were combined, evaporated to dryness and reconstituted in 40  $\mu$ L acetonitrile containing 0.01% formic acid. For DAC study, recombinant CYP1B1 (100

pmol/mL) was incubated with AA (100  $\mu$ M) and NADPH (2mM) for 10 min. Also, human recombinant CYP2J2 (100 pmol/mL), which is the ortholog of the commercially unavailable rat CYP2J3, was incubated with 12-HPETE (4  $\mu$ g/mL) for 10 min, with or without NADPH (2mM). Incubations were conducted at 37°C in a shaking water bath (90 rpm) after a 5-min pre-equilibration period, and AA metabolites were extracted as described above.

### **2.13. Chromatographic Purification and Structural Elucidation**

Incubates of CYP2J2 with 12-HPETE performed as described above, were resolved on a reverse phase C18 column (Alltima HP, 250  $\times$  2.1 mm) at 25 °C. The mobile phase consisted of acetonitrile:water:formic acid (55:45:0.003) at a flow rate of 0.3 mL/min. Detection was performed by UV at 210 nm. Column eluate corresponding to peaks of interest was collected for further analysis with MS. The source temperature was 150 °C, and cone voltage was 25 V.

### **2.14. Selective Chemical Inhibition of cytochrome P450-Mediated AA Metabolism**

In order to determine the contribution of CYP1As to AA metabolism, the effect of CYP1As inhibition on rat heart, lungs, kidneys and liver microsomal-mediated AA metabolism was studied. Chemical-inhibition by selective CYP1As inhibitor ( $\alpha$ -NF) was used. 100  $\mu$ g of microsomal protein was incubated with 0, 40 and 160 nM of  $\alpha$ -NF for 10 min on ice (all samples contained a fixed concentration of 0.1% dimethylsulfoxide). AA (75  $\mu$ M) was added, and the reaction was initiated by the addition of NADPH and terminated and extracted as described above. Similarly, to determine the effect of selective P450 inhibitors on AA metabolism mediated by human microsomes, AA (75  $\mu$ M) was incubated with human liver microsomes (150  $\mu$ g) in the absence or presence of different concentrations of each of the following selective P450 inhibitors:  $\alpha$ -NF (40 and

160 nM), Res (0.03-1000  $\mu$ M), MS-PPOH (5 and 50  $\mu$ M), Flu (0.1 to 375  $\mu$ M), Tic (10 and 100  $\mu$ M), Ser (30 and 300  $\mu$ M), Dan (20 and 200 nM), HET0016 (50 nM and 1  $\mu$ M) and PTU (0.1 and 1 mM). In P450 inhibition experiments, all samples contained a fixed concentration of 0.1% of dimethylsulfoxide, and inhibitors were incubated with recombinant enzymes or microsomes for 15 min on ice before the addition of AA. Also, the same experiment was repeated for CYP4A11, CYP4F2 or CYP4F3B in the presence of 0.01-1000  $\mu$ M Res. Background control samples containing the same corresponding incubation mixture but without NADPH were prepared. The reaction was initiated by the addition of NADPH and terminated and extracted as described above

### **2.15. Immunoinhibition of cytochrome P450-Mediated AA Metabolism**

The inhibitory effect of P450-specific antibodies on P450-mediated AA metabolism in heart, lung, kidney and liver microsomes was determined. 20  $\mu$ g of rabbit anti-rat CYP1A1, mouse anti-rat CYP2Bs or mouse anti-rat CYP4As antibodies were incubated with 30  $\mu$ g of heart, lung, kidney or liver microsomal protein; whereas, 9  $\mu$ g of rabbit anti-rat CYP2C11 and rabbit anti-rat CYP2C23 antibodies were incubated with 15  $\mu$ g of rat heart, lung, kidney or liver microsomal protein. Goat anti-rat GAPDH antibody was used as non-P450-specific antibody and was added in the same amount of the P450-specific antibodies and served as control incubates. The incubation was performed initially on ice for 30 min, then, AA was added to a concentration of 75  $\mu$ M for kidneys and liver and 100  $\mu$ M for heart and lungs and final volume was 50  $\mu$ L. The incubates were moved to 37°C shaking water bath (90 rpm), equilibrated for 10 min, and the reaction was initiated by the addition of NADPH. The incubation time was 30 min for kidneys and liver and 60 min for heart and lungs, and the reaction was terminated by the addition of acetonitrile. The incubation mixtures were double extracted with 1 ml ethyl acetate; thereafter the

organic extracts were combined, evaporated to dryness and reconstituted in 50  $\mu$ L of acetonitrile.

## 2.16. Selective Induction of CYP1As-Mediated AA Metabolism

CYP1As were induced in rats by treatment with 3-MC, 0.5 mg/mL of microsomal protein separated from 3-MC-treated and corn-oil-treated rat hearts, lungs, kidneys or livers was incubated with AA (75  $\mu$ M) for 30 min. Incubations were conducted at 37°C in a shaking water bath (90 rpm) after a 5-min pre-equilibration period. The reaction was initiated by the addition of the cofactor NADPH (final concentration 2 mM) and terminated by the addition of 600  $\mu$ L ice-cold acetonitrile containing 0.01% formic acid and 0.001% butylated hydroxytoluene and extracted as described above.

## 2.17. Data Fitting

To determine the enzyme kinetics of P450-mediated AA metabolism by rat heart, lung, kidney and liver microsomal preparations, the rate of AA metabolite formation versus AA concentration in each organ were fitted to three models of enzyme kinetics: one site saturation Michaelis-Menten-sigmoidal model (eq. 1), one site saturation + linear nonspecific component (eq. 2), and two site saturation Michaelis-Menten model (eq. 3). The nonlinear regressions were performed using SigmaPlot software, version 11.0.

$$\text{Rate of formation} = \frac{V_{max} \times [AA]^h}{K_m^h + [AA]^h} \dots\dots\dots(\text{eq. 1})$$

$$\text{Rate of formation} = \frac{V_{max} \times [AA]}{K_m + [AA]} + NS \times [AA] \dots\dots\dots(\text{eq. 2})$$

$$\text{Rate of formation} = \frac{V_{max1} \times [AA]}{K_{m1} + [AA]} + \frac{V_{max2} \times [AA]}{K_{m2} + [AA]} \dots\dots\dots(\text{eq. 3})$$

Where  $V_{max}$  is the maximal rate of formation,  $K_m$  is the affinity constant,  $[AA]$  is the concentration of AA,  $h$  is the shape factor of a value of “1” or other values to fit the data, and NS represents the nonspecific activity. In the two binding sites model, two  $K_m$  ( $K_{m1}$  and  $K_{m2}$ ) and two  $V_{max}$  ( $V_{max1}$  and  $V_{max2}$ ) were used. The optimal enzyme kinetics model was determined by the Akaike information criterion as a measure of the goodness of fit. The intrinsic clearance ( $Cl_{int}$ ) for P450-derived AA metabolite formation was calculated as  $V_{max}/K_m$ .

To determine the kinetics of P450-mediated AA metabolism by recombinant P450 enzymes, nonlinear regression was performed using GraphPad Prism (version 5.01; GraphPad Software, Inc., La Jolla, CA). The rate of AA metabolite formation versus AA concentration data were fitted to several models of enzyme kinetics: Michaelis-Menten model (eq. 4), and its modified version to include homotropic cooperativity, Hill equation (eq. 5), were used (Kramer and Tracy 2008). It is estimated that in about 20% of enzymatic reactions, enzyme activity is inhibited by the presence of excess substrate. Therefore, substrate inhibition models, Haldane’s equation (eq. 6), and its modified version to include homotropic cooperativity (eq. 7) were also used (LiCata and Allewell 1997, Kapelyukh, Paine et al. 2008, Reed, Lieb et al. 2010).

$$\text{Rate of formation} = \frac{V_{max} \times [AA]}{K_m + [AA]} \dots\dots\dots(\text{eq. 4})$$

$$\text{Rate of formation} = \frac{V_{max} \times [AA]^h}{K_m^h + [AA]^h} \dots\dots\dots(\text{eq. 5})$$

$$\text{Rate of formation} = \frac{V_{max} \times [AA]}{K_m + [AA] + \frac{[AA]^2}{K_{si}}} \dots\dots\dots(\text{eq. 6})$$

$$\text{Rate of formation} = \frac{V_{max} \times [AA]^h}{K_m^h + [AA]^h + \frac{[AA]^{2h}}{K_{si}^h}} \dots\dots\dots(\text{eq. 7})$$

Where  $V_{max}$  is the maximal rate of formation,  $K_m$  is the affinity constant,  $[AA]$  is the concentration of AA,  $h$  is Hill coefficient, and  $K_{si}$  is the inhibition constant. The optimal enzyme kinetics model was determined by the Akaike information criterion as a measure of the goodness of fit. The intrinsic clearance ( $Cl_{int}$ ) for P450-derived AA metabolite formation was calculated as  $V_{max}/K_m$ .

Furthermore, to characterize the inhibition kinetics of Res and Flu in human microsomes, inhibitor concentration required for 50% inhibition ( $IC_{50}$ ) and maximal inhibition ( $I_{max}$ ) were determined by Enzyme Kinetics module from GraphPad Prism (version 5.0; GraphPad software, San Diego, CA). The following equation was used:

$$\text{Residual activity} = \text{Bottom} + \frac{I_{max}}{1 + 10^{\frac{\text{Log}[I] - \text{Log}[IC_{50}]}{h}}} \dots\dots\dots(\text{eq. 8})$$

Where Bottom is the lowest residual P450-mediated AA metabolizing activity.

## 2.18. Monte Carlo Simulation

Monte Carlo simulation is a highly valued tool to bridge pharmacokinetic data with pharmacodynamic data, in order to make a prediction about the fraction of human

population that would attain the targeted biological response.(Ferro, Meletiadis et al. 2015, Siopi, Siafakas et al. 2015) Accordingly, we performed Monte Carlo simulations (10,000 subjects) to calculate the expected residual AA-metabolizing activity in 90% of the human population using a random number generation module from SigmaPlot, version 11 (Systat Software, San Jose, CA, USA). Log-normal distribution was used to describe the dispersion of human plasma concentrations, as well as the parameters of enzyme inhibition kinetics around the mean values; whereas uniform distribution was used with the ratios of hepatic tissue to plasma concentration. The following equation was stochastically solved by Monte Carlo method:

$$Residual\ activity = (100 - I_{max}) + \frac{I_{max}}{1 + 10^{Log[liver:plasma\ ratio.C_{max}] - Log[IC50]}}$$

## 2.19. Statistical analysis

Statistical analysis was performed by SigmaPlot software, version 11.0 or GraphPad Prism, version 5.01. Data are presented as mean  $\pm$  S.E.M for experimental data; whereas data are presented as mean  $\pm$  S.E.E. for data generated by fitting. Student t test or one-way analysis of variance followed by a Tukey's post hoc test was performed in all data sets. All results were considered statistically significant where  $p < 0.05$ . Spearman correlation coefficients (r) were used for evaluating the possible association between AA metabolite formation and P450 enzymes expression.

## **CHAPTER 3: RESULTS**

## **1. Determination of the Dominant Arachidonic Acid Cytochrome P450 Monooxygenases in Untreated Rat Heart, Lungs, Kidneys and Liver**

### **1.1. Protein Expression of Cytochrome P450 Enzymes in Rat Heart, Lungs, Kidneys and Liver**

The P450 protein expression in the heart, lungs, kidneys and liver was determined by Western blot analysis. The four organs expressed all of the investigated P450 enzymes, albeit at different levels. The protein expression profiles of the main P450 epoxygenase enzymes (CYP2Bs, CYP2C11, CYP2C23, and CYP2J3) and P450  $\omega$ -hydroxylase (CYP4As and CYP4Fs) were found to be organ specific. Figure 3.1 depicts this profile for the heart, lungs and kidneys compared to the liver. It is apparent that CYP2C11 and CYP2J3 were the main epoxygenases to be expressed in the heart in levels comparable to their levels in lungs and kidneys; on the other hand, CYP2BS, CYP2C11 and CYP2J3 were expressed in the lungs (Fig. 3.1). For the kidneys, CYP2BS was negligibly expressed compared to the liver or the lungs. Kidneys were the organ with the highest expression of CYP2J3 (Fig. 3.1). Also, CYP2C23 has a predominant expression in the kidneys compared to CYP2C11 (Fig. 3.1). The liver was found to be the organ with the highest expression of all the tested P450-AA epoxygenases, with the exception of CYP2J3; the expression level of CYP2J3 was higher in the heart and kidneys than in the liver (Fig. 3.1).

With respect to the P450 hydroxylase activity,  $\omega$ -hydroxylation of AA has been attributed to CYP4AS and CYP4Fs (Xu, Falck et al. 2004). We found that the protein levels of CYP4AS as well as CYP4Fs in the lungs were ~25% of their levels in the liver (Fig. 3.1). CYP4AS were highly expressed in the kidneys compared to the other organs (Fig. 3.1). CYP4Fs were the highest in the liver followed by the lungs and then the kidneys (Fig.

3.1). Regarding the heart, CYP4AS and CYP4Fs expression was significantly lower compared to other organs (Fig. 3.1).

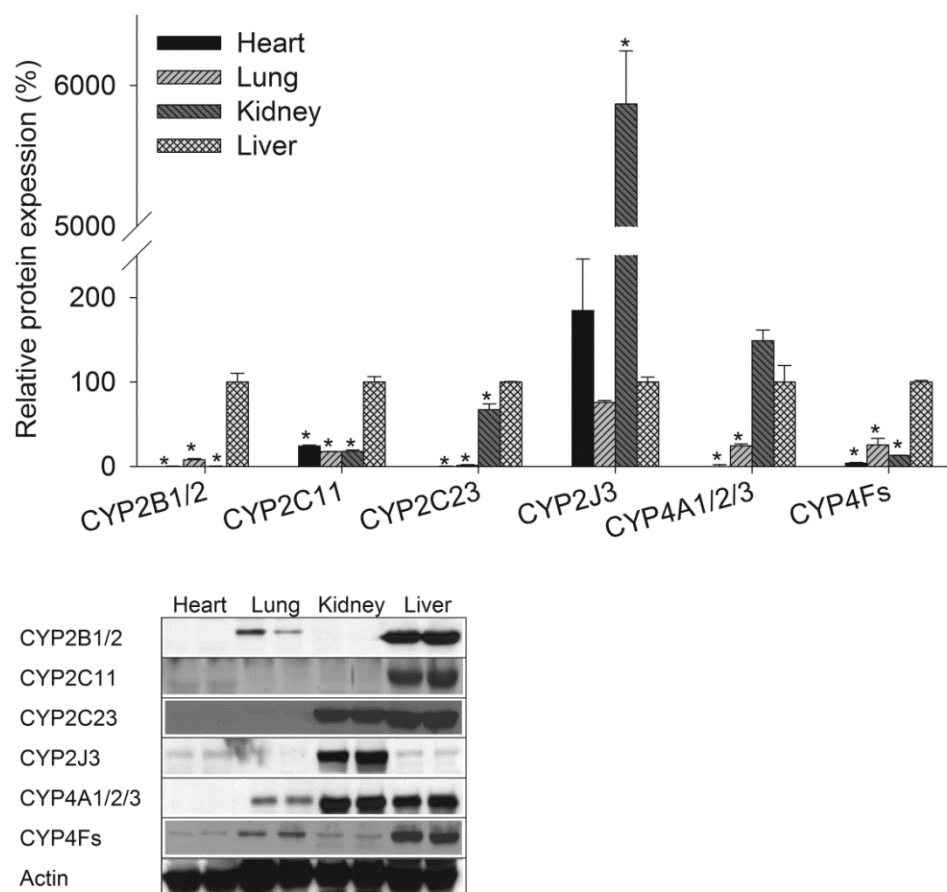


**Figure 3.1. P450 Protein Expression in Untreated Rat Heart, Lungs, Kidneys and Liver.** Microsomal protein was isolated from the heart, lungs, kidneys and liver and separated on a 10% SDS-PAGE. CYP2B1/2, CYP2C11, CYP2C23, CYP2J3, CYP4A1/2/3, CYP4Fs, and actin proteins were detected by the enhanced chemiluminescence method. The graph represents the amount of protein normalized to the loading control (mean  $\pm$  S.E.M., n = 3), and the results are expressed as a percentage of the liver protein expression value. One-way analysis of variance followed by a Tukey's post hoc test (\* P < 0.05 compared with the liver).

## 1.2. Determination of the Kinetic Parameters of Cytochrome P450-Mediated AA Metabolism in Untreated Rat Heart, Lungs, Kidneys and Liver

The AA concentration ranges needed for the full kinetic profile were up to 922  $\mu\text{M}$  for heart and lungs and up to 182  $\mu\text{M}$  for kidneys and liver, as shown in Figures 3.2 and 3.3. In comparison, the reported endogenous AA concentration was up to 100  $\mu\text{M}$  (Brash 2001). Moreover, the kinetic model that provided the best fit was the simple or the sigmoidal Michaelis-Menten models rather than the more complex models, for all metabolites in all organs (Figs. 3.2 & 3.3). This indicates that the formation of a metabolite was either controlled by a single P450 enzyme, or by more than one P450 enzymes of similar  $K_m$  and  $V_{max}$  values. The enzyme kinetics parameters values,  $V_{max}$ , and  $K_m$  are shown in Table 3.1. Again, the  $K_m$  values of the EET formation in the heart in addition to the 14,15-EET formation in the lungs are substantially higher than the reported endogenous AA concentration (Brash 2001). 19-HETE was identified by its retention time (14.6 min) which was consistent with the authentic standard. Linearity for 19-HETE was in the range between 0.01 and 4  $\mu\text{g/ml}$  and the lower limit of detection was 0.001  $\mu\text{g/ml}$ .

In the heart, P450-mediated metabolism of AA was mainly through epoxygenation (Fig. 3.2), whereas, 20-HETE was formed at a significantly lower rate (Fig. 3.3). Heart microsomal fraction formed minor amounts of 19-HETE which was below the limit of quantification.  $Cl_{int}$  values were 0.18, 0.12, 0.28 and 0.26  $\mu\text{L/min/mg}$  protein for 5,6-, 8,9-, 11,12- and 14,15-EET, respectively, and 0.01  $\mu\text{L/min/mg}$  protein for 20-HETE (Table 3.1). The  $K_m$  values were 268, 310, 271 and 570  $\mu\text{M}$  for 5,6-, 8,9-, 11,12- and 14,15-EET, respectively (Table 3.1). While the  $V_{max}$  values were 49.3, 38.2, 76.6 and 146  $\text{pmol/min/mg}$  protein by the same order (Table 3.1). The  $V_{max}$  and  $K_m$  values for the 20-HETE formation were 0.73  $\text{pmol/min/mg}$  protein and 59.6  $\mu\text{M}$ , respectively (Table 3.1).

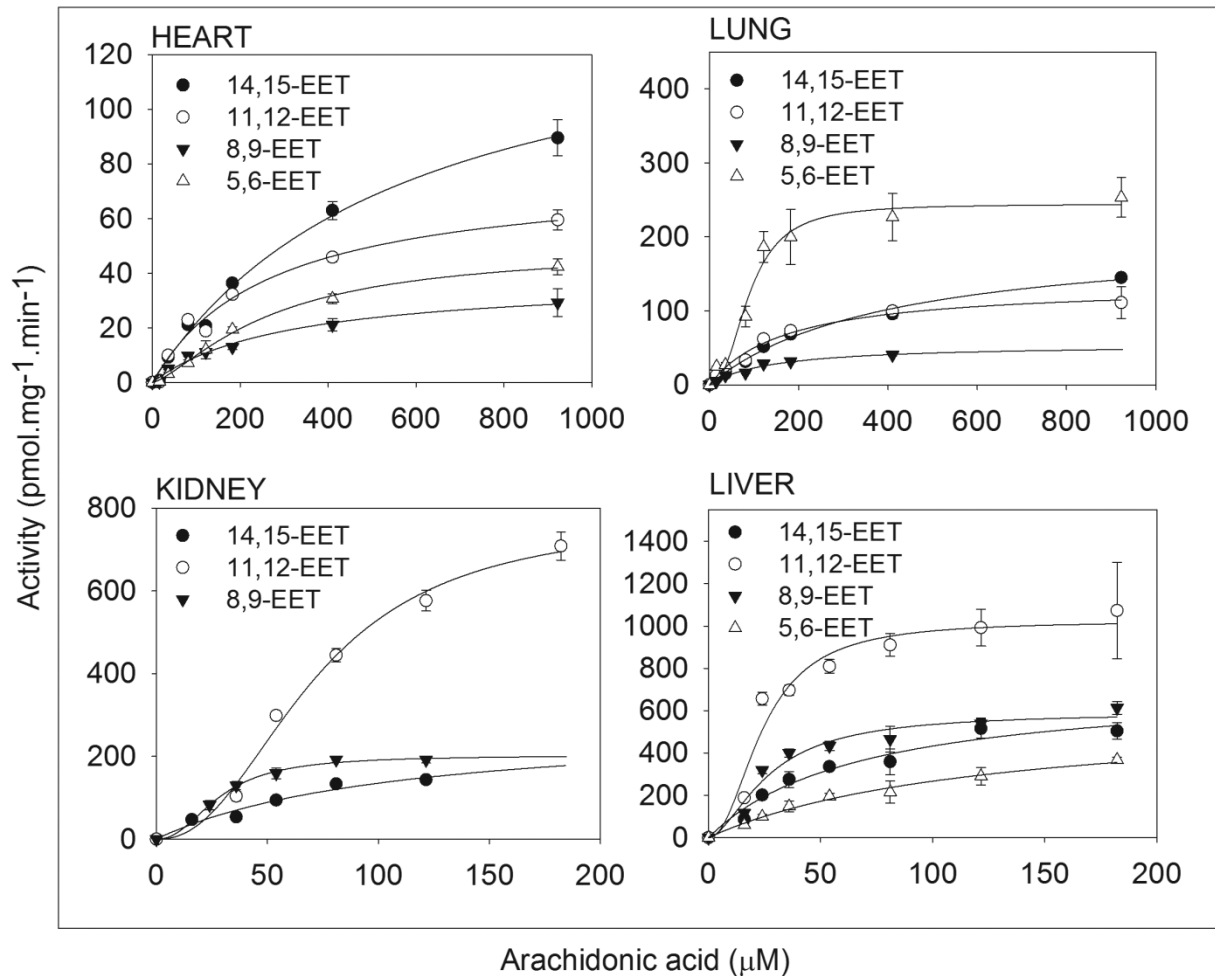


**Figure 3.2. Kinetic Profiles of EET Formation by Microsomes Separated from Untreated Rat Heart, Lungs, Kidneys and Liver.** In a 200 μL total volume, 200 μg (heart and lungs) and 100 μg (kidneys and liver) of microsomal protein pooled from 5 rats incubated with arachidonic acid for 30 min for heart and lungs and 15 min for kidneys and liver. The experimental values for arachidonic acid metabolism were expressed as mean ± S.E.M. Each point was measured in triplicate.

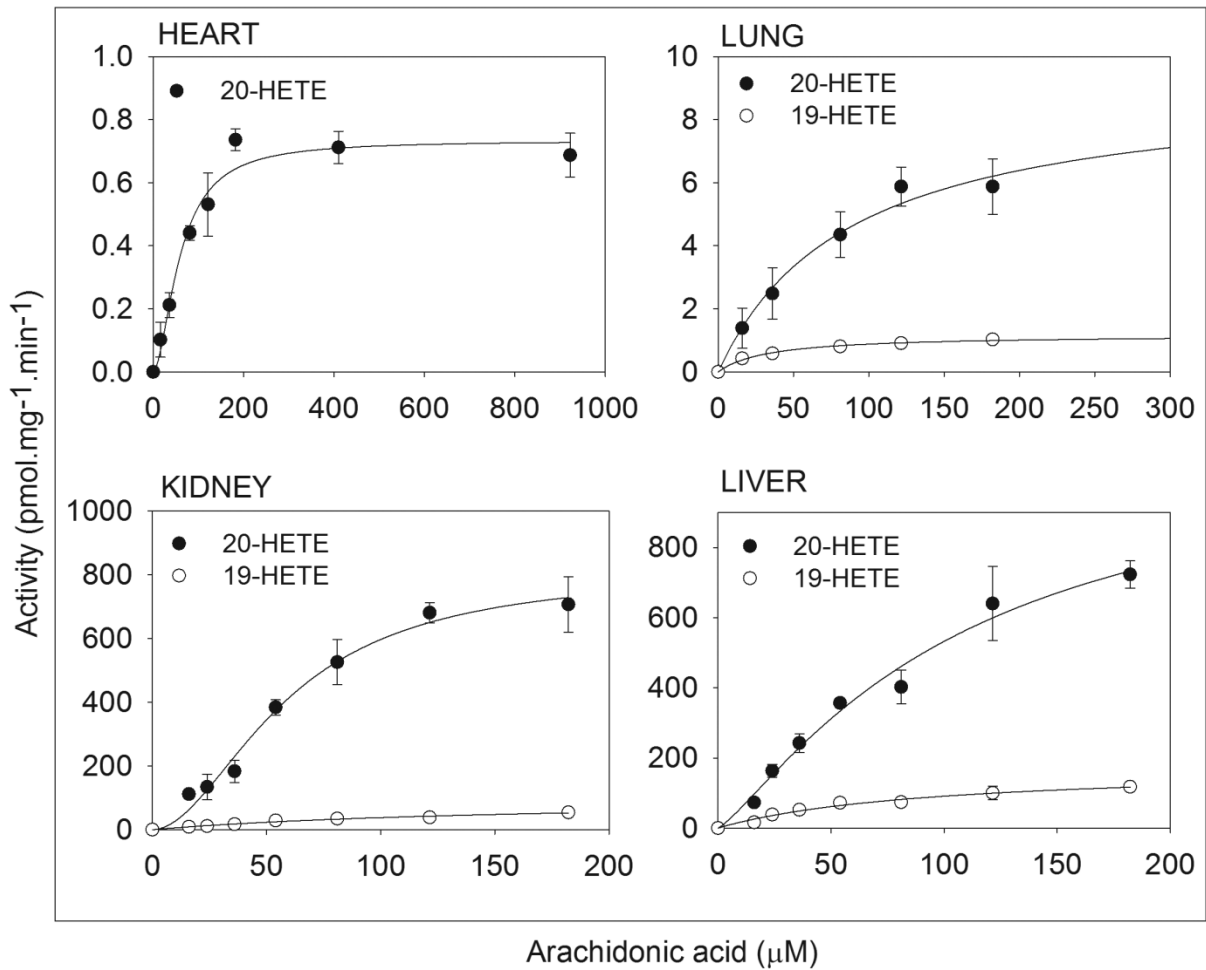


**Figure 3.3. Kinetic Profiles of 19- and 20-HETE Formation by Microsomes Separated from Untreated Rat Heart, Lungs, Kidneys and Liver.** In a 200  $\mu\text{L}$  total volume, 200  $\mu\text{g}$  (heart and lungs) and 100  $\mu\text{g}$  (kidneys and liver) of microsomal protein pooled from 5 rats incubated with arachidonic acid for 30 min for heart and lungs and 15 min for kidneys and liver. The experimental values for arachidonic acid metabolism were expressed as mean  $\pm$  S.E.M. Each point was measured in triplicate.

Similar to the heart, the epoxygenase activity in the lungs was higher than that of the hydroxylase (Fig. 3.2 & 3.3).  $Cl_{int}$  values were 2.74, 0.39, 0.79 and 0.51  $\mu\text{L}/\text{min}/\text{mg}$  protein for 5,6-, 8,9-, 11,12- and 14,15-EET, and 0.03 and 0.1  $\mu\text{L}/\text{min}/\text{mg}$  protein for 19- and 20-HETE, respectively (Table 3.1). The  $K_m$  values were 89.2, 141, 172 and 401  $\mu\text{M}$  and the  $V_{max}$  values were 244, 55.1, 136 and 204  $\text{pmol}/\text{min}/\text{mg}$  protein for 5,6-, 8,9-, 11,12- and 14,15-EET, respectively (Table 3.1). The  $V_{max}$  and  $K_m$  values for the 19-HETE formation were 1.18  $\text{pmol}/\text{min}/\text{mg}$  protein and 33.8  $\mu\text{M}$  and for 20-HETE were 9.19  $\text{pmol}/\text{min}/\text{mg}$  protein and 87.8  $\mu\text{M}$ , respectively (Table 3.1).

AA hydroxylation in the kidneys and liver was substantially higher than those of the heart or the lungs (Fig. 3.3). For the kidneys, 5,6-EET formation was below the limit of quantification in the kidneys but not in the other three organs.  $Cl_{int}$  values were 7.15, 10.9 and 2.59  $\mu\text{L}/\text{min}/\text{mg}$  protein for 8,9-, 11,12- and 14,15-EET, and 0.6 and 13.9  $\mu\text{L}/\text{min}/\text{mg}$  protein for 19- and 20-HETE, respectively (Table 3.1). The  $K_m$  values were 28.3, 71.3, and 109  $\mu\text{M}$  and the  $V_{max}$  values were 202, 775 and 283  $\text{pmol}/\text{min}/\text{mg}$  protein for 8,9-, 11,12- and 14,15-EET, respectively (Table 3.1). The  $V_{max}$  and  $K_m$  values for the 19-HETE formation were 100  $\text{pmol}/\text{min}/\text{mg}$  protein and 166  $\mu\text{M}$  and for 20-HETE were 812  $\text{pmol}/\text{min}/\text{mg}$  protein and 58.7  $\mu\text{M}$ , respectively (Table 3.1).

For the liver,  $Cl_{int}$  values were 4.83, 22, 42.4 and 10.7  $\mu\text{L}/\text{min}/\text{mg}$  protein for 5,6-, 8,9-, 11,12- and 14,15-EET, and 1.87 and 10.4  $\mu\text{L}/\text{min}/\text{mg}$  protein for 19- and 20-HETE, respectively (Table 3.1). The  $K_m$  values were 124, 26.9, 24.2 and 68.4  $\mu\text{M}$  and the  $V_{max}$  values were 596, 592, 1024 and 729  $\text{pmol}/\text{min}/\text{mg}$  protein for 5,6-, 8,9-, 11,12- and 14,15-EET, respectively (Table 3.1). The  $V_{max}$  and  $K_m$  values for the 19-HETE formation were 177  $\text{pmol}/\text{min}/\text{mg}$  protein and 94.6  $\mu\text{M}$  and for 20-HETE were 1118  $\text{pmol}/\text{min}/\text{mg}$  protein and 108  $\mu\text{M}$ , respectively (Table 3.1).

**Table 3.1. Enzyme Kinetic Parameters (mean  $\pm$  S.E.E) for the Formation of EETs and HETEs by Microsomes Separated from Untreated Rat Heart, Lungs, Kidneys and Liver.**

Parameters		Heart	Lungs	Kidneys	Liver
<b>5,6-EET</b>	<b>V<sub>max</sub></b>	49.3 $\pm$ 3.4	244 $\pm$ 11	-	596 $\pm$ 71
	<b>h</b>	1.40 $\pm$ 0.13	2.41 $\pm$ 0.45	-	1.0
	<b>K<sub>m</sub></b>	268 $\pm$ 35	89.2 $\pm$ 7.1	-	124 $\pm$ 26
	<b>Cl<sub>int</sub></b>	0.18	2.74	-	4.83
	<b>R<sup>2</sup></b>	0.99	0.95	-	0.95
<b>8,9-EET</b>	<b>V<sub>max</sub></b>	38.2 $\pm$ 2.7	55.1 $\pm$ 3.1	202 $\pm$ 8	592 $\pm$ 35
	<b>h</b>	1.0	1.0	2.25 $\pm$ 0.33	1.71 $\pm$ 0.33
	<b>K<sub>m</sub></b>	310 $\pm$ 50	141 $\pm$ 18	28.3 $\pm$ 1.4	26.9 $\pm$ 2.8
	<b>Cl<sub>int</sub></b>	0.12	0.39	7.15	22
	<b>R<sup>2</sup></b>	0.96	0.98	0.99	0.95
<b>11,12-EET</b>	<b>V<sub>max</sub></b>	76.6 $\pm$ 4	136 $\pm$ 7	775 $\pm$ 40	1024 $\pm$ 57
	<b>h</b>	1.0	1.0	2.30 $\pm$ 0.23	2.13 $\pm$ 0.50
	<b>K<sub>m</sub></b>	270 $\pm$ 33	172 $\pm$ 24	71.3 $\pm$ 4.5	24.2 $\pm$ 2.4
	<b>Cl<sub>int</sub></b>	0.28	0.79	10.9	42.4
	<b>R<sup>2</sup></b>	0.97	0.96	0.99	0.92
<b>14,15-EET</b>	<b>V<sub>max</sub></b>	146 $\pm$ 8	204 $\pm$ 8	283 $\pm$ 44	729 $\pm$ 60
	<b>h</b>	1.0	1.0	1.0	1.0
	<b>K<sub>m</sub></b>	570 $\pm$ 60	401 $\pm$ 32	109 $\pm$ 29	68.4 $\pm$ 12.6
	<b>Cl<sub>int</sub></b>	0.26	0.51	2.59	10.7
	<b>R<sup>2</sup></b>	0.99	0.99	0.96	0.94
<b>19-HETE</b>	<b>V<sub>max</sub></b>	-	1.18 $\pm$ 0.03	100 $\pm$ 19	177 $\pm$ 18
	<b>h</b>	-	1.0	1.0	1.0
	<b>K<sub>m</sub></b>	-	33.8 $\pm$ 3.5	166 $\pm$ 52	94.6 $\pm$ 19
	<b>Cl<sub>int</sub></b>	-	0.03	0.60	1.87
	<b>R<sup>2</sup></b>	-	0.97	0.91	0.94
<b>20-HETE</b>	<b>V<sub>max</sub></b>	0.73 $\pm$ 0.03	9.19 $\pm$ 1.28	812 $\pm$ 62	1118 $\pm$ 264
	<b>h</b>	1.77 $\pm$ 0.27	1.0	1.91 $\pm$ 0.26	1.23 $\pm$ 0.22
	<b>K<sub>m</sub></b>	59.6 $\pm$ 6.1	87.8 $\pm$ 27.1	58.7 $\pm$ 6.7	108 $\pm$ 45
	<b>Cl<sub>int</sub></b>	0.01	0.10	13.9	10.4
	<b>R<sup>2</sup></b>	0.95	0.93	0.97	0.96

V<sub>max</sub> (pmol/min/mg protein), K<sub>m</sub> ( $\mu$ M) and h were determined as per simple Michaelis-Menten or sigmoidal model (eq. 1); Cl<sub>int</sub> ( $\mu$ L/min/mg protein) was calculated as V<sub>max</sub>/K<sub>m</sub>.

Interestingly, the K<sub>m</sub> values for all metabolites were significantly different between the organs except in three cases (Table 3.1), namely the K<sub>m</sub> values of 8,9-EET formation between liver and kidneys, and the K<sub>m</sub> values of 20-HETE formation between heart and kidneys and between lungs and liver.

### 1.3. Determination of the Regioselectivity of AA Metabolism in Rat Heart, Lungs, Kidneys and Liver

The regioselectivity of AA metabolism mediated by each organ was determined for different AA concentrations. The concentrations used ranged between 16 and 81  $\mu\text{M}$  to reflect the endogenous AA level. Figure 3.4 depicts the relative formation of four EET regioisomers, as well as, the 19- and 20-HETE formation rate, represented as a percentage of the total measured AA metabolite formation. In the heart, 20-HETE formation represented 0.7 % of total metabolites (Fig. 3.4). There were two main EET regioisomers, 14,15- and 11,12-EETs, whose formation was 34.2 and 37.1 % of the total EETs (Fig. 3.4); then the 8,9- and 5,6-EET which contributed to 17.1 and 11.6 %, respectively (Fig. 3.4). Only a minute amount of 19-HETE was observed but could not be accurately quantified (Fig. 3.4). While the lungs formed 19-HETE and 20-HETE at a rate of 0.66 and 2.72 % of the total measured AA metabolites, respectively (Fig. 3.4). Interestingly, the main EET was 5,6-EET which represented 45.4 % of the total EETs in the lungs. 11,12- and 14,15-EETs represented 24 and 18.7 % of the total EETs, respectively (Fig. 3.4). The least EET to be formed was 8,9-EET which represented 11.9 % of total EETs in the lungs.

Regarding the kidneys, quantification of 5,6-EET was problematic due to its low rate of formation. The main EET formed in the kidneys was 11,12-EET followed by 8,9-EET and lastly 14,15-EET, and they represented 49.6, 33, and 17.4 % of the total EET formation, respectively (Fig. 3.4). 20-HETE formation represented 35.3 % compared to total metabolites formed, while 19-HETE represented 2.73% (Fig. 3.4). A similar pattern was observed for the liver, the EET regioisomers formation was: 10.3, 25.2, 46.5 and 18.1 % for 5,6-, 8,9-, 11,12- and 14,15-EET, respectively (Fig. 3.4). 19- and 20-HETE represented 2.98 and 14.3 % of the total measured AA metabolite formation (Fig. 3.4).

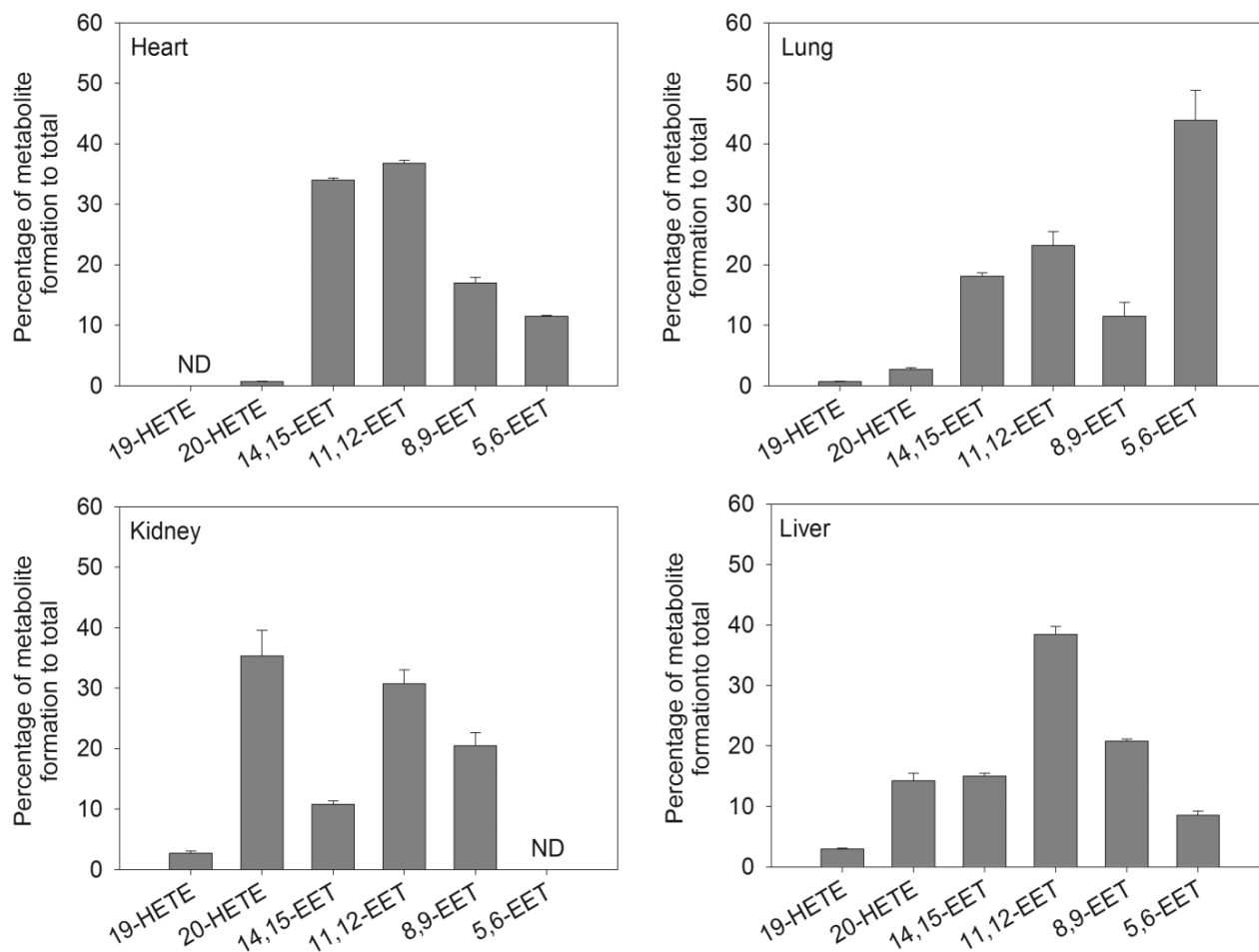


**Figure 3.4. Regioselectivity of Arachidonic Acid Epoxygenation and Hydroxylation Mediated by Microsomes Separated from Untreated Rat Heart, Lungs, Kidneys and Liver.** AA (16, 36 or 81  $\mu$ M) was incubated with 200  $\mu$ g (heart and lungs) and 100  $\mu$ g (kidneys and liver) of microsomal protein pooled from 5 rats for 30 min for heart and lungs and 15 min for kidneys and liver. The y-axis indicates the percentage of each metabolite formation to total sum of the formation rates of investigated P450-derived arachidonic acid metabolite. Data were expressed as mean  $\pm$  S.E.M. Each point was measured in triplicate.

#### **1.4. Immunoinhibition of Cytochrome P450-Mediated AA Epoxygenation and Hydroxylation Activity**

In order to gain insight on the role of P450 enzymes across rat heart, lungs, kidneys and liver, the effect of the selective inhibition of different P450 enzymes by antibodies on AA metabolism was determined. Anti-CYP2C11 antibody efficiently inhibited AA epoxygenation in the heart and liver by 89 and 88.5 %, respectively (Table 3.2). Anti-CYP2B8 antibody caused predominant inhibition of AA epoxygenation in the lungs by 46 % (Table 3.2). For anti-CYP2C23 antibody, it inhibited AA epoxygenation in the kidneys by 72.5 % and the liver by 62.6 % (Table 3.2). Anti-CYP4As inhibited AA hydroxylation in the four organs. The percentage of inhibition was 76, 23.9, 71.5 and 35.1 % for the heart, lungs, kidneys and liver, respectively (Table 3.2).

**Table 3.2. Immunoinhibition of P450-Mediated AA Epoxygenation and Hydroxylation in Untreated Rat Heart, Lung, Kidney and Liver Microsomes. Data are the Mean  $\pm$  S.E.M. Each point was measured in triplicate.**

Antibody	% Inhibition							
	Heart		Lungs		Kidneys		Liver	
	Epoxygenation	Hydroxylation	Epoxygenation	Hydroxylation	Epoxygenation	Hydroxylation	Epoxygenation	Hydroxylation
<b>Anti-CYP2BS</b>	4.48 $\pm$ 3.63	8.20 $\pm$ 4.17	46 $\pm$ 14	20.5 $\pm$ 3.9	11.2 $\pm$ 5.5	21.5 $\pm$ 11.6	14.5 $\pm$ 9.8	8.00 $\pm$ 9.43
<b>Anti-CYP2C11</b>	89 $\pm$ 25	11 $\pm$ 5	17.5 $\pm$ 6.6	15.2 $\pm$ 6.8	58.1 $\pm$ 22.8	25.4 $\pm$ 21.9	88.5 $\pm$ 26.5	30.2 $\pm$ 7.1
<b>Anti-CYP2C23</b>	5.02 $\pm$ 3.66	8.87 $\pm$ 4.18	9.51 $\pm$ 6.02	3.02 $\pm$ 2.38	72.5 $\pm$ 16.9	4.73 $\pm$ 6.93	62.6 $\pm$ 28	27.3 $\pm$ 8.4
<b>Anti-CYP4AS</b>	17.5 $\pm$ 4.2	76 $\pm$ 28	23 $\pm$ 10	23.9 $\pm$ 15.8	27.7 $\pm$ 23.7	71.5 $\pm$ 27.3	21.4 $\pm$ 6.1	35.1 $\pm$ 10.1

## **2. Alterations in Cytochrome P450-Derived Arachidonic Acid Metabolism During Pressure Overload-Induced Cardiac Hypertrophy**

### **2.1. Effect of DAC on the Development of Cardiac Hypertrophy**

5 weeks post-surgery, DAC animals showed a 28% increase in left ventricle weight to tibial length ratio compared to sham (Fig. 3.5A). Echocardiographic analysis showed a significant thickening of the left ventricle posterior wall thickness and interventricular septal wall thickness by 31, and 28%, respectively in DAC hearts compared to sham (Fig. 3.5A). On the other hand, left ventricle volume showed a significant decrease by 14% in DAC hearts compared to sham (Fig. 3.5A). Regarding heart functions, the percentage of fractional shortening and the percentage of ejection fraction did not change, while, Tei index showed a significant increase by 14% in DAC hearts compared to sham (Fig. 3.5B). Additionally, the expression of hypertrophic markers, ANP, BNP and  $\beta/\alpha$ -MHC ratio, were significantly increased by 0.66-, 6.78- and 36.58-fold, respectively, in DAC hearts compared to sham (Fig. 3.5C). Our results showed that compensated cardiac hypertrophy was developed 5 weeks post-surgery.

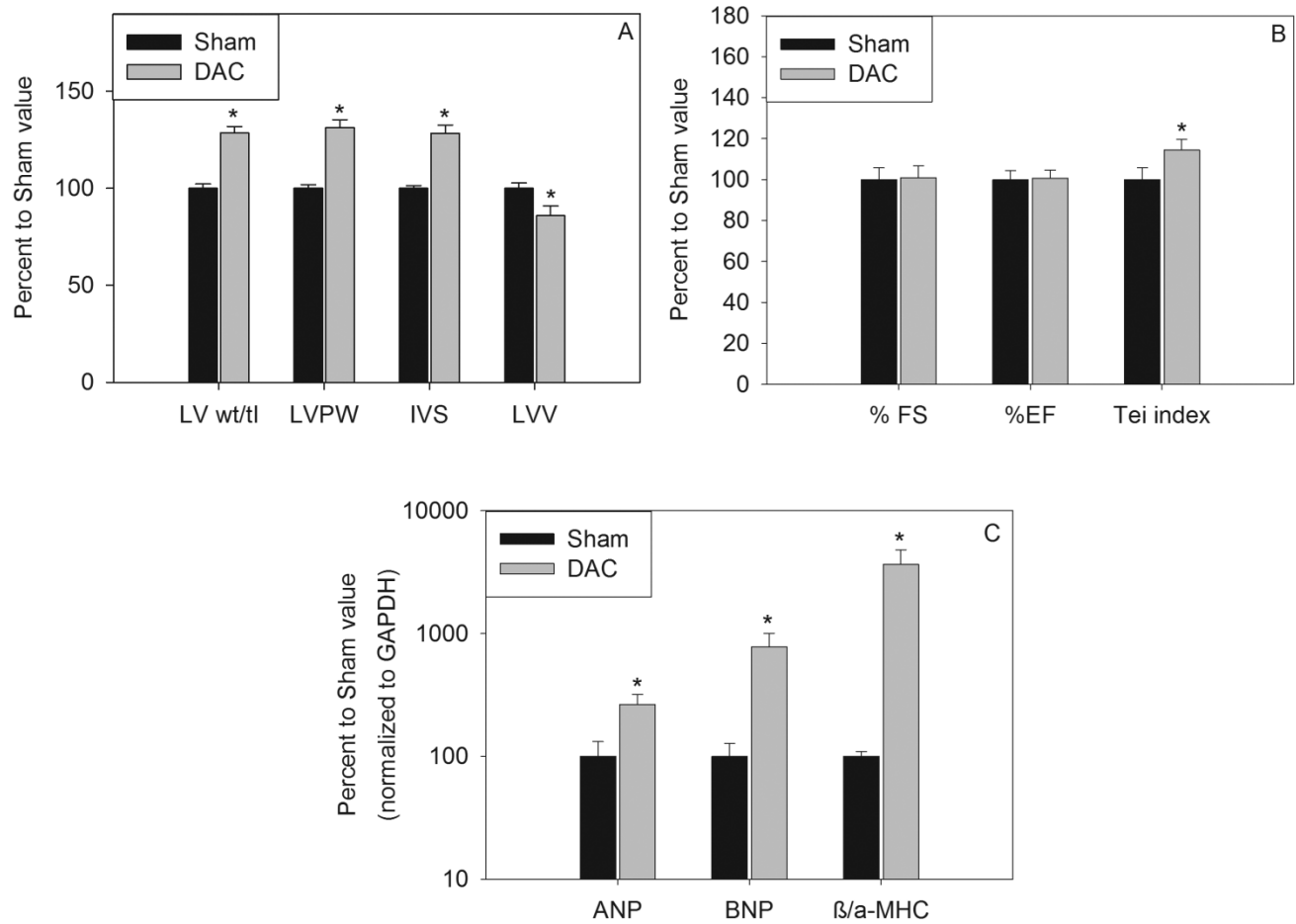


**Figure 3.5. Assessment of Cardiac Hypertrophy in Rats.** 5 weeks post-surgery, rats were weighed and mildly anesthetized for echocardiography to measure: Heart dimensions parameters (A), namely left ventricular weight to tibial length (LV wt/tl), LVPW, IVS, and LVV during diastole. Heart functions (B), namely %FS, %EF, and Tei index. Thereafter, hearts were harvested and total RNA was isolated from hearts of sham and DAC animals. Gene expressions were determined by real-time PCR for hypertrophic markers (C), namely ANP, BNP,  $\beta$ -MHC and  $\alpha$ -MHC. The  $\beta/\alpha$ -MHC ratio was calculated as  $\beta$ -MHC/ $\alpha$ -MHC gene expression. Results are expressed as mean  $\pm$  S.E.M. Student t test (\*  $P < 0.05$  compared with sham group). Sham rats (n=6) and DAC rats (n=9).

## 2.2. Effect of Cardiac Hypertrophy on the Levels of AA Metabolites in Heart Tissue

The HPLC method provided good resolution for all formed metabolites, 4 EETs, 4 DHETs, 3 mid-chain and 5 terminal and subterminal HETEs, except the co-elution of 16- and 17-HETE, and 8- and 12-HETE. The retention time, and ions monitored are shown in Table 3.3. Both EETs and DHETs quantification has been a challenging task due to their low levels in heart tissue. We measured EETs levels indirectly after their conversion to DHET, therefore, the measured levels were, in fact, the sum of EET and its corresponding DHET levels. Thus, it reflected the level of endogenous epoxy-metabolites of AA in heart tissue. There was a significant increase in cardiac 5,6-, 8,9-, 11,12- and 14,15-EET+DHET levels by 89, 76, 62 and 69% respectively, in DAC animals compared to sham (Fig. 3.6A).

**Table 3.3. The Retention Times, and Ions Monitored for the Analyzed P450-Derived AA Metabolites.**

Metabolite	Retention time (min)	m/z
14,15-DHET	16.8	337
14,15-DHET-D11	16.4	348
11,12-DHET	18.4	337
8,9-DHET	19.6	337
5,6-DHET	21.2	337
19-HETE	21	319
20-HETE	21.6	319
18-HETE	22.6	319
16/17-HETE	23.5	319
15-HETE	26	319
15-HETE-D8	25.4	327
8/12-HETE	28.3	319
5-HETE	30	319
14,15-EET	32.7	319
14,15-EET-D11	32.4	330
11,12-EET	34.6	319
8,9-EET	35.5	319
5,6-EET	36.2	319

Mid-chain HETEs, 5-, 8/12-, and 15-HETE, were found to be higher in heart tissue compared to EETs or DHETs (Fig. 3.6). In DAC heart there was a significant increase in 5-, 8/12-, and 15-HETE levels by 52, 100 and 31%, respectively compared to sham (Fig. 3.6B). With respect to terminal and subterminal HETEs, the endogenous concentrations of 16-, 17-, 18-, and 19-HETE could not be detected in either DAC or sham hearts (Fig. 3.6C). While for 20-HETE, its cardiac level was comparable to EETs and DHETs, and there was a significant increase in its level in heart tissue of DAC animals by 3.41-fold compared to sham (Fig. 3.6C).

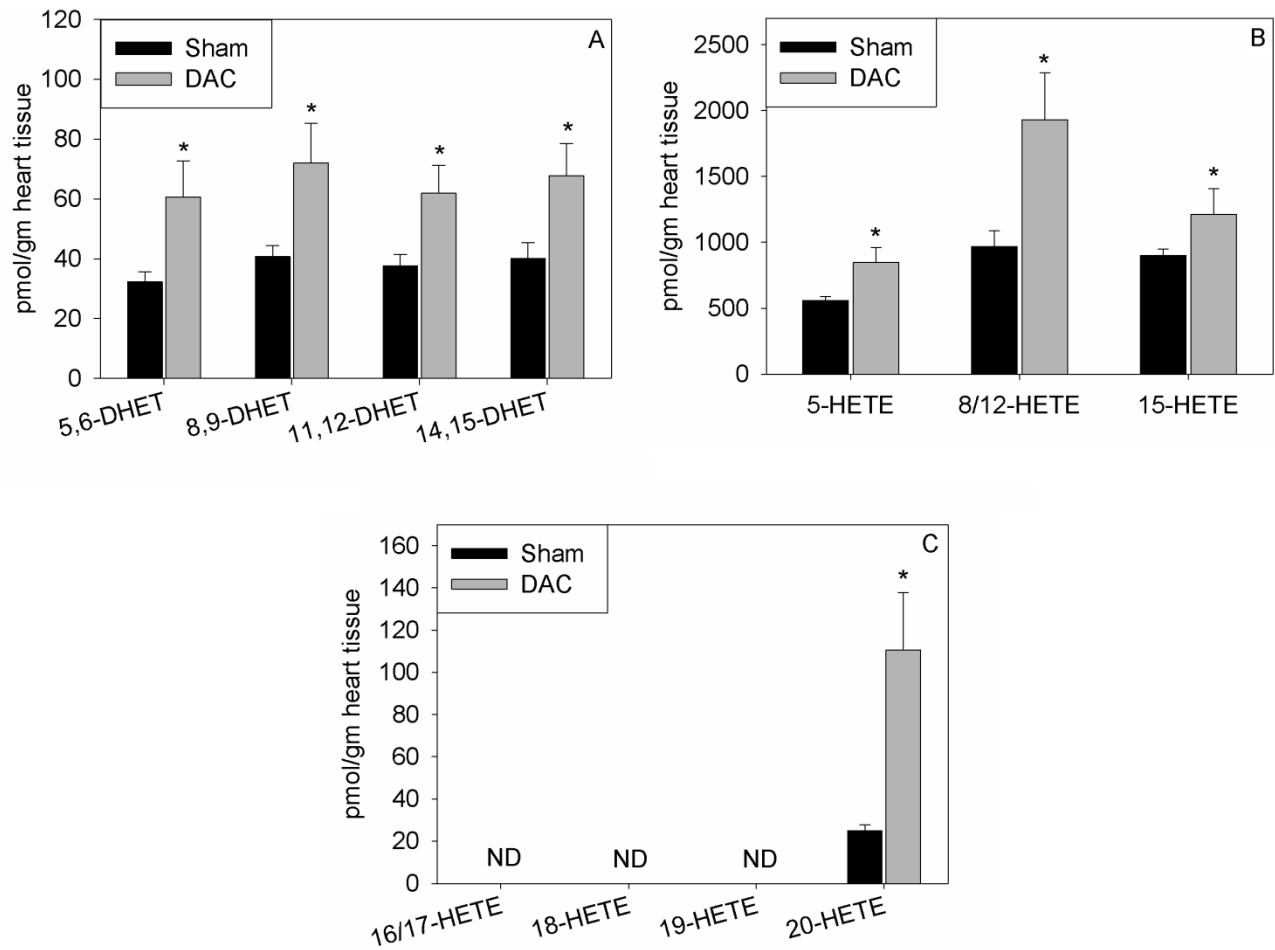


**Figure 3.6. Effect of Cardiac Hypertrophy on Rat Cardiac AA Metabolites Levels.**

Heart tissue was homogenized on ice with potassium phosphate buffer, then, centrifuged at 10,000 g for 15 min at 0 °C. After spiking with internal standards, AA metabolites were extracted from the resultant supernatant by solid-phase cartridge (Oasis HLB). The sum of each EETs and its corresponding DHET (A), mid-chain HETEs (B), and terminal and subterminal HETEs (C) were measured using LC-ESI-MS as described under *Materials and Methods*. Results are expressed as mean  $\pm$  S.E.M. Student t test (\* P < 0.05 compared with sham group). ND, not detected. Sham rats (n=6) and DAC rats (n=9).

### **2.3. Effect of Cardiac Hypertrophy on the Formation and Degradation of EETs**

With respect to EET formation rate, there was a 1-, 1.79-, 1.79- and 3.03-fold increase in 5,6-, 8,9-, 11,12-, and 14,15-EET formation rate, respectively in DAC hearts compared to sham (Fig. 3.7A). Moreover, there was an alteration in the regioselectivity of epoxide group insertion. Regioselectivity expressed as 14,15-EET:11,12-EET:8,9-EET ratio was 1.2:1.2:1 for normal and 1.7:1.2:1 for DAC hearts (Fig. 3.7A). The observed increase in EET formation rate was in line with the observed increase in the levels of EETs + DHETs in heart tissue during cardiac hypertrophy.

In order to determine whether or not cardiac hypertrophy also altered the degradation of EETs to DHETs, sEH activity, and expression were measured. sEH is the dominant enzyme responsible for catalyzing the transformation of EETs to DHETs. Interestingly, the activity of sEH significantly decreased by 30% in DAC hearts compared to sham (Fig. 3.7B). Additionally, EPHX2 gene expression was significantly decreased in DAC heart by 98% compared to sham (Fig. 3.7C).

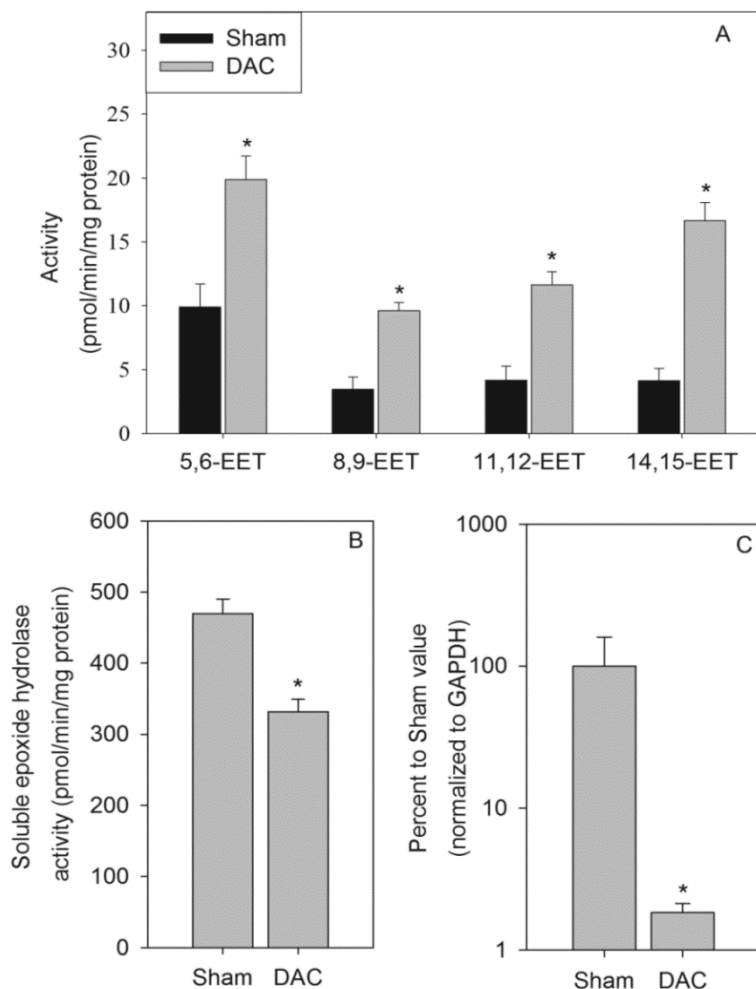


**Figure 3.7. Effect of Cardiac Hypertrophy on the Formation and Degradation of EETs by Microsomes and Cytosols Separated from Rat Heart.** Heart microsomal fraction was incubated with 50  $\mu$ M arachidonic acid to determine EET formation (A). Also, heart cytosol was incubated with 2  $\mu$ g/ml 14,15-EET to determine sEH activity, i.e. EETs degradation (B). sEH activity was determined by measuring the formation rate of 14,15-DHET. AA metabolites were injected into LC-ESI-MS as described under *Materials and Methods*. Total RNA was isolated from hearts of sham and DAC animals for the determination of EPHX2 gene expression (C) by real-time PCR. Results are expressed as mean  $\pm$  S.E.M. Student t test (\*  $P < 0.05$  compared with sham group). Sham rats (n=6) and DAC rats (n=9).

## 2.4. Effect of Cardiac Hypertrophy on the Formation of HETEs

Lipoxygenases are also known to catalyze the formation of mid-chain HETEs, therefore, the formation of mid-chain HETEs, 5-, 8/12-, and 15-HETE was determined in microsomal incubates with and without P450 activation by NADPH. Despite lipoxygenases are mainly cytosolic, lipoxygenases activity was previously reported in microsomal fraction (Breitbart, Sofer et al. 1996). In consistence with the published data, the heart microsomal fraction was able to form only the 8/12-HETE without NADPH (Fig. 3.8A). By adding NADPH, the rate of 8/12-HETE formation was significantly increased, whereas, 5- and 15-HETE formations were still below the detection limit (Fig. 3.8A). 8/12-HETE formation mediated by the microsomal fraction of sham hearts was 4.48 and 3.64 pmol/min/mg protein with and without NADPH, respectively (Fig. 3.8A). For DAC hearts, 8/12-HETE formation was 11.41 and 6.64 pmol/min/mg protein with and without NADPH, respectively. In DAC hearts, there was a significant increase in NADPH-dependent 8/12-HETE formation rate by 3.7-fold compared to sham (Fig. 3.8A).

In contrast, terminal and subterminal HETEs were formed by heart microsomes only after P450 activation by NADPH. Except for 18-HETE, the formation of 16/17-, 19-, and 20-HETE could be detected in DAC, and sham hearts (Fig. 3.8B). Albeit, 16/17-HETE formation rate showed no significant changes, 19-HETE formation rate decreased significantly by 41% in DAC hearts compared to sham (Fig. 3.8B). On the other hand, 20-HETE formation rate was slightly higher but did not reach the statistical significance ( $p=0.06$ ), in DAC hearts compared to sham (Fig. 3.8B).

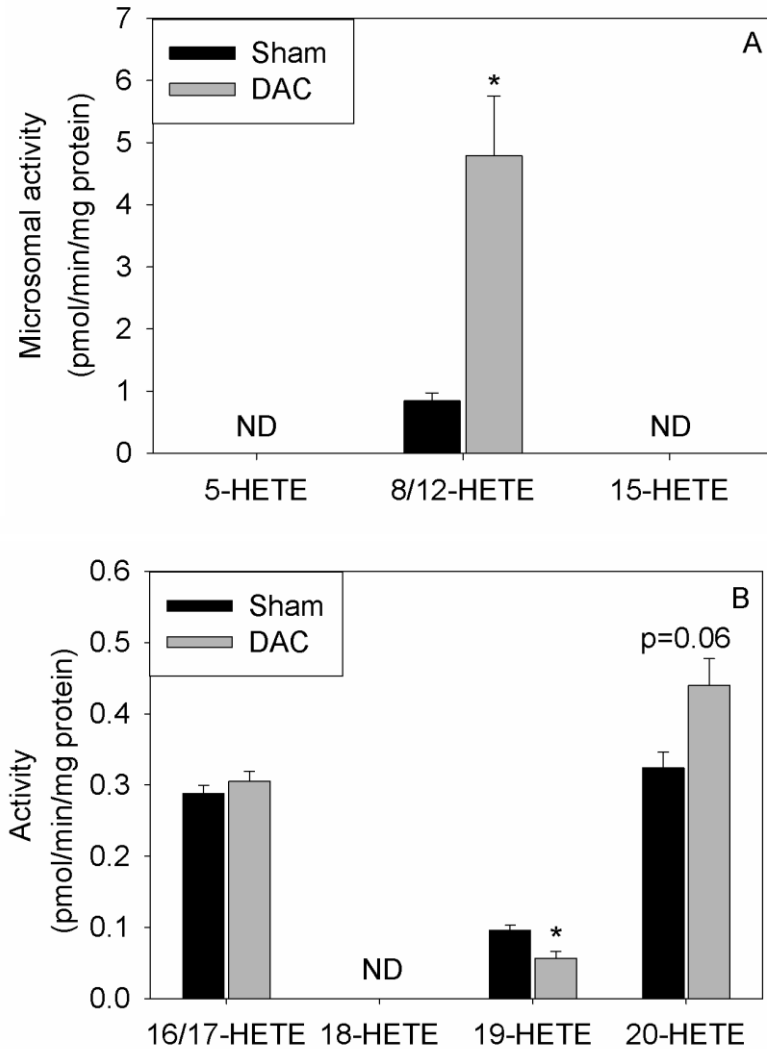


**Figure 3.8. Effect of Cardiac Hypertrophy on the Formation of HETEs by Microsomes Separated from Rat Heart.** Heart microsomal fraction was incubated with 100  $\mu$ M arachidonic acid. The reaction was lasted for 30 min, then, metabolites were extracted by ethyl acetate. Mid-chain HETEs (A), as well as, terminal and subterminal HETEs (B) were measured using LC-ESI-MS as described under *Materials and Methods*. 18-HETE standard curve were used to interpret the signals of co-eluted metabolites, 16- and 17-HETE, since standard curves for all HETEs were nearly identical. Results are expressed as mean  $\pm$  S.E.M. Student t test (\*  $P < 0.05$  compared with sham group). ND, not detected. Sham rats (n=6) and DAC rats (n=9).

## **2.5. Effect of Cardiac Hypertrophy on Cytochrome P450 Protein Expression**

In order to determine main P450 enzymes involved in the observed alteration in AA metabolism, two-step analysis was performed. First, the effect of DAC-induced cardiac hypertrophy on P450 protein expression was determined by Western blot analysis. Second, we tested the correlation between P450 expression and the measured AA metabolite formation rates, as previously described (Castle, Merdink et al. 1995, Baldwin, Clarke et al. 1999).

Regarding P450 expression in the cardiac microsomal fraction, several P450 enzymes, namely CYP1As, CYP1B1, CYP2Bs, CYP2C11, CYP2E1, CYP2J3, and CYP4As, were measured using Western blot analysis (Fig. 3.9). For CYP1 family, CYP1As expression was significantly decreased by 76%, whereas CYP1B1 expression was significantly induced by 100% in DAC hearts compared to sham (Fig. 3.9). With regard to CYP2 family, CYP2Bs expression significantly increased by 72% in DAC hearts compared to sham (Fig. 3.9), whereas, CYP2J3 expression was significantly decreased by 31% in DAC hearts compared to sham (Fig. 3.9). CYP2C11, and CYP2E1 expressions were not significantly altered by cardiac hypertrophy (Fig. 3.9). For CYP4 family, CYP4As expression was decreased by 65% in DAC hearts compared to sham, while the expression of CYP4Fs was not altered (Fig. 3.9).

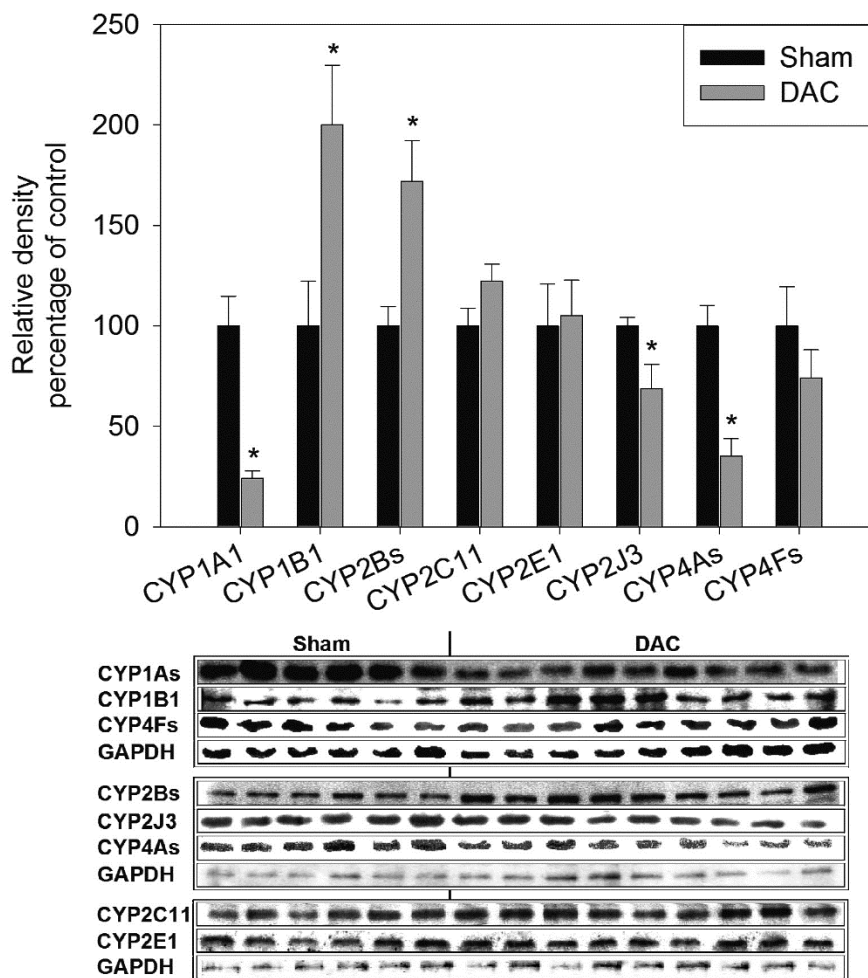


**Figure 3.9. Effect of Cardiac Hypertrophy on P450 Protein Expression in Rat Heart.**

Microsomal protein was isolated from the heart and separated on a 10% sodium dodecyl sulfate-polyacrylamide gel. CYP1As, CYP1B1, CYP2Bs, CYP2C11, CYP2E1, CYP2J3, CYP4As, CYP4Fs, and GAPDH proteins were detected by the enhanced chemiluminescence method as described under *Materials and Methods*. The graph represents the amount of protein normalized to the loading control (GAPDH) (mean  $\pm$  S.E.M.), and expressed as a percentage of the sham group. Student t test (\*  $P < 0.05$  compared with sham group). Sham rats (n=6) and DAC rats (n=9).

The correlation analysis based on the fact that if a P450 enzyme is predominantly involved in the formation of a specific AA metabolite, we will observe that the higher the expression of this enzyme, the higher the formation rate of its metabolites, and vice versa. Using non-parametric correlation analysis, CYP2Bs was found to be correlated significantly with 5,6-, 8,9-, 11,12- and 14,15-EET; r values were 0.61, 0.71, 0.78 and 0.72, respectively (Fig. 3.10). Significant correlation was observed between CYP1B1 and 8/12-HETE suggesting that CYP1B1 was involved in 8/12-HETE formation; r value was 0.73 (Fig. 3.10). Furthermore, CYP4As was found to correlate significantly with 19-HETE (r=0.61) (Fig. 3.10). Interestingly, CYP2J3 expression exhibited significant inverse correlation with 8/12-HETE, r value was -0.67 (Fig. 3.10).

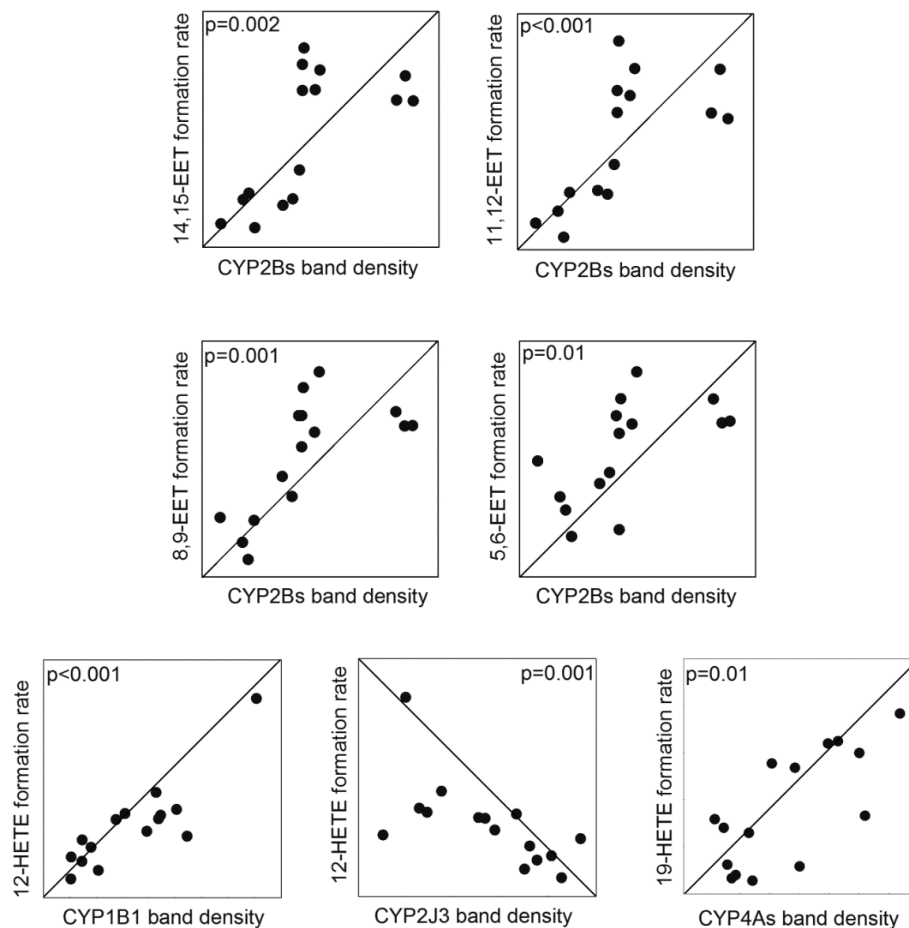


**Figure 3.10. Correlation between P450 Protein Expression Levels and the Formation Rate of P450-Derived AA Metabolites by Microsomes Separated from Rat Heart.** Heart microsomal fraction was incubated with 50 or 100  $\mu\text{M}$  arachidonic acid. The reaction was lasted for 30 min, then, metabolites were extracted by ethyl acetate. Spearman rank correlation coefficients ( $r$ ) were used for evaluating the possible association. Tendency of correlation is indicated by ascending or descending lines. Spearman correlation analysis is a non-parametric method used to evaluate the association between metabolite formation rate and P450 protein expression, which is not necessarily linear. Correlations shown were statistically significant according to P-value ( $P < 0.05$ ).

## 2.6. Role of CYP1B1 and CYP2J2 in Mid-Chain HETEs Metabolism

In order to gain insight about the role of CYP1B1, and CYP2J3 in mid-chain HETE formation, recombinant CYP1B1, and CYP2J2 were examined. CYP1B1 was found to mediate the metabolism of AA to 5-, 8/12-, and 15-HETE in a rate comparable to that of 8/12-HETE formation by the cardiac microsomal fraction (Fig. 3.11). On the other hand, CYP2J2 did not catalyze the degradation of mid-chain HETEs, 5-, 12-, and 15-HETE. We hypothesized that CYP2J2 decreases the formation of 12-HETE by consuming its precursor, 12-HPETE. To test this hypothesis, we incubated 12-HPETE with CYP2J2. Our results showed that CYP2J2 did catalyze the degradation of 12-HPETE to hepoxilins, which are hydroxyepoxyeicosatrienoic acids, based on its retention time and its mass spectrum (Fig. 3.12). Only after the addition of NADPH, hepoxilins peak was detected in CYP2J2-12-HPETE chromatogram (Fig. 3.12A). The CYP2J2-mediated formation of hepoxilins was accompanied by a consumption of 12-HPETE (Fig. 3.12B). The mass spectrum showed that the base peak corresponds to hepoxilin molecular ion,  $[M-H]^-$ , at  $m/z = 335$  and two fragment ions peaks at  $m/z = 317$  and  $273$  correspond to  $[M-H-H_2O]^-$  and  $[M-H-H_2O-CO_2]^-$ , respectively (Fig. 3.12C). This is consistent with the reported mass spectrum of hepoxilins (Chawengsub, Gauthier et al. 2009).

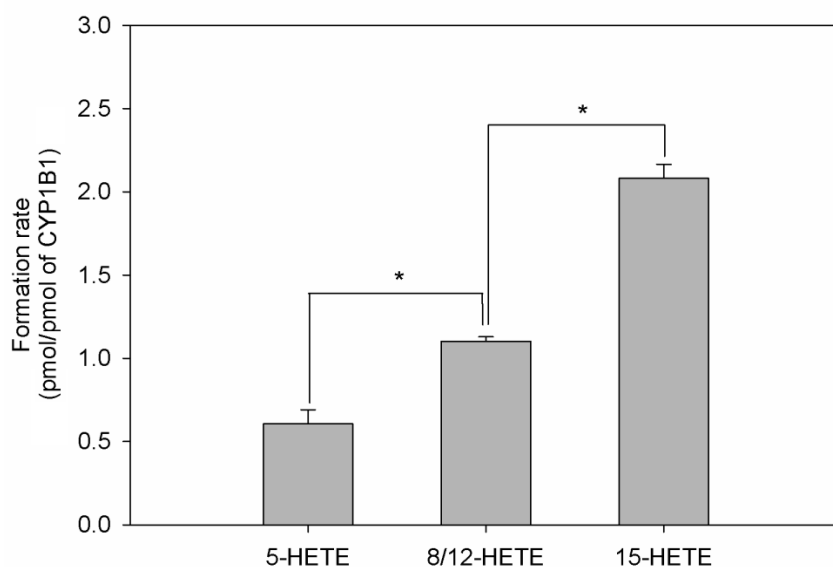


**Figure 3.11. Formation of Mid-Chain HETEs by Recombinant Human CYP1B1.** The reconstituted system consisted of 20 pmol CYP1B1, and 100  $\mu$ M arachidonic acid with 40 pmol cytochrome  $b_5$ , co-incubated for 10 min. Metabolites were extracted by ethyl acetate and dried. Reconstituted metabolites were injected into LC-ESI-MS as described under *Materials and Methods*. Results are expressed as mean  $\pm$  S.E.M. One-way analysis of variance followed by a Tukey's post hoc test (\*  $P < 0.05$ ). The experiment was performed 3 times.

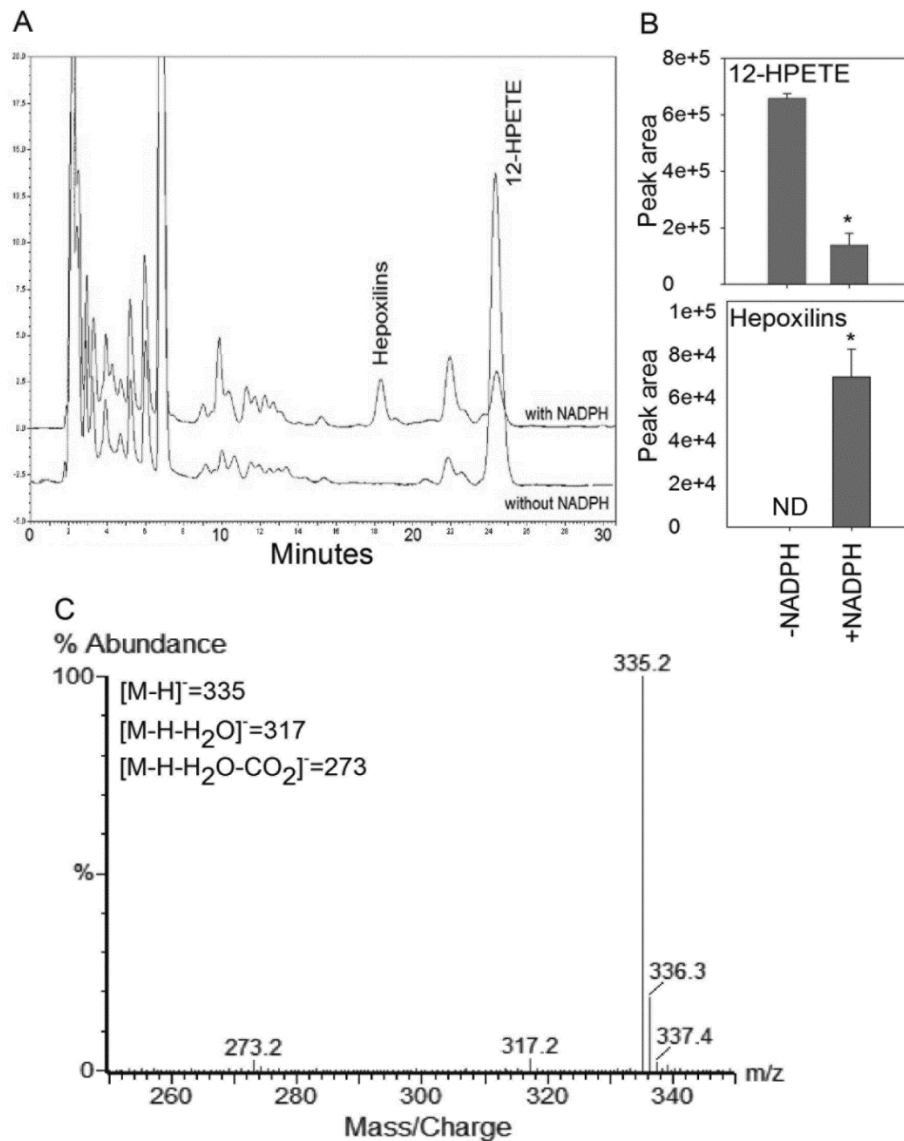


**Figure 3.12. Degradation of 12-HPETE by Recombinant Human CYP2J2.** The reconstituted system consisted of 20 pmol CYP2J2 and 4  $\mu\text{g/mL}$  12-HPETE with and without NADPH as described under *Materials and Methods*. The chromatograms (A) and peak areas for 12-HPETE and hepoxilins (B) with and without NADPH were determined as described under *Materials and Methods*. Mass spectrum (C) was determined by collecting column eluate corresponding to hepoxilins peak for further analysis with ESI-MS as described under *Materials and Methods*. Results are expressed as mean  $\pm$  S.E.M. Student t test (\* P < 0.05). The experiment was performed 3 times.

### **3. Characterization of Arachidonic Acid Metabolism by Rat Cytochrome P450 Enzymes**

#### **3.1. LC-ESI-MS Method Development and Validation**

Previous reverse-phase LC methods used gradient elution of acidified acetonitrile or methanol with water for separating P450-derived AA metabolites. However, the co-elution of mid-chain HETEs, in addition to, the co-elution of terminal and subterminal HETEs was the common drawback for all these methods (Choudhary, Jansson et al. 2004). Therefore, additional normal-phase LC or gas chromatographic methods were utilized to achieve the complete resolution of P450-derived AA metabolites by reanalyzing the eluate collected from an initial reverse-phase separation (Carroll, Balazy et al. 1997, Kiss, Schutte et al. 2000, Schwarz, Kisselev et al. 2004). Tandem MS detection could be another way to achieve successful one-step resolution of mid-chain HETE, as well as terminal and subterminal HETEs (Norris, Reichart et al. 2011, Edpuganti and Mehvar 2013). Therefore, we aimed to develop a reverse-phase LC method for one-step, simultaneous separation of all P450-derived AA metabolites without the expensive tandem MS equipment or the complications of normal-phase chromatography.

**Table 3.4. The Retention Times ( $R_t$ ), Ions Monitored, Sensitivity and Linearity Results of P450-Derived AA Metabolites Analysis.**

Compound	SIM (m/z)	$R_t$ (min)	Range (ng)	Equation	$r^2$	LLOQ (ng)
AA	303	53.5	1.37-244	$Y=0.53X+1.33$	0.999	1.37
5-HETE	319	45.5	0.45-45	$Y=0.46X-0.03$	0.999	0.45
8-HETE	319	42.5	0.05-45	$Y=0.65X-0.02$	0.999	0.05
9-HETE	319	43.5	0.05-45	$Y=0.89X+0.04$	0.999	0.05
11-HETE	319	40.5	0.05-45	$Y=0.89X+0.11$	0.999	0.05
12-HETE	319	42	0.05-45	$Y=0.60X+0.02$	0.999	0.05
15-HETE	319	38	0.45-45	$Y=0.55X-0.02$	0.999	0.45
16-HETE	319	33	0.45-45	$Y=0.69X+0.04$	0.999	0.45
17-HETE	319	32	0.45-45	$Y=0.54X+0.12$	0.999	0.45
18-HETE	319	30.5	0.05-45	$Y=0.69X+0.04$	0.999	0.05
19-HETE	319	28	0.45-45	$Y=0.54X+0.04$	0.999	0.45
20-HETE	319	29.5	0.45-45	$Y=0.46X+0.06$	0.999	0.45
5,6-EET	319	49.5	0.45-45	$Y=0.49X+0.03$	0.999	0.45
8,9-EET	319	48.5	0.45-45	$Y=0.58X-0.03$	0.999	0.45
11,12-EET	319	48	0.05-45	$Y=0.42X-0.01$	0.999	0.05
14,15-EET	319	46.5	0.05-45	$Y=0.39X-0.02$	0.999	0.05

We found that methanol-based gradient elution gave very poor resolution for 16-, 17-, 18-, 19- and 20-HETE, and 8-, 9-, 11- and 12-HETE. For acetonitrile-based elution, it could not resolve 8-HETE from 12-HETE and 16-HETE from 17-HETE. Adding isopropanol to either methanol or acetonitrile led to the co-elution of 5-HETE with 14,15-EET and 18-HETE with 20-HETE. Resolution of AA and its 15 P450-derived AA metabolites was achieved by adding 16% of equivolume mixture of methanol and isopropanol to acetonitrile as the organic mobile phase. With respect to P450-derived AA metabolites, the retention time, and the linear range that extended over 4 orders of

magnitude are shown in Table 3.4. Three internal standards, AA-D8 for AA quantification, 14,15-EET-D11 for EETs quantification and 15-HETE-D8 for HETEs quantification, were monitored at  $m/z=311$ , 330 and 327, respectively, and their retention time were 53.5, 46 and 37 min, respectively. The lower limit of quantitation of the assay based on the mean %error and CV% results was in the range of 0.05 to 0.45 ng (Table 3.4). Above the lower limit of detection, the intraday and interday precision determined at all concentration levels did not exceed  $\pm 15\%$  of the CV (Table 3.5). Also, with respect to intraday and interday accuracy (Table 3.5), the mean %error did not exceed  $\pm 15\%$  for all concentration levels.

**Table 3.5. Precision and Accuracy Results of Representative P450-Derived AA Metabolites.**

Compound	Nominal conc. ( $\mu\text{g/mL}$ )	CV%		%error	
		Intraday	Interday	Intraday	Interday
AA	0.14	1.22	10.40	-11.25	3.67
	1.37	1.82	7.56	-19.52	-7.16
	13.7	2.81	0.56	1.53	-7.05
	68.5	0.97	10.67	14.89	-9.59
15-HETE	0.005	2.45	4.53	11.38	24.27
	0.045	1.75	3.29	-6.91	2.25
	0.45	1.02	3.75	10.61	1.70
	4.5	0.75	2.89	9.03	0.06
18-HETE	0.005	15.66	10.30	-0.02	16.19
	0.045	2.11	1.20	-11.15	4.88
	0.45	2.19	1.70	5.09	4.41
	4.5	1.80	5.01	0.02	0.24
8,9-EET	0.005	3.87	1.22	-3.18	22.91
	0.045	5.02	7.94	-9.53	9.03
	0.45	2.40	5.02	3.92	5.19
	4.5	2.30	5.10	0.04	0.18

### **3.2. Determination of AA-Metabolizing Activity and Metabolic Profile of Cytochrome P450 Enzymes**

Ten rat recombinant P450 enzymes were included in our experiments, selected from different families and subfamilies to get a good idea about the differences in AA-metabolizing activity among rat P450 enzymes. There was no NADPH-independent formation of AA metabolites mediated by Supersomes preparation. Also, there was no formation of AA metabolites mediated by NADPH-P450 reductase or *cyb<sub>5</sub>*. Upon the addition of NADPH, all the tested P450 enzymes were able to metabolize AA but with substantial difference in their rates. 75  $\mu$ M of AA was used to reflect the *in vivo* situation. CYP2C11 metabolized AA with the highest rate (19.9 pmol/pmol P450/min), whereas CYP2A1 had the lowest rate (0.35 pmol/pmol P450/min) (Fig. 3.13). Interestingly, CYP1A1, CYP1A2 and CYP2C6 that have largely been ignored in P450-AA studies were among the P450 of the highest activity (Fig. 3.13). In contrast, CYP2A1, CYP2B1 and CYP2E1 that are of the interest of P450-AA studies were of relatively lower activity (Fig. 3.13).

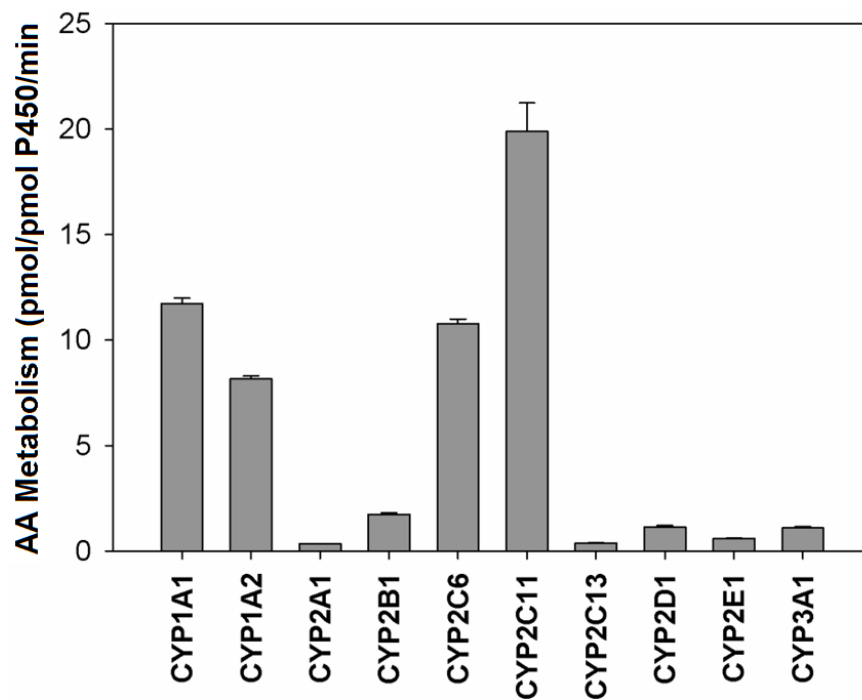


**Figure 3.13. P450-mediated AA-Metabolizing Activity of Rat Recombinant P450 Enzymes.** P450 enzymes (50-100 pmol/mL) were incubated with AA (75  $\mu$ M) for 15-25 min as described under *Materials and Methods*. AA was measured by LC-ESI-MS. Results are presented as mean percentage, and S.E.M and are based on at least 3 individual experiments.

With respect to P450 regioselectivity, all the tested P450 enzymes preferentially mediated AA hydroxylation more than olefin epoxygenation, except CYP2C11 (Figs. 3.14 & 3.15). Interestingly, CYP1A1, and CYP1A2 produced mainly subterminal HETEs by 88.7% and 62.7%, respectively (Fig. 3.14). For CYP2C6, the major metabolites were mid-chain HETEs (48.3%), and EETs (29.4%) (Fig. 3.14). While for CYP2C11, EETs represented 61.3% of the total P450-derived AA metabolites formed, while mid-chain HETEs and terminal and subterminal HETEs represented 23.6% and 15.1%, respectively (Fig. 3.14). Moreover, terminal and subterminal HETEs were the major metabolites for CYP2A1, CYP2B1 and CYP2E1 as 56.1%, 52.1% and 68.7% of the total metabolites formed, respectively (Fig. 3.15). Whereas, mid-chain HETEs were the predominant for CYP2C13, CYP2D1 and CYP3A1 as 45%, 47.3% and 81.8% of the total metabolites formed (Fig. 3.15). Also, P450 enzymes were found to exhibit regioselective oxidation of AA. For CYP1A1, it preferentially oxidized AA to produce 19-HETE, while CYP1A2 produced mainly 16-HETE (Fig. 3.14). The main epoxy-metabolite for CYP2C11, and CYP2C6 were 11,12- and 14,15-EET, respectively (Fig. 3.14).

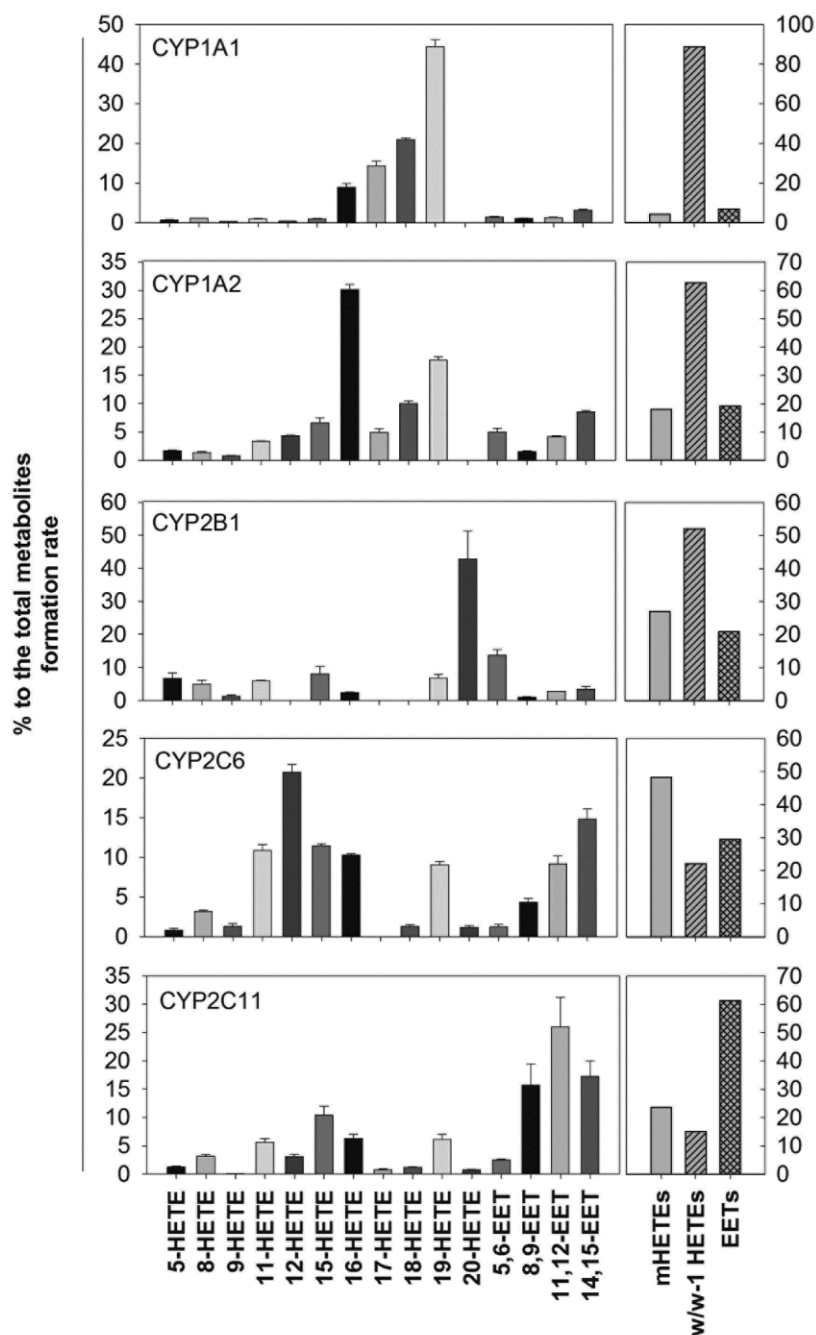


**Figure 3.14. The Metabolic Profile/Regioselectivity of P450-Mediated AA Metabolism by Rat CYP1A1/2, CYP2B1 and CYP2C6/11.** P450 enzymes (50-100 pmol/mL) were incubated with AA (75  $\mu$ M) for 15-25 min and measured by LC-ESI-MS as described under *Materials and Methods*. Results are presented as mean percentage to the total metabolite formation, and S.E.M. and are based on at least 3 individual experiments.

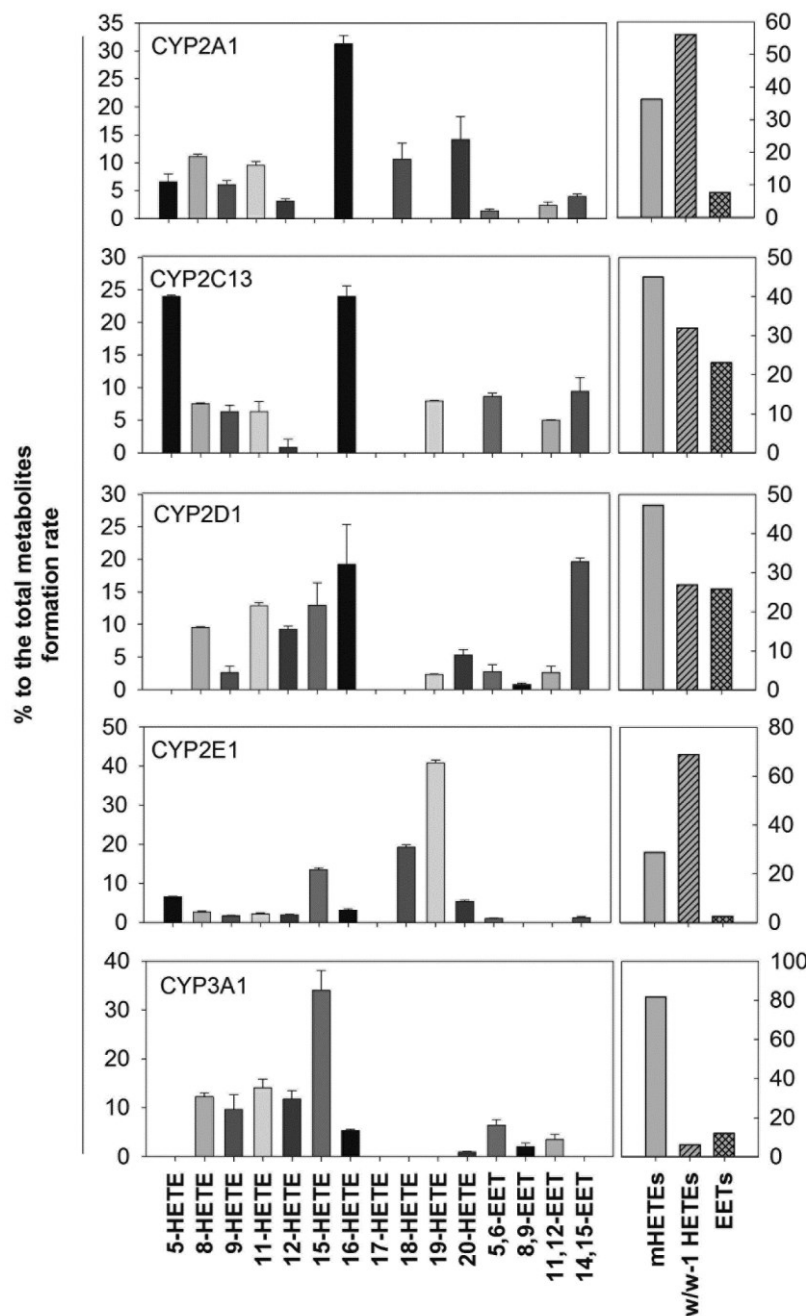


**Figure 3.15. The Metabolic Profile/Regioselectivity of P450-Mediated AA Metabolism by Rat CYP2A1, CYP2C13, CYP2D1, CYP2E1 and CYP3A1.** P450 enzymes (50-100 pmol/mL) were incubated with AA (75  $\mu$ M) for 15-25 min and measured by LC-ESI-MS as described under *Materials and Methods*. Results are presented as mean percentage to the total metabolite formation, and S.E.M. and are based on at least 3 individual experiments.

### 3.3. Determination of the Kinetic Profile of CYP1A1/2- and CYP2C6/11-Mediated AA Metabolism

The high activity toward AA metabolism showed by CYP1A1, CYP1A2, CYP2C6 and CYP2C11 (Fig. 3.13) implies the predominant role of these P450 in AA metabolism *in vivo*. Therefore, the kinetic profile of CYP1A1/2 and CYP2C6/11 was determined. The rate of formation of P450-derived AA metabolites was measured at varied concentration of AA. An inhibition in P450 activity was observed by the excess addition of AA for all the tested P450 enzymes indicating substrate inhibition kinetics. The model that demonstrated the best goodness of fit was eq. 7. The equation describes substrate inhibition in addition to homotropic cooperativity, indicating the binding of more than one AA molecule to the tested enzymes. It was assumed a shared value for  $K_{si}$  among the metabolites for each P450 enzymes;  $K_{si}$  value was 132, 121, 142 and 82.9  $\mu\text{M}$  for CYP1A1, CYP1A2, CYP2C6 and CYP2C11, respectively (Table 3.6). Kinetic parameters mean values are shown for the 4 major metabolites of each enzyme (Table 3.6). The  $K_m$  values were ranging from 40 to 52  $\mu\text{M}$  for the major metabolites of CYP1A1 and from 10 to 11  $\mu\text{M}$  for the major metabolites of CYP1A2 (Table 3.6). On the other hand,  $K_m$  values were ranging from 13 to 36  $\mu\text{M}$  for the major metabolites of CYP2C6 and from 60 to 90  $\mu\text{M}$  for the major metabolites of CYP2C11 (Table 3.6).

**Table 3.6. Enzyme Kinetic Parameters (Mean  $\pm$  S.E.E.) for the Formation of Major Metabolites of CYP1A1/2 and CYP2C6/11.**

		$V_{max}$	$K_m$	$K_{si}$	h	$Cl_{int}$	$R^2$
<b>CYP1A1</b>	16-HETE	1.79 $\pm$ 0.36	41.55 $\pm$ 9.32	131.9 $\pm$ 14.98	2.46 $\pm$ 0.61	0.04	0.88
	17-HETE	2.39 $\pm$ 0.45	51.56 $\pm$ 10.53	131.9 $\pm$ 14.98	2.30 $\pm$ 0.44	0.05	0.96
	18-HETE	3.77 $\pm$ 0.60	48.31 $\pm$ 7.32	131.9 $\pm$ 14.98	2.37 $\pm$ 0.32	0.08	0.96
	19-HETE	7.75 $\pm$ 1.04	39.50 $\pm$ 4.77	131.9 $\pm$ 14.98	2.27 $\pm$ 0.22	0.20	0.96
<b>CYP1A2</b>	16-HETE	2.18 $\pm$ 0.13	10.07 $\pm$ 0.82	121.0 $\pm$ 5.33	2.71 $\pm$ 0.44	0.22	0.98
	17-HETE	0.44 $\pm$ 0.14	11.25 $\pm$ 6.53	121.0 $\pm$ 5.33	2.00 $\pm$ 0.55	0.04	0.99
	18-HETE	0.73 $\pm$ 0.11	9.92 $\pm$ 2.31	121.0 $\pm$ 5.33	2.71 $\pm$ 1.41	0.07	0.98
	19-HETE	1.17 $\pm$ 0.11	9.76 $\pm$ 1.26	121.0 $\pm$ 5.33	3.00 $\pm$ 1.00	0.12	0.98
<b>CYP2C6</b>	12-HETE	2.65 $\pm$ 0.29	18.28 $\pm$ 2.84	141.6 $\pm$ 5.91	2.39 $\pm$ 0.55	0.14	0.96
	15-HETE	0.82 $\pm$ 0.13	13.01 $\pm$ 2.02	141.6 $\pm$ 5.91	5.40 $\pm$ 2.33	0.06	0.93
	11,12-EET	1.49 $\pm$ 0.40	35.93 $\pm$ 18.48	141.6 $\pm$ 5.91	1.44 $\pm$ 0.54	0.04	0.97
	14,15-EET	2.10 $\pm$ 0.39	31.92 $\pm$ 11.07	141.6 $\pm$ 5.91	1.46 $\pm$ 0.38	0.07	0.97
<b>CYP2C11</b>	5,6-EET	4.99 $\pm$ 1.26	90.21 $\pm$ 43.70	82.94 $\pm$ 5.05	1.33 $\pm$ 0.42	0.06	0.90
	8,9-EET	8.36 $\pm$ 1.25	65.57 $\pm$ 10.56	82.94 $\pm$ 5.05	2.13 $\pm$ 0.29	0.13	0.97
	11,12-EET	12.01 $\pm$ 1.38	60.05 $\pm$ 6.78	82.94 $\pm$ 5.05	2.18 $\pm$ 0.20	0.20	0.96
	14,15-EET	7.77 $\pm$ 1.14	62.34 $\pm$ 11.19	82.94 $\pm$ 5.05	1.89 $\pm$ 0.28	0.12	0.98

Data are the mean and S.E.E.  $V_{max}$  (in picomoles per picomoles P450 per minute),  $K_m$  and  $K_{si}$  (in micromolars), and h were determined as per (Eq. 7).  $Cl_{int}$  (in microliters per minute per picomoles P450 of protein) was calculated as  $V_{max}/K_m$ .

### **3.4. Determination of P450-mediated AA Metabolic Profile of Rat Heart, Lungs, Kidneys and Liver Microsomes**

We showed that individual rat recombinant P450 enzymes are able to mediate oxidation of AA to several EETs and HETEs. In order to get insight on whether this also occurs in *in vivo* condition of competing co-expressed P450 enzymes, we studied AA metabolism by heart, lungs, kidneys and liver microsomes. The formation of the three groups of P450-derived AA metabolites, mid-chain HETEs, terminal and subterminal HETEs and EETs, were found to be mediated by heart, lungs, kidneys and liver microsomes (Table 3.7 and Fig. 3.16). EETs were the major metabolites formed, of which 11,12-EET was the most abundant, for heart, kidneys and liver (Table 3.7 and Fig. 3.16). Whereas, for lungs, mid-chain HETEs were the major metabolites, of which 15-HETE was the most abundant (Table 3.7 and Fig. 3.16). As expected, liver exhibited the highest AA-metabolizing activity due to its high P450 content followed by kidneys compared with heart and lungs that exhibited comparable low activity (Table 3.7). For subterminal HETEs, which are the major metabolites for CYP1A1 and CYP1A2, liver had the highest activity then kidneys followed by lungs and heart (Table 3.7).

**Table 3.7. The Formation Rate of P450-derived AA Metabolites Mediated by Heart, Lung, Kidney and Liver Microsomal Fractions Separated from Untreated Rat.**

	Formation rate (pmol/mg protein/min)			
	Heart	Lungs	Kidneys	Liver
<b>5-HETE</b>	-	74.9±6.69	75.6±5.42	60.9±2.67
<b>8-HETE</b>	6.28±0.42	23.4±1.61	27.5±1.81	51.4±2.93
<b>9-HETE</b>	5.34±0.46	20.9±1.22	21.4±1.11	19.5±1.38
<b>11-HETE</b>	6.40±0.41	24.8±2.39	24.9±1.46	103±7.97
<b>12-HETE</b>	7.15±0.48	34.6±2.21	24.3±1.30	84.0±6.98
<b>15-HETE</b>	-	81.3±5.47	90.1±5.33	202±12.8
<b>16-HETE</b>	2.49±0.23	2.47±0.17	25.5±1.44	234±6.68
<b>17-HETE</b>	-	-	-	70.3±1.79
<b>18-HETE</b>	-	-	-	-
<b>19-HETE</b>	0.1±0.03	0.45±0.02	20.0±1.46	181±6.96
<b>20-HETE</b>	0.49±0.07	1.85±0.11	258±14.5	546±29.4
<b>5,6-EET</b>	7.98±0.86	19.1±1.18	15.4±1.68	256±6.79
<b>8,9-EET</b>	11.8±0.80	10.2±0.57	126±6.97	505±31.8
<b>11,12-EET</b>	26.6±1.04	20.5±1.20	225±15.6	883±47.8
<b>14,15-EET</b>	22.6±1.41	16.0±1.27	86.8±5.55	364±35.8

Data are the mean ± S.E.M. based on at least 3 individual experiments.

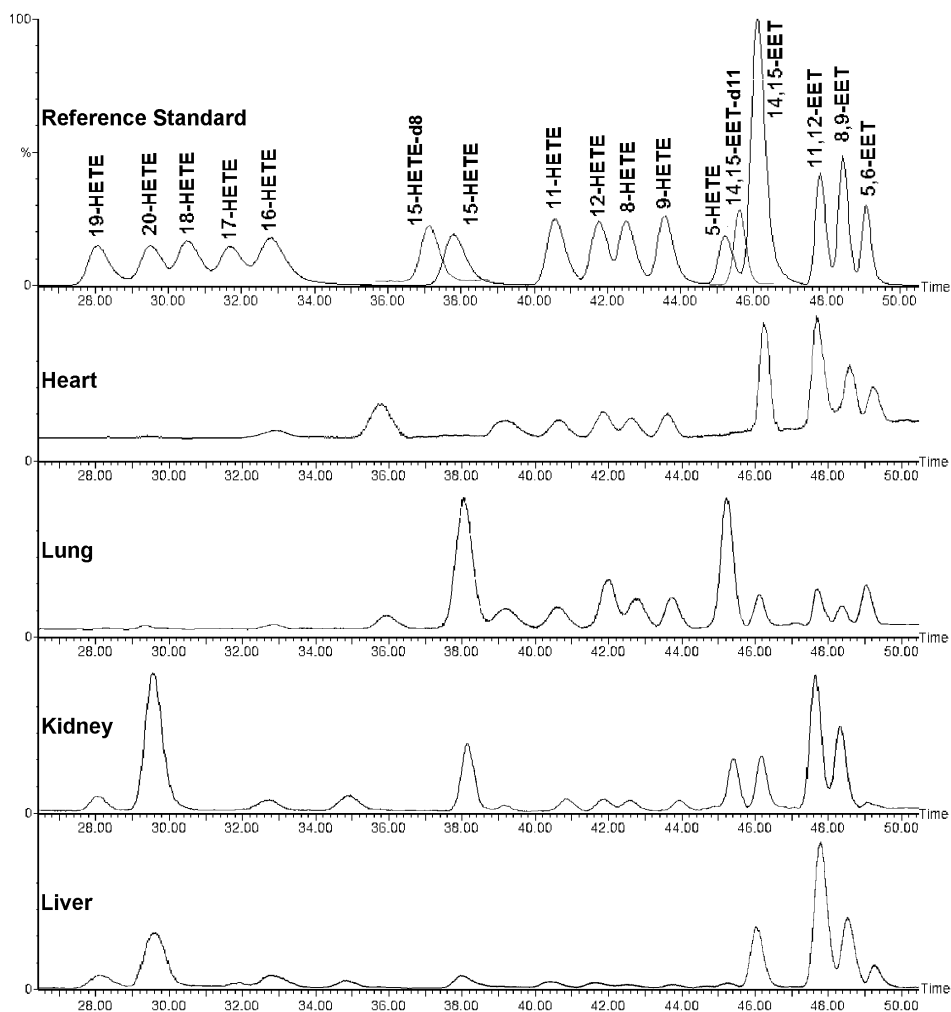


**Figure 3.16. P450-Mediated AA Metabolite Formation by Heart, Lung, Kidney and Liver Microsomes Separated from Untreated Rats.** Microsomal protein of heart, lungs, kidneys or liver (100  $\mu\text{g}$ ) was incubated with AA (75  $\mu\text{M}$ ) for 30 min, injected to LC-ESI-MS, and the resulted chromatograms and the reference standard were determined as described under *Materials and Methods*.

### **3.5. Determination of the Contribution of CYP1A1/2 to AA Metabolism in Rat Heart, Lungs, Kidneys and Liver**

Our findings showed that CYP1A1 and CYP1A2 have high AA-metabolizing activity compared with other rat P450. However, the contribution of CYP1A1 and CYP1A2 to tissue-mediated AA metabolism has never been studied before. Accordingly, the role of CYP1A1 and CYP1A2 in AA metabolism has been underestimated. In order to determine the contribution of these two enzymes to AA metabolism in rat organs, we determined; 1) The effect of CYP1As inhibition by selective CYP1As chemical inhibitor,  $\alpha$ -NF, and by anti-CYP1As antibodies, and 2) the effect of CYP1As induction by an aryl hydrocarbon receptor agonist, (3-MC), on the metabolism of AA mediated by microsomal fractions of heart, lungs, kidneys and liver. Combining the results of these three experiments would allow the determination of the specific contribution of CYP1As to AA metabolism in different rat organs.

With respect to CYP1As chemical inhibition, 6  $\alpha$ -NF concentrations were tested for CYP1As inhibition by 7-ER and 7-MR dealkylation assays. Consequently, 40 and 160 nM of  $\alpha$ -NF, which caused a 28% and 95% inhibition of 7-ER dealkylation activity, respectively, and a 41% and 63% inhibition of 7-MR dealkylation activity, respectively, were tested for their effect on AA metabolism.  $\alpha$ -NF at 40 nM significantly inhibited liver-mediated formation of 16- and 19-HETE by 24.3% and 25.9%, respectively (Table 3.8). Whereas,  $\alpha$ -NF at 160 nM significantly inhibited lung-mediated formation of 16- and 19-HETE by 37.5% and 80.2%, respectively, as well as liver-mediated formation of 16- and 19-HETE by 43.6% and 52%, respectively (Table 3.8).

**Table 3.8. The Inhibitory Effect of CYP1As Inhibitor,  $\alpha$ -Naphthoflavone on P450-Mediated AA Metabolism by Heart, Lung, Kidney and Liver Microsomal Fractions Separated from Untreated Rat.**

	% Difference							
	Heart		Lungs		Kidneys		Liver	
	40 nM	160 nM	40 nM	160 nM	40 nM	160 nM	40 nM	160 nM
<b>5-HETE</b>	-	-	-12.1±7.7	-15.3±2.6	4.0±4.3	1.9±5.9	-3.6±2.6	-6.6±4.8
<b>8-HETE</b>	3.3±4.7	-7.3±1.2	9.5±8.8	14.1±7.8	8.6±1.7	-3.2±7.4	-2.8±2.3	-1.3±2.0
<b>9-HETE</b>	0.2±0.7	-12.5±2.5	-12.0±8.3	-16.1±3.3	0.1±1.9	-4.5±5.0	-4.3±1.8	-9.1±6.1
<b>11-HETE</b>	12.8±4.3	-3.7±7.3	17.0±10.0	-9.4±2.5	14.8±12.0	5.5±1.9	-2.3±1.9	-4.5±2.1
<b>12-HETE</b>	9.0±1.0	-1.0±3.8	-28.7±17.8	-9.5±5.7	8.1±1.9	-0.2±5.8	-3.4±2.6	-9.6±0.2*
<b>15-HETE</b>	-	-	-25.6±8.2	-18.6±3.3	11.7±4.8	4.7±4.2	-1.7±2.1	-7.5±4.9
<b>16-HETE</b>	13.8±12.7	-8.7±6.0	-15.3±5.6	-37.5±1.0*	18.0±6.1	21.3±12.2	-24.3±0.7*	-43.6±2.2*
<b>19-HETE</b>	3.6±6.5	-8.0±8.9	-36.6±37.5	-80.2±18.8*	21.8±9.7	10.0±2.4	-25.9±0.5*	-52.0±1.2*
<b>20-HETE</b>	20.3±2.6	-15.8±4.9	-10.3±4.7	-18.2±5.2	23.1±15.8	7.5±3.1	-1.8±1.3	-7.9±4.4
<b>5,6-EET</b>	-5.8±2.6	-15.4±13.7	-34.2±17.1	4.8±8.8	22.7±8.4	23.4±14.6	-1.3±6.2	-8.6±6.8
<b>8,9-EET</b>	-1.2±4.1	-11.1±6.8	-7.8±11.7	10.1±3.5	16.7±9.0	7.5±5.4	-9.0±4.3	-9.2±8.8
<b>11,12-EET</b>	2.6±10.5	-22.6±1.2*	-8.6±5.8	5.2±5.2	11.5±7.6	4.6±5.4	-7.6±7.6	-7.8±4.1
<b>14,15-EET</b>	-6.7±4.7	-13.2±10.0	27.6±8.8	-7.0±5.9	6.0±3.9	5.3±5.4	-5.4±5.4	-15.8±1.8*

Data are based on at least 3 individual experiments. \* indicates the inhibition was significant at  $p < 0.05$  compared to control incubates.

In agreement with chemical inhibition results, immunoinhibition of CYP1As resulted in a significant decrease in lung-, kidney- and liver-mediated formation of 19-HETE by 83.9%, 26.5% and 66.2%, respectively (Table 3.9). Also, liver-mediated formation of 16-HETE was also significantly decreased by 41.2% (Table 3.9). CYP1As inhibition resulted in more pronounced effects on liver-mediated AA metabolism, which included not only terminal and subterminal HETEs but also mid-chain HETEs and EET formation (Table 3.9). 14,15-EET formation was significantly inhibited (15.8%) by  $\alpha$ -NF, whereas, EET formation was significantly inhibited (52% average) by anti-CYP1As antibodies. For mid-chain HETEs, 12-HETE was significantly inhibited (9.6%) by  $\alpha$ -NF, whereas, 8-, 11-, 12- and 15-HETE formation was significantly inhibited (38% average) by anti-CYP1As antibodies (Table 3.9). For heart, inhibition of CYP1As did not result in any significant alteration in AA metabolism, except the inhibition of 11,12-EET formation (22.6%) by  $\alpha$ -NF (Tables 3.8 & 3.9).

**Table 3.9. The Inhibitory Effect of Anti-CYP1As Antibodies on P450-Mediated AA Metabolism by Heart, Lung, Kidney and Liver Microsomal Fractions Separated from Untreated Rat.**

	% Difference			
	Heart	Lungs	Kidneys	Liver
<b>5-HETE</b>	-	5.4±2.2	11.3±4.8	15.6±5.0
<b>8-HETE</b>	14.1±3.2	14.3±1.6	-5.7±5.7	-30.9±4.5*
<b>9-HETE</b>	17.1±2.9	12.9±1.5	0.3±3.1	-13.8±6.7
<b>11-HETE</b>	14.3±0.3	17.2±6.3	-5.2±3.2	-41.7±4.2*
<b>12-HETE</b>	14.0±0.7	11.6±3.0	-6.7±1.2	-35.6±4.8*
<b>15-HETE</b>	-	14.4±6.9	-0.6±1.2	-39.7±1.8*
<b>16-HETE</b>	17.9±10.0	5.2±2.4	-7.5±0.9	-41.2±2.1*
<b>17-HETE</b>	-	-	-	-
<b>18-HETE</b>	-	-	-	-
<b>19-HETE</b>	5.6±8.7	-84.0±4.6*	-26.5±1.2*	-66.2±3.6*
<b>20-HETE</b>	7.8±4.6	-14.0±2.1	-12.0±4.2	-15.4±4.1
<b>5,6-EET</b>	-8.0±2.8	11.7±0.3	0.9±2.1	-43.4±3.1*
<b>8,9-EET</b>	15.5±2.7	16.9±0.8	-19.4±12.2	-59.1±0.9*
<b>11,12-EET</b>	12.2±1.0	4.0±1.5	-22.7±32.3	-54.5±1.6*
<b>14,15-EET</b>	17.5±8.6	3.9±2.6	-24.6±6.8	-51.6±0.8*

Data are based on at least 3 individual experiments. \* indicates the inhibition was significant at  $p < 0.05$ .

On the other hand, 3-day treatment of 3-MC led to a significant induction in CYP1As activities in all four organs compared with corn-oil-treated (control) group. In heart, lungs, kidneys and liver, CYP1A1 activity measured by 7-ER dealkylation assay showed a 13500%, 2070%, 1120% and 1160% induction, whereas, CYP1A2 activity measured by 7-MR dealkylation showed a 300%, 310%, 510% and 3600% induction, respectively, compared with control group (Fig. 3.17). This observed induction in CYP1As resulted in a significant increase in subterminal HETE formation for all four organs. The

formation of 16-, 17-, 18- and 19-HETE was significantly increased by 131%, 183%, 415% and 750%, respectively, for heart, 171%, 1200%, 364% and 844%, respectively, for lungs, and 200%, 404%, 2570% and 213%, respectively, for liver, compared with control group (Fig. 3.18). For kidneys, the formation rate of 17- and 18-HETE was significantly increased by 1380% and 536%, compared with control group (Fig. 3.18). Additionally, there was a 142% increase in 12-HETE formation, while, there was a 51% and 34% decrease in 11,12-EET and 20-HETE formation, respectively, in 3-MC-treated livers compared with control livers (Fig. 3.18).

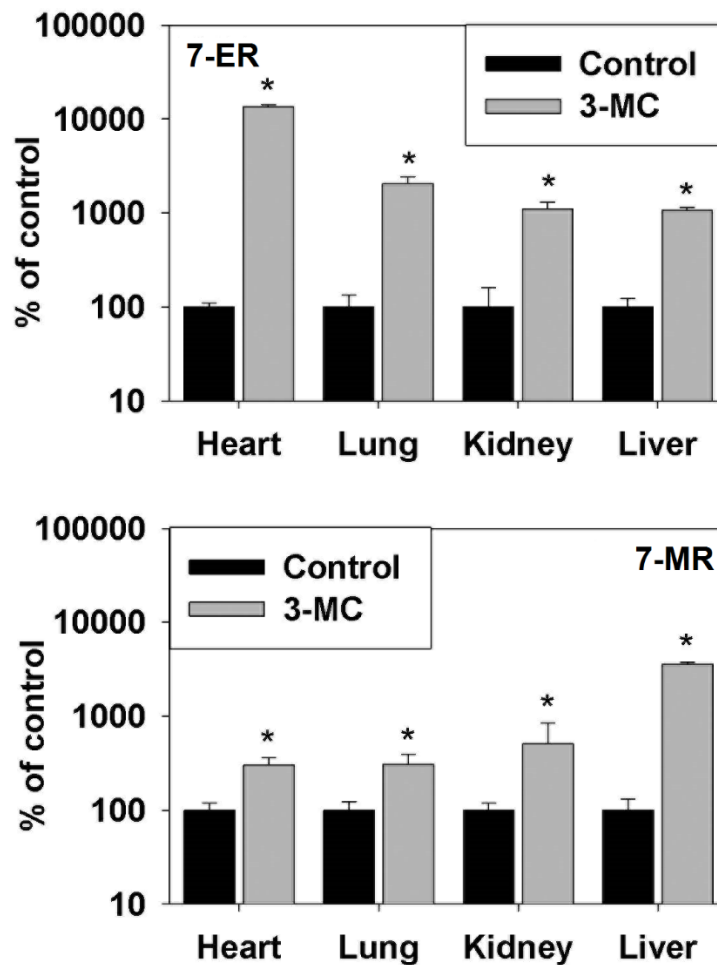


**Figure 3.17. The Effect of 3-MC Treatment on CYP1A1 and CYP1A2 Activity of Rat Heart, Lung, Kidney and Liver Microsomes.** Microsomal protein of heart, lungs, kidneys or liver was incubated with 7-ER or 7-MR for 30 min as described under *Materials and Methods*. Fluorescence associated with resorufin formation was measured at excitation and emission wavelengths of 535 and 585 nm Results are presented as mean and S.E.M. (n=4). \* indicates the difference was significant at  $p < 0.05$ .

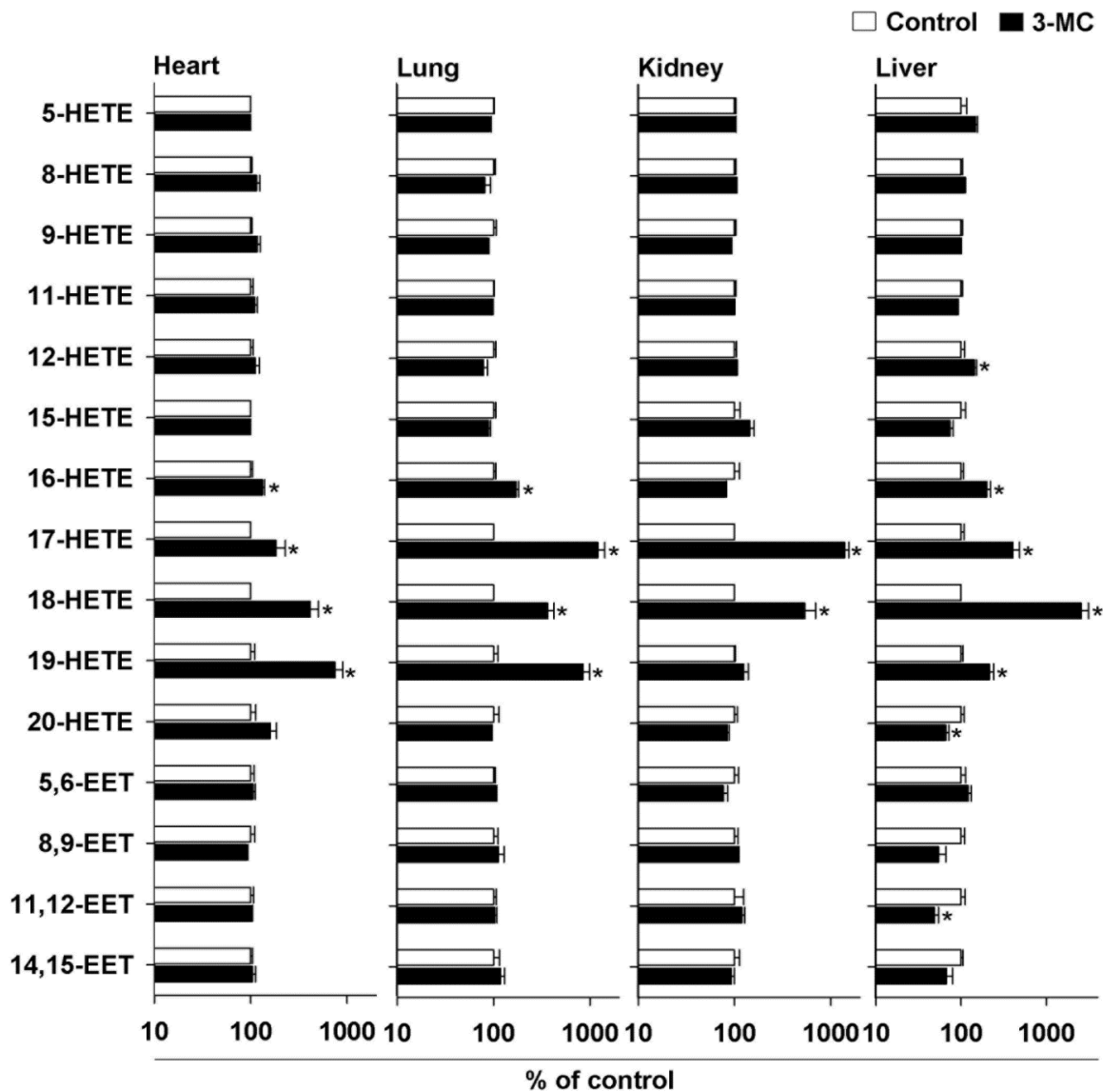


**Figure 3.18. The Effect of 3-MC Treatment on P450-mediated AA Metabolism by Rat Heart, Lung, Kidney and Liver Microsomes.** Microsomal protein of heart, lungs, kidneys or liver was incubated with AA for 30 min, and AA metabolites were measured by LC-ESI-MS as described under *Materials and Methods*. The amounts of undetectable metabolites in control samples were assumed to be 0.05 ng (the lowest lower limit of quantitation) per injection volume. Results are presented as mean and S.E.M. (n=4). Student t test (\* P < 0.05 compared with control group).

## **4. Repurposing Resveratrol and Fluconazole to Modulate Human Cytochrome P450-Mediated Arachidonic Acid Metabolism**

### **4.1. AA-Metabolizing Activity and Metabolic Profile of Recombinant Cytochrome P450 Enzymes**

In the current study, we tested a large group of human recombinant P450 enzymes for their AA-metabolizing activities and metabolic profiles. Interestingly, we found that all tested P450 enzymes were able to mediate AA-metabolism, but with variable activities and characteristic profiles. On the other hand, there was no detectable formation of P450-derived AA metabolites by NADPH reductase and cyb5 alone in control samples.

Among the tested P450 enzymes, CYP2C19 was of the highest activity followed by CYP1A1 and CYP4F3B, and then CYP4A11 and CYP4F2 (Fig. 3.19). The rate of CYP2C19-mediated AA consumption was 32.2 pmol/pmol P450/min. In contrast, CYP3A4 exhibited the lowest AA-metabolizing activity, whose rate was 0.95 pmol/pmol P450/min (Fig. 3.19). CYP4 family, collectively, showed the highest activity toward AA compared with CYP1, CYP2 and CYP3 families. Noteworthy, all tested P450 enzymes, except CYP1A2, mediated the hydroxylation of AA (mid-chain, terminal and subterminal HETE formation) more efficiently than AA epoxidation (Fig. 3.19). For AA epoxidation, CYP2C19 was the highest P450 enzyme in the formation rates of the four EETs, 1.7, 5.54, 1.68, 4.88 pmol/pmol P450/min for 5,6-, 8,9-, 11,12-, and 14,15-EET, respectively (Fig. 3.20). Also, CYP1A2, followed by CYP1A1, showed high EET-formation activity emphasizing their importance as P450 epoxygenase (Figs. 3.19 & 3.20). CYP2J2 was ranked the third highest enzyme in EET formation rate (Fig. 3.19); CYP2J2-mediated formation rate of 5,6-, 8,9-, 11,12-, and 14,15-EET was 0.05, 0.12, 0.09, and 0.21 pmol/pmol P450/min, respectively (Fig. 3.20). With respect to hydroxylation, almost all P450 enzymes mediated

the hydroxylation of AA at its terminal and subterminal regions more efficiently than at the double bond region (mid-chain HETEs). Although CYP1A1, CYP1A2, CYP2C19, CYP2C9 and CYP4F12 showed the highest mid-chain HETE formation rates, only CYP1B1 and CYP2C18 mediated the formation of mid-chain HETEs more than the formation of EETs or terminal and subterminal HETEs (Fig. 3.19). Their mid-chain HETE formation rates were 0.38, and 0.62 pmol/pmol P450/min for CYP1B1, and CYP2C18, respectively (Fig. 3.19). With respect to terminal hydroxylation, CYP1A1 was the most active enzyme among tested P450 enzymes in the formation of 16-, 17-, and 18-HETE (1.81, 1.1 and 3 pmol/pmol P450/min, respectively), and the second most active enzyme for 19-HETE (6.6 pmol/pmol P450/min) after CYP2C19 (Fig. 3.19). CYP2C19 also mediated the formation of 16-, 17-, 18-, and 19-HETE at a specific activity of 0.46, 0.31, 0.62, and 11.34 pmol/pmol P450/min, respectively (Fig. 3.20). On the other hand, the most active 20-HETE forming P450 enzymes were CYP4A11, CYP4F2, CYP4F3A and CYP4F3B with specific activity of 7.17, 5.94, 1.06, and 16.25 pmol/pmol P450/min, respectively (Fig. 3.20).

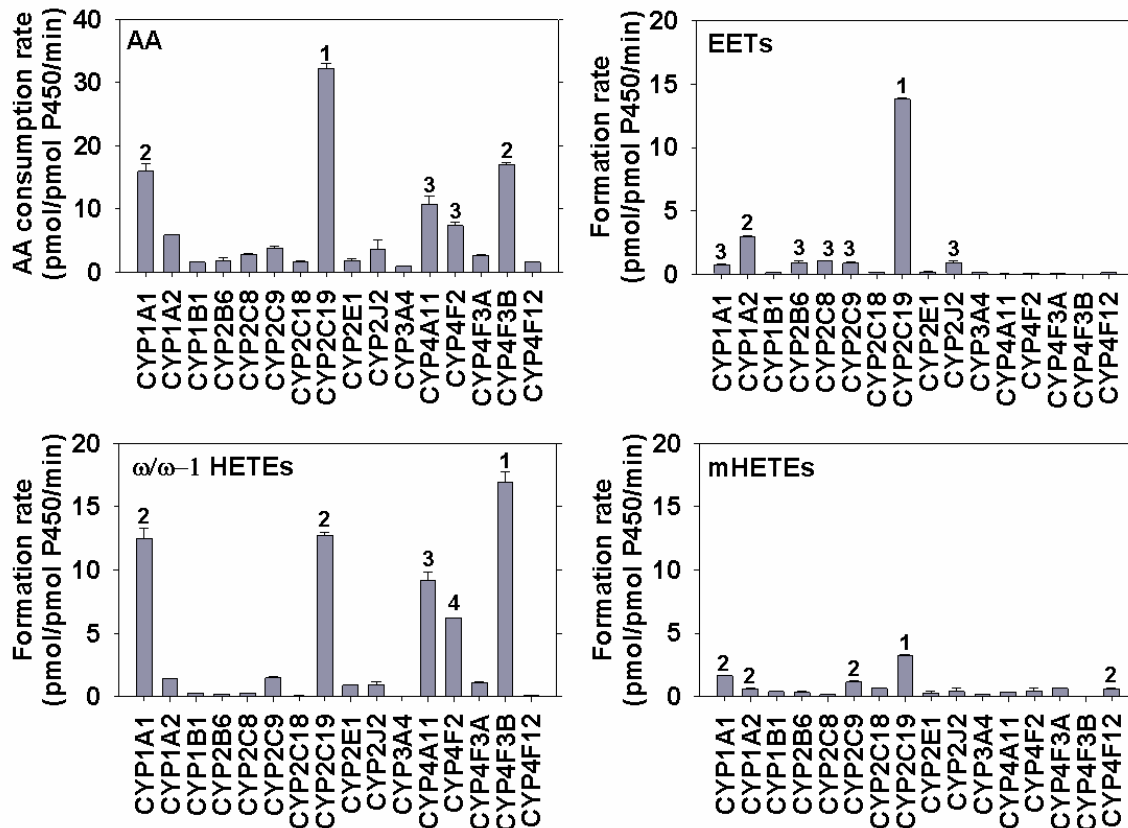


**Figure 3.19. The Metabolizing Activity of Human Recombinant P450 Enzymes: AA Consumption, and EETs, Mid-Chain HETEs (mHETE) and Terminal and Subterminal HETEs ( $\omega/\omega-1$  HETEs) Formation.** Recombinant P450 enzymes were incubated with AA (75  $\mu$ M) for 15-20 min, and AA and its metabolites were measured by LC-ESI-MS, as described under *Materials and Methods*. Results are presented as mean and S.E.M., based on at least 3 individual experiments. Using one-way analysis of variance followed by a Tukey's post hoc test, the five most active P450 enzymes were identified (indicated by Arabic numbers); different numbers indicate significantly different activities at  $p < 0.05$ .

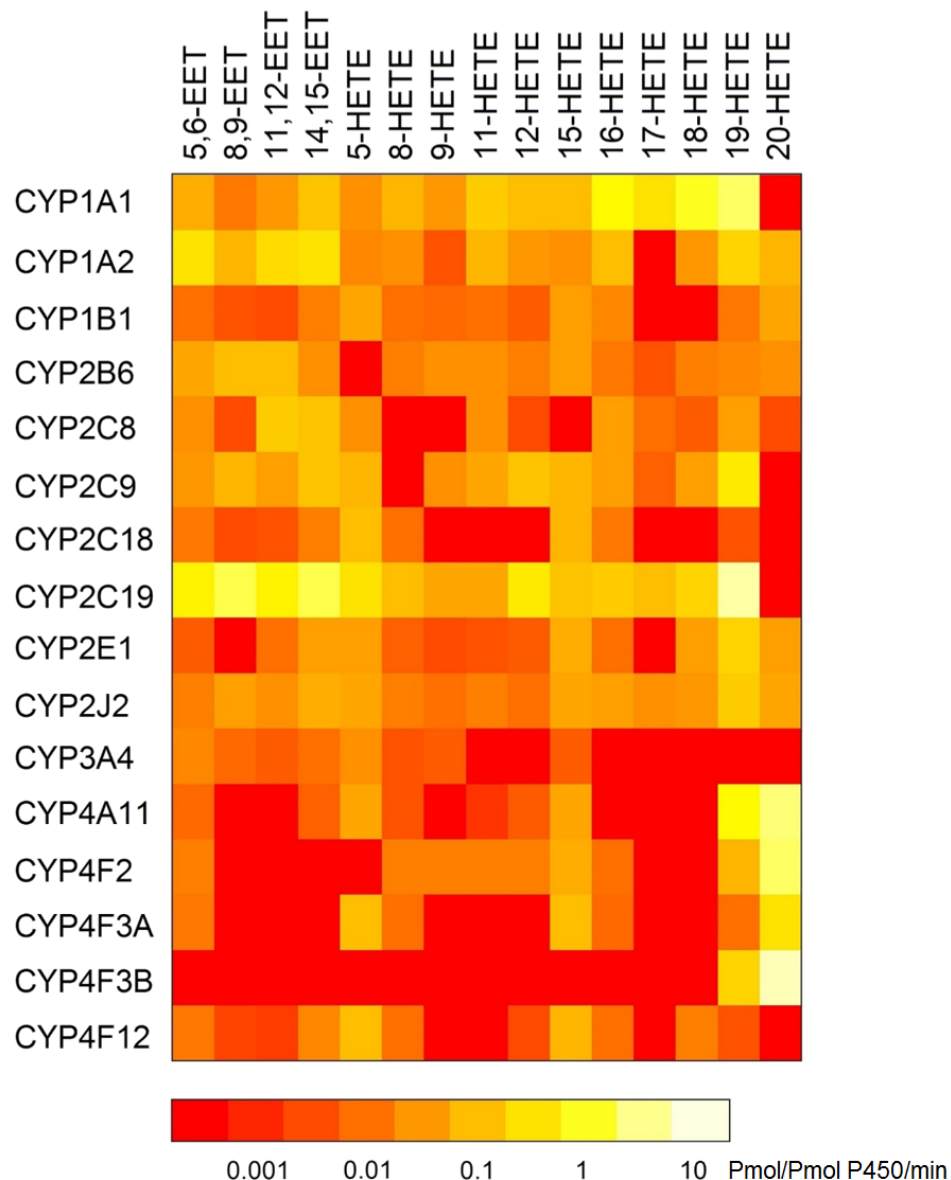


**Figure 3.20. Heat Map of the Activities of P450-Derived AA Metabolite Formation of Human Recombinant P450 Enzymes.** Recombinant P450 enzymes were incubated with AA for 15-20 min, and P450-derived AA metabolites were measured by LC-ESI-MS, as described under *Materials and Methods*. Results are presented referring to the color key at the right side. The numerical values are shown in the supplementary Tables S1, S2 and S3.

#### 4.2. AA-Metabolizing Activity and Metabolic Profile of Human Microsomes

We investigated the AA-metabolism by microsomes separated from human liver and kidneys. There was low NADPH-independent formation of mid-chain HETEs, and therefore they were subtracted from the rates of P450-dependent formation of mid-chain HETEs. Liver microsomes showed, expectedly, the highest overall AA-metabolizing activity at all AA concentrations; liver-mediated AA metabolism was 2-fold higher than that of kidneys at 75  $\mu$ M AA (Fig. 3.21). Increasing AA concentration from 7.5 to 75  $\mu$ M led to an increase in metabolite formation rates, while increasing AA concentration from 75 to 750  $\mu$ M led to the same formation rates of almost all metabolites (Fig. 3.21). In the kidneys, we only detected the formation of 5,6- and 8,9-EET and 18-HETE at 75  $\mu$ M AA but not at 7.5 or 750  $\mu$ M (Fig. 3.21). The most prominent metabolites for both liver and kidneys was 20-HETE (111 and 64 pmol/mg protein/min at 75 $\mu$ M AA, respectively), followed by 19-HETE (18 and 10 pmol/mg protein/min at 75 $\mu$ M AA, respectively) (Fig. 3.21).

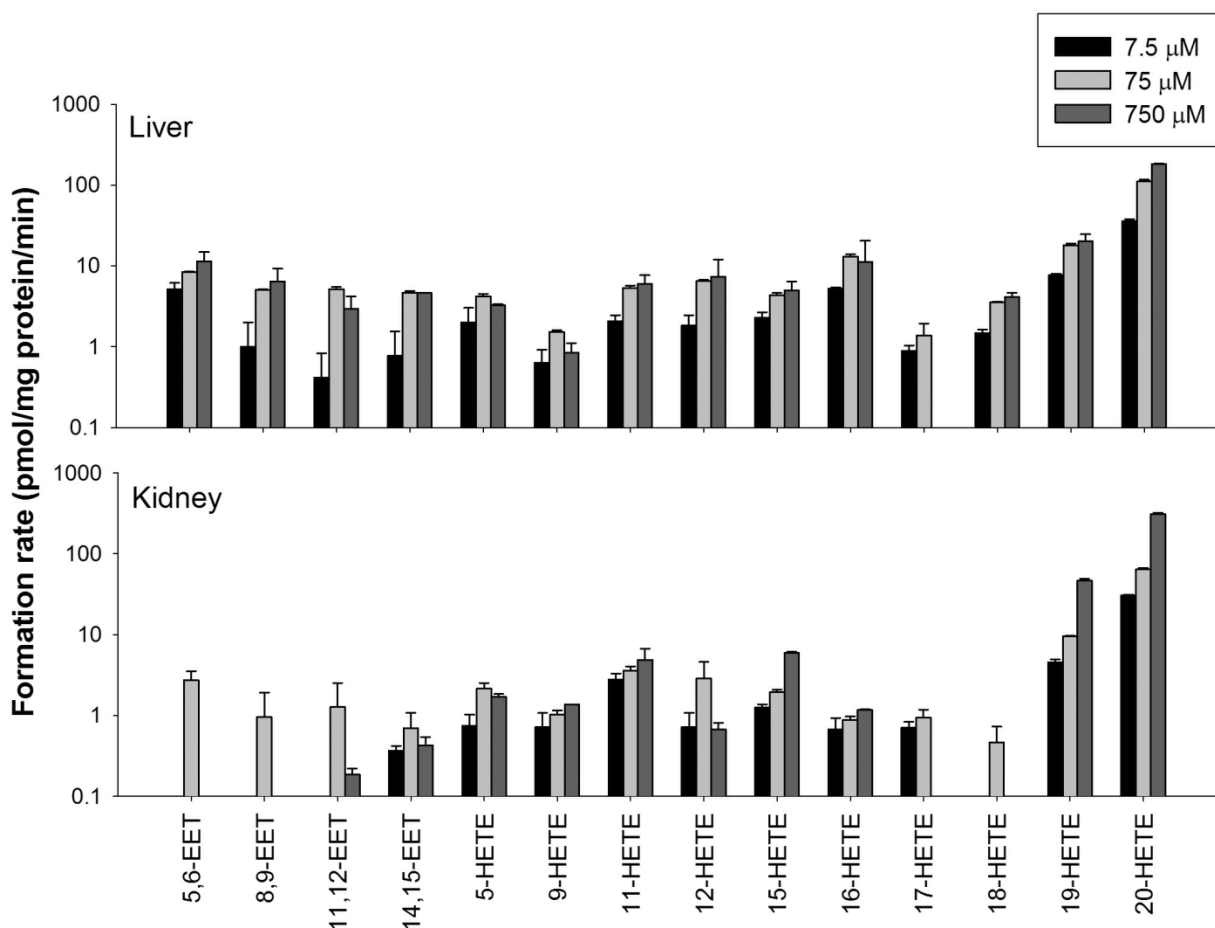


**Figure 3.21. The Formation of P450-Derived AA Metabolites Mediated by Human Liver and Kidney Microsomes.** Microsomal protein from liver or kidneys was incubated with 7.5, 75 and 750  $\mu$ M of AA for 30 minutes, and P450-derived AA metabolites were measured by LC-ESI-MS, as described under *Materials and Methods*. Results are presented as mean and S.E.M., based on at least 3 individual experiments.

### 4.3. Effect of Cytochrome P450 Inhibition on P450-mediated AA-Metabolism by Human Liver Microsomes

In *in vitro* and animal studies, three investigational agents are widely used to modulate P450-mediated AA metabolism, namely MS-PPOH to inhibit P450 epoxygenases (Liu, Li et al. 2011), HET0016 to inhibit P450  $\omega$ -hydroxylases (Miyata, Taniguchi et al. 2001), and  $\alpha$ -NF to inhibit CYP1 family and subterminal HETE formation (Huang, Temple et al. 2007, Food-and-Drug-Administration 2014). We tested the effect of these investigational agents on AA metabolism to help evaluate the selectivity and effectiveness of the tested clinically-approved drugs.

With respect to MS-PPOH, its effect on hepatic AA metabolism was selective to 11,12- and 14,15-EETs and 12-HETE at either the low (5  $\mu$ M) or the high (50  $\mu$ M) concentrations (Table 3.10). The formation rates of these metabolites were significantly inhibited by an average of 22% and 51% by 5 and 50  $\mu$ M of MS-PPOH, respectively (Table 3.10). On the other hand, HET0016 selectivity was impaired by increasing its concentration from 50 nM to 1  $\mu$ M. At 50 nM, HET0016 caused a significant inhibition by 9 and 67% of the hepatic formation rate of 19- and 20-HETEs, respectively (Table 3.10). While at 1  $\mu$ M, HET0016 significantly altered the formation of 5,6-EET and 5-, 11-, 12-, and 15-HETEs in addition to 9-, 19- and 20-HETEs (Table 3.10). For 5,6-EET and 9-, 19- and 20-HETEs, there was an inhibition in the formation rate by 35, 35, 30 and 98%, respectively, and for 5-, 11-, 12-, and 15-HETEs, there was an increase in the formation rate by 36, 18, 27 and 46%, respectively, by HET0016 (Table 3.10). Regarding  $\alpha$ -NF, it significantly and selectively inhibited the formation of subterminal HETEs, 16- and 18-HETEs in liver by 14% at the low concentration (40 nM); whereas, at 160 nM,  $\alpha$ -NF lost its selectivity and inhibited the formation of 5 other metabolites in addition to 16- and 18-HETEs (Table 3.10).

**Table 3.10. Effect (Mean  $\pm$  S.E.M.) of Different Selective Investigational P450 Inhibitors on P450-Mediated AA Metabolism by Human Liver Microsomes Based on at Least 3 Individual Experiments.**

P450 inhibitor		% Difference <sup>a</sup>												
		5,6-EET	8,9-EET	11,12-EET	14,15-EET	5-HETE	9-HETE	11-HETE	12-HETE	15-HETE	16-HETE	18-HETE	19-HETE	20-HETE
$\alpha$ -NF	40 nM	23 $\pm$ 10	13 $\pm$ 9	16 $\pm$ 4	28 $\pm$ 17	-1 $\pm$ 7	25 $\pm$ 10	29 $\pm$ 19	32 $\pm$ 26	10 $\pm$ 3	-14 $\pm$ 2*	-14 $\pm$ 3*	5 $\pm$ 2	4 $\pm$ 1
	160 nM	-64 $\pm$ 2*	-9 $\pm$ 5	32 $\pm$ 11	-21 $\pm$ 4*	-20 $\pm$ 6*	-4 $\pm$ 6	-20 $\pm$ 4*	15 $\pm$ 3	-17 $\pm$ 3*	-32 $\pm$ 6*	-17 $\pm$ 4*	-8 $\pm$ 5	0 $\pm$ 4
MS-PPOH	5 $\mu$ M	-29 $\pm$ 15	-12 $\pm$ 7	-15 $\pm$ 4*	-18 $\pm$ 5*	-9 $\pm$ 18	-52 $\pm$ 19	-30 $\pm$ 11	-32 $\pm$ 6*	-22 $\pm$ 10	13 $\pm$ 16	-4 $\pm$ 19	-10 $\pm$ 6	-8 $\pm$ 6
	50 $\mu$ M	-33 $\pm$ 30	-28 $\pm$ 10	-46 $\pm$ 5**	-51 $\pm$ 5**	-26 $\pm$ 20	-49 $\pm$ 23	-55 $\pm$ 37	-57 $\pm$ 9*	-48 $\pm$ 21	-16 $\pm$ 19	14 $\pm$ 17	5 $\pm$ 5	-1 $\pm$ 7
HET0016	50 nM	7 $\pm$ 9	8 $\pm$ 2	26 $\pm$ 9	18 $\pm$ 5	6 $\pm$ 3	-22 $\pm$ 3	4 $\pm$ 10	2 $\pm$ 7	29 $\pm$ 12	3 $\pm$ 5	10 $\pm$ 7	-9 $\pm$ 2*	-67 $\pm$ 7**
	1000 nM	-35 $\pm$ 1**	5 $\pm$ 2	21 $\pm$ 13	28 $\pm$ 7	36 $\pm$ 2**	-35 $\pm$ 5*	18 $\pm$ 2*	27 $\pm$ 2*	46 $\pm$ 4**	3 $\pm$ 1	31 $\pm$ 18	-30 $\pm$ 2**	-98 $\pm$ 7**

<sup>a</sup> Data are based on at least three individual experiments; \* significant at P = 0.05; \*\* significant at P = 0.01.

According to our recombinant P450 data, CYP1As, CYP2Cs and CYP4s have the most prominent activity toward AA metabolism. Consequently, clinically-approved drugs we tested in our study are: Res to inhibit CYP1As (Chang, Chen et al. 2001), Flu to inhibit CYP2C9 and to a lower extent CYP2C19 (Niwa, Shiraga et al. 2005), Tic to inhibit CYP2C19 and to a lower extent CYP2C9 (Ko, Desta et al. 2000). Regarding CYP4s, we could not find a direct inhibitor for them; however, it has been previously reported that  $\omega$ -hydroxylation of fatty acids by CYP4s is dependent on cyb5 (Wang, Stec et al. 1996, Adas, Salaun et al. 1999, Xu, Falck et al. 2004). Therefore, we explored the effect of cyb5 inhibition on hepatic AA metabolism by PTU, reported to exhibit selective inhibitory activity against cyb5 (Lee and Kariya 1986). Also, we used Dan to inhibit CYP2J2 and Ser to inhibit CYP2B6 (Walsky, Astuccio et al. 2006, Lee, Jones et al. 2012).

Res at low and high concentrations significantly and selectively inhibited the formation rate of 16-, 18- and more interestingly 20-HETE by an average of 22 and 46%, respectively (Table 3.11). A significant decrease was observed in the hepatic formation rates of 8,9- and 14,15-EETs by low concentration of Flu by an average of 24% (Table 3.11). At high concentration of Flu, the formation rates of 11-, 12- and 15-HETEs in addition to 8,9- and 14,15-EETs were significantly decreased by an average of 49% (Table 3.11). At low concentration of Tic, the formation rates of 5,6- and 8,9-EET and 9-, 16-, 18- and 19-HETE were significantly decreased in the liver, whereas, at high concentration of Tic, the formation rates of almost all metabolites were decreased (Table 3.11). The inhibition of CYP2B6 by Ser and inhibition of CYP2J2 by Dan led to modest effects on AA-metabolism. Low concentration of Ser only decreased the formation rate of 18-HETE in liver by 15%, while high concentration of Ser decreased 11,12-EET and 9- and 18-HETEs by an average of 25% (Table 3.11). Similarly, Dan decreased the formation rate of 19-HETE at its high concentration in the liver by 11% (Table 3.11). With respect to PTU, it

did not cause any significant alteration in the hepatic formation rates of the tested metabolites except 20-HETE, whose formation rate was significantly increased by 49% (Table 3.11).

**Table 3.11. Effect (mean ± S.E.M) of Different Selective Clinically-approved P450 Inhibitors on P450-Mediated AA Metabolism by Human Liver Microsomes**

P450 inhibitor		% Difference <sup>a</sup>												
		5,6-EET	8,9-EET	11,12-EET	14,15-EET	5-HETE	9-HETE	11-HETE	12-HETE	15-HETE	16-HETE	18-HETE	19-HETE	20-HETE
<b>Res</b>	<b>1 µM</b>	18±16	-12±7	10±8	0±7	-7±11	-4±5	-17±8	-4±6	34±13	-21±6*	-33±6*	6±1	-12±1**
	<b>10 µM</b>	-28±19	-13±17	-16±8	-9±8	-15±18	-6±2	-23±6	-33±15	-40±18	-40±5**	-65±2**	-5±7	-32±6*
<b>Flu</b>	<b>10 µM</b>	16±5	-22±4*	-9±6	-26±2**	-16±4	-21±12	-19±10	-15±4	-15±9	2±1	2±0	2±4	14±4
	<b>100 µM</b>	-9±9	-61±1**	-21±8	-43±3**	41±40	-12±20	-41±1**	-61±1**	-38±2**	-17±36	-8±10	-11±10	18±13
<b>Tic</b>	<b>10 µM</b>	-49±4**	-29±2**	38±11	-3±7	-5±5	-47±5*	1±5	14±13	-7±3	-14±2*	-10±2*	-18±2*	1±2
	<b>100 µM</b>	-85±3**	-50±15*	32±30	-54±14*	-1±3	-57±5**	-30±4*	-28±13	-36±6*	-27±6*	-41±4**	-43±4**	-21±5
<b>Ser</b>	<b>30 µM</b>	23±11	37±31	11±12	0±4	6±9	-15±10	0±0	31±5	0±5	14±4	-15±3*	20±7	17±5
	<b>300 µM</b>	32±35	-1±11	-19±0**	38±24	34±12	-34±1**	0±0	53±33	21±37	7±12	-21±1**	2±7	46±37
<b>Dan</b>	<b>20 nM</b>	3±10	6±8	24±7	32±10	4±9	-10±9	2±10	5±7	5±3	1±9	-10±4	5±6	2±8
	<b>200 nM</b>	-8±6	2±2	1±1	-2±1	-1±1	-10±3	-3±1	-2±1	-7±3	2±2	-13±5	-11±2*	-1±2
<b>PTU</b>	<b>0.1 mM</b>	-42±17	-6±7	6±5	5±6	32±20	1±8	-4±9	2±4	-12±10	45±20	18±16	2±8	6±7
	<b>1 mM</b>	-36±20	7±9	7±7	17±7	39±17	-23±11	7±6	-7±1	14±15	22±14	14±11	8±5	49±5**

<sup>a</sup> Data are based on at least three individual experiments; \* significant at P = 0.05; \*\* significant at P = 0.01.

#### 4.4. Kinetics of Cytochrome P450-Mediated AA Metabolism Inhibition

To explain how Res decreased the formation rate of 20-HETE, varied concentration of Res (0.03-1000  $\mu\text{M}$ ) was incubated with the dominant hepatic 20-HETE-forming P450 enzymes, CYP4A11, CYP4F2 and CYP4F3B. We found that Res was able to inhibit all of the three P450 enzymes but with different kinetics (Fig. 3.22). For CYP4F2, the  $I_{\text{max}}$  and  $IC_{50}$  mean values were 92% and 4  $\mu\text{M}$ , respectively (Fig. 3.22). Whereas, for CYP4A11, the  $I_{\text{max}}$  and  $IC_{50}$  mean values were 81% and 90  $\mu\text{M}$ , respectively, and for CYP4F3B, the  $I_{\text{max}}$  and  $IC_{50}$  mean values were 100% and 109  $\mu\text{M}$ , respectively (Fig. 3.22).

Also, the kinetics of P450-mediated AA metabolism inhibition by Res and Flu were determined, because their selectivity and effectiveness were comparable to MS-PPOH and HET0016. We found that the formation rates of 11,12- and 14,15-EETs and 16-, 18-, 19- and 20-HETEs showed a significant inverse non-parametric Spearman rank correlation with Res concentration. The  $I_{\text{max}}$  mean values of Res were 99, 100, 79, 69, 61 and 54% for 11,12- and 14,15-EETs and 16-, 18-, 19- and 20-HETEs, respectively (Fig. 3.23). Whereas, the  $IC_{50}$  mean values of Res were 60, 68, 17, 5, 104 and 3  $\mu\text{M}$  for 11,12- and 14,15-EETs and 16-, 18-, 19- and 20-HETEs, respectively (Fig. 3.23). For Flu, the formation rates of 8,9- and 14,15-EETs and 11-, 12- and 15-HETEs were significantly correlated with Flu concentration. The  $I_{\text{max}}$  mean values of Flu were 61, 64, 67, 80 and 57% for 8,9- and 14,15-EETs and 11-, 12- and 15-HETEs, respectively (Fig. 3.23). Whereas, the  $IC_{50}$  mean values of Flu were 13, 27, 28, 28 and 36  $\mu\text{M}$  for 8,9- and 14,15-EETs and 11-, 12- and 15-HETEs, respectively (Fig. 3.23).

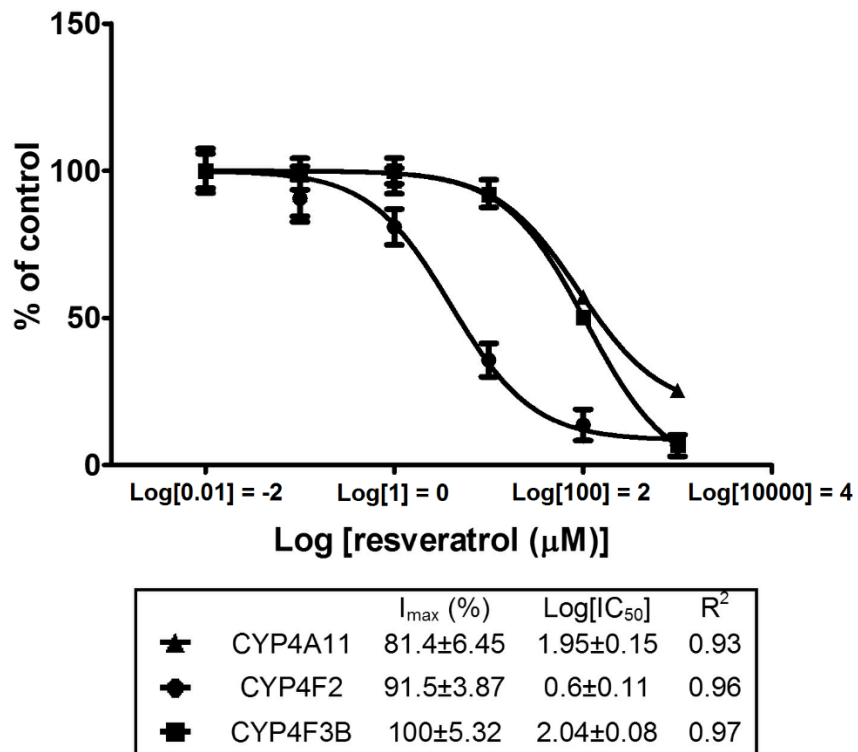
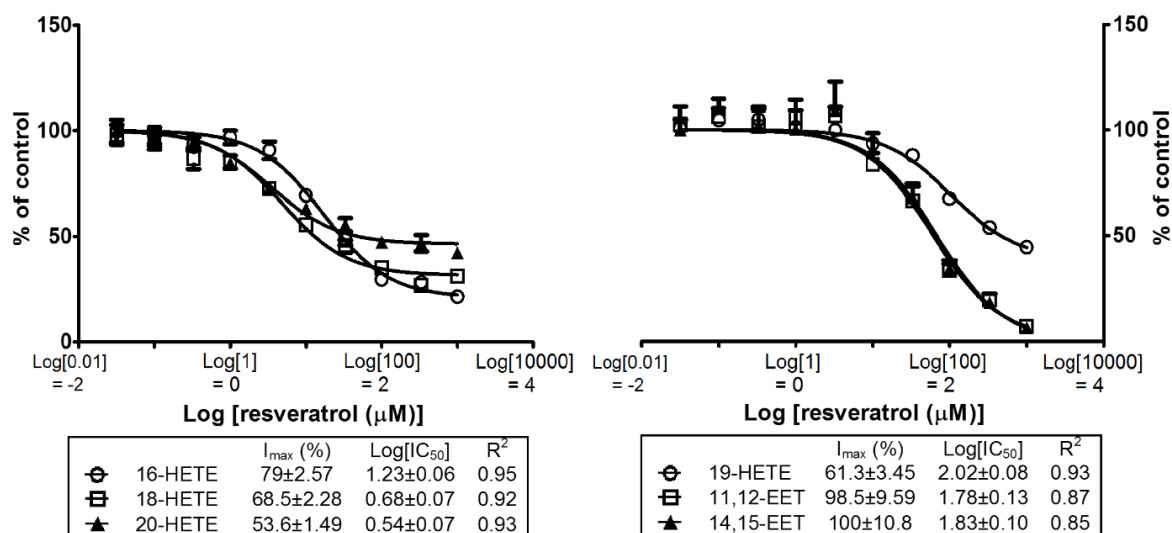


**Figure 3.22. Concentration-Dependent Inhibition of CYP4A11-, CYP4F2- and CYP4F3B-Mediated 20-HETE Formation by Res.** Recombinant P450 enzymes were incubated with AA for 15-20 min and 0.01-1000  $\mu\text{M}$  of Res, and 20-HETE was measured by LC-ESI-MS, as described under *Materials and Methods*. Results are presented as mean and S.E.M., based on at least 3 individual experiments.  $\text{Log}(IC_{50})$  and  $I_{max}$  mean  $\pm$  S.E.E. were determined by Enzyme Kinetics module from GraphPad Prism, version 5.0.

## Resveratrol



## Fluconazole

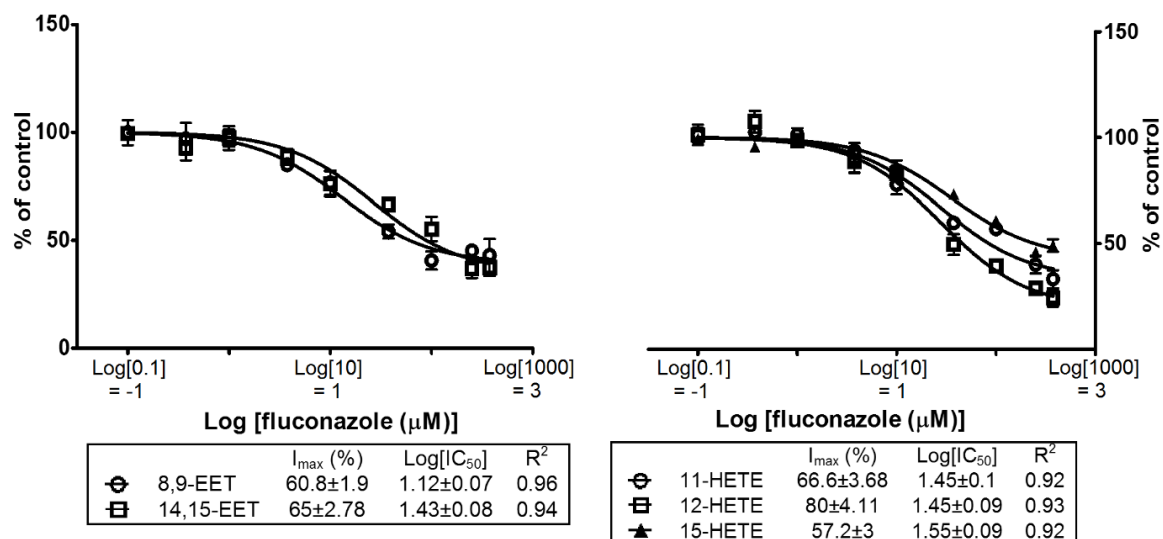


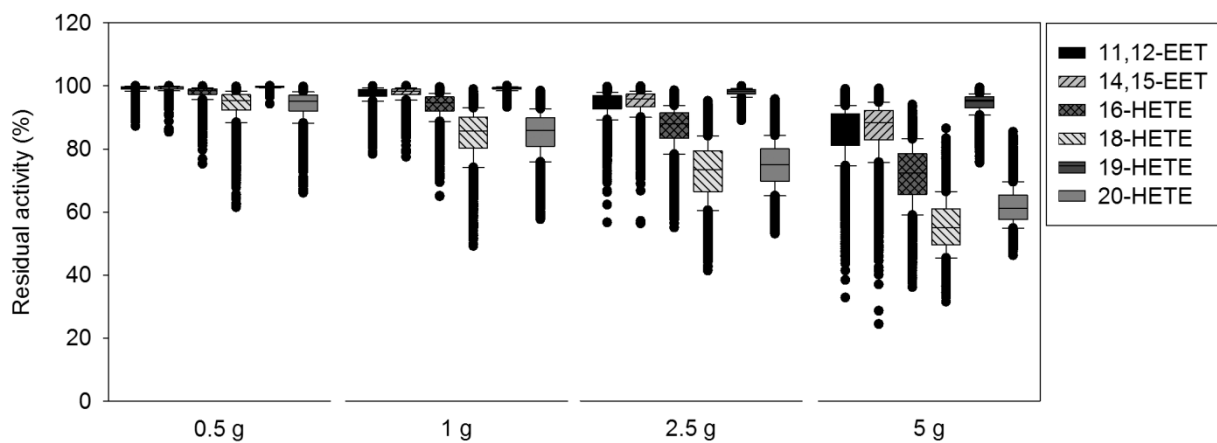
**Figure 3.23. Concentration-Dependent Inhibition of Hepatic Microsomal-Mediated Formation of P450-Derived AA Metabolites by Res and Flu.** Microsomal protein from liver was incubated with AA for 30 minutes, and P450-derived AA metabolites were measured by LC-ESI-MS, as described under *Materials and Methods*. Results are presented as mean and S.E.M, based on at least 3 individual experiments.  $\text{Log}(IC_{50})$  and  $I_{max}$  mean  $\pm$  S.E.E. were determined by Enzyme Kinetics module from GraphPad Prism, version 5.0.

#### 4.5. Simulating the Inhibition of Cytochrome P450-Mediated AA Metabolism after Safe Oral Doses of Res and Flu

To gain insight about the expected inhibition in P450-mediated AA metabolism in humans after safe oral doses of Res and Flu, Monte Carlo simulation was performed to simulate 10,000 human subjects orally administered 0.5, 1, 2.5 or 5 g daily of Res, or 50, 150 or 400 mg of Flu. We used the previously reported human plasma and tissue concentration data combined with the kinetics of AA metabolism inhibition shown above. It has been reported that maximum plasma concentration mean values and SD are  $0.19\pm 0.17$ ,  $0.62\pm 0.43$ ,  $1.45\pm 0.86$  and  $4.24\pm 2.27$   $\mu\text{M}$  for 0.5, 1, 2.5 or 5 g daily of Res, respectively, in humans (Brown, Patel et al. 2010). Also, the reported liver to plasma ratio of Res is 2.49 in humans (Sale, Verschoyle et al. 2004), and uniform distribution of  $\pm 20\%$  was assumed. For Flu, the reported maximum plasma concentration mean values and SD of  $3.04\pm 0.42$ ,  $8.78\pm 1.4$  and  $27.85\pm 5.1$   $\mu\text{M}$  for 50, 150 or 400 mg daily of Flu, respectively, in humans (Ripa, Ferrante et al. 1993, Berl, Wilner et al. 1995), and the reported liver to plasma ratio is 3.4 in humans (Felton, Troke et al. 2014), with  $\pm 20\%$  uniform distribution.

Our simulations predicted that 90% of the human population would experience 2-12%, 6-22% and 17-41% inhibition in 16-HETE, 7-26%, 16-39% and 34-55% in 18-HETE and 7-26%, 16-35% and 31-46% in 20-HETE formation rates after 1, 2.5 and 5 g daily of Res, respectively (Fig. 3.24). In contrast, Res at 0.5 g daily caused very modest inhibitory effect. Similarly, 11,12- and 14,15-EETs as well as 19-HETE were not effectively inhibited by Res at any of the tested doses (Fig. 3.24). For Flu, 50, 150 and 400 mg of Flu led to an inhibition of 22-31%, 37-46% and 50-56% for 8,9-EET, 14-23%, 28-40% and 45-55% for 14,15-EET, 13-23%, 23-41% and 45-57% for 11-HETE, 16-27%, 34-49% and 54-68% for 12-HETE and 9-17%, 20-31% and 36-46% for 15-HETE, respectively, in 90% of human population (Fig. 3.24).

## Resveratrol



## Fluconazole

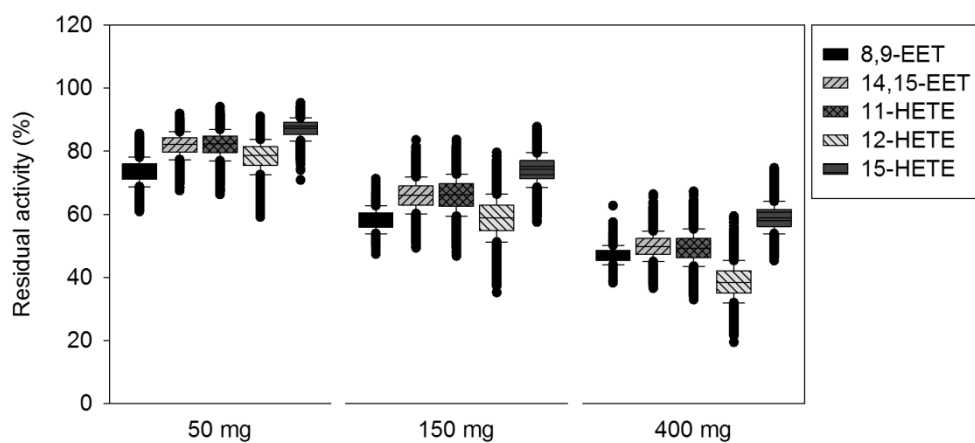


**Figure 3.24. Box Plot Showing Monte Carlo Simulations of P450-Mediated AA Metabolism Modulation by Different Doses of Res and Flu.** Monte Carlo simulations of 10,000 human subjects were performed using random number generation module from SigmaPlot, version 11, as described under *Materials and Methods*. Results are presented as median and 10<sup>th</sup>, 25<sup>th</sup>, 75<sup>th</sup> and 90<sup>th</sup> percentiles; circles represent outliers.

## CHAPTER 4: DISCUSSION

## **1. Determination of the Dominant Arachidonic Acid Cytochrome P450 Monooxygenases in Rat Heart, Lungs, Kidneys and Liver**

P450-derived AA metabolites, most notably EETs and 20-HETE, have been shown to play pivotal physiological roles in various organs (Quigley, Baum et al. 2000, Sudhahar, Shaw et al. 2010). AA is metabolized to 5,6-, 8,9-, 11,12-, and 14,15-EET by P450 enzymes (Wu, Moomaw et al. 1996), among which, CYP2B, CYP2C, and CYP2J3 isoforms are considered major P450 epoxygenases (Capdevila, Falck et al. 2000). On the other hand, P450 hydroxylation has been generally attributed to CYP4A and CYP4F isoforms (Capdevila, Falck et al. 2000, Xu, Falck et al. 2004). Other P450s, such as CYP1As, CYP1B1, CYP2As, and CYP2E1, are believed to contribute to AA monooxygenation as well; CYP1A1 and CYP1B1 were reported to exhibit some activity toward AA metabolism. They catalyze the formation of HETEs other than the 20-HETE, especially mid-chain HETEs for CYP1B1 (Capdevila, Falck et al. 2000, Choudhary, Jansson et al. 2004). CYP2A isoforms were also reported to have a very low epoxygenase activity (Imaoka, Hashizume et al. 2005). For CYP2E1, it has a substantial contribution to  $\omega$ -1-hydroxylation activity in the liver but not in the kidneys of rats and rabbits; however this was reported only after its induction and not at the constitutive state (Laethem, Balazy et al. 1993, Capdevila, Falck et al. 2000, Poloyac, Tortorici et al. 2004). Despite the documented physiological and pathophysiological role of P450-derived AA metabolites, the organ-specific kinetic properties of the P450 epoxygenases and hydroxylases activities have not been investigated.

Our results have demonstrated that AA is metabolized to EETs and HETEs in all organs tested, albeit with different levels of metabolic activity. In the heart, the P450 epoxygenase activity was 84 times the P450  $\omega$ -hydroxylase activity based on  $Cl_{int}$  (Table 3.1). In agreement with our results, it has been previously reported that P450 epoxygenase activity

was greater than P450  $\omega$ -hydroxylase activity in the heart microsomal fraction of mice (Theken, Deng et al. 2011).

In line with our observations, it has been previously reported that P450 epoxygenase activity is higher than P450 hydroxylase activity in the lungs of mice (Theken, Deng et al. 2011). We found that CYP4As and CYP4Fs exhibited moderate expressions in the lungs, representing ~25% of their relative expression in liver (Fig. 3.1). Consequently, the pulmonary 20-HETE formation rate was expected to be about 25% of that in the liver at saturating concentration of AA, given the linearity between metabolite formation rate and enzyme concentration. However, our observed hydroxylase activity was lower than what was expected based on protein expression. The explanation is that CYP4A and CYP4F isoforms are widely varied with respect to AA metabolism activity; CYP4A3, CYP4F5, and CYP4F6 have no or very low activity (Nguyen, Wang et al. 1999, Capdevila, Falck et al. 2000, Xu, Falck et al. 2004). The unexpected results could be due to the relatively greater concentrations of these inactive isoforms are in the lung microsomes compared with the liver.

In rat kidneys, as reported elsewhere, HETEs and EETs are formed in considerable amounts (Carroll, Balazy et al. 1997). Our results demonstrated that the kidneys exhibit P450 hydroxylase activity comparable to that of the epoxygenase activity based on  $Cl_{int}$  (Table 3.1). This can be attributed to the high expressions of CYP2C23, CYP2J3 and CYP4As found in the kidneys (Fig. 3.1). Similar to what was seen in the heart and kidneys, enzyme activities in the liver correlated well with protein expression. Based on  $Cl_{int}$ , P450 epoxygenase activity was 6.5 times the hydroxylase activity (Table 3.1). In agreement with previously published results (Sacerdoti, Gatta et al. 2003), P450 epoxygenases (CYP2B8, CYP2C11, CYP2C23 and CYP2J3) and P450 hydroxylases (CYP4As and CYP4Fs) were both highly expressed in the liver.

Another objective of the current study was to identify P450 epoxygenases and hydroxylases that have the major contribution to the formation of EETs and HETEs in the heart, lung, kidney, and liver microsomes. Our strategy was to compare the regioselectivity of organ microsomes with the available previously reported regioselectivity of the individual P450 enzymes; this comparison would indicate the P450 enzymes most probably have the highest contribution to AA metabolism in each organ. The identity of these P450 enzymes was further confirmed by specific immunoinhibition of P450 enzymes and by the kinetic characteristics of AA metabolism.

In rat heart, the expression levels of the P450 epoxygenases, CYP2C11 and CYP2J3, were comparable to the other organs (Fig. 3.1). It has been previously demonstrated that recombinant CYP2J3 produces EETs as a mixture of regioisomers with relative ratios of 1.5:1:1 of 14,15-, 11,12- and 8,9-EET, respectively (Wu, Chen et al. 1997); while for CYP2C11, the corresponding ratios were 1:1:0.5, respectively (Holla, Makita et al. 1999). Compared with the regioselectivity of the microsomal incubates, we can conclude that CYP2C11 dominates the EET formation in rat heart (Fig. 3.4). In agreement with our conclusion, it has been previously reported that CYP2C11 and especially CYP2J3 are highly expressed in rat heart, however, CYP2C11 activity is many fold higher than CYP2J3 (Imig 2012). On the other hand, 20-HETE formation could be attributed to the constitutive expression of CYP4Fs and/or CYP4AS.

With respect to rat lungs, CYP2B5, CYP2C11 and CYP2J3 proteins were found to be significantly expressed. Lungs produce a mixture of 14,15-, 11,12- and 8,9-EET in a ratio of 0.8:1:0.5. Therefore, CYP2J3 and CYP2B2 could be excluded due to their different pattern of regioselectivity (Capdevila, Karara et al. 1990, Wu, Chen et al. 1997). As aforementioned, CYP2C11 has a characteristic feature of producing equal amounts of 14,15- and 11,12-EET. For CYP2B1, it produces a mixture of 14,15-, 11,12-, and 8,9-EET in a ratio of 0.8:1:0.7, as previously reported (Capdevila, Karara et al. 1990). Regioselectivity suggests that CYP2B1

dominates EET formation in the lungs, although CYP2C11 may also play a role (Fig. 3.4). This is consistent with an earlier study that showed high CYP2B1 expression in the lungs (Imaoka, Hashizume et al. 2005). Concerning HETE formation, it can be catalyzed by CYP4AS and/or CYP4F isoforms.

Rat kidneys express several epoxygenases, CYP2C11, CYP2C23, and CYP2J3, in addition to CYP4AS and CYP4Fs as hydroxylases (Fig. 3.1). Kidneys produced EET mixture of 0.3:1:0.6 corresponding to 14,15-, 11,12- and 8,9-EET, respectively (Fig. 3.4). There is a close similarity between the regioselectivity of kidney microsomal fraction and CYP2C23, which produces 14,15-, 11,12- and 8,9-EET in a ratio of 0.2:1:0.4 (Holla, Makita et al. 1999). CYP2C24 which is believed to be an important epoxygenase in the kidneys have a substantially different ratio of 1:1:0.4 (Holla, Makita et al. 1999). This suggests that CYP2C23 is the most dominant epoxygenase in the kidneys, which is consistent with previously published studies (Imig, Navar et al. 1996, Imig 2012). It was previously suggested that CYP4As are the major  $\omega$ -hydroxylases in the kidneys (Ito, Nakamura et al. 2006); therefore, it was expected to have similar regioselectivity in the kidneys to what was reported elsewhere for CYP4A2, which is the formation of 19- and 20-HETE in a ratio of 1:3.6 (Capdevila, Karara et al. 1990, Helvig, Dishman et al. 1998, Nguyen, Wang et al. 1999). However, this ratio does not conform to our results that the kidney microsomal fraction produce 19- and 20-HETE in a ratio of 1:12.9, which, on the other hand, is close to the reported CYP4A1 19-/20-HETE ratio of 1:12.6 (Fig. 3.4) (Nguyen, Wang et al. 1999). Hence, CYP4A1 but not CYP4A2 seems to be the major enzyme contributed to the rat renal 19/20-HETE formation. This conclusion is consistent with an earlier study demonstrating no inhibitory effect of specific CYP4A2 antisense oligonucleotides on renal 20-HETE production; whereas specific CYP4A1 antisense oligonucleotides were able to inhibit 20-HETE production *in vivo* (Wang, Guan et al. 1999).

In rat liver, all epoxygenases, CYP2Bs, CYP2C11, CYP2C23, and CYP2J3, and hydroxylases, CYP4A1s and CYP4Fs were highly expressed (Fig. 3.1). Therefore, deriving a conclusion regarding the dominant CYP epoxygenases and CYP hydroxylases was difficult. However, regioselectivity of liver microsomal incubate was found to be 0.4:1:0.5 for 14,15-, 11,12-, and 8,9-EET, respectively (Fig. 3.4). From the aforementioned regioselectivity of CYP2B1, CYP2C11, and CYP2C23, probably CYP2C23 together with CYP2C11 are the main epoxygenases in the liver. In this regard, it was previously reported that CYP2C11 is a major epoxygenase in the male rat liver (Imig 2000).

The statistical analysis that was performed on  $K_m$  values was in agreement with the activity and protein expression of P450. Our conclusion based on regioselectivity was further supported by the fact that there are statistical differences in epoxygenation kinetics between the four organs. Moreover, these differences were less apparent between kidneys and liver, especially for 8,9-EET which did not significantly differ. This could be attributed to CYP2C23 which is shared between the kidneys and the liver. On the other hand, 19-HETE formation kinetics significantly differed between lungs, kidneys, and liver, suggesting the involvement of different P450s. 20-HETE formation kinetics did not differ between heart and kidneys, or between lungs and liver. Therefore, enzyme kinetics confirm that the dominant epoxygenases are CYP2C11, CYP2B1, CYP2C23 and CYP2C23/CYP2C11 for the heart, lungs, kidneys, and liver, respectively. Also, the results suggest that CYP4As are the main  $\omega$ -hydroxylase in the heart and kidneys, whereas CYP4A2 and/or CYP4F isoforms are the main  $\omega$ -hydroxylase enzymes in the lungs and liver. In addition, our preliminary immunoinhibition experiments suggest that CYP2C11 is the dominant epoxygenase in the heart; whereas CYP2Bs is the dominant in lungs. In addition, CYP2C23 and CYP2C23/CYP2C11 are the dominant epoxygenases in the kidneys and liver, respectively. On the other hand, CYP4As plays a significant role in AA hydroxylation in the kidneys and heart.

## **2. Alterations in Cytochrome P450-Derived Arachidonic Acid Metabolism During Pressure Overload-Induced Cardiac Hypertrophy**

In the current study, we constricted the descending aorta to induce compensated cardiac hypertrophy in SD rats. Progression of cardiac hypertrophy was gradual over 5 weeks as assessed by multiple echocardiography, with no sign of the development of heart failure. The absence of systolic heart functions deterioration indicated that the heart was able to compensate the pressure overload via cardiac remodeling (Sasayama, Kihara et al. 1999). Several cardiac hypertrophic models have been used to examine the alteration in the formation rates of some P450-derived AA metabolites (Zordoky, Aboutabl et al. 2008, Aboutabl, Zordoky et al. 2009, Zordoky, Anwar-Mohamed et al. 2010, Anwar-Mohamed, El-Sherbeni et al. 2012). The cardiac hypertrophy model, the DAC model, used in the current study has several advantages over the previously used models; notably, no exogenous agents, such as isoproterenol or doxorubicin, were given to induce hypertrophy. These exogenous agents may have their own effect on P450-mediated AA metabolism. Moreover, cardiac hypertrophy is developed over relatively longer period of time, thus, the DAC model more clearly mimics the clinical setting (Patten and Hall-Porter 2009).

The alterations in P450-mediated AA metabolism during cardiac hypertrophy were determined by measuring the primary oxygenation products of the AA-P450 monooxygenase. The cardiac levels and formation rates of 16 metabolites, 4 EETs, 4 DHETs, 3 mid-chain and 5 terminal and subterminal HETEs, were quantified. Good resolution was obtained by the HPLC method used in the current study for the targeted metabolites except the co-elution of 16- and 17-HETE. 18-HETE standard curve were used to interpret the signals of co-eluted metabolites, since standard curves for all HETEs were nearly identical. The instability problem of 5,6-EET led to a general notion that 5,6-EET role is underestimated (Nusing, Schweer et al. 2007, Kaspera and Totah 2009). Therefore, a previously published method was used to solve this

instability problem (Fulton, Falck et al. 1998), thereby, 5,6-EET alteration was accurately evaluated for the first time during cardiac hypertrophy. The scope of the current study was limited to P450-derived metabolites, therefore, cyclooxygenases and lipoxygenases expression and activity were not measured.

Pressure overload-induced cardiac hypertrophy led to a significant increase in EETs levels in the heart tissue. This increase in cardiac EETs levels was also confirmed *in vitro* by measuring their formation and degradation rates by cardiac microsomal and cytosolic fractions, respectively. The induction of EETs in hypertrophied hearts was not reported before. In fact, isoproterenol-, doxorubicin-, benzo(a)pyrene-, and arsenic-induced cardiac hypertrophy were found to decrease EET formation (Zordoky, Aboutabl et al. 2008, Aboutabl, Zordoky et al. 2009, Zordoky, Anwar-Mohamed et al. 2010, Anwar-Mohamed, El-Sherbeni et al. 2012). Several factors may explain why pressure overload model of cardiac hypertrophy causes an increase in EETs levels. First, the stretching of cardiomyocytes by pressure overload itself could directly increase EETs levels, since it has been previously reported that shear stress in smooth muscles was able to increase the levels of EETs (Huang, Sun et al. 2005, Sun, Yan et al. 2007). Second, the longer duration of time needed to develop cardiac hypertrophy in DAC model may alter the response on EETs. The previous models developed acute cardiac hypertrophy within hours or few days, in contrast, DAC induced cardiac hypertrophy over a longer period of time (several weeks). In this context, it has been previously reported that there was an increase in EETs plasma levels, and a decrease of sEH activity in patients with chronic cardiovascular disease compared to healthy volunteers which is in agreement with our results (Theken, Schuck et al. 2012). Our results may explain the failure of sEH inhibitors in the prevention or treatment of pressure overload-induced cardiac hypertrophy (Morgan, Olzinski et al. 2012), despite the success of these inhibitors in acute models of cardiac hypertrophy (Althurwi, Tse et al. 2012, Anwar-Mohamed, El-Sherbeni et al. 2012). Evidently, EETs have cardioprotective effects

against cardiac hypertrophy (Imig 2012). Therefore, we believe that EETs induction is an adaptive response to pressure overload insult.

With respect to terminal and subterminal HETEs, only the 20-HETE level was found to increase in heart tissue during cardiac hypertrophy, whereas, other terminal and subterminal HETEs, 16-, 17-, 18- and 19-HETE were undetectable. Also, the formation of 18-HETE was not detected in cardiac microsomal incubates, therefore, we can conclude that SD heart tissue does not produce substantial amounts of 18-HETE. The formation rate of 16/17-HETE was not altered during cardiac hypertrophy, consequently, it is expected that their levels in heart tissue would not be altered. For the 19-HETE, there was a significant decrease in its formation rate during cardiac hypertrophy, hence, an equivalent decrease in its cardiac level is expected. In summary, there was a significant increase in the cardiotoxic 20-HETE and a decrease in its endogenous antagonist, 19-HETE, during pressure overload-induced cardiac hypertrophy. The observed increase in 20-HETE is in agreement with the previously reported data for cardiac hypertrophy regardless of the model of cardiac hypertrophy used (Zordoky, Aboutabl et al. 2008, Alsaad, Zordoky et al. 2012, Althurwi, Tse et al. 2012, Anwar-Mohamed, El-Sherbeni et al. 2012)

Despite the significant increase in the endogenous levels of mid-chain HETEs in heart tissue during cardiac hypertrophy, only the increase in 8/12-HETE could be linked to P450 enzymes. However, the role of P450 in regulating mid-chain HETEs levels in heart tissue requires further investigation. It is worth noting that the percent increase in 8/12-HETE level in heart tissue was about 1/5 of the percent increase in the formation of 8/12-HETE by heart microsomal fraction. To our knowledge, this is the first time to report that pressure overload-induced cardiac hypertrophy is associated with an increase in the cardiac mid-chain HETEs levels. However, several previous studies did report the detrimental role of mid-chain HETEs in the development of cardiac hypertrophy and heart failure (Wen, Gu et al. 2001, Wen, Gu et al. 2003, Jenkins, Cedars et al. 2009, Kayama, Minamino et al. 2009).

As aforementioned above, cardiac levels of P450-derived AA metabolites were altered during cardiac hypertrophy. Apparently, these metabolites have a role in the pathogenesis and progression of cardiac hypertrophy, most probably by inducing inflammation and fibrosis in the heart. In fact, inflammation and fibrosis represent key events in cardiac hypertrophy. Evidently, the expression of inflammatory markers has been shown to precede any manifestation of cardiac hypertrophy (Smeets, Teunissen et al. 2008). Also, several reports demonstrated the association between the magnitude of the expression of inflammatory markers and the deterioration of heart functions (Bayes-Genis 2007, Frustaci, Verardo et al. 2007, Masiha, Sundstrom et al. 2013). Furthermore, the induction and prevention of cardiac hypertrophy were reported to be achievable by altering inflammatory mediators *in vivo* and *in vitro* (Bozkurt, Kribbs et al. 1998, Ha, Li et al. 2005, Smeets, Teunissen et al. 2008, Miguel-Carrasco, Zambrano et al. 2010). In contrast to inflammation, fibrosis is not associated with the initial stages of cardiac hypertrophy, but involved in the deterioration of heart functions (Conrad, Brooks et al. 1995, Nicoletti and Michel 1999). The stiffness of the heart muscles due to fibrosis leads to an increase in the relative workload per myocyte, resulting in further damage (Nicoletti and Michel 1999). Thereby, progressive deterioration in the heart functions occurs during the transition from compensated to decompensated cardiac hypertrophy that eventually leads to heart failure. Collectively, we suggest that the increase in cardiac levels of mid-chain and 20-HETEs mediate, at least in part, the pathogenesis and the progression of cardiac hypertrophy. In addition, the cardiotoxic effects of 20-HETE should be more pronounced due to the decrease in the cardiac levels of 19-HETE, which is the endogenous antagonist for 20-HETE (Alonso-Galicia, Falck et al. 1999, Zhang, Deng et al. 2005).

To identify novel targets for the prevention and treatment of cardiac hypertrophy and heart failure, we attempted to identify the P450 enzymes involved in the observed alteration in P450-mediated AA metabolism. We found previously that EET formation in healthy hearts

microsomes reflects the regioselectivity of CYP2C11. In hypertrophied hearts, we found that regioselectivity was altered for 14,15-EET:11,12-EET:8,9-EET ratio from 1.20:1.21:1 to 1.73:1.20:1 during cardiac hypertrophy. CYP2C11 has a characteristic feature of producing comparable amounts of 11,12- and 14,15-EET (Capdevila, Falck et al. 2000). Only CYP2J3 and CYP2Bs are characterized by the formation of 14,15-EET as the major EETs (Wu, Chen et al. 1997, Capdevila, Falck et al. 2000). Therefore, it was expected to observe an induction in CYP2J3 and/or CYP2Bs expression in hypertrophied hearts. In the current study, CYP2J3 enzyme was downregulated, while CYP2Bs was induced. Moreover, using non-parametric correlation analysis, CYP2Bs expression was significantly associated with EET formation rate. These data strongly suggest that the increase in EET formation was mainly due to CYP2Bs induction.

CYP1As, CYP2E1 and CYP4A2 were reported to produce 19-HETE (Falck, Lumin et al. 1990, Laethem, Balazy et al. 1993, Capdevila, Falck et al. 2000). In the current study, the decrease in 19-HETE was only correlated with CYP4As expression, which may suggest that CYP4A is involved in 19-HETE formation. CYP4A subfamily includes three enzymes, CYP4A1 which hydroxylates AA at C20 mainly (Capdevila, Falck et al. 2000), as well as CYP4A2 and CYP4A3 which produce 19-HETE (Nguyen, Wang et al. 1999).

With respect to mid-chain HETEs, correlation analysis showed that CYP1B1 was involved in 8/12-HETE formation, whereas, CYP2J3 was involved in 8/12-HETE degradation. The recombinant CYP1B1 catalyzed the formation of 5, 12- and 15-HETEs similar to what has been previously reported (Choudhary, Jansson et al. 2004). Hence, CYP1B1 is responsible, in part, for 8/12-HETE endogenous formation. For CYP2J3, it has been previously reported that CYP2J2 exhibits hydroperoxide isomerase activity and can metabolize 15-HPETE to hepoxilins before being transformed to mid-chain HETEs (Chawengsub, Gauthier et al. 2009). Here, we reported that the metabolism of 12-HPETE to hepoxilins can also occur via CYP2J2.

Accordingly, one of the beneficial roles of CYP2Js in the heart is mediating the degradation of the cardiotoxic 12- and 15-HETE in favor of the formation of the cardioprotective metabolite, hepoxilins.

### 3. Characterization of Arachidonic Acid Metabolism by Rat Cytochrome P450 Enzymes

Recently, P450-derived AA metabolites have been reported to have numerous physiological and pathological effects. Therefore, pharmacological modulation of P450-mediated AA metabolism has great potential for treatment and control of several diseases and pathological conditions. In this regard, performing a comparison between the AA-metabolizing activities of several P450 would provide important information. In the current study, a simple HPLC method was developed and validated for determining the formation of mid-chain, subterminal and 20-HETEs and EETs by P450 enzymes. We selected 10 recombinant rat P450 enzymes from 3 different families including enzymes that have not been studied before, such as CYP2D1 and CYP3A1, to be characterized. The AA-metabolizing activities of these enzymes were measured and the kinetic profiles of P450 enzymes of the highest activity were determined. One interesting finding was the high AA-metabolizing activity of CYP1A1 and CYP1A2, consequently, we investigated the involvement of CYP1A1 and CYP1A2 in AA metabolism in rat heart, lungs, kidneys and liver.

Interestingly, P450 enzymes tested in the current study were able to metabolize AA, including CYP2C6, CYP2C13, CYP2D1 and CYP3A1 that have never been studied before. In several previously published papers, CYP2C6 and CYP2C13 were considered as AA epoxygenases (Holla, Makita et al. 1999, Iliff, Jia et al. 2010). However, our results showed that CYP2C6, as well as CYP2C13, mainly mediates AA hydroxylation. Despite CYP2C6, CYP2C11 and CYP2C13 are of the same subfamily, there was substantial variation in their AA-metabolizing activities; CYP2C6 and CYP2C11 were among the highest, whereas CYP2C13 was among the lowest. In agreement with our results, it has been reported that CYP2C11 is the main epoxygenase in rats (Imig 2012). It mediates AA metabolism to EETs as about 2/3 of total metabolites and its regioselectivity was in the order of 11,12-EET $\geq$ 14,15-EET>8,9-EET>>5,6-EET (Capdevila, Falck et al. 2000). Also, the observation made by Bylund *et al* that CYP3A1

could mediate mid-chain hydroxylation based on immunoinhibition data was confirmed by our results that mid-chain HETEs are the major metabolites for CYP3A1 (Bylund, Kunz et al. 1998). In previously published studies, CYP2A1-mediated formation of EETs and 19- and 20-HETEs could not be detected, c.f. other CYP2 enzymes, and this is consistent with our finding that CYP2A1 has the lowest AA-metabolizing activity among the tested enzymes (Imaoka, Hashizume et al. 2005).

Several P450 enzymes can mediate the metabolism of AA, however the contribution of each one of them to overall AA metabolism has to be varied significantly. P450 expression and their catalytic activities are the two factors that dictate the contribution of a P450 enzyme to AA metabolism in a tissue. With respect to P450 expression, substantial differences have been reported between different tissues and organs (Zordoky, Aboutabl et al. 2008). Additionally, AA-metabolizing activity demonstrated great variation among P450 enzymes. Normally, a highly expressed P450 enzyme with high activity will have a greater contribution to AA metabolism than a low expressed or low activity P450 enzyme. Apparently, CYP1As and CYP2Cs have a substantial role in AA metabolism, due to their high AA-metabolizing activity. Also, it has been reported that CYP1As are constitutively expressed in different rat organs, including heart, lungs, kidneys and liver. CYP1As activity is remarkably higher in the liver compared with heart, lungs and kidneys (Elsherbiny, El-Kadi et al. 2010). This is in line with our results that the liver has the highest formation rate of CYP1As major metabolites, subterminal HETEs, while the heart has the lowest. We found that the expression of CYP2Cs to be the highest in rat liver followed by rat kidneys, and the lowest in rat heart and lungs. This was in agreement with the rate of EET formation, which is the highest in the liver followed by the kidneys, then the heart and lungs. Noteworthy, the liver has the highest formation rate of all groups of P450-derived AA metabolites, which is consistent with the fact that the liver has the highest P450 content among body organs. Being an important P450 metabolizing enzyme in

mammals (Martignoni, Groothuis et al. 2006), CYP2E1 has been considered to be a major subterminal AA hydroxylase. However, experimentally, CYP2E1 contribution to the constitutive formation of subterminal HETEs has been reported to be minor (Laethem, Balazy et al. 1993, Capdevila, Falck et al. 2000, Poloyac, Tortorici et al. 2004). This contradiction is explainable by our results that CYP2E1 has one of the lowest AA-metabolizing activities among the tested P450 enzymes.

In the current study, CYP1A1-, CYP1A2-, CYP2C6- and CYP2C11-mediated AA metabolism has been determined to follow substrate inhibition kinetics. Using this atypical model to describe enzyme activity allows more accurate estimation of kinetic parameters values (Houston and Kenworthy 2000). The mechanism by which the excess substrate can inhibit the activity of an enzyme is not fully elucidated (Lin, Lu et al. 2001). Probably, the decrease in enzyme activity can be attributed to reaction products themselves (Lin, Lu et al. 2001). In agreement with our results, Xu *et al* reported that CYP4F1-, and CYP4F4-mediated  $\omega$ -hydroxylation of AA follows substrate inhibition kinetics (Xu, Falck et al. 2004). The phenomenon of substrate inhibition has been reported to have a regulatory role in several metabolic pathways (Reed, Lieb et al. 2010).

P450-derived AA metabolites have multifaceted roles in the regulation of several biological functions. Interestingly, the reported experimental effects of P450 modulations on biological systems can be explainable in light of P450 AA metabolizing activities. Considering that EETs and subterminal HETEs are more cytoprotective, whereas mid-chain HETEs and 20-HETE are more cytotoxic, we can suggest that CYP1A1, CYP1A2 and CYP2C11 play cytoprotective roles in biological systems. In this context it has been previously reported that the induction of CYP2C11 protects rats from ischemic brain injury (Alkayed, Goyagi et al. 2002, Liu and Alkayed 2005), which can be explainable by the predominant role of CYP2Cs in the formation of EETs *in vivo* we found previously. Also, in consistence with our explanation, an

increase in blood pressure has been reported in *cyp1a1*-knockout mice (Agbor, Walsh et al. 2012). Moreover, cardiac hypertrophy has been reported in aryl hydrocarbon-receptor-knockout mice, which show decreased levels of *cyp1a1* and *cyp1a2* (Lund, Goens et al. 2003). While, CYP1A1 and CYP1A2 induction was reported to protect rats from hyperoxic pulmonary toxicity, and knocking-out *cyp1a1* and *cyp1a2* increased pulmonary toxicity in mice (Couroucli, Welty et al. 2002, Jiang, Welty et al. 2004). Also, liver fibrosis was reported to be increased in aryl hydrocarbon-receptor-knockout mice (Fernandez-Salguero, Pineau et al. 1995, Peterson, Hodgson et al. 2000). On the other hand, the observed low AA-metabolizing activity of CYP2E1 and CYP3A1 can explain at least in part why *cyp2e1*- and *cyp3a*-knockout mice did not show any physiological abnormalities compared with wild-type mice (Lee, Buters et al. 1996, van Herwaarden, Wagenaar et al. 2007).

In the current study, we determined CYP1As involvement in AA metabolism in the microsomes of heart, lungs, kidneys and liver. Because AA metabolism is mediated by several P450 enzymes, we preferred to utilize multiple approaches together, in order to make the determination of the specific contribution of CYP1As to AA metabolism more reliable. Generally, inhibiting CYP1As by  $\alpha$ -NF or by anti-CYP1As antibodies, or inducing CYP1As by 3-MC is considered valid and selective methods by their own for determining the involvement of CYP1As in the metabolism of a compound (Nakajima, Wang et al. 1992, Carlson, Hynes et al. 1998, Reid, Kuffel et al. 1999, Kondraganti, Jiang et al. 2008). The effects of chemical inhibition and immunoinhibition on AA metabolism were in agreement that CYP1As is a major contributor to subterminal HETE formation *in vivo* as evident by recombinant CYP1A1 and CYP1A2 results. Also, the induction of CYP1As levels resulted in a remarkable increase in subterminal HETE formation in all organs. Interestingly, even at the constitutive level, CYP1As had a significant contribution to subterminal HETE formation in the liver and to a lower extent in the lungs. On the other hand, anti-CYP1As antibodies inhibited the formation of all EETs and  $\alpha$ -NF inhibited

the formation of 14,15-EET in the liver, while the induction of CYP1As led to an inhibition of the formation of 11,12-EET in the liver. This may be due to non-selective modulation of P450 enzymes other than CYP1As. However, we cannot exclude the possibility that CYP1A2 may also play a role in the hepatic formation of AA metabolites, other than subterminal HETEs. It is well known that CYP1A2 is one of the major P450 in the mammalian liver (Yeung, Shen et al. 2014).

#### **4. Repurposing Resveratrol and Fluconazole to Modulate Human Cytochrome P450-Mediated Arachidonic Acid Metabolism**

In the current study, we determined the AA-metabolizing activity of 16 recombinant human P450 enzymes belong to different P450 families and subfamilies to get a good idea about the differences in AA-metabolizing activity among human P450 enzymes. Tested P450 enzymes were untagged, expressed in the same expression system and previously validated for activity studies. Noteworthy, there are P450 enzymes, such as CYP4F11, have been reported to metabolize AA at a low rate (Kalsotra, Turman et al. 2004), and they were commercially unavailable to us at the time to be included in the current study. Interestingly, CYP4 family was collectively the most active P450 family with regard to AA-metabolizing activity. CYP4 family is one of the most antique within the P450 enzymes, which implies its importance in biological systems (Lewis, Watson et al. 1998). AA-metabolizing activities were variable among the tested P450 enzymes; there was a 34-fold difference in AA-metabolizing activity between P450 enzyme of the highest activity (CYP2C19) and of the lowest activity (CYP3A4). The activity of an enzyme toward a substrate is governed by two factors: the volume of the active site, and the amino acids forming the active site. Our results suggest that there is an optimum volume for P450 active site to get the highest AA-metabolizing activity. With respect to CYP1s, the volume of active site is decreasing from 524 Å<sup>3</sup> for CYP1A1, to 469 Å<sup>3</sup> for CYP1A2 and 441 Å<sup>3</sup> for CYP1B1 (Walsh, Szklarz et al. 2013), which is correlated with the decreasing trend of AA metabolizing activities among CYP1s. CYP2E1 has one of the smallest active site volume among P450 enzymes (~ 250 Å<sup>3</sup>) (Miller 2008, Walsh, Szklarz et al. 2013), and it showed low AA-metabolizing activity. On the other hand, large active site volume may negatively affect AA-metabolizing activity. CYP2C8 has one of the largest active site volumes (~ 1450 Å<sup>3</sup>) among P450 enzymes, and showed low AA-metabolizing activity. The closely related CYP2C19 has smaller active site (estimated to be ~850 Å<sup>3</sup>) as well as CYP2C9, whose active site volume is

~1250 Å<sup>3</sup> (Williams, Cosme et al. 2003), and this again is correlated with their AA-metabolizing activities (CYP2C19>CYP2C9>CYP2C8) (Reynald, Sansen et al. 2012). It has been reported that CYP2C8 simultaneously binds to two molecules of retinoic acid, which is structurally similar to AA (Schoch, Yano et al. 2008). Therefore, we can insightfully postulate that this unusual binding may restrain the AA-metabolizing activity of CYP2C8, compared with the closely related CYP2C19 and CYP2C9. This was also true for CYP3A4, whose active site volume is the largest among P450 enzymes (~ 1600Å<sup>3</sup>), and its AA metabolizing activity was the lowest (Lee, Neul et al. 2010). Likewise, CYP2J2 has a large active site volume of 1420 Å<sup>3</sup>, which is comparable to CYP3A4 and CYP2C8, but, it has been reported that CYP2J2 active site is narrower than CYP3A4 near the heme iron (Lee, Neul et al. 2010); as a result, CYP2J2 showed a higher AA-metabolizing activity compared with CYP3A4.

AA is a C20 unsaturated fatty acid that has four double bonds at C5, C8, C11 and C14. Oxidation of AA by P450 includes either hydroxylation or epoxidation; hydroxylation, theoretically, can occur at any of methinyl, methylene or the terminal methyl groups of AA, whereas, epoxidation of AA occurs only at one of its four double bonds. Therefore, AA epoxidation depends on steric factors dictating the conformation of AA in the active site, and hence, the proximity of any of the double bonds to the ferryl oxygen. Epoxidation is thermodynamically favored over hydroxylation at the region of double bonds; it has been reported that epoxidation involves a smaller energy barrier (14 kcal/mol) compared with hydroxylation (>20 kcal/mol) (de Visser, Ogliaro et al. 2002). Therefore, at the region of the double bonds, i.e. mid-chain (C5-C15), AA hydroxylation should occur at a lower rate, compared with AA epoxidation (de Visser, Ogliaro et al. 2002), and this was in agreement with our results (Fig. 3.20).

Both the AA-metabolizing activity and the amount expressed in a tissue of each P450 enzymes, dictate the tissue-specific metabolism of AA. In rats, we previously found that

differences in the metabolic and kinetic profiles of AA metabolism by untreated rat liver, kidneys lung and heart microsomes can be explained by differences in tissue-specific expression of P450 enzymes . In humans, due to their high AA-metabolizing activity, CYP1As, CYP2C19 and CYP4s are potentially dominating the P450-mediated AA metabolism. With respect to CYP1As, liver has the highest expression of CYP1A2 among human organs, whereas CYP1A1, despite it was also detected in the liver (Drahushuk, McGarrigle et al. 1998), is considered mainly an extrahepatic enzyme (Androustopoulos, Tsatsakis et al. 2009). Being the major metabolites of recombinant CYP1As, subterminal HETEs and EET formation was significantly reduced by CYP1As selective inhibition by  $\alpha$ -NF, while Res reduced the formation of subterminal HETEs. Similar to CYP1As, previous reports found CYP2C19 is mainly hepatic and no or little expression was reported in kidneys (Lasker, Chen et al. 2000, Lash, Putt et al. 2008). In agreement, the formation of EETs in kidneys is in a much lower rate than liver, and additionally, inhibition of CYP2C19 by Tic or Flu led to wide inhibition in the formation of AA metabolites, most importantly the major metabolites of CYP2C19, viz. 8,9- and 14,15-EETs. While, the low AA-metabolizing activity of recombinant CYP2B6 and CYP2J2 is in agreement with the weak inhibitory effect of their selective inhibitors, Ser and Dan, respectively. With respect to CYP4s, their expression in either liver or kidneys is comparable, but no or little expression of CYP4s was noted in other tissues (Lasker, Chen et al. 2000, Edson and Rettie 2013). Consistent with our findings that CYP4s have the highest AA-metabolizing activity, the formation rate of 19- and 20-HETE formation was the highest in both human liver and kidneys compared with all other P450-derived AA metabolites. Also, the high 20-HETE formation rates of recombinant human CYP4 family are consistent with the inhibitory effect of HET0016 on 20-HETE formation. Interestingly, the almost complete inhibition of 20-HETE formation by HET0016 could be the explanation of the unexpected increase in the formation rates of mid-chain HETEs, namely 5-, 11-, 12- and 15-HETEs, by HET0016. Blocking CYP4s from mediating the hepatic formation of 20-HETE, which is the dominant metabolite in the liver, made AA more available to the other

still-active P450-enzymes. Consequently, all P450-derived AA metabolites, other than 5,6-EET and 9-, 19- and 20-HETEs, showed an increase in their formation rates, which was only significant for 5-, 11-, 12- and 15-HETEs. Similarly, there was a significant increase in the formation rate of 20-HETE, which was the only observed alteration in liver-mediated AA metabolism by PTU. Therefore, we believe that PTU increased 20-HETE formation by activating CYP4s through heterotropic cooperativity (Kramer and Tracy 2008).

Our results show that the addition of the tested clinically-approved drugs induced significant alterations in P450-mediated AA metabolism in the liver, comparable to the alterations induced by investigational agents in term of magnitude and selectivity. As a result, HET0016 and MS-PPOH, which have been used extensively in *in vitro* and animal studies as selective inhibitors for 20-HETE and EET formation, respectively (Miyata, Taniguchi et al. 2001, Liu, Li et al. 2011), can be easily replaced with Res and Flu, respectively, in clinical studies. The other clinically-approved drugs were either of low inhibitory activity or of low selectivity toward AA metabolism. As mentioned above CYP4 family has the major contribution to 19- and 20-HETE formation in humans. Therefore, we could not initially explain how Res as a CYP1s inhibitor significantly decreased the formation of 20-HETE (Chang, Chen et al. 2001). We found thereafter that Res does inhibit all of the hepatic CYP4s; however, at low Res concentration, Res selectively inhibits CYP4F2 with statistically the same  $IC_{50}$  value determined for Res inhibition of liver-mediated 20-HETE formation. Likewise, the  $IC_{50}$  values of Res inhibition of liver- and CYP4A11-mediated 19-HETE formation are not significantly different, which is also in agreement with recombinant CYP4A11 data. The reported  $IC_{50}$  values for CYP1As inhibition by Res are in line with our  $IC_{50}$  values for liver-mediated formation of 16- and 18-HETEs (Chang, Chen et al. 2001). For Flu, it inhibits 8,9- and 14,15-EETs and 11-, 12- and 15-HETEs with  $IC_{50}$  values very similar to the reported  $IC_{50}$  values of Flu inhibition of CYP2C9/19 (Niwa, Shiraga et al. 2005).

Based on our results, several P450 enzymes can mediate AA-metabolism, and therefore the *in vivo* modulation of P450-mediated AA-metabolism requires highly selective P450 inhibitors. Also, it is important to note the substantial loss of selectivity by the increase in the concentration of the tested P450 inhibitors, which highlights the importance of identifying the optimum doses to retain selectivity. Our simulations show that Res may maintain its selectivity and magnitude of inhibition when given to human subjects at a relatively high but safe oral dose of 2.5 g daily (Vang, Ahmad et al. 2011). Whereas, for Flu, selectivity and magnitude of inhibition may be maintained by low oral dose of 50 mg (Debruyne 1997). Because liver has the highest P450 content in the body, it has been reported that hepatic P450-mediated AA metabolism controls the systemic levels of P450-derived AA metabolites (Diani-Moore, Ma et al. 2014, Schuck, Zha et al. 2014). Elevated levels of 20-HETE has been associated with several diseases, especially cardiovascular and renal diseases (Muroya, Fan et al. 2015, Zhao, Qi et al. 2015); whereas, elevated levels of EETs has been reported to promote cancer progression due to EET-induced angiogenesis (Wang and Dubois 2012).

## 5. Summary and General Conclusions

In the current work, our ultimate goal was to pave the way for the clinical use of pharmacological P450-modulators as new therapeutic modalities, especially for the treatment of cardiac hypertrophy. We used rodent model, SD rat, to expand our knowledge on P450-mediated AA metabolism in different organs, and how it was altered during cardiac hypertrophy.

First, we provided a comparison of the total P450 epoxygenase and P450 hydroxylase activity of microsomes separated from rat heart, lungs, kidneys, and liver. We concluded that AA is metabolized to EETs and HETEs in all organs tested, but with varying metabolic activities. We found P450 epoxygenase activity in rat heart and lungs to be higher than the P450 hydroxylase activity of the same organ; while, P450 hydroxylase activity in rat liver is significantly higher than its P450 epoxygenase activity. Similar P450 epoxygenase and hydroxylase activities were found in rat kidneys. In light of our results, CYP2C11 may be the predominant epoxygenase in rat heart; whereas CYP2Bs may be the predominant in rat lungs. In addition, our data suggest that CYP2C23 and CYP2C23/CYP2C11 may be the dominant epoxygenases in rat kidneys and liver, respectively. CYP4As are probably the major hydroxylase in rat kidneys and heart. On the other hand, CYP4A and/or CYP4F families are probably the dominant  $\omega$ -hydroxylases in rat liver and lungs. Our data showed that different rat tissues can mediate the formation of their own P450-derived AA metabolites with organ-distinct metabolic and kinetic profiles, indicating that developing organ-specific modulators of P450-mediated AA metabolism could be feasible.

Second, we found that pressure overload-induced cardiac hypertrophy caused several alterations in the normal P450-mediated AA metabolic profile. These alterations were characterized, which include the significant increase in EETs, and midchain and 20-HETEs cardiac levels. We also identified the alterations in P450 enzymes that may lead to the observed alteration in P450-mediated AA metabolism. Our conclusions were that in cardiac hypertrophy

CYP1B1 may have a detrimental effect on the heart by mediating the formation of the cardiotoxic mid-chain HETEs. On the other hand, CYP2Bs, CYP2J3 and CYP4As may play cardioprotective roles; our data suggest that CYP2Bs may play a major role in the formation of the cardioprotective EETs during cardiac hypertrophy, whereas, CYP4As could mediate the formation of the cardioprotective metabolite, 19-HETE. Interestingly, CYP2J3 could mediate the decrease in the cardiotoxic mid-chain HETEs levels, and the formation of the cardioprotective hepoxilins, in addition to its reported contribution to the formation of cardioprotective metabolite, EETs. Therefore, we were able to identify cardiac P450 enzymes that are altered and may significantly impact P450-mediated AA metabolism during cardiac hypertrophy in SD rats.

Third, we found that the individual rat recombinant P450 enzymes to show significant differences in AA-metabolizing activity and regioselectivity. Our results suggest that CYP1As and CYP2C11 could have beneficial effects, since CYP1As are a predominant subterminal AA-hydroxylases, while CYP2C11 is a predominant AA epoxygenases. Furthermore, it seems that AA metabolism is dominated by relatively small group of P450, and therefore, altering certain metabolites by the pharmacological modulation of a single P450 is possible. Our results suggest that CYP1A1 and CYP1A2 are of high importance because of their inducibility and their significant contribution to AA metabolism. However, further investigation is needed to determine the potential beneficial effects of pharmacological modulation of CYP1A1 and CYP1A2 enzymes *in vivo*. Our results link alterations in P450 expression to pathological and physiological changes in tissues levels of P450-derived AA metabolites, and thus, could present protein targets for pharmacological modulation.

Collectively, we were able to identify number of protein and chemical targets that would have potentially beneficial effects on cardiac hypertrophy. It was the efforts of my other colleagues in our laboratory to validate these potential targets *in vivo*. Based on our work that 19-HETE, which is the prominent AA metabolite of CYP2E1, CYP2E1 could have a protective effect in cardiac hypertrophy, Elkhatali *et al* showed that CYP2E1 inducer, isoniazid, protects SD rats from angiotensin II-induced cardiac hypertrophy (Elkhatali, El-Sherbeni et al. 2015). Also, based on our work that mid-chain HETEs, especially 8/12-HETE, mainly formed by CYP1B1 in SD rats, CYP1B1 could have a detrimental effect in cardiac hypertrophy, Maayah *et al* showed that CYP1B1 inhibition by TMS protects SD rats from doxorubicin-induced cardiotoxicity (Maayah, Althurwi et al. 2016). Our final efforts were to pose and validate an interesting translational concept, which is to repurpose drugs known to cause inhibition of P450-mediated metabolism of concurrently-administered drugs to control P450-mediated AA metabolism. We showed that the utilization of these drugs produced effective and specific alteration in P450-mediated AA metabolism by human liver microsomes. Their repurposing may provide already clinically-approved new P450-based treatments.

In conclusion, pharmacological modulation of P450-mediated AA metabolism, similar to cyclooxygenase and lipoxygenase-mediated metabolism, could have great potential for clinical uses. Recently, soluble epoxide hydrolase inhibitors, which increase EETs levels, have been successfully used for prevention and treatment of several diseases and pathological conditions (Morisseau and Hammock 2013). Likewise, targeting P450 enzymes to alter P450-derived AA metabolites starts to be in the focus of biomedical research (Evangelista, Kaspera et al. 2013). The advantage of repurposing clinically-approved drugs is that their dosage and human safety profile are known. Upon determining which drug is the best candidate as a treatment of heart enlargement and heart failure, that drug could be easily introduced to clinical

trials. In this regard, we systematically identified potentially safe doses of Res and Flu to modulate P450-mediated AA metabolism in humans.

## 6. Limitations and Pitfalls

We would like to point out the limitations of the current work. First of all, we used pooled microsomes separated from different rat and human organs to study P450-mediated AA metabolism in several experiments. Pooled microsomal fractions for each organ were used to determine the kinetics, regioselectivity and activity of P450-mediated AA metabolism that represent the average rat/human individual; however, it cannot be used to determine the inter-individual variability in P450-mediated AA metabolism, which was not the scope of our work. We recognize that individual animals may differ in their expression levels and/or enzymatic activity of P450 enzymes. On the other hand, the inter-individual variability was an important aspect to be determined for rats undergone DAC or exposed to 3-MC, therefore, we did not pool the microsomes, but we used individually separated microsomes corresponding to individual rats. Also, the formation of each EET was determined as EET plus the corresponding DHET, and the microsomal incubations were performed without adding sEH inhibitor, since the inhibition of sEH may activate the other pathways of EETs degradation (Imig 2012). We would like to point out that 5,6-EET has been reported to be slightly unstable in physiological buffer and may spontaneously degrade to 5,6- $\delta$ -lactone, which may lead to the underestimation of P450-mediated 5,6-EET formation activity; therefore, 5,6-EET data shown should be interpreted with some degree of caution. To avoid this problem when we measured 5,6-EET in hypertrophied hearts, we used previously published method to transform 5,6- $\delta$ -lactone to the stable 5,6-DHET (Fulton, Falck et al. 1998). In an interesting study by Edpuganti and Mehvar, it has been reported that storing fresh tissue even at low temperature, as well as tissue freeze-thaw, can increase the free concentration of P450-derived AA metabolites in the tissues (Edpuganti and Mehvar 2013). Therefore, we acknowledge that our determination of the free cardiac levels of P450-derived AA metabolites may be slightly higher than their real *in vivo* levels.

## 7. Future Research Directions

In the current work, we have extensively studied the metabolizing activity, regioselectivity and kinetic profile of AA metabolism by P450 enzymes. Also, we identified new promising drug targets in the cascade of P450-mediated AA metabolism, and posed a novel strategy based on the repurposing of old drugs to target P450-mediated AA metabolism in humans. However, several points still have to be covered, in order to bring new P450-based therapeutic modalities a step closer to the clinic, of which the following interesting points:

1. To investigate the stereoselectivity of AA metabolism by organ-specific microsomes and recombinant P450 enzymes.
2. To investigate the contribution of CYP2Js to hepoxilin formation and mid-chain HETEs degradation, and the crosstalk between CYP2Js and lipoxygenases and its role in the development of cardiac hypertrophy.
3. To investigate the effects of tryptophan-derived endogenous aryl hydrocarbon receptor agonists, such as 6-formylindolo[3,2-b]carbazole, on the development of cardiac hypertrophy, based on our findings that aryl hydrocarbon receptor agonists increase 19-HETE levels.
4. To confirm our *in vitro* predictions with respect to Res and Flu selective effect on 20-HETE and EETs levels, respectively, clinically by giving human subjects safe doses of Res or Flu and measure plasma P450-derived AA metabolites.
5. To continue screening and identifying old drugs that can be repurposed to target P450-mediated AA metabolism.

6. To investigate the P450-mediated linoleic acid metabolism during cardiac hypertrophy and its role in the development of cardiac hypertrophy.

## REFERENCES

Aboutabl, M. E., B. N. Zordoky and A. O. El-Kadi (2009). "3-methylcholanthrene and benzo(a)pyrene modulate cardiac cytochrome P450 gene expression and arachidonic acid metabolism in male Sprague Dawley rats." Br J Pharmacol **158**(7): 1808-1819.

Aboutabl, M. E., B. N. Zordoky, B. D. Hammock and A. O. El-Kadi (2011). "Inhibition of soluble epoxide hydrolase confers cardioprotection and prevents cardiac cytochrome P450 induction by benzo(a)pyrene." J Cardiovasc Pharmacol **57**(3): 273-281.

Adas, F., J. P. Salaun, F. Berthou, D. Picart, B. Simon and Y. Amet (1999). "Requirement for omega and (omega;-1)-hydroxylations of fatty acids by human cytochromes P450 2E1 and 4A11." J Lipid Res **40**(11): 1990-1997.

Agbor, L. N., M. T. Walsh, J. R. Boberg and M. K. Walker (2012). "Elevated blood pressure in cytochrome P4501A1 knockout mice is associated with reduced vasodilation to omega-3 polyunsaturated fatty acids." Toxicol Appl Pharmacol **264**(3): 351-360.

Alexander, S. P., D. Fabbro, E. Kelly, N. Marrion, J. A. Peters, H. E. Benson, E. Faccenda, A. J. Pawson, J. L. Sharman, C. Southan, J. A. Davies and C. Collaborators (2015). "The Concise Guide to PHARMACOLOGY 2015/16: Enzymes." Br J Pharmacol **172**(24): 6024-6109.

Alkayed, N. J., T. Goyagi, H. D. Joh, J. Klaus, D. R. Harder, R. J. Traystman and P. D. Hurn (2002). "Neuroprotection and P450 2C11 upregulation after experimental transient ischemic attack." Stroke **33**(6): 1677-1684.

Alonso-Galicia, M., J. R. Falck, K. M. Reddy and R. J. Roman (1999). "20-HETE agonists and antagonists in the renal circulation." Am J Physiol **277**(5 Pt 2): F790-796.

Alsaad, A. M., B. N. Zordoky, A. A. El-Sherbeni and A. O. El-Kadi (2012). "Chronic doxorubicin cardiotoxicity modulates cardiac cytochrome P450-mediated arachidonic acid metabolism in rats." Drug Metab Dispos **40**(11): 2126-2135.

Alsaad, A. M., B. N. Zordoky, M. M. Tse and A. O. El-Kadi (2013). "Role of cytochrome P450-mediated arachidonic acid metabolites in the pathogenesis of cardiac hypertrophy." Drug Metab Rev **45**(2): 173-195.

Althurwi, H. N., O. H. Elshenawy and A. O. El-Kadi (2014). "Fenofibrate modulates cytochrome P450 and arachidonic acid metabolism in the heart and protects against isoproterenol-induced cardiac hypertrophy." J Cardiovasc Pharmacol **63**(2): 167-177.

Althurwi, H. N., Z. H. Maayah, O. H. Elshenawy and A. O. El-Kadi (2015). "Early Changes in CYP and their Associated Arachidonic Acid Metabolites Play a Crucial Role in the Initiation of Cardiac Hypertrophy Induced by Isoproterenol." Drug Metab Dispos.

Althurwi, H. N., M. M. Tse, G. Abdelhamid, B. N. Zordoky, B. D. Hammock and A. O. El-Kadi (2012). "Soluble epoxide hydrolase inhibitor, tups, protects against isoproterenol-induced cardiac hypertrophy." Br J Pharmacol.

Althurwi, H. N., M. M. Tse, G. Abdelhamid, B. N. Zordoky, B. D. Hammock and A. O. El-Kadi (2013). "Soluble epoxide hydrolase inhibitor, TUPS, protects against isoprenaline-induced cardiac hypertrophy." Br J Pharmacol **168**(8): 1794-1807.

Alvares, A. P. and P. Siekevitz (1973). "Gel electrophoresis of partially purified cytochromes P450 from liver microsomes of variously-treated rats." Biochem Biophys Res Commun **54**(3): 923-929.

Anandatheerthavarada, H. K., N. B. Sepuri and N. G. Avadhani (2009). "Mitochondrial targeting of cytochrome P450 proteins containing NH<sub>2</sub>-terminal chimeric signals involves an unusual TOM20/TOM22 bypass mechanism." J Biol Chem **284**(25): 17352-17363.

Andersen, M. E. (1981). "Saturable metabolism and its relationship to toxicity." Crit Rev Toxicol **9**(2): 105-150.

Androutsopoulos, V. P., A. M. Tsatsakis and D. A. Spandidos (2009). "Cytochrome P450 CYP1A1: wider roles in cancer progression and prevention." BMC Cancer **9**: 187.

Annalora, A. J., D. B. Goodin, W. X. Hong, Q. Zhang, E. F. Johnson and C. D. Stout (2010). "Crystal structure of CYP24A1, a mitochondrial cytochrome P450 involved in vitamin D metabolism." J Mol Biol **396**(2): 441-451.

Anwar-Mohamed, A., A. A. El-Sherbeni, S. H. Kim, H. N. Althurwi, B. N. Zordoky and A. O. El-Kadi (2012). "Acute arsenic toxicity alters cytochrome P450 and soluble epoxide hydrolase and their associated arachidonic acid metabolism in C57Bl/6 mouse heart." Xenobiotica.

Anwar-Mohamed, A., A. A. El-Sherbeni, S. H. Kim, H. N. Althurwi, B. N. Zordoky and A. O. El-Kadi (2012). "Acute arsenic toxicity alters cytochrome P450 and soluble epoxide hydrolase and their associated arachidonic acid metabolism in C57Bl/6 mouse heart." Xenobiotica **42**(12): 1235-1247.

Anzenbacher, P. and E. Anzenbacherova (2001). "Cytochromes P450 and metabolism of xenobiotics." Cell Mol Life Sci **58**(5-6): 737-747.

Anzenbacher, P. and U. M. Zanger (2012). Metabolism of drugs and other xenobiotics. Weinheim, Wiley-VCH.

Araya, Z., M. Norlin and H. Postlind (1996). "A possible role for CYP27 as a major renal mitochondrial 25-hydroxyvitamin D3 1 alpha-hydroxylase." FEBS Lett **390**(1): 10-14.

Axen, E., H. Postlind, H. Sjoberg and K. Wikvall (1994). "Liver mitochondrial cytochrome P450 CYP27 and recombinant-expressed human CYP27 catalyze 1 alpha-hydroxylation of 25-hydroxyvitamin D3." Proc Natl Acad Sci U S A **91**(21): 10014-10018.

Baldwin, S. J., S. E. Clarke and R. J. Chenery (1999). "Characterization of the cytochrome P450 enzymes involved in the in vitro metabolism of rosiglitazone." Br J Clin Pharmacol **48**(3): 424-432.

Barakat, M. M., A. O. El-Kadi and P. du Souich (2001). "L-NAME prevents in vivo the inactivation but not the down-regulation of hepatic cytochrome P450 caused by an acute inflammatory reaction." Life Sci **69**(13): 1559-1571.

Bayes-Genis, A. (2007). "Hypertrophy and inflammation: too much for one heart." Eur Heart J **28**(6): 661-663.

Bednar, M. M., C. E. Gross, M. K. Balazy, Y. Belosludtsev, D. T. Colella, J. R. Falck and M. Balazy (2000). "16(R)-hydroxy-5,8,11,14-eicosatetraenoic acid, a new arachidonate metabolite in human polymorphonuclear leukocytes." Biochem Pharmacol **60**(3): 447-455.

Benassayag, C., T. M. Mignot, M. Haourigui, C. Civel, J. Hassid, B. Carbonne, E. A. Nunez and F. Ferre (1997). "High polyunsaturated fatty acid, thromboxane A2, and alpha-fetoprotein concentrations at the human feto-maternal interface." J Lipid Res **38**(2): 276-286.

Berl, T., K. D. Wilner, M. Gardner, R. A. Hansen, B. Farmer, B. A. Baris and W. L. Henrich (1995). "Pharmacokinetics of fluconazole in renal failure." J Am Soc Nephrol **6**(2): 242-247.

Bernhardt, R. (2006). "Cytochromes P450 as versatile biocatalysts." J Biotechnol **124**(1): 128-145.

Bibi, Z. (2008). "Role of cytochrome P450 in drug interactions." Nutrition & metabolism **5**(1): 1.

Blewett, A. J., D. Varma, T. Gilles, J. R. Libonati and S. A. Jansen (2008). "Development and validation of a high-performance liquid chromatography-electrospray mass spectrometry method for the simultaneous determination of 23 eicosanoids." J Pharm Biomed Anal **46**(4): 653-662.

Borhan, B., A. D. Jones, F. Pinot, D. F. Grant, M. J. Kurth and B. D. Hammock (1995). "Mechanism of soluble epoxide hydrolase. Formation of an alpha-hydroxy ester-enzyme intermediate through Asp-333." J Biol Chem **270**(45): 26923-26930.

Bozkurt, B., S. B. Kribbs, F. J. Clubb, Jr., L. H. Michael, V. V. Didenko, P. J. Hornsby, Y. Seta, H. Oral, F. G. Spinale and D. L. Mann (1998). "Pathophysiologically relevant concentrations of tumor necrosis factor-alpha promote progressive left ventricular dysfunction and remodeling in rats." Circulation **97**(14): 1382-1391.

Brash, A. R. (2001). "Arachidonic acid as a bioactive molecule." J Clin Invest **107**(11): 1339-1345.

Breitbart, E., Y. Sofer, A. Shainberg and S. Grossman (1996). "Lipoxygenase activity in heart cells." FEBS Lett **395**(2-3): 148-152.

Brodie, B. B., J. R. Gillette and B. N. La Du (1958). "Enzymatic metabolism of drugs and other foreign compounds." Annu Rev Biochem **27**(3): 427-454.

Brown, V. A., K. R. Patel, M. Viskaduraki, J. A. Crowell, M. Perloff, T. D. Booth, G. Vasilinin, A. Sen, A. M. Schinas, G. Piccirilli, K. Brown, W. P. Steward, A. J. Gescher and D. E. Brenner (2010). "Repeat dose study of the cancer chemopreventive agent resveratrol in healthy volunteers: safety, pharmacokinetics, and effect on the insulin-like growth factor axis." Cancer Res **70**(22): 9003-9011.

Buczynski, M. W., D. S. Dumlao and E. A. Dennis (2009). "Thematic Review Series: Proteomics. An integrated omics analysis of eicosanoid biology." J Lipid Res **50**(6): 1015-1038.

Bureik, M., B. Schiffler, Y. Hiraoka, F. Vogel and R. Bernhardt (2002). "Functional expression of human mitochondrial CYP11B2 in fission yeast and identification of a new internal electron transfer protein, etp1." Biochemistry **41**(7): 2311-2321.

Burke, J. E. and E. A. Dennis (2009). "Phospholipase A2 structure/function, mechanism, and signaling." J Lipid Res **50** Suppl: S237-242.

Bylund, J., T. Kunz, K. Valmsen and E. H. Oliw (1998). "Cytochromes P450 with bisallylic hydroxylation activity on arachidonic and linoleic acids studied with human recombinant enzymes and with human and rat liver microsomes." J Pharmacol Exp Ther **284**(1): 51-60.

Capdevila, J., L. Gil, M. Orellana, L. J. Marnett, J. I. Mason, P. Yadagiri and J. R. Falck (1988). "Inhibitors of cytochrome P-450-dependent arachidonic acid metabolism." Arch Biochem Biophys **261**(2): 257-263.

Capdevila, J. H. (2007). "Regulation of ion transport and blood pressure by cytochrome p450 monooxygenases." Curr Opin Nephrol Hypertens **16**(5): 465-470.

Capdevila, J. H., J. R. Falck and R. C. Harris (2000). "Cytochrome P450 and arachidonic acid bioactivation. Molecular and functional properties of the arachidonate monooxygenase." J Lipid Res **41**(2): 163-181.

Capdevila, J. H., A. Karara, D. J. Waxman, M. V. Martin, J. R. Falck and F. P. Guengerich (1990). "Cytochrome P-450 enzyme-specific control of the regio- and enantiofacial selectivity of the microsomal arachidonic acid epoxygenase." J Biol Chem **265**(19): 10865-10871.

Carlson, G. P., D. E. Hynes and N. A. Mantick (1998). "Effects of inhibitors of CYP1A and CYP2B on styrene metabolism in mouse liver and lung microsomes." Toxicol Lett **98**(3): 131-137.

Carroll, M. A., M. Balazy, D. D. Huang, S. Rybalova, J. R. Falck and J. C. McGiff (1997). "Cytochrome P450-derived renal HETEs: storage and release." Kidney Int **51**(6): 1696-1702.

Castle, P. J., J. L. Merdink, J. R. Okita, S. A. Wrighton and R. T. Okita (1995). "Human liver lauric acid hydroxylase activities." Drug Metab Dispos **23**(10): 1037-1043.

Caterina, P., D. P. Antonello, C. Chiara, L. Giacomo, S. Antonio and G. Luca (2013). "Pharmacokinetic drug-drug interaction and their implication in clinical management." Journal of research in medical sciences **18**(7): 600-609.

Chang, T. K., J. Chen and W. B. Lee (2001). "Differential inhibition and inactivation of human CYP1 enzymes by trans-resveratrol: evidence for mechanism-based inactivation of CYP1A2." J Pharmacol Exp Ther **299**(3): 874-882.

Chawengsub, Y., K. M. Gauthier, K. Nithipatikom, B. D. Hammock, J. R. Falck, D. Narsimhaswamy and W. B. Campbell (2009). "Identification of 13-hydroxy-14,15-epoxyeicosatrienoic acid as an acid-stable endothelium-derived hyperpolarizing factor in rabbit arteries." J Biol Chem **284**(45): 31280-31290.

Chevalier, D., D. Allorge, J. M. Lo-Guidice, C. Cauffiez, C. Lepetit, F. Migot-Nabias, A. Kenani, M. Lhermitte and F. Broly (2002). "Sequence analysis, frequency and ethnic distribution of VNTR polymorphism in the 5'-untranslated region of the human prostacyclin synthase gene (CYP8A1)." Prostaglandins Other Lipid Mediat **70**(1-2): 31-37.

Choudhary, D., I. Jansson, I. Stoilov, M. Sarfarazi and J. B. Schenkman (2004). "Metabolism of retinoids and arachidonic acid by human and mouse cytochrome P450 1b1." Drug Metab Dispos **32**(8): 840-847.

Chuang, S. S., C. Helvig, M. Taimi, H. A. Ramshaw, A. H. Collop, M. Amad, J. A. White, M. Petkovich, G. Jones and B. Korczak (2004). "CYP2U1, a novel human thymus- and brain-specific cytochrome P450, catalyzes omega- and (omega-1)-hydroxylation of fatty acids." J Biol Chem **279**(8): 6305-6314.

Chun, Y. J., S. Kim, D. Kim, S. K. Lee and F. P. Guengerich (2001). "A new selective and potent inhibitor of human cytochrome P450 1B1 and its application to antimutagenesis." Cancer Res **61**(22): 8164-8170.

Conrad, C. H., W. W. Brooks, J. A. Hayes, S. Sen, K. G. Robinson and O. H. Bing (1995). "Myocardial fibrosis and stiffness with hypertrophy and heart failure in the spontaneously hypertensive rat." Circulation **91**(1): 161-170.

Couroucli, X. I., S. E. Welty, R. S. Geske and B. Moorthy (2002). "Regulation of pulmonary and hepatic cytochrome P4501A expression in the rat by hyperoxia: implications for hyperoxic lung injury." Mol Pharmacol **61**(3): 507-515.

Daff, S. N., S. K. Chapman, K. L. Turner, R. A. Holt, S. Govindaraj, T. L. Poulos and A. W. Munro (1997). "Redox control of the catalytic cycle of flavocytochrome P-450 BM3." Biochemistry **36**(45): 13816-13823.

de Montellano, P. R. O. and M. A. Correia (1995). Inhibition of cytochrome P450 enzymes. Cytochrome P450, Springer: 305-364.

de Visser, S. P., F. Ogliaro, P. K. Sharma and S. Shaik (2002). "What factors affect the regioselectivity of oxidation by cytochrome p450? A DFT study of allylic hydroxylation and double bond epoxidation in a model reaction." J Am Chem Soc **124**(39): 11809-11826.

Deb, S. and S. M. Bandiera (2009). "Characterization and expression of extrahepatic CYP2S1." Expert Opin Drug Metab Toxicol **5**(4): 367-380.

Debruyne, D. (1997). "Clinical pharmacokinetics of fluconazole in superficial and systemic mycoses." Clin Pharmacokinet **33**(1): 52-77.

Decker, M., M. Adamska, A. Cronin, F. Di Giallonardo, J. Burgener, A. Marowsky, J. R. Falck, C. Morisseau, B. D. Hammock, A. Gruzdev, D. C. Zeldin and M. Arand (2012). "EH3 (ABHD9): the first member of a new epoxide hydrolase family with high activity for fatty acid epoxides." J Lipid Res **53**(10): 2038-2045.

Decker, M., M. Arand and A. Cronin (2009). "Mammalian epoxide hydrolases in xenobiotic metabolism and signalling." Arch Toxicol **83**(4): 297-318.

Delozier, T. C., G. E. Kissling, S. J. Coulter, D. Dai, J. F. Foley, J. A. Bradbury, E. Murphy, C. Steenbergen, D. C. Zeldin and J. A. Goldstein (2007). "Detection of human CYP2C8, CYP2C9, and CYP2J2 in cardiovascular tissues." Drug Metab Dispos **35**(4): 682-688.

Deng, J., I. Carbone and R. A. Dean (2007). "The evolutionary history of cytochrome P450 genes in four filamentous Ascomycetes." BMC Evol Biol **7**: 30.

Denisov, I. G., T. M. Makris, S. G. Sligar and I. Schlichting (2005). "Structure and chemistry of cytochrome P450." Chem Rev **105**(6): 2253-2277.

Diani-Moore, S., Y. Ma, S. S. Gross and A. B. Rifkind (2014). "Increases in levels of epoxyeicosatrienoic and dihydroxyeicosatrienoic acids (EETs and DHETs) in liver and heart in vivo by 2,3,7,8-tetrachlorodibenzo-p-dioxin (TCDD) and in hepatic EET:DHET ratios by cotreatment with TCDD and the soluble epoxide hydrolase inhibitor AUDA." Drug Metab Dispos **42**(2): 294-300.

Doligalski, C. T., A. Tong Logan and A. Silverman (2012). "Drug interactions: a primer for the gastroenterologist." Gastroenterol Hepatol (N Y) **8**(6): 376-383.

Dorokhov, Y. L., A. V. Shindyapina, E. V. Sheshukova and T. V. Komarova (2015). "Metabolic methanol: molecular pathways and physiological roles." Physiol Rev **95**(2): 603-644.

Drahushuk, A. T., B. P. McGarrigle, K. E. Larsen, J. J. Stegeman and J. R. Olson (1998). "Detection of CYP1A1 protein in human liver and induction by TCDD in precision-cut liver slices incubated in dynamic organ culture." Carcinogenesis **19**(8): 1361-1368.

Draper, A. J. and B. D. Hammock (2000). "Identification of CYP2C9 as a human liver microsomal linoleic acid epoxygenase." Arch Biochem Biophys **376**(1): 199-205.

Dubrac, S., S. R. Lear, M. Ananthanarayanan, N. Balasubramanian, J. Bollineni, S. Shefer, H. Hyogo, D. E. Cohen, P. J. Blanche, R. M. Krauss, A. K. Batta, G. Salen, F. J. Suchy, N. Maeda and S. K. Erickson (2005). "Role of CYP27A in cholesterol and bile acid metabolism." J Lipid Res **46**(1): 76-85.

Dufek, M. B., A. S. Bridges and D. R. Thakker (2013). "Intestinal first-pass metabolism by cytochrome p450 and not p-glycoprotein is the major barrier to amprenavir absorption." Drug Metab Dispos **41**(9): 1695-1702.

Edpuganti, V. and R. Mehvar (2013). "UHPLC-MS/MS analysis of arachidonic acid and 10 of its major cytochrome P450 metabolites as free acids in rat livers: Effects of hepatic ischemia." J Chromatogr B Analyt Technol Biomed Life Sci.

Edson, K. Z. and A. E. Rettie (2013). "CYP4 enzymes as potential drug targets: focus on enzyme multiplicity, inducers and inhibitors, and therapeutic modulation of 20-hydroxyeicosatetraenoic acid (20-HETE) synthase and fatty acid omega-hydroxylase activities." Curr Top Med Chem **13**(12): 1429-1440.

Eldrup, A. B., F. Soleymanzadeh, S. J. Taylor, I. Muegge, N. A. Farrow, D. Joseph, K. McKellop, C. C. Man, A. Kukulka and S. De Lombaert (2009). "Structure-based optimization of arylamides as inhibitors of soluble epoxide hydrolase." J Med Chem **52**(19): 5880-5895.

Elkhatali, S., A. A. El-Sherbeni, O. H. Elshenawy, G. Abdelhamid and A. O. El-Kadi (2015). "19-Hydroxyeicosatetraenoic acid and isoniazid protect against angiotensin II-induced cardiac hypertrophy." Toxicol Appl Pharmacol **289**(3): 550-559.

Elsherbin, M. E., A. O. El-Kadi and D. R. Brocks (2010). "The effect of beta-naphthoflavone on the metabolism of amiodarone by hepatic and extra-hepatic microsomes." Toxicol Lett **195**(2-3): 147-154.

Enayetallah, A. E., R. A. French, M. Barber and D. F. Grant (2006). "Cell-specific subcellular localization of soluble epoxide hydrolase in human tissues." J Histochem Cytochem **54**(3): 329-335.

Evangelista, E. A., R. Kaspera, N. A. Mokadam, J. P. Jones, 3rd and R. A. Totah (2013). "Activity, inhibition, and induction of cytochrome P450 2J2 in adult human primary cardiomyocytes." Drug Metab Dispos **41**(12): 2087-2094.

Falck, J. R., S. Lumin, I. Blair, E. Dishman, M. V. Martin, D. J. Waxman, F. P. Guengerich and J. H. Capdevila (1990). "Cytochrome P-450-dependent oxidation of arachidonic acid to 16-, 17-, and 18-hydroxyeicosatetraenoic acids." J Biol Chem **265**(18): 10244-10249.

Fan, D., A. Takawale, J. Lee and Z. Kassiri (2012). "Cardiac fibroblasts, fibrosis and extracellular matrix remodeling in heart disease." Fibrogenesis Tissue Repair **5**(1): 15.

Fan, F., Y. Muroya and R. J. Roman (2015). "Cytochrome P450 eicosanoids in hypertension and renal disease." Curr Opin Nephrol Hypertens **24**(1): 37-46.

Felton, T., P. F. Troke and W. W. Hope (2014). "Tissue penetration of antifungal agents." Clin Microbiol Rev **27**(1): 68-88.

Fernandez-Salguero, P., T. Pineau, D. M. Hilbert, T. McPhail, S. S. Lee, S. Kimura, D. W. Nebert, S. Rudikoff, J. M. Ward and F. J. Gonzalez (1995). "Immune system impairment and hepatic fibrosis in mice lacking the dioxin-binding Ah receptor." Science **268**(5211): 722-726.

Ferro, B. E., J. Meletiadis, M. Wattenberg, A. de Jong, D. van Soelingen, J. W. Mouton and J. van Ingen (2015). "Clofazimine Prevents the Regrowth of Mycobacterium abscessus and Mycobacterium avium Type Strains Exposed to Amikacin and Clarithromycin." Antimicrob Agents Chemother **60**(2): 1097-1105.

Fleming, I. (2014). "The pharmacology of the cytochrome P450 epoxygenase/soluble epoxide hydrolase axis in the vasculature and cardiovascular disease." Pharmacol Rev **66**(4): 1106-1140.

Food-and-Drug-Administration. (2014). "Drug Development and Drug Interactions: Table of Substrates, Inhibitors and Inducers." Retrieved May 10, 2015, from <http://www.fda.gov/drugs/developmentapprovalprocess/developmentresources/druginteractions/abeling/ucm093664.htm>.

Fowler, S. and H. Zhang (2008). "In vitro evaluation of reversible and irreversible cytochrome P450 inhibition: current status on methodologies and their utility for predicting drug-drug interactions." AAPS J **10**(2): 410-424.

Fretland, A. J. and C. J. Omiecinski (2000). "Epoxide hydrolases: biochemistry and molecular biology." Chem Biol Interact **129**(1-2): 41-59.

Frey, N., H. A. Katus, E. N. Olson and J. A. Hill (2004). "Hypertrophy of the heart: a new therapeutic target?" Circulation **109**(13): 1580-1589.

Frey, N. and E. N. Olson (2003). "Cardiac hypertrophy: the good, the bad, and the ugly." Annu Rev Physiol **65**: 45-79.

Frustaci, A., R. Verardo, M. Caldarulo, M. C. Acconcia, M. A. Russo and C. Chimenti (2007). "Myocarditis in hypertrophic cardiomyopathy patients presenting acute clinical deterioration." Eur Heart J **28**(6): 733-740.

Fulton, D., J. R. Falck, J. C. McGiff, M. A. Carroll and J. Quilley (1998). "A method for the determination of 5,6-EET using the lactone as an intermediate in the formation of the diol." J Lipid Res **39**(8): 1713-1721.

Gan, L. S., A. L. Acebo and W. L. Alworth (1984). "1-Ethynylpyrene, a suicide inhibitor of cytochrome P-450 dependent benzo[a]pyrene hydroxylase activity in liver microsomes." Biochemistry **23**(17): 3827-3836.

Garfinkel, D. (1958). "Studies on pig liver microsomes. I. Enzymic and pigment composition of different microsomal fractions." Arch Biochem Biophys **77**(2): 493-509.

Gauthier, K. M., C. Deeter, U. M. Krishna, Y. K. Reddy, M. Bondlela, J. R. Falck and W. B. Campbell (2002). "14,15-Epoxyeicosa-5(Z)-enoic acid: a selective epoxyeicosatrienoic acid antagonist that inhibits endothelium-dependent hyperpolarization and relaxation in coronary arteries." Circ Res **90**(9): 1028-1036.

Gharavi, N. and A. O. El-Kadi (2005). "tert-Butylhydroquinone is a novel aryl hydrocarbon receptor ligand." Drug Metab Dispos **33**(3): 365-372.

Gill, S. S. and B. D. Hammock (1980). "Distribution and properties of a mammalian soluble epoxide hydrolase." Biochem Pharmacol **29**(3): 389-395.

Golan, D. E. (2012). Principles of pharmacology : the pathophysiologic basis of drug therapy. Philadelphia, Wolters Kluwer/Lippincott Williams & Wilkins.

Gomez, G. A., C. Morisseau, B. D. Hammock and D. W. Christianson (2004). "Structure of human epoxide hydrolase reveals mechanistic inferences on bifunctional catalysis in epoxide and phosphate ester hydrolysis." Biochemistry **43**(16): 4716-4723.

Grant, D. F., D. H. Storms and B. D. Hammock (1993). "Molecular cloning and expression of murine liver soluble epoxide hydrolase." J Biol Chem **268**(23): 17628-17633.

Guengerich, F. P. (2008). "Cytochrome p450 and chemical toxicology." Chem Res Toxicol **21**(1): 70-83.

Gugler, R. and H. Allgayer (1990). "Effects of antacids on the clinical pharmacokinetics of drugs. An update." Clin Pharmacokinet **18**(3): 210-219.

Ha, T., Y. Li, X. Gao, J. R. McMullen, T. Shioi, S. Izumo, J. L. Kelley, A. Zhao, G. E. Haddad, D. L. Williams, I. W. Browder, R. L. Kao and C. Li (2005). "Attenuation of cardiac hypertrophy by inhibiting both mTOR and NFkappaB activation in vivo." Free Radic Biol Med **39**(12): 1570-1580.

Hammarstrom, S., M. Hamberg, B. Samuelsson, E. A. Duell, M. Stawiski and J. J. Voorhees (1975). "Increased concentrations of nonesterified arachidonic acid, 12L-hydroxy-5,8,10,14-eicosatetraenoic acid, prostaglandin E2, and prostaglandin F2alpha in epidermis of psoriasis." Proc Natl Acad Sci U S A **72**(12): 5130-5134.

Hammock, B. D., D. F. Grant and D. H. Storms (1997). Epoxide hydrolases  
Elsevier Science Ltd, Oxford.

Hannemann, F., A. Bichet, K. M. Ewen and R. Bernhardt (2007). "Cytochrome P450 systems--biological variations of electron transport chains." Biochim Biophys Acta **1770**(3): 330-344.

He, J., C. Wang, Y. Zhu and D. Ai (2016). "Soluble epoxide hydrolase: A potential target for metabolic diseases." J Diabetes **8**(3): 305-313.

Helvig, C., E. Dishman and J. H. Capdevila (1998). "Molecular, enzymatic, and regulatory characterization of rat kidney cytochromes P450 4A2 and 4A3." Biochemistry **37**(36): 12546-12558.

Hoch, U. and P. R. Ortiz De Montellano (2001). "Covalently linked heme in cytochrome p450<sub>4A</sub> fatty acid hydroxylases." J Biol Chem **276**(14): 11339-11346.

Holla, V. R., K. Makita, P. G. Zaphiropoulos and J. H. Capdevila (1999). "The kidney cytochrome P-450 2C23 arachidonic acid epoxygenase is upregulated during dietary salt loading." J Clin Invest **104**(6): 751-760.

Houston, J. B. and K. E. Kenworthy (2000). "In vitro-in vivo scaling of CYP kinetic data not consistent with the classical Michaelis-Menten model." Drug Metab Dispos **28**(3): 246-254.

Huang, A., D. Sun, A. Jacobson, M. A. Carroll, J. R. Falck and G. Kaley (2005). "Epoxyeicosatrienoic acids are released to mediate shear stress-dependent hyperpolarization of arteriolar smooth muscle." Circ Res **96**(3): 376-383.

Huang, H., M. Al-Shabrawey and M. H. Wang (2016). "Cyclooxygenase- and cytochrome P450-derived eicosanoids in stroke." Prostaglandins Other Lipid Mediat **122**: 45-53.

Huang, S. M., R. Temple, D. C. Throckmorton and L. J. Lesko (2007). "Drug interaction studies: study design, data analysis, and implications for dosing and labeling." Clin Pharmacol Ther **81**(2): 298-304.

Hye Khan, M. A., T. S. Pavlov, S. V. Christain, J. Neckar, A. Staruschenko, K. M. Gauthier, J. H. Capdevila, J. R. Falck, W. B. Campbell and J. D. Imig (2014). "Epoxyeicosatrienoic acid analogue lowers blood pressure through vasodilation and sodium channel inhibition." Clin Sci (Lond) **127**(7): 463-474.

Iliff, J. J., J. Jia, J. Nelson, T. Goyagi, J. Klaus and N. J. Alkayed (2010). "Epoxyeicosanoid signaling in CNS function and disease." Prostaglandins Other Lipid Mediat **91**(3-4): 68-84.

Imaoka, S., T. Hashizume and Y. Funae (2005). "Localization of rat cytochrome P450 in various tissues and comparison of arachidonic acid metabolism by rat P450 with that by human P450 orthologs." Drug Metab Pharmacokin **20**(6): 478-484.

Imig, J. D. (2000). "Epoxygenase metabolites. Epithelial and vascular actions." Mol Biotechnol **16**(3): 233-251.

Imig, J. D. (2012). "Epoxides and soluble epoxide hydrolase in cardiovascular physiology." Physiol Rev **92**(1): 101-130.

Imig, J. D., A. Elmarakby, K. Nithipatikom, S. Wei, J. H. Capdevila, V. R. Tuniki, B. Sangras, S. Anjaiah, V. L. Manthathi, D. Sudarshan Reddy and J. R. Falck (2010). "Development of epoxyeicosatrienoic acid analogs with in vivo anti-hypertensive actions." Front Physiol **1**: 157.

Imig, J. D. and B. D. Hammock (2009). "Soluble epoxide hydrolase as a therapeutic target for cardiovascular diseases." Nat Rev Drug Discov **8**(10): 794-805.

Imig, J. D., L. G. Navar, R. J. Roman, K. K. Reddy and J. R. Falck (1996). "Actions of epoxygenase metabolites on the preglomerular vasculature." J Am Soc Nephrol **7**(11): 2364-2370.

Inoue, Y., A. M. Yu, S. H. Yim, X. Ma, K. W. Krausz, J. Inoue, C. C. Xiang, M. J. Brownstein, G. Eggertsen, I. Bjorkhem and F. J. Gonzalez (2006). "Regulation of bile acid biosynthesis by hepatocyte nuclear factor 4alpha." J Lipid Res **47**(1): 215-227.

Ioannides, C. (2002). Enzyme systems that metabolise drugs and other xenobiotics. Chichester ; New York, J. Wiley.

Ioannides, C. (2008). Cytochromes P450 role in the metabolism and toxicity of drugs and other xenobiotics. Issues in toxicology. Cambridge, RSC Pub.: 1 online resource (xviii, 521 p.).

Ito, O., Y. Nakamura, L. Tan, T. Ishizuka, Y. Sasaki, N. Minami, M. Kanazawa, S. Ito, H. Sasano and M. Kohzuki (2006). "Expression of cytochrome P-450 4 enzymes in the kidney and liver: regulation by PPAR and species-difference between rat and human." Mol Cell Biochem **284**(1-2): 141-148.

Jefcoate, C. R., R. Hume and G. S. Boyd (1970). "Separation of two forms of cytochrome P450 adrenal cortex mitochondria." FEBS Lett **9**(1): 41-44.

Jenkins, C. M., A. Cedars and R. W. Gross (2009). "Eicosanoid signalling pathways in the heart." Cardiovasc Res **82**(2): 240-249.

Jiang, W., S. E. Welty, X. I. Couroucli, R. Barrios, S. R. Kondraganti, K. Muthiah, L. Yu, S. E. Avery and B. Moorthy (2004). "Disruption of the Ah receptor gene alters the susceptibility of mice to oxygen-mediated regulation of pulmonary and hepatic cytochromes P4501A expression and exacerbates hyperoxic lung injury." J Pharmacol Exp Ther **310**(2): 512-519.

Juric, D., P. Wojciechowski, D. K. Das and T. Netticadan (2007). "Prevention of concentric hypertrophy and diastolic impairment in aortic-banded rats treated with resveratrol." Am J Physiol Heart Circ Physiol **292**(5): H2138-2143.

Kalsotra, A., C. M. Turman, Y. Kikuta and H. W. Strobel (2004). "Expression and characterization of human cytochrome P450 4F11: Putative role in the metabolism of therapeutic drugs and eicosanoids." Toxicol Appl Pharmacol **199**(3): 295-304.

Kapelyukh, Y., M. J. Paine, J. D. Marechal, M. J. Sutcliffe, C. R. Wolf and G. C. Roberts (2008). "Multiple substrate binding by cytochrome P450 3A4: estimation of the number of bound substrate molecules." Drug Metab Dispos **36**(10): 2136-2144.

Karlgren, M., A. Gomez, K. Stark, J. Svard, C. Rodriguez-Antona, E. Oliw, M. L. Bernal, S. Ramon y Cajal, I. Johansson and M. Ingelman-Sundberg (2006). "Tumor-specific expression of the novel cytochrome P450 enzyme, CYP2W1." Biochem Biophys Res Commun **341**(2): 451-458.

Kaspera, R. and R. A. Totah (2009). "Epoxyeicosatrienoic acids: formation, metabolism and potential role in tissue physiology and pathophysiology." Expert Opin Drug Metab Toxicol **5**(7): 757-771.

Katholi, R. E. and D. M. Couri (2011). "Left ventricular hypertrophy: major risk factor in patients with hypertension: update and practical clinical applications." Int J Hypertens **2011**: 495349.

Kayama, Y., T. Minamino, H. Toko, M. Sakamoto, I. Shimizu, H. Takahashi, S. Okada, K. Tateno, J. Moriya, M. Yokoyama, A. Nojima, M. Yoshimura, K. Egashira, H. Aburatani and I. Komuro (2009). "Cardiac 12/15 lipoxygenase-induced inflammation is involved in heart failure." J Exp Med **206**(7): 1565-1574.

Kehat, I. and J. D. Molkentin (2010). "Molecular pathways underlying cardiac remodeling during pathophysiological stimulation." Circulation **122**(25): 2727-2735.

Kim, S., H. Ko, J. E. Park, S. Jung, S. K. Lee and Y. J. Chun (2002). "Design, synthesis, and discovery of novel trans-stilbene analogues as potent and selective human cytochrome P450 1B1 inhibitors." J Med Chem **45**(1): 160-164.

Kiss, L., H. Schutte, K. Mayer, H. Grimm, W. Padberg, W. Seeger and F. Grimminger (2000). "Synthesis of arachidonic acid-derived lipoxygenase and cytochrome P450 products in the intact human lung vasculature." Am J Respir Crit Care Med **161**(6): 1917-1923.

Klingenberg, M. (1958). "Pigments of rat liver microsomes." Arch Biochem Biophys **75**(2): 376-386.

Knijff-Dutmer, E. A., G. A. Schut and M. A. van de Laar (2003). "Concomitant coumarin-NSAID therapy and risk for bleeding." Ann Pharmacother **37**(1): 12-16.

Ko, J. W., Z. Desta, N. V. Soukhova, T. Tracy and D. A. Flockhart (2000). "In vitro inhibition of the cytochrome P450 (CYP450) system by the antiplatelet drug ticlopidine: potent effect on CYP2C19 and CYP2D6." Br J Clin Pharmacol **49**(4): 343-351.

Kodani, S. D. and B. D. Hammock (2015). "The 2014 Bernard B. Brodie award lecture-epoxide hydrolases: drug metabolism to therapeutics for chronic pain." Drug Metab Dispos **43**(5): 788-802.

Kondraganti, S. R., W. Jiang, A. K. Jaiswal and B. Moorthy (2008). "Persistent induction of hepatic and pulmonary phase II enzymes by 3-methylcholanthrene in rats." Toxicol Sci **102**(2): 337-344.

Kramer, M. A. and T. S. Tracy (2008). "Studying cytochrome P450 kinetics in drug metabolism." Expert Opin Drug Metab Toxicol **4**(5): 591-603.

Kuhn, H., S. Banthiya and K. van Leyen (2015). "Mammalian lipoxygenases and their biological relevance." Biochim Biophys Acta **1851**(4): 308-330.

Lacourciere, G. M., V. N. Vakharia, C. P. Tan, D. I. Morris, G. H. Edwards, M. Moos and R. N. Armstrong (1993). "Interaction of hepatic microsomal epoxide hydrolase derived from a recombinant baculovirus expression system with an azarene oxide and an aziridine substrate analogue." Biochemistry **32**(10): 2610-2616.

Laethem, R. M., M. Balazy, J. R. Falck, C. L. Laethem and D. R. Koop (1993). "Formation of 19(S)-, 19(R)-, and 18(R)-hydroxyeicosatetraenoic acids by alcohol-inducible cytochrome P450 2E1." J Biol Chem **268**(17): 12912-12918.

Lash, L. H., D. A. Putt and H. Cai (2008). "Drug metabolism enzyme expression and activity in primary cultures of human proximal tubular cells." Toxicology **244**(1): 56-65.

Lasker, J. M., W. B. Chen, I. Wolf, B. P. Blowski, P. D. Wilson and P. K. Powell (2000). "Formation of 20-hydroxyeicosatetraenoic acid, a vasoactive and natriuretic eicosanoid, in human kidney. Role of Cyp4F2 and Cyp4A11." J Biol Chem **275**(6): 4118-4126.

LeBrun, L. A., U. Hoch and P. R. Ortiz de Montellano (2002). "Autocatalytic mechanism and consequences of covalent heme attachment in the cytochrome P4504A family." J Biol Chem **277**(15): 12755-12761.

Lee, C. A., J. P. Jones, 3rd, J. Katayama, R. Kaspera, Y. Jiang, S. Freiwald, E. Smith, G. S. Walker and R. A. Totah (2012). "Identifying a selective substrate and inhibitor pair for the evaluation of CYP2J2 activity." Drug Metab Dispos **40**(5): 943-951.

Lee, C. A., D. Neul, A. Clouser-Roche, D. Dalvie, M. R. Wester, Y. Jiang, J. P. Jones, 3rd, S. Freiwald, M. Zientek and R. A. Totah (2010). "Identification of novel substrates for human cytochrome P450 2J2." Drug Metab Dispos **38**(2): 347-356.

Lee, E. and K. Kariya (1986). "Propylthiouracil, a selective inhibitor of NADH-cytochrome b5 reductase." FEBS Lett **209**(1): 49-51.

Lee, S. S., J. T. Buters, T. Pineau, P. Fernandez-Salguero and F. J. Gonzalez (1996). "Role of CYP2E1 in the hepatotoxicity of acetaminophen." J Biol Chem **271**(20): 12063-12067.

Lewis, D. F., E. Watson and B. G. Lake (1998). "Evolution of the cytochrome P450 superfamily: sequence alignments and pharmacogenetics." Mutat Res **410**(3): 245-270.

LiCata, V. J. and N. M. Allewell (1997). "Is substrate inhibition a consequence of allostery in aspartate transcarbamylase?" Biophys Chem **64**(1-3): 225-234.

Lin, Y., P. Lu, C. Tang, Q. Mei, G. Sandig, A. D. Rodrigues, T. H. Rushmore and M. Shou (2001). "Substrate inhibition kinetics for cytochrome P450-catalyzed reactions." Drug Metab Dispos **29**(4 Pt 1): 368-374.

Liu, M. and N. J. Alkayed (2005). "Hypoxic preconditioning and tolerance via hypoxia inducible factor (HIF) 1alpha-linked induction of P450 2C11 epoxygenase in astrocytes." J Cereb Blood Flow Metab **25**(8): 939-948.

Liu, X., C. Li, D. Gebremedhin, S. H. Hwang, B. D. Hammock, J. R. Falck, R. J. Roman, D. R. Harder and R. C. Koehler (2011). "Epoxyeicosatrienoic acid-dependent cerebral vasodilation evoked by metabotropic glutamate receptor activation in vivo." Am J Physiol Heart Circ Physiol **301**(2): H373-381.

Livak, K. J. and T. D. Schmittgen (2001). "Analysis of relative gene expression data using real-time quantitative PCR and the 2(-Delta Delta C(T)) Method." Methods **25**(4): 402-408.

Lorell, B. H. and B. A. Carabello (2000). "Left ventricular hypertrophy: pathogenesis, detection, and prognosis." Circulation **102**(4): 470-479.

Lowry, O. H., N. J. Rosebrough, A. L. Farr and R. J. Randall (1951). "Protein measurement with the Folin phenol reagent." J Biol Chem **193**(1): 265-275.

Lozada, A. and C. A. Dujovne (1994). "Drug interactions with fibric acids." Pharmacol Ther **63**(2): 163-176.

Lu, A. Y., K. W. Junk and M. J. Coon (1969). "Resolution of the cytochrome P-450-containing omega-hydroxylation system of liver microsomes into three components." J Biol Chem **244**(13): 3714-3721.

Lu, A. Y., R. Kuntzman, S. West and A. H. Conney (1971). "Reconstituted liver microsomal enzyme system that hydroxylates drugs, other foreign compounds and endogenous substrates. I. Determination of substrate specificity by the cytochrome P-450 and P-448 fractions." Biochem Biophys Res Commun **42**(6): 1200-1206.

Lu, A. Y., W. Levin, S. B. West, M. Jacobson, D. Ryan, R. Kuntzman and A. H. Conney (1973). "Reconstituted liver microsomal enzyme system that hydroxylates drugs, other foreign compounds, and endogenous substrates. VI. Different substrate specificities of the cytochrome P450 fractions from control and phenobarbital-treated rats." J Biol Chem **248**(2): 456-460.

Lund, A. K., M. B. Goens, N. L. Kanagy and M. K. Walker (2003). "Cardiac hypertrophy in aryl hydrocarbon receptor null mice is correlated with elevated angiotensin II, endothelin-1, and mean arterial blood pressure." Toxicol Appl Pharmacol **193**(2): 177-187.

Maayah, Z. H., G. Abdelhamid and A. O. El-Kadi (2015). "Development of cellular hypertrophy by 8-hydroxyeicosatetraenoic acid in the human ventricular cardiomyocyte, RL-14 cell line, is implicated by MAPK and NF-kappaB." Cell Biol Toxicol **31**(4-5): 241-259.

Maayah, Z. H., H. N. Althurwi, G. Abdelhamid, G. Lesyk, P. Jurasz and A. O. El-Kadi (2016). "CYP1B1 inhibition attenuates doxorubicin-induced cardiotoxicity through a mid-chain HETEs-dependent mechanism." Pharmacol Res **105**: 28-43.

Maayah, Z. H. and A. O. El-Kadi (2016). "5-, 12- and 15-Hydroxyeicosatetraenoic acids induce cellular hypertrophy in the human ventricular cardiomyocyte, RL-14 cell line, through MAPK- and NF-kappaB-dependent mechanism." Arch Toxicol **90**(2): 359-373.

Makia, N. L. and J. A. Goldstein (2016). "CYP2C8 Is a Novel Target of Peroxisome Proliferator-Activated Receptor alpha in Human Liver." Mol Pharmacol **89**(1): 154-164.

Marji, J. S., M. H. Wang and M. Laniado-Schwartzman (2002). "Cytochrome P-450 4A isoform expression and 20-HETE synthesis in renal preglomerular arteries." Am J Physiol Renal Physiol **283**(1): F60-67.

Martignoni, M., G. M. Groothuis and R. de Kanter (2006). "Species differences between mouse, rat, dog, monkey and human CYP-mediated drug metabolism, inhibition and induction." Expert Opin Drug Metab Toxicol **2**(6): 875-894.

Masiha, S., J. Sundstrom and L. Lind (2013). "Inflammatory markers are associated with left ventricular hypertrophy and diastolic dysfunction in a population-based sample of elderly men and women." J Hum Hypertens **27**(1): 13-17.

McMullen, J. R. and G. L. Jennings (2007). "Differences between pathological and physiological cardiac hypertrophy: novel therapeutic strategies to treat heart failure." Clin Exp Pharmacol Physiol **34**(4): 255-262.

Midzak, A., N. Akula, L. Lecanu and V. Papadopoulos (2011). "Novel androstenediol interacts with the mitochondrial translocator protein and controls steroidogenesis." J Biol Chem **286**(11): 9875-9887.

Miguel-Carrasco, J. L., S. Zambrano, A. J. Blanca, A. Mate and C. M. Vazquez (2010). "Captopril reduces cardiac inflammatory markers in spontaneously hypertensive rats by inactivation of NF- $\kappa$ B." J Inflamm (Lond) **7**: 21.

Mihl, C., W. R. Dassen and H. Kuipers (2008). "Cardiac remodelling: concentric versus eccentric hypertrophy in strength and endurance athletes." Neth Heart J **16**(4): 129-133.

Miksys, S. and R. F. Tyndale (2013). "Cytochrome P450-mediated drug metabolism in the brain." J Psychiatry Neurosci **38**(3): 152-163.

Miller, G. P. (2008). "Advances in the interpretation and prediction of CYP2E1 metabolism from a biochemical perspective." Expert Opin Drug Metab Toxicol **4**(8): 1053-1064.

Mitchell, L. A., J. H. Moran and D. F. Grant (2002). "Linoleic acid, cis-epoxyoctadecenoic acids, and dihydroxyoctadecadienoic acids are toxic to Sf-21 cells in the absence of albumin." Toxicol Lett **126**(3): 187-196.

Miyata, N., T. Seki, Y. Tanaka, T. Omura, K. Taniguchi, M. Doi, K. Bandou, S. Kametani, M. Sato, S. Okuyama, L. Cambj-Sapunar, D. R. Harder and R. J. Roman (2005). "Beneficial effects of a new 20-hydroxyeicosatetraenoic acid synthesis inhibitor, TS-011 [N-(3-chloro-4-morpholin-4-yl) phenyl-N'-hydroxyimido formamide], on hemorrhagic and ischemic stroke." J Pharmacol Exp Ther **314**(1): 77-85.

Miyata, N., K. Taniguchi, T. Seki, T. Ishimoto, M. Sato-Watanabe, Y. Yasuda, M. Doi, S. Kametani, Y. Tomishima, T. Ueki, M. Sato and K. Kameo (2001). "HET0016, a potent and selective inhibitor of 20-HETE synthesizing enzyme." Br J Pharmacol **133**(3): 325-329.

Mizrachi, D., Z. Wang, K. K. Sharma, M. K. Gupta, K. Xu, C. R. Dwyer and R. J. Auchus (2011). "Why human cytochrome P450c21 is a progesterone 21-hydroxylase." Biochemistry **50**(19): 3968-3974.

Moran, J. H., G. Nowak and D. F. Grant (2001). "Analysis of the toxic effects of linoleic acid, 12,13-cis-epoxyoctadecenoic acid, and 12,13-dihydroxyoctadecenoic acid in rabbit renal cortical mitochondria." Toxicol Appl Pharmacol **172**(2): 150-161.

Moran, J. H., R. Weise, R. G. Schnellmann, J. P. Freeman and D. F. Grant (1997). "Cytotoxicity of linoleic acid diols to renal proximal tubular cells." Toxicol Appl Pharmacol **146**(1): 53-59.

Morgan, L. A., A. R. Olzinski, J. J. Upson, S. Zhao, T. Wang, S. H. Eisennagel, B. Hoang, J. R. Tunstead, J. P. Marino, Jr., R. N. Willette, B. M. Jucker and D. J. Behm (2012). "Soluble epoxide hydrolase inhibition does not prevent cardiac remodeling and dysfunction following aortic constriction in rats and mice." J Cardiovasc Pharmacol.

Morisseau, C. (2013). "Role of epoxide hydrolases in lipid metabolism." Biochimie **95**(1): 91-95.

Morisseau, C., G. Du, J. W. Newman and B. D. Hammock (1998). "Mechanism of mammalian soluble epoxide hydrolase inhibition by chalcone oxide derivatives." Arch Biochem Biophys **356**(2): 214-228.

Morisseau, C., M. H. Goodrow, D. Dowdy, J. Zheng, J. F. Greene, J. R. Sanborn and B. D. Hammock (1999). "Potent urea and carbamate inhibitors of soluble epoxide hydrolases." Proc Natl Acad Sci U S A **96**(16): 8849-8854.

Morisseau, C. and B. D. Hammock (2005). "Epoxide hydrolases: mechanisms, inhibitor designs, and biological roles." Annu Rev Pharmacol Toxicol **45**: 311-333.

Morisseau, C. and B. D. Hammock (2007). "Measurement of soluble epoxide hydrolase (sEH) activity." Curr Protocol Toxicol **33**: 1-18.

Morisseau, C. and B. D. Hammock (2013). "Impact of soluble epoxide hydrolase and epoxyeicosanoids on human health." Annu Rev Pharmacol Toxicol **53**: 37-58.

Muerhoff, A. S., D. E. Williams, N. O. Reich, C. A. CaJacob, P. R. Ortiz de Montellano and B. S. Masters (1989). "Prostaglandin and fatty acid omega- and (omega-1)-oxidation in rabbit lung. Acetylenic fatty acid mechanism-based inactivators as specific inhibitors." J Biol Chem **264**(2): 749-756.

Muir, A. I., L. Chamberlain, N. A. Elshourbagy, D. Michalovich, D. J. Moore, A. Calamari, P. G. Szekeres, H. M. Sarau, J. K. Chambers, P. Murdock, K. Steplewski, U. Shabon, J. E. Miller, S. E.

Middleton, J. G. Darker, C. G. Larminie, S. Wilson, D. J. Bergsma, P. Emson, R. Faull, K. L. Philpott and D. C. Harrison (2001). "AXOR12, a novel human G protein-coupled receptor, activated by the peptide KiSS-1." J Biol Chem **276**(31): 28969-28975.

Muller, D. N., J. Theuer, E. Shagdarsuren, E. Kaergel, H. Honeck, J. K. Park, M. Markovic, E. Barbosa-Sicard, R. Dechend, M. Wellner, T. Kirsch, A. Fiebeler, M. Rothe, H. Haller, F. C. Luft and W. H. Schunck (2004). "A peroxisome proliferator-activated receptor-alpha activator induces renal CYP2C23 activity and protects from angiotensin II-induced renal injury." Am J Pathol **164**(2): 521-532.

Muroya, Y., F. Fan, K. R. Regner, J. R. Falck, M. R. Garrett, L. A. Juncos and R. J. Roman (2015). "Deficiency in the Formation of 20-Hydroxyeicosatetraenoic Acid Enhances Renal Ischemia-Reperfusion Injury." J Am Soc Nephrol **26**(10): 2460-2469.

Murray, G. I., W. T. Melvin, W. F. Greenlee and M. D. Burke (2001). "Regulation, function, and tissue-specific expression of cytochrome P450 CYP1B1." Annu Rev Pharmacol Toxicol **41**: 297-316.

Nagata, K., R. Liao, F. R. Eberli, N. Satoh, B. Chevalier, C. S. Apstein and T. M. Suter (1998). "Early changes in excitation-contraction coupling: transition from compensated hypertrophy to failure in Dahl salt-sensitive rat myocytes." Cardiovasc Res **37**(2): 467-477.

Nakajima, T., R. S. Wang, E. Elovaara, S. S. Park, H. V. Gelboin and H. Vainio (1992). "A comparative study on the contribution of cytochrome P450 isozymes to metabolism of benzene, toluene and trichloroethylene in rat liver." Biochem Pharmacol **43**(2): 251-257.

Nakamura, S., M. Yoshimura, M. Nakayama, T. Ito, Y. Mizuno, E. Harada, T. Sakamoto, Y. Saito, K. Nakao, H. Yasue and H. Ogawa (2004). "Possible association of heart failure status with synthetic balance between aldosterone and dehydroepiandrosterone in human heart." Circulation **110**(13): 1787-1793.

Nebert, D. W., M. Adesnik, M. J. Coon, R. W. Estabrook, F. J. Gonzalez, F. P. Guengerich, I. C. Gunsalus, E. F. Johnson, B. Kemper, W. Levin and et al. (1987). "The P450 gene superfamily: recommended nomenclature." DNA **6**(1): 1-11.

Nebert, D. W., K. Wikvall and W. L. Miller (2013). "Human cytochromes P450 in health and disease." Philos Trans R Soc Lond B Biol Sci **368**(1612): 20120431.

Nelson, D. R. (2006). "Cytochrome P450 nomenclature, 2004." Methods Mol Biol **320**: 1-10.

Nelson, D. R. (2009). "The cytochrome p450 homepage." Hum Genomics **4**(1): 59-65.

Nelson, J. W., R. M. Subrahmanyam, S. A. Summers, X. Xiao and N. J. Alkayed (2013). "Soluble epoxide hydrolase dimerization is required for hydrolase activity." J Biol Chem **288**(11): 7697-7703.

Newman, J. W., C. Morisseau and B. D. Hammock (2005). "Epoxide hydrolases: their roles and interactions with lipid metabolism." Prog Lipid Res **44**(1): 1-51.

Nguyen, X., M. H. Wang, K. M. Reddy, J. R. Falck and M. L. Schwartzman (1999). "Kinetic profile of the rat CYP4A isoforms: arachidonic acid metabolism and isoform-specific inhibitors." Am J Physiol **276**(6 Pt 2): R1691-1700.

Nicoletti, A. and J. B. Michel (1999). "Cardiac fibrosis and inflammation: interaction with hemodynamic and hormonal factors." Cardiovasc Res **41**(3): 532-543.

Nithipatikom, K., A. J. Grall, B. B. Holmes, D. R. Harder, J. R. Falck and W. B. Campbell (2001). "Liquid chromatographic-electrospray ionization-mass spectrometric analysis of cytochrome P450 metabolites of arachidonic acid." Anal Biochem **298**(2): 327-336.

Niwa, T., T. Shiraga and A. Takagi (2005). "Effect of antifungal drugs on cytochrome P450 (CYP) 2C9, CYP2C19, and CYP3A4 activities in human liver microsomes." Biol Pharm Bull **28**(9): 1805-1808.

Norris, P. C., D. Reichart, D. S. Dumlao, C. K. Glass and E. A. Dennis (2011). "Specificity of eicosanoid production depends on the TLR-4-stimulated macrophage phenotype." J Leukoc Biol **90**(3): 563-574.

Norwood, S., J. Liao, B. D. Hammock and G. Y. Yang (2010). "Epoxyeicosatrienoic acids and soluble epoxide hydrolase: potential therapeutic targets for inflammation and its induced carcinogenesis." Am J Transl Res **2**(4): 447-457.

Nusing, R. M., H. Schweer, I. Fleming, D. C. Zeldin and M. Wegmann (2007). "Epoxyeicosatrienoic acids affect electrolyte transport in renal tubular epithelial cells: dependence on cyclooxygenase and cell polarity." Am J Physiol Renal Physiol **293**(1): F288-298.

Oesch, F., J. G. Hengstler and M. Arand (2004). "Detoxication strategy of epoxide hydrolase-the basis for a novel threshold for definable genotoxic carcinogens." Nonlinearity Biol Toxicol Med **2**(1): 21-26.

Oesch, F., D. Raphael, H. Schwind and H. R. Glatt (1977). "Species differences in activating and inactivating enzymes related to the control of mutagenic metabolites." Arch Toxicol **39**(1-2): 97-108.

Oka, T., H. Akazawa, A. T. Naito and I. Komuro (2014). "Angiogenesis and cardiac hypertrophy: maintenance of cardiac function and causative roles in heart failure." Circ Res **114**(3): 565-571.

Oliw, E. H. (1994). "Oxygenation of polyunsaturated fatty acids by cytochrome P450 monooxygenases." Prog Lipid Res **33**(3): 329-354.

Omura, T. and R. Sato (1962). "A new cytochrome in liver microsomes." J Biol Chem **237**: 1375-1376.

Ortiz de Montellano, P. R. (2005). *Cytochrome P450 structure, mechanism, and biochemistry*. New York, Kluwer Academic/Plenum Publishers: xx, 689 p.

Ozawa, T., M. Nishikimi, S. Sugiyama, F. Taki, M. Hayakawa and H. Shionoya (1988). "Cytotoxic activity of leukotoxin, a neutrophil-derived fatty acid epoxide, on cultured human cells." Biochem Int **16**(2): 369-373.

Palakodety, R. B., L. A. Clejan, G. Krikun, D. E. Feerman and A. I. Cederbaum (1988). "Characterization and identification of a pyrazole-inducible form of cytochrome P-450." J Biol Chem **263**(2): 878-884.

Pandak, W. M., P. B. Hylemon, S. Ren, D. Marques, G. Gil, K. Redford, D. Mallonee and Z. R. Vlahcevic (2002). "Regulation of oxysterol 7 $\alpha$ -hydroxylase (CYP7B1) in primary cultures of rat hepatocytes." Hepatology **35**(6): 1400-1408.

Pandey, A. V., P. Kempna, G. Hofer, P. E. Mullis and C. E. Fluck (2007). "Modulation of human CYP19A1 activity by mutant NADPH P450 oxidoreductase." Mol Endocrinol **21**(10): 2579-2595.

Pang, W., N. Li, D. Ai, X. L. Niu, Y. F. Guan and Y. Zhu (2011). "Activation of peroxisome proliferator-activated receptor-gamma downregulates soluble epoxide hydrolase in cardiomyocytes." Clin Exp Pharmacol Physiol **38**(6): 358-364.

Patten, R. D. and M. R. Hall-Porter (2009). "Small animal models of heart failure: development of novel therapies, past and present." Circ Heart Fail **2**(2): 138-144.

Peterson, T. C., P. Hodgson, P. Fernandez-Salguero, M. Neumeister and F. J. Gonzalez (2000). "Hepatic fibrosis and cytochrome P450: experimental models of fibrosis compared to AHR knockout mice." Hepatol Res **17**(2): 112-125.

Pinot, F., D. F. Grant, J. L. Spearow, A. G. Parker and B. D. Hammock (1995). "Differential regulation of soluble epoxide hydrolase by clofibrate and sexual hormones in the liver and kidneys of mice." Biochem Pharmacol **50**(4): 501-508.

Piver, B., F. Berthou, Y. Dreano and D. Lucas (2001). "Inhibition of CYP3A, CYP1A and CYP2E1 activities by resveratrol and other non volatile red wine components." Toxicol Lett **125**(1-3): 83-91.

Podolin, P. L., B. J. Bolognese, J. F. Foley, E. Long, 3rd, B. Peck, S. Umbrecht, X. Zhang, P. Zhu, B. Schwartz, W. Xie, C. Quinn, H. Qi, S. Sweitzer, S. Chen, M. Galop, Y. Ding, S. L. Belyanskaya, D. I. Israel, B. A. Morgan, D. J. Behm, J. P. Marino, Jr., E. Kurali, M. S. Barnette, R. J. Mayer, C. L. Booth-Genthe and J. F. Callahan (2013). "In vitro and in vivo characterization of a novel soluble epoxide hydrolase inhibitor." Prostaglandins Other Lipid Mediat **104-105**: 25-31.

Poloyac, S. M., M. A. Tortorici, D. I. Przychodzin, R. B. Reynolds, W. Xie, R. F. Frye and M. A. Zemaitis (2004). "The effect of isoniazid on CYP2E1- and CYP4A-mediated hydroxylation of arachidonic acid in the rat liver and kidney." Drug Metab Dispos **32**(7): 727-733.

Porter, T. D. and C. B. Kasper (1986). "NADPH-cytochrome P-450 oxidoreductase: flavin mononucleotide and flavin adenine dinucleotide domains evolved from different flavoproteins." Biochemistry **25**(7): 1682-1687.

Powell, P. K., I. Wolf, R. Jin and J. M. Lasker (1998). "Metabolism of arachidonic acid to 20-hydroxy-5,8,11, 14-eicosatetraenoic acid by P450 enzymes in human liver: involvement of CYP4F2 and CYP4A11." J Pharmacol Exp Ther **285**(3): 1327-1336.

Preskorn, S. H., J. Alderman, M. Chung, W. Harrison, M. Messig and S. Harris (1994). "Pharmacokinetics of desipramine coadministered with sertraline or fluoxetine." J Clin Psychopharmacol **14**(2): 90-98.

Public Health Agency of Canada. (2009). 2009 tracking heart disease and stroke in Canada. Ottawa, Public Health Agency of Canada.

Quigley, R., M. Baum, K. M. Reddy, J. C. Griener and J. R. Falck (2000). "Effects of 20-HETE and 19(S)-HETE on rabbit proximal straight tubule volume transport." Am J Physiol Renal Physiol **278**(6): F949-953.

Reddy, M. A., P. R. Thimmalapura, L. Lanting, J. L. Nadler, S. Fatima and R. Natarajan (2002). "The oxidized lipid and lipoxygenase product 12(S)-hydroxyeicosatetraenoic acid induces hypertrophy and fibronectin transcription in vascular smooth muscle cells via p38 MAPK and cAMP response element-binding protein activation. Mediation of angiotensin II effects." J Biol Chem **277**(12): 9920-9928.

Reed, M. C., A. Lieb and H. F. Nijhout (2010). "The biological significance of substrate inhibition: a mechanism with diverse functions." Bioessays **32**(5): 422-429.

Reid, J. M., M. J. Kuffel, J. K. Miller, R. Rios and M. M. Ames (1999). "Metabolic activation of dacarbazine by human cytochromes P450: the role of CYP1A1, CYP1A2, and CYP2E1." Clin Cancer Res **5**(8): 2192-2197.

Reynald, R. L., S. Sansen, C. D. Stout and E. F. Johnson (2012). "Structural characterization of human cytochrome P450 2C19: active site differences between P450s 2C8, 2C9, and 2C19." J Biol Chem **287**(53): 44581-44591.

Ripa, S., L. Ferrante and M. Prena (1993). "Pharmacokinetics of fluconazole in normal volunteers." Chemotherapy **39**(1): 6-12.

Riviere, J. E. (2011). Comparative pharmacokinetics: principles, techniques and applications, John Wiley & Sons.

Roger, V. L., A. S. Go, D. M. Lloyd-Jones, E. J. Benjamin, J. D. Berry, W. B. Borden, D. M. Bravata, S. Dai, E. S. Ford, C. S. Fox, H. J. Fullerton, C. Gillespie, S. M. Hailpern, J. A. Heit, V. J. Howard, B. M. Kissela, S. J. Kittner, D. T. Lackland, J. H. Lichtman, L. D. Lisabeth, D. M. Makuc, G. M. Marcus, A. Marelli, D. B. Matchar, C. S. Moy, D. Mozaffarian, M. E. Mussolino, G. Nichol, N. P. Paynter, E. Z. Soliman, P. D. Sorlie, N. Sotoodehnia, T. N. Turan, S. S. Virani, N. D. Wong, D. Woo and M. B. Turner (2012). "Heart disease and stroke statistics--2012 update: a report from the American Heart Association." Circulation **125**(1): e2-e220.

Roman, R. J. (2002). "P-450 metabolites of arachidonic acid in the control of cardiovascular function." Physiol Rev **82**(1): 131-185.

Room, M. (2013, May 15, 2013). "Nomenclature Committee of IUBMB (NC-IUBMB) and IUPAC-IUBMB Joint Commission on Biochemical Nomenclature (JCBN)." from <http://iupac.org/cms/wp-content/uploads/2016/01/Joint-Commission-on-Biochemical-Nomenclature-JCBN-Meeting-Minutes-Dun-Laoghaire-May-2013.pdf>.

Rouzer, C. A. and L. J. Marnett (2009). "Cyclooxygenases: structural and functional insights." J Lipid Res **50 Suppl**: S29-34.

Roy, U., R. Joshua, R. L. Stark and M. Balazy (2005). "Cytochrome P450/NADPH-dependent biosynthesis of 5,6-trans-epoxyeicosatrienoic acid from 5,6-trans-arachidonic acid." Biochem J **390**(Pt 3): 719-727.

Ruan, K. H., P. Li, R. J. Kulmacz and K. K. Wu (1994). "Characterization of the structure and membrane interaction of NH<sub>2</sub>-terminal domain of thromboxane A<sub>2</sub> synthase." J Biol Chem **269**(33): 20938-20942.

Russo, G. L. (2009). "Dietary n-6 and n-3 polyunsaturated fatty acids: from biochemistry to clinical implications in cardiovascular prevention." Biochem Pharmacol **77**(6): 937-946.

Rustan, A. C. and C. A. Drevon (2001). "Fatty Acids: Structures and Properties." eLS.

Sacerdoti, D., A. Gatta and J. C. McGiff (2003). "Role of cytochrome P450-dependent arachidonic acid metabolites in liver physiology and pathophysiology." Prostaglandins Other Lipid Mediat **72**(1-2): 51-71.

Sadoshima, J. and S. Izumo (1993). "Mechanical stretch rapidly activates multiple signal transduction pathways in cardiac myocytes: potential involvement of an autocrine/paracrine mechanism." EMBO J **12**(4): 1681-1692.

Sale, S., R. D. Verschoyle, D. Boocock, D. J. Jones, N. Wilsher, K. C. Ruparelia, G. A. Potter, P. B. Farmer, W. P. Steward and A. J. Gescher (2004). "Pharmacokinetics in mice and growth-inhibitory properties of the putative cancer chemopreventive agent resveratrol and the synthetic analogue trans 3,4,5,4'-tetramethoxystilbene." Br J Cancer **90**(3): 736-744.

Salsali, M., A. Holt and G. B. Baker (2004). "Inhibitory effects of the monoamine oxidase inhibitor tranylcypramine on the cytochrome P450 enzymes CYP2C19, CYP2C9, and CYP2D6." Cell Mol Neurobiol **24**(1): 63-76.

Sasayama, S., Y. Kihara, A. Matsumori and K. Hasegawa (1999). "Transition from Compensated to Decompensated Cardiac Hypertrophy." Heart Failure Reviews **4**.

Schladt, L., R. Hartmann, C. Timms, M. Strolin-Benedetti, P. Dostert, W. Worner and F. Oesch (1987). "Concomitant induction of cytosolic but not microsomal epoxide hydrolase with peroxisomal beta-oxidation by various hypolipidemic compounds." Biochem Pharmacol **36**(3): 345-351.

Schoch, G. A., J. K. Yano, S. Sansen, P. M. Dansette, C. D. Stout and E. F. Johnson (2008). "Determinants of cytochrome P450 2C8 substrate binding: structures of complexes with montelukast, troglitazone, felodipine, and 9-cis-retinoic acid." J Biol Chem **283**(25): 17227-17237.

Schuck, R. N., W. Zha, M. L. Edin, A. Gruzdev, K. C. Vendrov, T. M. Miller, Z. Xu, F. B. Lih, L. M. DeGraff, K. B. Tomer, H. M. Jones, L. Makowski, L. Huang, S. M. Poloyac, D. C. Zeldin and C.

R. Lee (2014). "The cytochrome P450 epoxygenase pathway regulates the hepatic inflammatory response in fatty liver disease." PLoS One **9**(10): e110162.

Schwarz, D., A. Chernogolov and P. Kisselev (1999). "Complex formation in vesicle-reconstituted mitochondrial cytochrome P450 systems (CYP11A1 and CYP11B1) as evidenced by rotational diffusion experiments using EPR and ST-EPR." Biochemistry **38**(29): 9456-9464.

Schwarz, D., P. Kisselev, S. S. Ericksen, G. D. Szklarz, A. Chernogolov, H. Honeck, W. H. Schunck and I. Roots (2004). "Arachidonic and eicosapentaenoic acid metabolism by human CYP1A1: highly stereoselective formation of 17(R),18(S)-epoxyeicosatetraenoic acid." Biochem Pharmacol **67**(8): 1445-1457.

Shen, H. C. and B. D. Hammock (2012). "Discovery of inhibitors of soluble epoxide hydrolase: a target with multiple potential therapeutic indications." J Med Chem **55**(5): 1789-1808.

Shimada, T., J. Watanabe, K. Kawajiri, T. R. Sutter, F. P. Guengerich, E. M. Gillam and K. Inoue (1999). "Catalytic properties of polymorphic human cytochrome P450 1B1 variants." Carcinogenesis **20**(8): 1607-1613.

Shinkyō, R., T. Sakaki, M. Kamakura, M. Ohta and K. Inouye (2004). "Metabolism of vitamin D by human microsomal CYP2R1." Biochem Biophys Res Commun **324**(1): 451-457.

Shorr, R. I., W. A. Ray, J. R. Daugherty and M. R. Griffin (1993). "Concurrent use of nonsteroidal anti-inflammatory drugs and oral anticoagulants places elderly persons at high risk for hemorrhagic peptic ulcer disease." Arch Intern Med **153**(14): 1665-1670.

Siopi, M., N. Siafakas, S. Vourli, L. Zerva and J. Meletiadis (2015). "Optimization of polyene-azole combination therapy against aspergillosis using an in vitro pharmacokinetic-pharmacodynamic model." Antimicrob Agents Chemother **59**(7): 3973-3983.

Sladek, N. E. and G. J. Mannering (1966). "Evidence for a new P-450 hemoprotein in hepatic microsomes from methylcholanthrene treated rats." Biochem Biophys Res Commun **24**(5): 668-674.

Slavotinek, A. M., P. Mehrotra, I. Nazarenko, P. L. Tang, R. Lao, D. Cameron, B. Li, C. Chu, C. Chou, A. L. Marqueling, M. Yahyavi, K. Cordoro, I. Frieden, T. Glaser, T. Prescott, M. A. Morren, K. Devriendt, P. Y. Kwok, M. Petkovich and R. J. Desnick (2013). "Focal facial dermal dysplasia, type IV, is caused by mutations in CYP26C1." Hum Mol Genet **22**(4): 696-703.

Sligar, S. G. (1976). "Coupling of spin, substrate, and redox equilibria in cytochrome P450." Biochemistry **15**(24): 5399-5406.

Slim, R., B. D. Hammock, M. Toborek, L. W. Robertson, J. W. Newman, C. H. Morisseau, B. A. Watkins, V. Saraswathi and B. Hennig (2001). "The role of methyl-linoleic acid epoxide and diol metabolites in the amplified toxicity of linoleic acid and polychlorinated biphenyls to vascular endothelial cells." Toxicol Appl Pharmacol **171**(3): 184-193.

Smeets, P. J., B. E. Teunissen, A. Planavila, H. de Vogel-van den Bosch, P. H. Willemsen, G. J. van der Vusse and M. van Bilsen (2008). "Inflammatory pathways are activated during cardiomyocyte hypertrophy and attenuated by peroxisome proliferator-activated receptors PPARalpha and PPARdelta." J Biol Chem **283**(43): 29109-29118.

Spector, A. A. and H. Y. Kim (2015). "Cytochrome P450 epoxygenase pathway of polyunsaturated fatty acid metabolism." Biochim Biophys Acta **1851**(4): 356-365.

Stec, D. E., K. P. Gannon, J. S. Beaird and H. A. Drummond (2007). "20-Hydroxyeicosatetraenoic acid (20-HETE) stimulates migration of vascular smooth muscle cells." Cell Physiol Biochem **19**(1-4): 121-128.

Stuehr, D. J., J. Tejero and M. M. Haque (2009). "Structural and mechanistic aspects of flavoproteins: electron transfer through the nitric oxide synthase flavoprotein domain." FEBS J **276**(15): 3959-3974.

Stundl, U. M., I. Schmidt, U. Scheller, R. Schmid, W. H. Schunck and F. Schauer (1998). "Purification and characterization of cytosolic cytochrome P450 forms from yeasts belonging to the genus *Trichosporon*." Arch Biochem Biophys **357**(1): 131-136.

Sucharov, C. C., K. Dockstader and T. A. McKinsey (2008). "YY1 protects cardiac myocytes from pathologic hypertrophy by interacting with HDAC5." Mol Biol Cell **19**(10): 4141-4153.

Sudhahar, V., S. Shaw and J. D. Imig (2010). "Epoxyeicosatrienoic acid analogs and vascular function." Curr Med Chem **17**(12): 1181-1190.

Sun, D., C. Yan, A. Jacobson, H. Jiang, M. A. Carroll and A. Huang (2007). "Contribution of epoxyeicosatrienoic acids to flow-induced dilation in arteries of male ERalpha knockout mice: role of aromatase." Am J Physiol Regul Integr Comp Physiol **293**(3): R1239-1246.

Taegtmeyer, H., S. Sen and D. Vela (2010). "Return to the fetal gene program: a suggested metabolic link to gene expression in the heart." Ann N Y Acad Sci **1188**: 191-198.

Tamburini, P. P., H. A. Masson, S. K. Bains, R. J. Makowski, B. Morris and G. G. Gibson (1984). "Multiple forms of hepatic cytochrome P-450. Purification, characterisation and comparison of a

novel clofibrate-induced isozyme with other major forms of cytochrome P-450." Eur J Biochem **139**(2): 235-246.

Taxak, N., P. V. Desai, B. Patel, M. Mohutsky, V. J. Klimkowski, V. Gombar and P. V. Bharatam (2012). "Metabolic-intermediate complex formation with cytochrome P450: theoretical studies in elucidating the reaction pathway for the generation of reactive nitroso intermediate." J Comput Chem **33**(21): 1740-1747.

Theken, K. N., Y. Deng, M. A. Kannon, T. M. Miller, S. M. Poloyac and C. R. Lee (2011). "Activation of the acute inflammatory response alters cytochrome P450 expression and eicosanoid metabolism." Drug Metab Dispos **39**(1): 22-29.

Theken, K. N., R. N. Schuck, M. L. Edin, B. Tran, K. Ellis, A. Bass, F. B. Lih, K. B. Tomer, S. M. Poloyac, M. C. Wu, A. L. Hinderliter, D. C. Zeldin, G. A. Stouffer and C. R. Lee (2012). "Evaluation of cytochrome P450-derived eicosanoids in humans with stable atherosclerotic cardiovascular disease." Atherosclerosis **222**(2): 530-536.

Thomas, H., L. Schladt, M. Knehr and F. Oesch (1989). "Effect of diabetes and starvation on the activity of rat liver epoxide hydrolases, glutathione S-transferases and peroxisomal beta-oxidation." Biochem Pharmacol **38**(23): 4291-4297.

Thum, T. and J. Borlak (2002). "Testosterone, cytochrome P450, and cardiac hypertrophy." FASEB J **16**(12): 1537-1549.

Tran, D. T., A. Ohinmaa, N. X. Thanh, J. G. Howlett, J. A. Ezekowitz, F. A. McAlister and P. Kaul (2016). "The current and future financial burden of hospital admissions for heart failure in Canada: a cost analysis." CMAJ Open **4**(3): E365-E370.

Tripathy, S., J. D. Chapman, C. Y. Han, C. A. Hogarth, S. L. Arnold, J. Onken, T. Kent, D. R. Goodlett and N. Isoherranen (2016). "All-Trans-Retinoic Acid Enhances Mitochondrial Function in Models of Human Liver." Mol Pharmacol **89**(5): 560-574.

Tse, M. M., M. E. Aboutabl, H. N. Althurwi, O. H. Elshenawy, G. Abdelhamid and A. O. El-Kadi (2013). "Cytochrome P450 epoxygenase metabolite, 14,15-EET, protects against isoproterenol-induced cellular hypertrophy in H9c2 rat cell line." Vascul Pharmacol **58**(5-6): 363-373.

Ullrich, V., R. Brugger, F. Lottspeich and I. Siegle (1997). "Properties of prostacyclin synthase." Adv Exp Med Biol **400A**: 113-119.

van Herwaarden, A. E., E. Wagenaar, C. M. van der Kruijssen, R. A. van Waterschoot, J. W. Smit, J. Y. Song, M. A. van der Valk, O. van Tellingen, J. W. van der Hoorn, H. Rosing, J. H. Beijnen

and A. H. Schinkel (2007). "Knockout of cytochrome P450 3A yields new mouse models for understanding xenobiotic metabolism." J Clin Invest **117**(11): 3583-3592.

Van Vleet, T. R., D. W. Bombick and R. A. Coulombe, Jr. (2001). "Inhibition of human cytochrome P450 2E1 by nicotine, cotinine, and aqueous cigarette tar extract in vitro." Toxicol Sci **64**(2): 185-191.

Vang, O., N. Ahmad, C. A. Baile, J. A. Baur, K. Brown, A. Csiszar, D. K. Das, D. Delmas, C. Gottfried, H. Y. Lin, Q. Y. Ma, P. Mukhopadhyay, N. Nalini, J. M. Pezzuto, T. Richard, Y. Shukla, Y. J. Surh, T. Szekeres, T. Szkudelski, T. Walle and J. M. Wu (2011). "What is new for an old molecule? Systematic review and recommendations on the use of resveratrol." PLoS One **6**(6): e19881.

Vangaveti, V. N., H. Jansen, R. L. Kennedy and U. H. Malabu (2016). "Hydroxyoctadecadienoic acids: Oxidised derivatives of linoleic acid and their role in inflammation associated with metabolic syndrome and cancer." Eur J Pharmacol **785**: 70-76.

Vincent, B., N. Morellet, F. Fatemi, L. Aigrain, G. Truan, E. Guittet and E. Lescop (2012). "The closed and compact domain organization of the 70-kDa human cytochrome P450 reductase in its oxidized state as revealed by NMR." J Mol Biol **420**(4-5): 296-309.

Voznesensky, A. I. and J. B. Schenkman (1992). "The cytochrome P450 2B4-NADPH cytochrome P450 reductase electron transfer complex is not formed by charge-pairing." J Biol Chem **267**(21): 14669-14676.

Walsh, A. A., G. D. Szklarz and E. E. Scott (2013). "Human cytochrome P450 1A1 structure and utility in understanding drug and xenobiotic metabolism." J Biol Chem **288**(18): 12932-12943.

Walsky, R. L., A. V. Astuccio and R. S. Obach (2006). "Evaluation of 227 drugs for in vitro inhibition of cytochrome P450 2B6." J Clin Pharmacol **46**(12): 1426-1438.

Wang, D. and R. N. Dubois (2012). "Epoxyeicosatrienoic acids: a double-edged sword in cardiovascular diseases and cancer." J Clin Invest **122**(1): 19-22.

Wang, M. H., E. Brand-Schieber, B. A. Zand, X. Nguyen, J. R. Falck, N. Balu and M. L. Schwartzman (1998). "Cytochrome P450-derived arachidonic acid metabolism in the rat kidney: characterization of selective inhibitors." J Pharmacol Exp Ther **284**(3): 966-973.

Wang, M. H., H. Guan, X. Nguyen, B. A. Zand, A. Nasjletti and M. Laniado-Schwartzman (1999). "Contribution of cytochrome P-450 4A1 and 4A2 to vascular 20-hydroxyeicosatetraenoic acid synthesis in rat kidneys." Am J Physiol **276**(2 Pt 2): F246-253.

Wang, M. H., D. E. Stec, M. Balazy, V. Mastuygin, C. S. Yang, R. J. Roman and M. L. Schwartzman (1996). "Cloning, sequencing, and cDNA-directed expression of the rat renal CYP4A2: arachidonic acid omega-hydroxylation and 11,12-epoxidation by CYP4A2 protein." Arch Biochem Biophys **336**(2): 240-250.

Wen, Y., J. Gu, Y. Liu, P. H. Wang, Y. Sun and J. L. Nadler (2001). "Overexpression of 12-lipoxygenase causes cardiac fibroblast cell growth." Circ Res **88**(1): 70-76.

Wen, Y., J. Gu, X. Peng, G. Zhang and J. Nadler (2003). "Overexpression of 12-lipoxygenase and cardiac fibroblast hypertrophy." Trends Cardiovasc Med **13**(4): 129-136.

Werck-Reichhart, D. and R. Feyereisen (2000). "Cytochromes P450: a success story." Genome Biol **1**(6): REVIEWS3003.

Westphal, C., A. Konkel and W. H. Schunck (2015). "Cytochrome p450 enzymes in the bioactivation of polyunsaturated Fatty acids and their role in cardiovascular disease." Adv Exp Med Biol **851**: 151-187.

Wickramashighe, R. H. and C. A. Vilee (1975). "Early role during chemical evolution for cytochrome P450 in oxygen detoxification." Nature **256**(5517): 509-510.

Williams, P. A., J. Cosme, A. Ward, H. C. Angove, D. Matak Vinkovic and H. Jhoti (2003). "Crystal structure of human cytochrome P450 2C9 with bound warfarin." Nature **424**(6947): 464-468.

Wilson, L. D., S. B. Oldham and B. W. Harding (1968). "Cytochrome P450 and steroid 11beta-hydroxylation in mitochondria from human adrenal cortex." J Clin Endocrinol Metab **28**(8): 1143-1152.

Writing Group, M., D. Mozaffarian, E. J. Benjamin, A. S. Go, D. K. Arnett, M. J. Blaha, M. Cushman, S. R. Das, S. de Ferranti, J. P. Despres, H. J. Fullerton, V. J. Howard, M. D. Huffman, C. R. Isasi, M. C. Jimenez, S. E. Judd, B. M. Kissela, J. H. Lichtman, L. D. Lisabeth, S. Liu, R. H. Mackey, D. J. Magid, D. K. McGuire, E. R. Mohler, 3rd, C. S. Moy, P. Muntner, M. E. Mussolino, K. Nasir, R. W. Neumar, G. Nichol, L. Palaniappan, D. K. Pandey, M. J. Reeves, C. J. Rodriguez, W. Rosamond, P. D. Sorlie, J. Stein, A. Towfighi, T. N. Turan, S. S. Virani, D. Woo, R. W. Yeh, M. B. Turner, C. American Heart Association Statistics and S. Stroke Statistics (2016). "Heart Disease and Stroke Statistics-2016 Update: A Report From the American Heart Association." Circulation **133**(4): e38-60.

Wu, S., W. Chen, E. Murphy, S. Gabel, K. B. Tomer, J. Foley, C. Steenbergen, J. R. Falck, C. R. Moomaw and D. C. Zeldin (1997). "Molecular cloning, expression, and functional significance of a cytochrome P450 highly expressed in rat heart myocytes." J Biol Chem **272**(19): 12551-12559.

Wu, S., C. R. Moomaw, K. B. Tomer, J. R. Falck and D. C. Zeldin (1996). "Molecular cloning and expression of CYP2J2, a human cytochrome P450 arachidonic acid epoxygenase highly expressed in heart." J Biol Chem **271**(7): 3460-3468.

Xu, F., J. R. Falck, P. R. Ortiz de Montellano and D. L. Kroetz (2004). "Catalytic activity and isoform-specific inhibition of rat cytochrome p450 4F enzymes." J Pharmacol Exp Ther **308**(3): 887-895.

Xu, H., N. Valenzuela, S. Fai, D. Figeys and S. A. Bennett (2013). "Targeted lipidomics - advances in profiling lysophosphocholine and platelet-activating factor second messengers." FEBS J **280**(22): 5652-5667.

Yang, W., B. B. Holmes, V. R. Gopal, R. V. Kishore, B. Sangras, X. Y. Yi, J. R. Falck and W. B. Campbell (2007). "Characterization of 14,15-epoxyeicosatrienoyl-sulfonamides as 14,15-epoxyeicosatrienoic acid agonists: use for studies of metabolism and ligand binding." J Pharmacol Exp Ther **321**(3): 1023-1031.

Yeung, C. K., D. D. Shen, K. E. Thummel and J. Himmelfarb (2014). "Effects of chronic kidney disease and uremia on hepatic drug metabolism and transport." Kidney Int **85**(3): 522-528.

Zhang, D., G. Luo, X. Ding and C. Lu (2012). "Preclinical experimental models of drug metabolism and disposition in drug discovery and development." Acta Pharmaceutica Sinica B **2**(6): 549-561.

Zhang, D., X. Xie, Y. Chen, B. D. Hammock, W. Kong and Y. Zhu (2012). "Homocysteine upregulates soluble epoxide hydrolase in vascular endothelium in vitro and in vivo." Circ Res **110**(6): 808-817.

Zhang, F., H. Deng, R. Kemp, H. Singh, V. R. Gopal, J. R. Falck, M. Laniado-Schwartzman and A. Nasjletti (2005). "Decreased levels of cytochrome P450 2E1-derived eicosanoids sensitize renal arteries to constrictor agonists in spontaneously hypertensive rats." Hypertension **45**(1): 103-108.

Zhang, H., S. C. Im and L. Waskell (2007). "Cytochrome b5 increases the rate of product formation by cytochrome P450 2B4 and competes with cytochrome P450 reductase for a binding site on cytochrome P450 2B4." J Biol Chem **282**(41): 29766-29776.

- Zhang, W., Y. Ramamoorthy, T. Kilicarslan, H. Nolte, R. F. Tyndale and E. M. Sellers (2002). "Inhibition of cytochromes P450 by antifungal imidazole derivatives." Drug Metab Dispos **30**(3): 314-318.
- Zhao, H., G. Qi, Y. Han, X. Shen, F. Yao, C. Xuan, Y. Gu, S. Y. Qian, Q. Zeng, S. T. O'Rourke and C. Sun (2015). "20-Hydroxyeicosatetraenoic Acid Is a Key Mediator of Angiotensin II-induced Apoptosis in Cardiac Myocytes." J Cardiovasc Pharmacol **66**(1): 86-95.
- Zhao, L. and C. D. Funk (2004). "Lipoxygenase pathways in atherogenesis." Trends Cardiovasc Med **14**(5): 191-195.
- Zolk, O., F. Munzel and T. Eschenhagen (2004). "Effects of chronic endothelin-1 stimulation on cardiac myocyte contractile function." Am J Physiol Heart Circ Physiol **286**(4): H1248-1257.
- Zordoky, B. N., M. E. Aboutabl and A. O. El-Kadi (2008). "Modulation of cytochrome P450 gene expression and arachidonic acid metabolism during isoproterenol-induced cardiac hypertrophy in rats." Drug Metab Dispos **36**(11): 2277-2286.
- Zordoky, B. N., A. Anwar-Mohamed, M. E. Aboutabl and A. O. El-Kadi (2010). "Acute doxorubicin cardiotoxicity alters cardiac cytochrome P450 expression and arachidonic acid metabolism in rats." Toxicol Appl Pharmacol **242**(1): 38-46.
- Zou, A. P., J. T. Fleming, J. R. Falck, E. R. Jacobs, D. Gebremedhin, D. R. Harder and R. J. Roman (1996). "20-HETE is an endogenous inhibitor of the large-conductance Ca(2+)-activated K<sup>+</sup> channel in renal arterioles." Am J Physiol **270**(1 Pt 2): R228-237.
- Zou, J., B. M. Hallberg, T. Bergfors, F. Oesch, M. Arand, S. L. Mowbray and T. A. Jones (2000). "Structure of *Aspergillus niger* epoxide hydrolase at 1.8 Å resolution: implications for the structure and function of the mammalian microsomal class of epoxide hydrolases." Structure **8**(2): 111-122.

**Appendix: Supplement Materials**

**Table S1. The Formation Rate (pmol/pmol P450/min) of P450-Derived AA Metabolites Mediated by Human Recombinant CYP1s, CYP2B6 and CYP2C8 Enzymes.**

	<b>CYP1A1</b>	<b>CYP1A2</b>	<b>CYP1B1</b>	<b>CYP2B6</b>	<b>CYP2C8</b>
<b>5,6-EET</b>	0.194±0.01	0.988±0.032	0.035±0.001	0.157±0.028	0.08±0.008
<b>8,9-EET</b>	0.039±0.009	0.232±0.004	0.012±0.003	0.32±0.085	0.011±0.005
<b>11,12-EET</b>	0.099±0.032	0.76±0.026	0.011±0.001	0.325±0.087	0.522±0.014
<b>14,15-EET</b>	0.385±0.009	0.976±0.021	0.051±0.026	0.083±0.006	0.415±0.014
<b>5-HETE</b>	0.076±0.038	0.062±0.001	0.167±0.025	0±0	0.072±0.015
<b>8-HETE</b>	0.277±0.008	0.085±0.003	0.029±0.006	0.052±0.017	0±0
<b>9-HETE</b>	0.102±0.004	0.012±0.001	0.023±0.001	0.073±0.06	0±0
<b>11-HETE</b>	0.523±0.002	0.264±0.005	0.031±0.006	0.088±0.017	0.079±0.003
<b>12-HETE</b>	0.302±0.008	0.105±0.002	0.016±0.006	0.054±0.025	0.01±0.005
<b>15-HETE</b>	0.348±0.003	0.082±0.005	0.116±0.003	0.121±0.002	0±0
<b>16-HETE</b>	1.809±0.082	0.351±0.011	0.064±0.024	0.036±0.002	0.117±0.021
<b>17-HETE</b>	1.066±0.051	0±0	0±0	0.013±0.009	0.032±0.016
<b>18-HETE</b>	3.009±0.216	0.106±0.01	0±0	0.045±0.011	0.014±0.008
<b>19-HETE</b>	6.602±0.512	0.669±0.019	0.041±0.004	0.067±0.012	0.117±0.031
<b>20-HETE</b>	0±0	0.282±0.009	0.171±0.013	0.088±0	0.01±0.005

**Table S2. The Formation Rate (pmol/pmol P450/min) of P450-Derived AA Metabolites Mediated by Human Recombinant CYP2C9/18/19, CYP2E1 and CYP2J2 Enzymes.**

	<b>CYP2C9</b>	<b>CYP2C18</b>	<b>CYP2C19</b>	<b>CYP2E1</b>	<b>CYP2J2</b>
<b>5,6-EET</b>	0.108±0.012	0.044±0	1.701±0.045	0.015±0.001	0.034±0.008
<b>8,9-EET</b>	0.23±0.013	0.011±0.001	5.543±0.029	0±0	0.299±0.022
<b>11,12-EET</b>	0.13±0.009	0.012±0.001	1.685±0.023	0.029±0.001	0.143±0.01
<b>14,15-EET</b>	0.404±0.029	0.045±0.003	4.876±0.062	0.12±0.022	0.403±0.059
<b>5-HETE</b>	0.23±0.018	0.341±0.011	1.034±0.017	0.115±0.057	0.153±0.067
<b>8-HETE</b>	0±0	0.033±0.002	0.33±0.007	0.019±0.006	0.05±0.022
<b>9-HETE</b>	0.085±0.006	0±0	0.161±0.004	0.011±0.005	0.031±0.014
<b>11-HETE</b>	0.15±0.01	0±0	0.143±0.003	0.012±0.004	0.048±0.02
<b>12-HETE</b>	0.38±0.029	0±0	1.198±0.027	0.018±0.004	0.031±0.015
<b>15-HETE</b>	0.275±0.02	0.244±0.014	0.399±0.009	0.19±0.014	0.15±0.059
<b>16-HETE</b>	0.123±0.013	0.044±0.003	0.461±0.009	0.029±0.002	0.121±0.04
<b>17-HETE</b>	0.021±0.012	0±0	0.307±0.007	0±0	0.076±0.025
<b>18-HETE</b>	0.114±0.01	0±0	0.621±0.012	0.134±0.004	0.101±0.029
<b>19-HETE</b>	1.36±0.109	0.014±0.003	11.343±0.227	0.591±0.027	0.472±0.157
<b>20-HETE</b>	0±0	0±0	0±0	0.131±0.007	0.149±0.053

**Table S3. The Formation Rate (pmol/pmol P450/min) of P450-Derived AA Metabolites Mediated by Human Recombinant CYP3A4 and CYP4s Enzymes.**

	<b>CYP3A4</b>	<b>CYP4A11</b>	<b>CYP4F2</b>	<b>CYP4F3A</b>	<b>CYP4F3B</b>	<b>CYP4F12</b>
<b>5,6-EET</b>	0.057±0.011	0.023±0.013	0.05±0.027	0.039±0.002	0±0	0.036±0.002
<b>8,9-EET</b>	0.023±0.004	0±0	0±0	0±0	0±0	0.009±0.002
<b>11,12-EET</b>	0.016±0.002	0±0	0±0	0±0	0±0	0.006±0.001
<b>14,15-EET</b>	0.033±0.005	0.02±0.009	0±0	0±0	0±0	0.059±0.003
<b>5-HETE</b>	0.089±0	0.148±0.006	0±0	0.344±0.018	0±0	0.309±0.026
<b>8-HETE</b>	0.014±0.001	0.014±0.005	0.056±0.03	0.029±0.004	0±0	0.033±0.006
<b>9-HETE</b>	0.015±0.002	0±0	0.055±0.028	0±0	0±0	0±0
<b>11-HETE</b>	0±0	0.005±0.003	0.055±0.033	0±0	0±0	0±0
<b>12-HETE</b>	0±0	0.015±0.004	0.056±0.026	0±0	0±0	0.01±0.006
<b>15-HETE</b>	0.015±0.003	0.173±0.033	0.197±0.104	0.287±0.008	0±0	0.252±0.028
<b>16-HETE</b>	0±0	0±0	0.033±0.027	0.028±0	0±0	0.03±0.001
<b>17-HETE</b>	0±0	0±0	0±0	0±0	0±0	0±0
<b>18-HETE</b>	0±0	0±0	0±0	0±0	0±0	0.048±0.002
<b>19-HETE</b>	0±0	2.016±0.176	0.233±0.032	0.031±0	0.703±0.06	0.014±0.001
<b>20-HETE</b>	0±0	7.171±0.517	5.941±0.037	1.058±0.012	16.247±0.45	0±0